Nutrition modulates the interaction between the bacterium *Xenorhabdus nematophila* and its lepidopteran host *Spodoptera littoralis*

Robert Holdbrook

This dissertation is submitted for the degree of Doctor of Philosophy

April 2019

Lancaster Environment Centre

To my parents, who always pushed me to achieve my best

Thank you

Declaration

This thesis is the result of my own research and has not been submitted in support of an application for another degree at this or any other university. Many of the ideas in this thesis were the product of discussion with my supervisor Kenneth Wilson. All other collaborative involvement has been duly acknowledged.

Robert Holdbrook BSc. (Hons)

Lancaster University, UK

Abstract

Ecosystems consist of pairwise relationships that determine the characteristics of communities. Host-pathogen relationships are unique in ecological communities since hosts can also be considered as an ecosystem in which commensal microorganisms, parasites and host tissues compete for resources. At all ecosystem levels, resource availability produces bottom-up effects that can determine the outcome of competitive interactions. Nutrients are key resources due to their ability to influence life-history. Theories such as nutritional geometry provide a framework for the investigation of nutrient interactions with life-history traits. Insect models are common due to their economic importance as pests as well as some similarities with human biology, hence much of what is known about nutrition and immunity comes from insects.

Using the Egyptian cotton leafworm, *Spodoptera littoralis* (Lepidoptera: Noctuidae) and its natural pathogen *Xenorhabdus nematophilus* (Enterobacteriaceae) as a model system, this thesis investigates the influence of host nutrition on pathogen virulence and host resistance/tolerance.

Findings confirmed the role of dietary protein intake on *S. littoralis* resistance against pathogens (Chapter 2) and indicated possible carbohydrate-use by the caterpillar to tolerate infection (Chapter 3). Dietary macronutrient intake altered the proportion of key nutrient groups in the haemolymph as well as concentrations of individual nutrients (Chapter 4). Both *in vitro* and *in vivo*, *X. nematophilus* exploited host carbohydrates for growth, indicating direct competition for host resources (Chapters 3 & 5). *In vitro* assays also revealed direct inhibition of bacterial growth by host haemolymph protein (Chapter 5). Altogether these results allude to a greater significance for the self-medication behaviour displayed by *S. littoralis* during infection.

Acknowledgements

I have been lucky to have a big support network to help me through this process. Although I cannot name everyone here, I hope I have made you feel appreciated along the way. First, I would like to thank Sheena and Ken. You have been amazing mentors, both in and out of the lab, and you have both put up with more crazy waffling than I would like to admit.

Catherine and Yamini, the lab work would have been impossible without you. You made the start of the PhD feel like a natural process and problem solving became fun with your unique outlooks. Many thanks to Annabel, Clare, Mark, and Phil who have been my guiding forces and sources of wisdom at the worst of times. Thank you for listening patiently to all the rants and complaints.

Many thanks to everybody who has been a part of the insect culturing, especially Phil, who saves us from the little jobs so that we can focus on productivity.

I would like to thank Billy, Manyi and Anson as well as all my other housemates for keeping me sane outside the lab. Maria, I can't thank you enough for your unending faith in me. For sacrificing so much to see me through and for lifting me up at those times when I wasn't sure I would make it.

I am extremely grateful to my family who have been patient and enduring. You have all listened attentively and offered help whenever you can, even having no idea what I really do. Línive, you have been nothing but a blessing, and it has been mainly due to you that I have kept enough sanity to finish this. Finally, I give thanks and praise to God, who sustains me through His endless love and grace.

Contents

List of Tables

List of Figures

1 General Introduction

1.1 Ecosystems

1.1.1 Ecosystem divers and processes

Ecosystems consist of the biological community and the abiotic environment in which it exists (Rynkiewicz et al., 2015). The mixture of relationships that makes up a community gives it emergent properties that can be characterised and independently investigated (Begon et al., 2005). The physical factors acting on species can also be considered as constraining factors influencing species interactions (Tilman, 1986). Hence, a bi-directional relationship is formed in which the functions, and life-history of organisms influence their environment, whilst the structure of the community and resource availability determine the phenotypes and behaviours of its constituent individuals (Raubenheimer et al., 2009). The flow of energy, the main currency of an ecosystem, is determined by species interactions. Hence, communities are traditionally viewed as a complex network of pairwise relationships that are competitive, mutualistic, parasitic or predatory (Begon et al., 2005; McGill et al., 2006).

Mutualism and commensalism lead to a positive or neutral outcome for both species, whilst competition for a shared resource usually bears a cost for both species. Predation and parasitism stand out as relationships in which one organism uses another as a resource to its own benefit and to the detriment of its 'resource' (Holland and DeAngelis, 2009; Hughes et al., 2008; Polis et al., 1989). The influence of predation on a population results in top-down effects in which predator abundance and activity influences prey population structure. Prey responses to predation can in turn be mediated by the bottom-up effects of resource availability (Stoler and Relyea, 2013). These effects are the point at which the abiotic environment can determine community structure. For example, prey with better hiding locations or better-quality food resources can avoid predation more easily and so would make up a greater proportion of the

species composition. The carrying capacity (*K*) of an ecosystem reflects the number of individuals it can support and is limited by the energy inputs into the system, which is finite (Rynkiewicz et al., 2015). In this way, bottom-up effects of energy can be extrapolated from pairwise species relationships to the level of the ecosystem.

The primary focus of this project is the role of nutrient resources in the interaction between hosts and pathogenic microbes. This chapter aims to provide a brief introduction on the dynamics between the host and pathogen including pathogen resource requirements, host defence mechanisms, and how abiotic factors can alter the outcome of infection. The importance of nutrition in the mediation of infection will be introduced with a brief overview of current knowledge on how nutrients can improve host defence.

1.1.2 Microbial interactions

Ecosystems are full of microbial symbiotic relationships formed with organisms across various kingdoms of life (Stilwell et al., 2018). Although symbiosis can be commensal, mutualistic or parasitic, the term is normally used to describe mutualistic relationships between two individuals that have evolved to provide benefits to each other (Hughes et al., 2008; Vásquez et al., 2012). Microbial symbionts have been found to affect nutrition, reproduction, development and pathogen defence in insects (Chen et al., 2016; Tang et al., 2012; Vásquez et al., 2012). For example, the human body contains roughly 1.3 bacterial cells to every human cell, and these symbionts collectively possess 100 times the number of human genes (Gilbert et al., 2018). The intestinal tract alone contains a trillion microbial cells (Blum, 2017). As well as their aid in the metabolism of dietary nutrients, the human microbiota also reduces the pathogenic effects of parasites (Ayres and Schneider, 2008). Lepidopteran larvae of the species, *Spodoptera littoralis* and *Helicoverpa armigera* contain a microflora consisting of the families

Enterococci, Lactobacilli, Clostridia, the composition of which varies in response to host diet (Tang et al., 2012). Host defence has even evolved to accommodate symbionts. A study in the fruit fly, *Drosophila melanogaster*, found activation of the intestinal homeobox transcription factor, *Caudal*, represses antimicrobial peptide production. Inhibition of this pathway through RNA interference led to a significant reduction in the prevalence of Acetobacteraceae, a family of gut bacteria (Ryu et al., 2008; Silverman and Paquette, 2008).

1.2 Disease

1.2.1 Parasitic interactions

Pathogenic microorganisms are those that normally colonize a host and multiply to a density that results in disease; the reduction of functional abilities below typical efficacy (Emson, 1987; Smith and Holt, 1996; Wake and Morgan, 1986). Not all infections are caused by colonizing pathogens; opportunistic infections are those caused by resident microbes that have entered an uncontrolled state of replication. At the same time, not all colonization events lead to an infection. Pathogenic microbes only cause infection upon overcoming one or multiple facets of the host-defence (Wake and Morgan, 1986). Virulence is a term used to describe parasitic behaviour that leads to a loss of host fitness (Hughes et al., 2008). Parasites and pathogens can impact life-history evolution, sexual selection and population dynamics (Sheldon and Verhulst, 1996). Parasitic interactions are not always binary (a winner and loser) and may contain elements of other interactions such as competition for a shared resource (Holland and DeAngelis, 2009; Muñoz-Elías and McKinney, 2006).

In most cases, host-pathogen relationships fall under the bracket of interference competition in which one individual prevents another from exploiting resources in a

shared environment (Begon et al., 2005). The outcome of a host-parasite relationship can be dictated by the degree of overlap in the demand of shared resources; at different resource levels and demands, the hosts might win, the host and parasites may co-exist or the parasite might overcome the host (Rynkiewicz et al., 2015). As well as the availability of resources, hosts and pathogens are also constrained by the dependence of their growth rate on resource availability, the rate at which they may be consumed by other species, and physical limitations (Tilman, 1986).

During an infection, the host and pathogen both depend on host resources (Ponton et al., 2011b), which are further limited by metabolic demands of host immune responses (Cressler et al., 2014). Resource competition theory can be applied to host-pathogen systems and has been suggested based on evidence in mammalian biomedicine (Smith and Holt, 1996). The outcome of pathogenic interactions can be altered by nutrient availability, since within-host nutrients potentially limit pathogen growth (Smith and Holt, 1996). In a study of the nutritional demands placed on a host, Hall et al., (2009) found increasing mortality in the crustacean *Daphnia dentifera* with increasing nutrient provision, due to its fungal parasite, *Metschnikowia bicuspidata*, acting as a consumer and growing faster on the excess resources.

Consumption of resources by the host immune system limits pathogen replication ability and vice versa (Cressler et al., 2014). The advantage of limiting resources available to pathogens is confirmed by the occurrence of illness-induced anorexia across multiple phyla (Adamo, 2006). This response, involving host reduction of feeding upon infection, has been shown to increase host survival (Adamo et al., 2010). Although, the response is not consistent; some studies found a reduction in survival of diet restricted hosts (Miller and Cotter, 2017). Advantages to the host may be context specific, depending on the resource requirements of an invading pathogen in relation to its own.

The survival of diet-restricted *D. melanogaster* increased when infected with *Salmonella typhimurium*, but decreased during *Listeria monoctyogenes* infection (Ayres and Schneider, 2009). Ayres and Schneider, (2009) attributed the difference in outcome to the immune strategy employed by the fruit flies, highlighting the complexity in the role of resource availability in host-pathogen relationships.

Reflecting the need to adapt to resource availability, pathogenic organisms display phenotypic plasticity in reaction to variation in the host environment (Mideo and Reece, 2011). Phenotypic plasticity is the change of a phenotype for a given genotype in response to changes in environmental conditions (Begon et al., 2005; Reece et al., 2009). Costs associated with plasticity occur due to a diversion of resources from key growth and reproduction processes to the maintenance of sensory systems, information processing systems and infrastructure for the expression of varying phenotypes (Pigliucci and Pigliucci, 2001). There is, therefore, a selection process that results in genotype-related or population-related plastic responses (Reece et al., 2009). Parasites have developed infection strategies as part of the infection process due to an evolutionary pressure produced by host defences, selecting against individuals with inferior mechanisms (Behnke et al., 1992; Huffman, 2003).

1.2.2 Pathogen resistance

There is a lot of diversity in the physiological strategies hosts have evolved to defend against parasites, which range from the cell-mediated complex vertebrate immune system, to the simpler cellular and humoral invertebrate systems (Sheldon and Verhulst, 1996). The primary challenges faced by the immune system are distinguishing diverse potential pathogens from self, and responding to the constant evolution of pathogens. Pathogen recognition receptors have adapted to recognize conserved motifs on

prokaryotes, important to biological function and so protected from mutation (Aderem and Ulevitch, 2000). Host-defence triggers include lipopolysaccharide (LPS) from the cell-wall of gram-negative bacteria, lipopeptides, mannans from yeast cell walls, teichoic acids from gram-positive bacterial cell-walls and zymosan from fungal cell walls (Aderem and Ulevitch, 2000; Bronstein and Conner, 1984; Chai et al., 2009; Medzhitov and Janeway Jr, 1998).

The vertebrate immune system consists of 2 distinct branches that work together; the innate or non-specific response and the adaptive or specific immune response. Innate immunity, usually the primary line of defence, is involved in the acute response of the host when a threat is detected (Solomon et al., 2005). This response involves phagocytosis, mediated by white blood cells such as neutrophils and macrophages (Aderem and Ulevitch, 2000). Phagocytosis is the process whereby an immune cell engulfs a pathogen (Ribeiro and Brehélin, 2006). The adaptive immune response is mediated by cells called B and T lymphocytes, that make antigen receptors able to bind specifically to immune threats, through a series of transcriptional and translational modifications (Iwasaki and Medzhitov, 2010; Zhao et al., 2009).

The innate immunity is thought to be the older branch of the immune response due to its similarity to the invertebrate immune system. The cellular branch of the invertebrate immune system depends on cells that circulate the haemolymph called haemocytes. They isolate pathogens through the processes of phagocytosis, nodulation and encapsulation (Lavine and Strand, 2002). Encapsulation and nodulation both involve haemocyte cells forming a layer that surrounds the pathogen, then undergoing apoptosis (cell death) and melanisation to produce a permanent barrier between the pathogen and the host (Lapointe et al., 2012). The humoral response depends on free receptors and transmembrane pathogen recognition receptors detecting an immune elicitor. Binding to

an immune elicitor initiates a transcription cascade that leads to antimicrobial peptide (AMP) production (Kleino and Silverman, 2014). There is a specificity provided through the signalling cascades that lead to AMP production. Depending on whether the Toll, JNK or immune deficiency (IMD) signalling pathway is activated, a directed response can be produced for different pathogens (Petersen et al., 2012; Tanji et al., 2007). AMPs are attracted to the negatively-charged bacterial membrane through their positive domains. Once bound, they disrupt the membrane integrity through a range of mechanisms (Boman and Hultmark, 1987; Hoffmann and Reichhart, 2002; Lemaitre and Hoffmann, 2007).

AMPs may be produced by the fat body or by the gut epithelial cells. The intestinal epithelial cells may also produce reactive oxygen species to combat pathogens with a low virulence (Silverman and Paquette, 2008). As well as AMPs, pathogens circulating the insect haemolymph are faced with two enzyme-controlled responses; lysozyme and the phenoloxidase (PO) cascade. Lysozyme is an enzyme found in insect haemolymph that hydrolyzes β-1,4 linkages between N-acetylmuramic acid and N-acetyl-D-glucosamine residues of peptidoglycan in bacterial cell walls. The peptidoglycan fragments created induce immune-effector production in the fat body (Chapman, 2012). The phenoloxidase enzyme circulates in the haemolymph freely as the inactive zymogen, pro-phenoloxidase. Once activated, it oxidises mono-phenols to o-diphenols and then to o-quinones. O-quinones form melanin, which can encapsulate the target pathogens (Ashida and Brey, 1995; Haine et al., 2008b). Melanin is a multi-purpose molecule involved in immune defence, cuticle hardening, wound healing, clot formation and maintenance of intestinal homeostasis (Stączek et al., 2017).

1.2.3 Pathogen tolerance

Resistance, the ability to limit pathogen burden, is normally treated as the default host defence strategy in immunology. Another host defence strategy, however, involves limiting the health impact caused by a pathogen, referred to as tolerance (Ayres and Schneider, 2008). Hosts may not always clear an infection (resistance) and may instead tolerate infections if the virulence of the parasite is low (Sheldon and Verhulst, 1996). An example of this is in nematode-human interactions. *Necator americanus* and *Onchocerca volvulus* infections can persist for over 15 years (Behnke et al., 1992) and tolerance may be the preferred strategy if clearing the infection is more energetically costly or more damaging as a result of immunopathology (self-harm caused by the immune response), than repairing the damage caused by the pathogen (Rynkiewicz et al., 2015). Tolerance also takes into account mechanisms that regulate immunopathology (Ayres and Schneider, 2008). Summing together a host's *tolerance* and *resistance* defines it's defensive capacity (Ayres and Schneider, 2008), referred to as *resilience* (Louie et al., 2016). Tolerance has so far been demonstrated in both vertebrates (Clough et al., 2016) and invertebrates (Corby-Harris et al., 2007; Miller and Cotter, 2017). Evidence for tolerance in invertebrates comes mainly from work in the model insect *D. melanogaster*. One study investigating the relationship between genotypic variation in pathogen clearance and survival, during infection with *Pseudomonas aeruginosa,* found that genotypes with a low pathogen burden were not necessarily the longest-lived (Corby-Harris et al., 2007). Corby-Harris et al., (2007) concluded that resistance alone could not explain host survival, indicating a significant role for tolerance as a predictor of fitness when fruit flies are infected with this pathogen.

In animals, the mechanisms involved in host resistance have been studied extensively to a molecular level, but limited investment has been made to elucidate the mechanisms

involved in damage avoidance, limitation and repair (Ayres and Schneider, 2008). However, tolerance and resistance are both well described in plant biology, providing a starting point for the exploration of resilience as a combination of strategies in animals. The definition of resistance as the inverse of pathogen burden is derived from the plant ecologist assessment of host fitness in response to pathogen load (Ayres and Schneider, 2008). Similarly, tolerance is described as the slope of the reaction norm; a measure of how a given genotype would produce varying phenotypes in response to environmental variation. Plants with higher tolerance present a lower negative health impact for a given pathogen load, producing a flatter slope (Ayres and Schneider, 2008). *Vigour* is a measure of the baseline health of an individual or population before infection, and can be compared using the slope of a relationship between a health or fitness measure, and the parasite burden (Ayres and Schneider, 2008; Louie et al., 2016). The difficulty in distinguishing resistance from tolerance experimentally is due to immunopathology. Effector molecules such as reactive oxygen species are important for fighting infections, thereby increasing resistance, but the damage they cause to the host's own tissues results in a reduction in tolerance. A trade-off in resistance and tolerance might be expected due to hosts having evolved to minimise self-damage to any extent possible (Ayres and Schneider, 2008).

1.2.4 Self-medication

Abiotic factors mediating infection include temperature, pH, salinity and nutrition in invertebrates (Joseph and Philip, 2007) and vertebrates (Marcogliese and Pietrock, 2011). Hosts may take advantage of any of these factors to reduce their parasite burden whilst minimizing the cost of mounting an immune defence. In response to the selection pressure placed on hosts by evolving parasites, hosts have also evolved diverse behavioural mechanisms to defend against parasitism. For example, baboons, *Papio*

cynocepahalus, regularly change their sleeping, feeding and drinking sites to avoid prolonged exposure to pathogens (Huffman, 2003).

Self-medication is defined as a specific therapeutic or prophylactic alteration occurring in feeding behaviour in response to disease or parasitism. Referred to in its early conception as 'zoopharmacognosy', it is based on the premise that animals use plant secondary compounds and other non-nutritional substances (such as sesquiterpenes, alkaloids and saponins) in disease resistance (Huffman, 2003). Chimpanzees with a high gut parasite load swallow leaves of *Aspilia* plants in increased quantities, which dislodges the parasite from their intestinal lining (Huffman and Caton, 2001). A prophylactic response was found by de Roode et al., (2011), who showed that feeding Monarch butterflies (*Danaus plexippus*) milkweed before and during infection, but not after, reduced pathogen load and aided the butterfly in fighting infection. The mechanisms involved could be interference with parasite invasion, decreasing initial load, or direct toxicity of plant matter to the parasite but not the host, reducing the virulence of the parasite (de Roode et al., 2011).

The plastic nature of the response indicates a fitness cost in the absence of disease, meaning the increase in fitness as a result of this behaviour outweighs the cost, during infection (Singer et al., 2009). *Grammia incorrupta* caterpillars actively avoid pyrrolizidine alkaloids (PAs), due to the ability of this plant metabolite to compromise immune function. However, during the latter stages of infection by parasitoids, larvae significantly increased PA consumption, thereby increasing survival (Singer et al., 2009; Smilanich et al., 2011). Herbivores may reduce the harm caused to themselves by altering their host plant.

1.3 Nutritional ecology

Due to its influence on homeostasis and performance in animals, several studies have focused on the impact of nutrition on other measures of evolutionary success, such as survival rate (Azeez et al., 2014; Raubenheimer et al., 2009). Nutritional ecology is the study of how animals have adapted to their nutritional environment through evolutionary, developmental and physiological processes (Evans and Claiborne, 2005; Raubenheimer et al., 2009; Sperfeld et al., 2016). The importance of nutrition indicates a selection pressure on organisms to optimise nutrient acquisition and utilisation. There is a lot of evidence showing that dietary regulation is important for nutrients to be allocated to the correct life history traits, e.g. growth and immunity (Simpson and Raubenheimer, 2012). For example, in fish, limited essential amino acid (EAA) uptake leads to impaired protein synthesis, and reduced growth performance, whilst excessive levels of EAA results in increased ammonia excretion. The amino acid arginine, is especially important since it is needed for several metabolic pathways including urea production and metabolism of glutamic acid, proline, glucose and fatty acids (Rahimnejad and Lee, 2014).

1.3.1 Nutritional immunology

Most plant food sources contain secondary compounds that can be utilized for defence, as well as nutrients important for host biological processes, making it difficult to interpret self-medication in animals. For example, 30% of the plant species identified as foods among the Hausa people of Nigeria are also used medicinally (Huffman, 2003). This is further complicated by the dependence of host immune responses on nutrient availability (Cressler et al., 2014; Hall et al., 2009; Smith and Holt, 1996). Under-nutrition in humans, predominantly in protein intake, has been associated with

increasing morbidity and mortality from infectious diseases, especially in developing countries (Ponton et al., 2011b; Smith, 1993; Smith and Holt, 1996).

The multi-dimensional nature of nutrition at different trophic levels, and of the immune system, as well as the multi-faceted interactions between the two have made it difficult to fully explore the importance of nutrition for immunity (Ponton et al., 2011b, 2013). Nutritional immunology is a field that integrates nutritional research and immunological advances, focusing on interactions between the two fields (Li et al., 2007; Ponton et al., 2011b, 2013). The complex nature of the immune system in both vertebrates and invertebrates implies complex dietary requirements. In a study using the Egyptian cotton leafworm, *Spodoptera littoralis*, Cotter et al., (2011) revealed trade-offs between the phenoloxidase cascade and lysozyme activity when larvae were fed 20 diets varying in their macronutrient ratios and concentrations; lysozyme activity peaked in a nutrient space high in dietary protein, whilst PO peaked in a space high in dietary carbohydrates.

Modern approaches in nutritional immunology aim to correct the treatment of diet as a single component, such as energy and carbon, by recognizing the complex nature of foods and the variation in dietary requirements of organisms (Raubenheimer et al., 2009). Studies accounting for nutrient ratios provided a more accurate depiction of nutritional effects than earlier studies that had treated nutrients as a unitary currency (Ponton et al., 2011b), and so early studies in this field focused on dietary ratios rather than concentration. For example, using isocaloric diets that varied across 5 ratios of protein and carbohydrate, Lee et al., (2006) found that *S. littoralis* larvae self-select diets high in protein to augment defence against nucleopolyhedrovirus (NPV). However, Cotter et al., (2011) highlight the importance of taking into account both dietary ratios and concentrations since they found the lysozyme response to vary when analyses were categorised by diet concentration.

1.3.2 Environmental stoichiometry

Ecological Stoichiometry can trace its ideas to the Law of the Minimum principle, developed in the 19th century. This principle postulates that the constraining factor on organismal growth is the element in lowest environmental supply relative to the organism's demands, assuming a finite universe (Hessen et al., 2013). The beginning of the field is normally attributed to Alfred Redfield, who noted that both seawater and phytoplankton biomass comprised the chemical ratios 106 Carbon(C): 16 Nitrogen (N): 1 Phosphorous (P) (Elser, 2006; Redfield, 1958). Stoichiometry is defined as the proportions of elements contained in the reactants and products of chemical reactions. Not all elements of the periodic table are necessary for life, and those that are (e.g. Oxygen, Carbon, Magnesium) do not exist in equal proportions. Hence ecological stoichiometry can be defined as the study of the proportions of elements and energetics in ecological interactions (Elser, 2006; Sterner and Elser, 2002). Transfer functions refer to the passage of nutrients through animals over time. It is hypothesised that, in situations involving limitations in nutrients necessary for growth and performance, organisms develop transfer functions to maximise nutrient retention. Conversely, when organisms are placed under time pressure (e.g. high rates of predation), rates of nutrient gain would be prioritised (Anderson et al., 2004; Raubenheimer and Simpson, 1998).

Organisms in ES models are considered based on their C:N:P ratios (Elser, 2006; Raubenheimer et al., 2009), which in turn is determined by biological components such as the form of structural support (Elser, 2006). For example, plant reliance on cellulose compared to animal reliance on bone structure for support would give plants a higher C:P ratio than animals (Elser, 2006). Since N is the limiting factor in terrestrial environments, organisms would preferentially use acquired N for growth processes, whilst C (the most abundant element), would be used primarily for catabolic processes.

As N becomes more limiting, the efficiency of its use would increase (Anderson et al., 2004).

Gross Growth Efficiency (GGE) is a term used to denote the efficiency with which an organism can convert assimilated nutrients into biomass (Anderson et al., 2004). So, organisms aim to meet their nutritional requirement for growth by consuming diets with a similar stoichiometric ratio to their own, allowing a high GGE. If presented diets with necessary nutrients in excess, organisms can lower their GGE by voiding excess nutrients (Raubenheimer et al., 2009). In its attempt to simplify biological systems, ES assumes a homeostatic nutrient balance. This creates an inconsistency when considering differences in organismal preferences in relation to nutritional requirements at a given time. Theories building on ES accounting for enzymatic rates of nutrient conversion, such as the dynamic energy budget (DEB), attempt to address this (Anderson et al., 2004). DEB models use differential equations to describe the rate at which organisms use energy acquired from food for biological processes such as growth and respiration (Kooijman, 2001; Nisbet et al., 2000; van der Meer, 2006).

1.3.3 Nutritional Geometry

Nutritional Geometry (NG) is a similar approach towards nutrition to the ES framework in its prioritisation of the components of a diet, rather than the treatment of diet as a single currency. The primary difference between NG and ES is the use of macromolecules, such as proteins and sugars, in NG compared to chemical elements, such as nitrogen and carbon, in ES. In so doing, NG accounts for one of the major shortcomings of ES in foraging and food selection models; the idea that foraging is based on the nutritional value of a food. The nutritional value of a food is more closely related to the macromolecules present in it than to its chemical composition (Raubenheimer et al., 2009). For example, an organism consuming plant material would

be consuming a food source with a high C:N ratio, however, if most of the C comes in the form of cellulose, most of the plant C would be indigestible and would therefore hold no nutritional value. Cellulose is a complex polysaccharide providing structural support in plants that most animals need to digest extensively and so cannot use efficiently (Anderson et al., 2004). In its simplest form, NG models the relationships between variables in nutritional ecology (Raubenheimer and Boggs, 2009; Simpson and Raubenheimer, 2012). It was a development on classical insect nutritional ecology (CINE), which had successfully introduced the paradigm of dietary self-selection based on nutritional content of the dietary source (Raubenheimer and Boggs, 2009).

Although CINE frameworks successfully integrated environmental factors, such as nutrients and temperature, with animal responses, such as feeding and growth, they failed to capture the interactions between them (Raubenheimer and Simpson, 1992). The Geometric Framework (GF) approach fixes this by creating a geometric landscape determined by nutrients, on which traits of interest can be plotted and compared (Raubenheimer and Boggs, 2009; Simpson and Raubenheimer, 2012). Furthermore, GF approaches incorporate the idea of optimality by estimating optimal values for nutrient uptake and utilization (Raubenheimer and Boggs, 2009). In GF terminology, an Intake Target (IT), is the concentration and ratio of two (or more) nutrients an organism needs, within an arbitrary period of time, to achieve maximal Darwinian fitness (**Figure 1.1a**). A nutritional rail is the balance of food choices and utilization that an animal makes to achieve a target; nutritionally balanced diets are those in which the nutritional rail passes through the IT. The growth target (GT) is where the IT is replaced with growth as the aim of nutrient acquisition and is important as a measure of the nutrients retained by the body. The nutrient target (NT) is a measure of nutrient intake that satisfies the GT as well as processes that involve the loss or utilization of nutrients (e.g. respiration

and secretion), thereby maximising fitness. A theoretically perfect animal would therefore have an NT equal to its IT (Raubenheimer and Boggs, 2009; Simpson and Raubenheimer, 2012).

The rule of compromise (RC) deals with the challenge of nutritionally imbalanced food choices an organism may be restricted to in nature. In this case, the organism will not achieve its IT but can get close to it by either under-ingesting its required nutrients or over-ingesting and excreting nutrients in surplus (Simpson and Raubenheimer, 2012). A generalist feeder that can utilize multiple food sources is likely to over-ingest and excrete undesired nutrients to achieve its intake target of a desired nutrient (1; **Figure 1.1b).** This is referred to as the equal distance rule of compromise, in contrast to the closest distance rule of compromise adopted by specialist feeders that are accustomed to a limited selection of nutritional sources (2; **Figure 1.1b**). They balance their nutrient intake to reach the closest point possible to their intake target (Raubenheimer and Simpson, 2003; Simpson and Raubenheimer, 1993a, 2012).

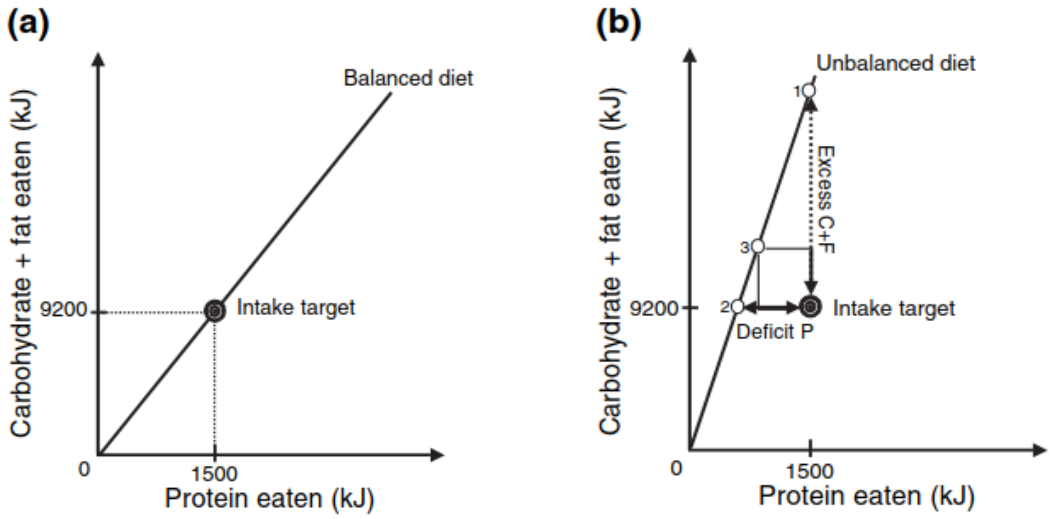

Figure 1.1: Models illustrating concepts of nutritional geometry. (a) Balanced diet. The Intake target (IT) is the concentration and ratio of protein (P) and carbohydrate+fat (C+F) an organism needs to eat within a given period of time to maximise fitness. In this case 1500 KJ of P and 9200 KJ of C+F. The line passing through the IT represents the nutritional rail, in this case a balanced diet. (b) Unbalanced diet. In this case the nutritional rail does not intersect the intake target, so an organism restricted to this diet must adopt a rule of compromise (RC). generalist feeders are expected to regulate their intake to point 1 which involves over ingesting C+F to meet theP target; the equal distance rule. A specialist feeder would regulate their diet intake to point 2 which meets the C+F requirement but P is under-eaten; closest distance rule. Point 3 represents a compromise with a surplus of C+F and a deficit of P that meets energy requirements. Adapted from Simpson and Raubenheimer (2005).

1.4 Medicinal nutrition

The IT is not a fixed point in nutrient space, but a flexible target that moves depending on the physiological demands placed on an organism. In relation to Darwinian fitness, the IT of an organism depends on the fitness traits being prioritised at a given time. The infection process is one such scenario in which an IT would move to match the heightened physiological demands placed on the organism both by the pathogen and its own immune defence (Simpson and Raubenheimer, 2012). At this stage there is a cross-over between self-medication and Nutritional Geometry in dietary choices made by animals, that increase survival if ingested before or during infection in greater quantities than would normally be observed. Although much research has been carried out on the immunological benefit of nutrition in both vertebrates and invertebrates, defining nutritional effects is only the first step towards understanding the role of nutrition on host-microbe interacts (Ponton et al., 2011b).

1.4.1 Micronutrients

The distinction between macro- and macro-nutrients is not a clear one, but rather refers to the relative quantities in which they are found in an animal (Simpson and Raubenheimer, 2012); the term micronutrients is normally used to describe vitamins and minerals (Chapman, 2012; Simpson and Raubenheimer, 2012). The importance of micronutrients, with regards to health, has been acknowledged since the 19th century (Semba, 2012). Classical diseases linked with deficiency in a micronutrient include scurvy (vitamin C), rickets (vitamin D), beriberi (thiamine) and anaemia (iron) (de Brito et al., 2014; Semba, 2012). Iron is crucial to mammalian biology due to its ability to exist in multiple states (Rang et al., 2011). Iron deficiency anaemia has been associated with immune impairment; reduced phagocytic activity, reduced immunoglobin levels, impaired T-cell response and IL-2 production have all been observed (Cunningham-

Rundles et al., 2005). Zinc plays important roles in the function of digestive enzymes, insulin synthesis, forms the core domains of nuclear receptors and is crucial in the ability of red blood cells to carry soluble CO_2 (Berne et al., 2010; Rang et al., 2011; Solomon et al., 2005). Deficiency in this mineral has implications for the immune system and can also cause anaemia, since it causes depletion in iron levels (de Brito et al., 2014; Solomon et al., 2005).

Comparatively little research has been carried out on the effects of micronutrients on health in invertebrates compared to vertebrates (Popham and Shelby, 2006). Selenium has been identified in defence against viruses in vertebrates (Beck et al., 2004) and invertebrates (Popham and Shelby, 2006). Larvae of the cabbage looper (*Trichoplusia ni*), and the tobacco budworm (*Heliothis virescens*) showed reduced growth rate but increased survival on diets supplemented with selenium when infected with a baculovirus (Popham et al., 2005). The mechanism involved could be due to augmentation of phagocytic or encapsulation responses. Zinc and calcium have both been shown to increase the lengths of haemocytes produced by *Manduca sexta* (Willott et al., 2002; Willott and Tran, 2002). Restricting iron levels in the wax moth, *Galleria mellonella* reduced the rate at which they cleared dead *Xenorhabdus nematophilus* and *Bacillus subtilis* cells, due to reduced haemocyte adhesion and PO activity.

1.4.2 Macronutrients

Nutritional research is limited by the availability of chemically-defined diets that would permit nutrient relationships to be teased apart. Chemically-defined diets allow the manipulation of single nutritional components, providing more flexibility in experimental design, however they are currently available for a limited number of species (Chapman, 2012). Although most of our understanding of animal nutrient

requirements comes from locusts, fruit flies and caterpillars, for which chemically-defined diets are available, relationships between macronutrients (e.g. proteins, carbohydrates, lipids and amino acids) and health have been found in a range of species. So far, a mixed picture has been revealed, with proteins, carbohydrates and lipids all proving important for different host defences, depending on the species. For example, there is evidence to suggest an important function of lipid carrier proteins in the clearance of LPS in humans, *Aedes aegypti* mosquitos and *G. mellonella* moths (Cheon et al., 2006). The accumulation of lipid stores in structures called lipid droplets forms an active part of the cellular immune response (Barletta et al., 2016). However, in *Gryllus texensis* crickets, there is a trade-off between lipid transport and the immune system, such that crickets with a high lipid intake presented a reduced immune response to the bacterium, *Serratia marcescens*.

Evidence from insects of the order Orthoptera suggests a role for dietary carbohydrate in immune defence. Migrating mormon crickets (*Anabrus simplex*) fed isocaloric diets varying in their protein-to-carbohydrate ratios exhibited stronger PO, lysozyme and encapsulation responses on a higher carbohydrate diet. In contrast, the Australian plague locust, *Chotoicetes terminifera* exhibited increased lytic activity and haemocyte densities on similar diets containing a higher proportion of dietary protein; only PO activity appeared to be unaffected by diet. However, the increased immune activity did not translate to overall survival, since a greater proportion of the locusts on higher-carbohydrate diets survived infection with the fungus *Metarhizium acridum*. The choice of high-carbohydrate diets by locusts supported the hypothesis that the fungal pathogen may be better at exploiting protein than the host (Graham et al., 2014). The cases presented so far do not provide a complete picture since carbohydrate is also used as an energy source to fuel the metabolic processes of resistance mechanisms (DeGrandi-Hoffman and Chen, 2015). For example, mosquitos of the genus *Anopheles* can use

dietary glucose to facilitate their melanisation immune response (Koella and Sørensen, 2002).

There is more widespread evidence for the use of protein and amino acids in immune defence than there is for carbohydrates or lipids. Evidence has been found for mammals (Clough et al., 2016; Kambara et al., 1993; Nnadi et al., 2010; Peck et al., 1992), including humans (Ambrus, 2004; Batool et al., 2013), birds (Lochmiller et al., 1993), fish (Goosen et al., 2014; Khosravi et al., 2015), lepidopteran larvae (Lee et al., 2006; Lee et al., 2008; Povey et al., 2014, 2009), dipteran flies (Fellous and Lazzaro, 2010), and hymenopteran bees (Brunner et al., 2014; Tritschler et al., 2017), amongst others. Treating protein as a generic term fails to take into account the constituent amino acids, which may produce variable effects. Lee et al., (2008b) found increased lysozyme activity in *S. littoralis* caterpillars on diets supplemented with casein, compared to those on diets supplemented with zein. The higher EAA content of casein makes it a superior dietary supplement to zein. *D. melanogaster* encapsulation of parasitoids eggs from *Asobara tabida* was increased when diets were supplemented with the EAA arginine (Kraaijeveld et al., 2011). The pathways involved in the use of arginine by cellular components of the immune response have been conserved through evolution, since arginine also affects mammalian lymphocyte activity (Li et al., 2007). Immunological research has identified roles for each of the amino acids in human immune responses (Li et al., 2007), providing a starting point for further investigation in other animals.

1.5 Nutritional physiology

1.5.1 Physiological adaptation for nutrient utilization

Invertebrates provide model systems for the study of the mechanisms underpinning host-microbe interactions (Stilwell et al., 2018). Often, a single measure of immune

function is used, such as AMP production, to estimate a host's disease response during invertebrate studies (Ayres and Schneider, 2008). Despite this method proving successful in the elucidation of host immune function, it makes certain assumptions, and findings must be interpreted with care. In their study of the relationship between genotype and infection in *D. melanogaster,* Corby-Harris et al., (2007) showed it was erroneous to assume that genotypes with a low host pathogen load would also be those with a high survival. Nevertheless, the mammalian immune system is more complicated due to its dual facets that communicate through a series of cytokines and receptors (Shi and Gao, 2012). Invertebrate models maintain a level of complexity, whilst raising less ethical and temporal issues, and reducing the cost of research (Ramarao et al., 2012).

Insects can satisfy their nutritional requirements through feedback mechanisms that involve components, such as olfactory and taste receptors, allowing them to associate nutrient levels of the food they ingest with nutrient requirements after absorption (Simcock et al., 2014; Simpson and Raubenheimer, 2012). In response to changes in the nutritional requirements of the body which may vary, insects will then alter their intake of certain nutrients to match increased/decreased demand. Sensilla, taste receptors in the mouthparts, respond to the free amino acid, sugar or inorganic salt content of plants or other nutritional sources (Chapman, 2003). Rather than just increasing or decreasing intake of certain nutrients, a host might alter its food source to one that has a different ratio of crucial nutrients to meet demand (Simpson and Raubenheimer, 2012). Digestion is carried out by protease, carbohydrase and lipase enzymes. Although some insects produce enzymatic secretions that begin digesting food extra-orally, most of the digestion process occurs in the midgut after ingestion (Chapman, 2012).

The primary sugar in the circulatory system of vertebrates is glucose, however insects and other invertebrates primarily use trehalose as an immediate energy source in the haemolymph, and it is homeostatically regulated (Friedman et al., 1991). In insects, carbohydrate is first converted into trehalose and then transported to the fat body where it can be stored as glycogen (Azeez et al., 2014). Before anabolism of carbohydrates and lipids can occur, glycogen must be converted back to trehalose for use in the haemolymph. Amino acids are also stored in the fat body and haemolymph. Lipids are stored as triacylglycerol from fatty acids that have in turn been hydrolysed from diacylglycerol. In the fat body, UDPglucose is used to synthesise both trehalose and glycogen, but trehalose-synthesizing enzymes have a higher affinity for the substrate. These enzymes are auto-inhibitory, with activity slowing down as trehalose concentrations increase. The result is that at high trehalose concentrations, glycogen is produced allowing automatic storage of carbohydrates (Friedman et al., 1991).

1.5.2 Haemolymph

The open circulatory system of insects allows oxygen from the tracheal tubes, and nutrients from the gut to be passively transported to metabolising cells and tissues. The Malpighian tubules and the gut regulate the volume and composition of the haemolymph, whilst the circulatory system keeps it in motion (Beyenbach, 2016). The diversity in insect environments and function generates more variable haemolymph homeostasis than is found in vertebrate blood. The regulation of osmotic pressure and the maintenance of haemolymph volume in adaptation to external environment or dietary intake is the primary challenge of haemolymph homeostasis.

The haemolymph generally contains a high level of intermediary metabolites needed for nutrient synthesis in the fat body (Thompson et al., 2001). The nutrient stores of the

haemolymph are consistently replenished by nutrients absorbed through the gut (Simpson and Raubenheimer, 1993). Unlike the more permanent fat body nutrient storage, the haemolymph nutrients fluctuate often in response to meal duration, feeding interval, and metabolic demands of tissues (Abisgold and Simpson, 1988, 1987; Simmonds et al., 1992). An advantage of the open circulatory system is the direct access to nutritional stores available to immune effectors. Although in low levels in the absence of infection, the haemolymph contains circulating haemocytes as well as a number of receptor proteins ready to activate PO, AMP and lysozyme activity upon the detection of a pathogen (Chapman, 2012).

1.5.3 Microbial nutrient use

Pathogen resource-use remains one of the poorly understood areas of immunological research (Muñoz-Elías and McKinney, 2006), mainly due to a host-focused paradigm in this field. As a result, only a few host nutrients important for pathogen proliferation have been identified (Steeb et al., 2013). In bacteria, the limited understanding of nutritional requirements during infection is due to the general assumption that *in vivo* nutrient requirements would not differ from *in vitro* requirements and would make poor targets for drug-development (Muñoz-Elías and McKinney, 2006). Due to limitations in membrane pore sizes, most bacteria secrete extracellular enzymes to partially digest organic molecules found in their environment to facilitate uptake (Cezairliyan and Ausubel, 2017). Steeb et al., (2013) identified 477 metabolic enzymes, produced by *Salmonella enterica* during an infection of laboratory mice, able to catalyse 925 metabolic reactions. Seventy-seven of these reactions were involved in 24 pathways for the utilization of carbohydrates, lipids, nucleosides and amino acids. Being heterotrophs, most pathogenic bacteria are able to catabolise a range of carbon sources to meet their energetic demands (Muñoz-Elías and McKinney, 2006). Iron is an

important element for micro-organisms since it is found either as insoluble hydroxides in the environment or bound by proteins in animals. As such, iron levels are tightly regulated by most bacteria; dedicated pathways such as the ferric dicitrate transport system in *E. coli* exist to scavange iron, whilst fur-iron protein complexes downregulate uptake to prevent toxicity at high concentrations (Crosa, 1997). Qurom sensing is a group of processes involving the production and sensing of small secreted molecules, called autoinducers, that regulate the secretion of enzymes useful in extracellular nutrient hydrolysis and uptake (Cezairliyan and Ausubel, 2017). Cezairliyan and Ausubel (2017) showed that for some pathogenic bacteria, such as *Pseudomonas aeruginosa*, proteases are secreted preferentially depending on the nutritional value of the environment.

In gram-negative bacteria, such as *E. coli*, water-soluble nutrients diffuse passively through the outer-cell membrane directly into the cell (Leisman et al., 1995). Bacteria regulate diffusion rates by modulating the type of pores in the extracellular membrane. These pores are formed by homotrimeric association of OmpF and OmpC porin proteins (Forst and Roberts, 1994). Expression of the porin proteins alters in response to osmolarity, pH and temperature of the growth medium (Leisman et al., 1995). At 37^{o}C, OmpF is predominantly expressed at low osmolalities, whilst OmpC dominates at high osmolality. This is significant since OmpF has a 10-fold higher diffusion rate than OmpC (Forst and Roberts, 1994), allowing faster absorption of nutrients. Solution osmolarity appears to be a shared sensor for both insects and their pathogens in regulation of their nutrient environments.

1.5.4 Microbial growth kinetics

To predict the outcome of infection, parasite identity, infection dynamics (including site and duration), previous and current infections, and host resource availability, must all be taken into account (Rynkiewicz et al., 2015). Microbial growth kinetics were first studied by Jacques Monod, who was interested in the relationship between sugar concentration and bacterial growth rate (Bren et al., 2013; Monod, 1949). The Monod Law was the result of his work:

$$\mu = \mu_0 \frac{S}{K_s + S}$$

where μ_0 represents the growth rate at substrate saturation S is the concentration of the limiting substrate for growth, and K_s is the substrate level at which growth rate is half the maximal rate (Monod, 1949). Monod's findings have led to the accepted assumption that growth rate in microorganisms is constrained by the limiting substrates in solution (Koch, 1982). Monod described bacterial growth in six phases (**Figure 1.2**) based on bacterial growth rates (Monod, 1949):

1. Lag phase: growth rate is zero, and population size is constant;
2. Acceleration phase: growth rate increases, and population size begins to increase;
3. Exponential phase: growth rate is constant, and population size increases;
4. Retardation phase: growth rate decreases, but population size increases;
5. Stationary phase: growth rate returns to zero, and population size plateaus;
6. Phase of decline: growth rate is negative, and population size declines.

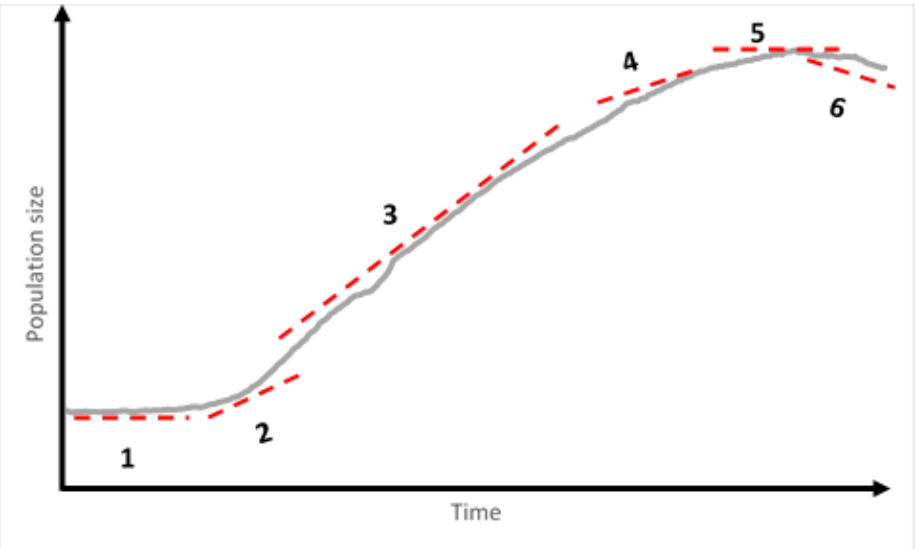

Figure 1.2: The phases of bacterial growth described by Monod (1949). (1) Lag phase. Growth rate is zero and there in no population growth. (2) Acceleration phase. Growth rate and the population size both begin to increase. (3) Exponential phase. Growth rate reaches its maximum and the population size increases. (4) Retardation phase. Growth rate begins to decline but population size increases. (5) Stationary phase. Growth rate declines to zero and the population size remains steady. (6) Phase of decline. Growth rate is negative and the population size declines.

Most studies measuring bacterial growth laws use a steady-state experimental set-up that involves batch-culture with constant nutrient replenishment, to avoid the complexities in evaluating growth in dynamical situations with depleting substrates (Bren et al., 2013). However, it is important to understand growth rates and substrate use in differing situations, to accurately depict infection outcomes for drug design. Studies investigating growth kinetics also vary a single nutrient at a time, normally opting to use generic media rich in nutrients, to meet the other nutritional demands of the microbe (Bowen et al., 2012; Kooliyottil et al., 2014). Pranaw, (2013) suggested the

use of a response surface methodology, which looks at multiple characteristics simultaneously, when optimizing metalloprotease production in the gram-negative bacterium *Xenorhabdus indica*. With more accurate modelling of the interactions occurring between chemicals in the growth media, they optimized *X. indica* protease production by 66%, arguing higher efficiency and more simplicity in the response surface methodology.

1.5.5 Microbial population ecology

An ecosystem is a theoretical concept, normally conceptualized at the scale of a geographical region, however, it can also consist of a smaller discrete habitat, such as a lake or a cave. Therefore, in host-parasite systems, the host can be considered as an ecosystem, whilst interactions can be observed between parasites, host symbiotic microbes and their shared environment (the host) (Rynkiewicz et al., 2015). As such, microbial growth and decline can be studied using conventional population ecology methods, providing an alternative to Monod's Law.

In population ecology, intrinsic rate of natural increase (r), is the change in population size per individual per unit time, or the rate at which a population increases in size in the absence of density-dependence (Begon et al., 2005). Due to intraspecific competition, as the population increases, per capita birth rate decreases and per capita death rate increases. The density at which these curves cross is referred to as the carrying capacity (K). The carrying capacity therefore represents the population size that environmental resources can maintain at a stable equilibrium. In a continuous breeding population, births and deaths do not follow a discrete pattern and so r is dependent on the population size at the time. The following logistic equation produces a Sigmoidal growth curve (**Figure 1.3**), in which at low population numbers, growth is exponential but at high population numbers growth becomes limited by intraspecific competition:

$$\frac{dN}{dt} = rN\left(\frac{K-N}{K}\right)$$

The primary caveat of the simplistic nature of this equation is the assumption of perfectly compensating density-dependence, in which *K* is always stable at equilibrium, creating a disparity with nature (Begon et al., 2005).

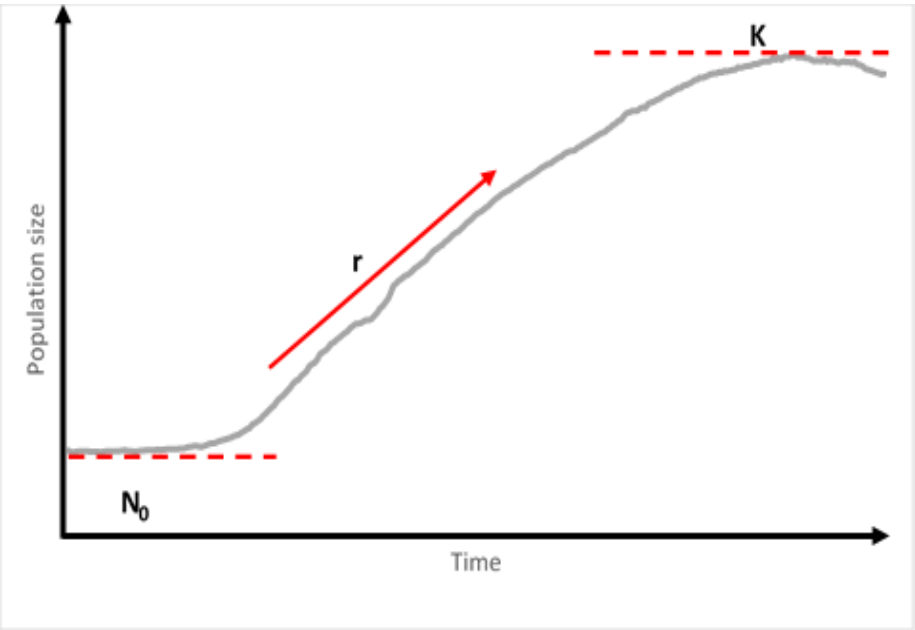

Figure 1.3: Sigmoidal growth curve produced by logistic equation, depicting population growth over time. N_0 represents the starting population size. *r* is the intrinsic growth rate of the population and *K* is the population carrying capacity.

1.6 Model systems

1.6.1 Spodoptera

The 160,000 described phytophagous lepidopterans makes them one of the most diverse insect taxa on Earth (Chen et al., 2016; Krenn, 2010). The host insect used in this thesis is *S. littoralis* (**Figure S1.1a**), a noctuid moth found in tropical regions (Brown and Dewhurst, 1975). It is a major crop pest across the Mediterranean, causing significant

economic damage to cotton crops in Egypt (Hosny et al., 1986). Cotton is only one of 40 host plants that *S. littoralis* is known to feed on (Novoselov et al., 2015); others include strawberry, artichoke, fodder crops, and maize. Being holometabolous, *S. littoralis* has four distinct life stages (**Figure 1.4**). Eggs hatch into larvae after 1 or 2 days. The larvae grow and moult through 6 instars using nutrients acquired through feeding. After about 10 days (depending on temperature), the larvae burrow into the soil and pupate, where they stay for 8-14 days, before emerging as mature adults, which live for 5-10 days (Chen et al., 2016; Salama and Shoukry, 1972). Females lay 300-500 eggs per cotton leaf (Hosny et al., 1986), and most of the hatched larvae feed on the leaves, retarding plant growth and production capabilities. Larvae feed on other sections of the plant including flowers and bolls during high infestation periods (Martinez et al., 2001).

Because of its importance as an agricultural pest, it is one of many moths used widely as

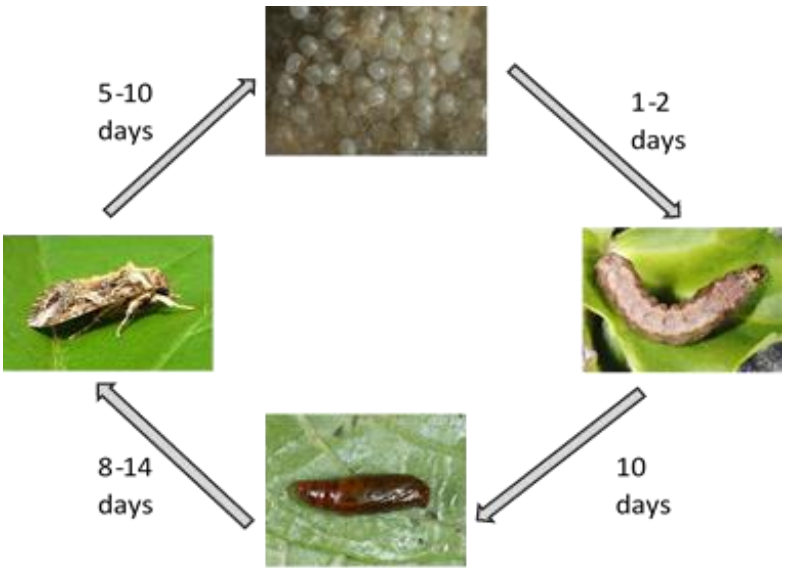

Figure 1.4: Life-cycle of Spodoptera littoralis. Eggs hatch into herbivorous caterpillars that pupate after 6 instars. Pupation is a non-feeding stage that occurs in the soil. Adults eclose from pupae within 2 weeks, and generally feed on nectar. Adults live for about 5-10 days.

a model system (Tang et al., 2012). Its polyphagous nature means it is exposed to a range of nutritional sources, relying on post-ingestive nutrient regulation for the control of its nutrient intake, especially when faced with nutrient-imbalance (Lee et al., 2004; Simpson and Raubenheimer, 2012). Correspondingly, larvae ingest small amounts of food they contact, irrespective of the diet nutritional content, in relation to their requirements (Simmonds et al., 1992). However, after the initial contact with diet, larvae regulate ingestion by altering feed duration to meet their intake target, IT (Lee et al., 2002; Simmonds et al., 1992). Lee et al., (2002) found that sixth-instar caterpillars regulated their diet to 57% protein and 43% carbohydrates when given a choice. As predicted for generalist feeders, food choice was consistent with the equal distance rule of compromise when individuals were unable to meet their IT (Lee et al., 2002; Simpson and Raubenheimer, 2012). The higher protein intake of the larval stage corresponds with the holometabolous life-cycle of Lepidoptera, which accumulate protein reserves during their larval stages, since their adult diets comprise mostly carbohydrates (Chapman and Boer, 2012; Lee et al., 2002). Most adult lepidopterans are nectar feeders, using their proboscis to uptake liquid substances (Krenn, 2010).

Consistent with ES theory, larvae were efficient in the conversion of dietary protein to pupal nitrogen stores, and conversion efficiency decreased with increasing dietary protein (Lee et al., 2002). Experimental infection with NPV revealed that higher proportions of dietary protein also increase survival of *S. littoralis* larvae. Resistance mechanisms upregulated by higher protein intake included lysozyme, the encapsulation response, and PO activity (Lee et al., 2006). Given a choice, larvae that maintained their IT through infection succumbed to the NPV infection, however those that altered intake to consume a relatively higher level of protein survived. This behaviour fits the definition of self-medication in the selection of diets usually sub-optimal to fitness (in

the absence of infection), in response to infection, that reduces the fitness costs of infection (Singer et al., 2009). Cotter et al., (2011) aimed to further investigate the nutrient effects on immunity found by Lee et al., (2006), due to the indication of a trade-off between growth and immunity, shown by these traits mapping onto different positions in the nutrient space. Using LPS to elicit an immune response, the authors found cuticular melanism, haemolymph protein and lysozyme activity to increase with increasing dietary protein. Phenoloxidase, being influenced by dietary carbohydrate, mapped this immune trait onto a different position in nutritional space, indicating a trade-off between different branches of the immune system, depending on nutrition (Cotter et al., 2011). Nutritional effects on tolerance are yet to be explored in this species.

1.6.2 Xenorhabdus

The genus *Xenorhabdus* consists of asporogenous, rod-shaped bacteria (Couche and Gregson, 1987), such as the pathogen in this thesis, Xenorhabdus nematophila (**Figure S1.1b**). *Xenorhabdus* belong to the family Enterobacteriaceae which comprises entirely gram-negative species (Thomas, 1979). The members of this genus normally form symbiotic relationships with entomopathogenic nematodes of the family *Steinernematidae* (Bird and Akhurst, 1983; Boemare et al., 1993; Forst et al., 1997). The life-cycle of *Steinernermatidae* consists of an egg stage, four juvenile stages and male/female adults (Nguyen and Smart, 1992). The infection cycle of these organisms starts with a third-stage juvenile (J3), also referred to as an infective juvenile (IJ), entering a host through the mouth, anus or spiracles (**Figure 1.5**). Once inside the host, the IJ make their way to the haemolymph, where they release the bacteria they carry in their intestines within 24 hours. Feeding on host nutrients, the IJ then mature to J4 (Nguyen and Smart, 1992). Nematode growth being optimal in the presence of its

symbiont indicates that the replicating bacteria also provide essential nutrients for proliferation of their hosts (Forst et al., 1997; Yamanaka et al., 1992). The J4 moult into first generation adult males and females within 60-72 hours, and the adult female nematodes produce eggs, which go through all the maturation stages to produce second-generation females (Nguyen and Smart, 1992). Eggs produced by the second-generation females only mature partway. The J2 or pre-infective juveniles re-assimilate bacteria, moult into non-feeding IJs and then exit the carcass into the soil, where they moult into IJs and stay at this stage until they infect another host (Forst et al., 1997).

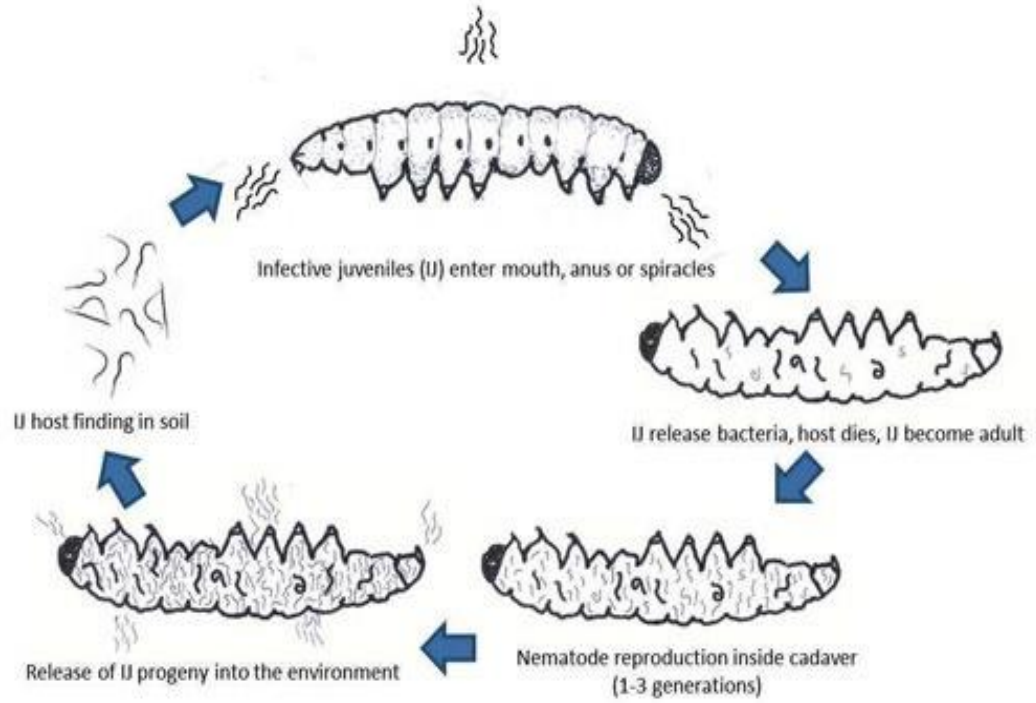

Figure 1.5: Life-cycle of entemopathogenic nematodes (Arthurs, 2018.)

Between 30 and 200 *Xenorhabdus* cells are carried in an intestinal pocket of the nematode called the receptacle, located between the pharynx and intestine (Richards and Goodrich-Blair, 2009; Snyder et al., 2007; Stilwell et al., 2018). It is thought that *Xenorhabdus* are obligate mutualists/pathogens since no variants have been found free-living in soil or water (Forst et al., 1997), although they can be cultured *in vitro* in the

absence of a host (Nielsen-LeRoux et al., 2012). The nematode also carries the bacteria monoxenically (Couche et al., 1987; Couche and Gregson, 1987), since the IJ excretes other bacterial species, including other species of *Xenorhabdus*, before exiting the cadaver (Bird and Akhurst, 1983). As the bacteria enter stationary phase, they start to produce protease, phospholipase and lipase enzymes that break down the macromolecules of the insect cadaver, providing the nematode with nutrients. They also produce antibiotics that supress the growth of other microorganisms to provide a sterile environment for their symbiont (Nielsen-LeRoux et al., 2012).

During *in vitro* culture, *Xenorhabdus* grows in two distinct forms, referred to as the phase I and phase II variants (Forst et al., 1997). These two forms are distinguished by colony morphology, pigmentation and antibiotic production (Couche and Gregson, 1987). Although both forms are pathogenic, only the phase I form is isolated from natural IJ populations (Couche and Gregson, 1987; Forst et al., 1997). Nutrient uptake differs depending on variant; Phase II *X. nematophilus* cells took up the amino acid proline faster than phase I cells, and were also quicker to recover from lag phase after starvation (Smigielski et al., 1994). Phenotypic variation generally involves the activity of regulatory cascades. One such transcriptional regulator identified in *X. nematophilus* is leucine-responsive regulatory protein (Lrp), which controls genes involved in amino acid biosynthesis, catabolism and transport. Lrp mutants are defective in infection, bacterial and nematode reproduction and transmission (Cowles et al., 2007). As such, nutrient biosynthesis and catabolism is important for both mutualistic and pathogenic activities of this bacterium. Multiple species of *Xenorhabdus* can use asparagine, cysteine, myo-inositol, mannose and trehalose (Yamanaka et al., 1992). Histidine catabolic genes are upregulated when *P. luminescence* sense host haemolymph (Münch et al., 2008), providing further evidence for amino acid requirements in these species.

Xenorhabdus along with their nematode hosts are widely used in insect pest control (Forst et al., 1997). Aside from their commercial importance, these bacteria are used to model pathogenicity since they can be directly injected into the haemocoel of the host to cause mortality (Yamanaka et al., 1992). Oral administration of toxins produced by *X. nematophila* were pathogenic in the white cabbage caterpillar *Pieris brassicae*, *A. aegypti* larvae, and the mustard beetle *Phaedon cochleariae* (Sergeant et al., 2006). Their ability to supress the insect immune system makes them potent killers and host mortality can occur within 48 hours (Goodrich-Blair and Clarke, 2007), adding to their importance as a biological control. *X. nematophila* inhibits both AMP production and nodulation (Richards and Goodrich-Blair, 2009), and *P. luminescens* produces a small-molecule antibiotic that inhibits PO in insect hosts (Eleftherianos et al., 2007). Despite the importance of nutrition in the pathogenicity and life cycle of these bacteria, little is known about their nutrient requirements (Münch et al., 2008; Pranaw, 2013). Although some work has been carried out on their use of carbohydrates (Bowen et al., 2012; Kooliyottil et al., 2014), there is even less information available about how they react to simultaneous variation of multiple nutrients as would occur in insect haemolymph during feeding (Pranaw, 2013).

1.7 Project aims

This project aims to establish the role of nutrition in the outcome of a host-pathogen interaction. It will build on previous work that shows that *Spodoptera* caterpillars self-select diets containing a higher ratio of protein-to-carbohydrate upon infection (Lee et al., 2006; Povey et al., 2009), and diets higher in protein can increase the host immune response (Cotter et al., 2011). A pathogen-focused perspective will be taken with the intention of capturing the bottom-up effects of shared nutritional resources. The host used will be *S. littoralis*, for which there is already a basis of information on its

nutritional requirements for growth and immune defence. The pathogen used will be *X. nematophila*, which is a parasite that relies heavily on the host as a nutritional resource. It can reduce competition from other pathogens and host-symbionts using antibiotics, limiting the number of confounding factors in its experimental use. Furthermore, being a haemolymph obligate parasite makes it subject to the fluctuating haemolymph nutrients that occur during host feeding and nutrition appears to be an important aspect of its pathogenicity. Experimental chapters will be as follows:

- Chapter 2: The initial aim of this chapter will be to examine the consistency of host diet effects under various parasite burdens by characterising host fitness (measured through survival and larval mass) when infected with different bacterial doses. 6 diets will be used varying in their protein and carbohydrate ratios as well as caloric content. This experiment will also investigate the time-course of infection by sampling bacterial load at multiple timepoints. The aim of this is to establish the key times at which host-diet affects pathogen proliferation. The primary outcome will be the quantification of parasite burden at the various timepoints across the 6 diets in the hope of making a direct connection between diet, parasite burden and host survival.
- Chapter 3: This chapter will aim to build on the findings of the previous chapter by increasing the coverage of the host nutrient-space that provides the investigation of infection dynamics. It will expand from a 6-diet set-up to a 20-diet set-up increasing our depth of understanding of the nutritional requirements of the host and pathogen. A pathogen LD50 will be used and pathogen load will once again be quantified to establish the effect of host macronutrient intake on pathogen performance.
- Chapter 4: The haemolymph is the site at which the host and this pathogen interacts. Being the primary means of nutrient transportation from the gut to

other host-tissues establishes this as the primary host location where any nutritional interactions would take place between the bacteria and its insect host. This chapter will aim to characterise the host nutritional status in the 20-diet nutrient space by measuring the haemolymph nutrient composition of caterpillars fed the 20 diets varying in their macronutrient ratios and concentrations. The macro- and micro-nutritional status of the host will be explored with the hopes of providing a picture of the internal nutritional resource pool available to both the host and pathogen.

- Chapter 5: The aim of this chapter will be to measure pathogen resource use. Based on the paradigm of the host haemolymph as a nutritional environment through which the pathogen can meet its nutritional requirements, a pair of experiments that measure pathogen nutrient use *in vitro* will be designed. The first experiment will use the information from Chapter 4, which quantified the host haemolymph nutritional content, to design a set of synthetic haemolymphs. There will be 20 haemolymphs, each matching the nutritional environment of the pathogen on each of the diets in Chapter 3. The use of synthetic haemolymphs will allow the removal of top down host effects. The information gained from the *in vitro* experiment will be compared to the *in vivo* pathogen data from Chapters 2 & 3. The second experiment will aim to isolate the requirements of the pathogen for each nutrient type that is variable in the host haemolymph, such as proteins and carbohydrates. It will also use a synthetic haemolymph design, however mean values will be used for the nutrients in solution except for the nutrient type being measured which will be varied within the range the pathogen is likely to experience *in vivo*.

The final chapter (Chapter 6) will attempt to synthesise and interpret the findings from the previous four data chapters.

1.8 Supplementary Material

(a) **(b)**

Figure S1.1: The photographs illustrate the host and pathogen. (a) *Spodoptera littoralis* (b) GFP labelled *Xenorhabdus nematophila* F1D3.

2 Dietary protein drives insect-pathogen interactions

Acknowledgements:

Experiments were carried out by Robert Holdbrook, Catherine Reavey & Yamini Tummala. The data were analysed by Robert Holdbrook & Kenneth Wilson. All authors contributed to the drafting of the final manuscript.

ABSTRACT

Recent research has suggested that the outcome of host-parasite interactions is dependent on the diet of the host, but few studies have attempted to disentangle the effects of energy (calories) from those of specific macronutrients (proteins, carbohydrates and lipids). Furthermore, previous studies have focussed on fitness outcomes for the host and the immune mechanisms that may drive those outcomes, without considering direct impacts of host nutrition on parasite establishment and proliferation. Here, using a model host-pathogen system (*Spodoptera littoralis* caterpillars and *Xenorhabdus nematophila* bacteria), we ask the question: how do the energy and macronutrient content of the host diet affect both pathogen and host fitness? To answer this question, caterpillars were restricted to diets that varied systematically in their protein to carbohydrate ratio and their energy density, they were exposed to a range of doses of *X. nematophila*, and their survival was monitored. Bacteria were quantified in the haemolymph of the host insect during the time-course of infection and at death. Our results clearly highlight the pre-eminence of protein in all aspects of the host-pathogen interaction. Low dietary protein resulted in increases in: the chances of pathogen establishment; pathogen replication rate; the likelihood of host death; and the speed of death. The energy content and amount of carbohydrate in the diet explained little variation in any of these measures of pathogen or host fitness. We discuss potential mechanisms underpinning these findings and their generality with respect to human and animal health.

2.1 INTRODUCTION

Nutrition is increasingly being seen as a key driver of the outcome of host-parasite interactions (Calder and Jackson, 2000; Cunningham-Rundles et al., 2005; Ponton et al., 2011b). Its effects may be mediated via a range of interacting mechanisms including host foraging behaviour and encounter rate with pathogens (Penczykowski et al., 2014), host immune function (both innate and adaptive immune responses), host diet-modulated pathogen replication rates (Frost et al., 2008; Serbus et al., 2015), interactions with the host microbiota (Nicholson et al., 2012; Pernice et al., 2014; Tremaroli and Bäckhed, 2012), and a range of other traits associated with the presence of a live pathogen, such as the repair of cells/tissues affected by the challenge (Allen and Wynn, 2011; Ayres and Schneider, 2009; Read et al., 2008). In the new field of nutritional immunology (Ponton et al., 2011b, 2013), an early focus was the effects of micronutrients on immune function, with elements such as zinc and iron being identified as having detrimental effects on immune function when limiting (Chandra, 1997; Cunningham-Rundles et al., 2005; Shankar and Prasad, 1998; Weinberg and Weinberg, 1995). Inspired by optimality theory, parallel research sought to identify the nutritional costs associated with mounting immune responses to combat infections, with much attention being focused on energy (food-derived calories) as the key currency (Lochmiller and Deerenberg, 2000). In the past decade, however, much of the focus has been on establishing the importance of the macronutrients that provide those calories – proteins, carbohydrates and lipids – in both constraining host immune function and determining the outcome of host-pathogen interactions.

Most recently, there has also been an appreciation of the need for greater complexity in diet-manipulation experiments (Ponton et al., 2011b, 2013). Early nutritional studies generally considered the effects of crude changes in host nutrition, such as food deprivation, calorie limitation, or changes in a single nutritional component (Moret and Schmid-Hempel, 2000; Popham and Shelby, 2006; Valtonen et al., 2010). For example, the nutritional costs associated with mounting an immune response in worker bumblebees was revealed by comparing immune-activated bees that had been starved with those that were allowed to feed on sugar-water *ad libitum* (Moret and Schmid-Hempel, 2000). Whilst these studies revealed important new insights into the nutritional ecology of host-parasite interactions, they were not designed to identify nutritional interactions (e.g. between different macronutrients) or to distinguish the effects of energy *per se* from the sources of energy in different dietary macronutrients. The geometric framework (GF) for nutritional ecology provides a useful structure for taming this complexity by making explicit the interactions between multiple nutritional components and by providing an experimental methodology to tease them apart (reviewed by Simpson and Raubenheimer, 2012, 1995). Specifically, the GF approach recognises that all organisms are driven by nutritional 'intake targets', which are the specific quantities and mixtures of nutrients that at any given time optimises its response to its environment (Simpson and Raubenheimer, 2012, 1995). The intake target for infected individuals is likely to differ greatly from that of healthy individuals, due to the nutritional requirements of the immune and tissue repair systems. Recognition of the fact that different (immune and life history) traits are likely to have different nutritional optima, resulting in trade-offs, is now a central feature of this

research area. For example, using the GF approach, Cotter *et al.* (2011) found that in larvae of the Egyptian cotton leafworm (*Spodoptera littoralis*), two important immune traits - phenoloxidase activity and lysozyme activity - peaked in different regions of macronutrient state-space, such that larval feeding behaviour that resulted in one trait being optimised would necessarily result in the other not being so.

The literature regarding the importance of macronutrients in modulating immune defense and determining the outcome of host-pathogen interactions provides a mixed picture. There is evidence for energy (Freitak et al., 2003), carbohydrate (Graham et al., 2014; Srygley and Lorch, 2011), protein (Cotter et al., 2011; Nnadi et al., 2010; Peck et al., 1992; Sakkas et al., 2011), lipid (Adamo et al., 2008; Cheon et al., 2006), and/or their ratios (Lee et al., 2006; Povey et al., 2014, 2009) all having a role to play in responses to parasitism. For example, in the human disease community, it is generally recognised that individuals in energy-deficit tend to have reduced immunocompetence and elevated susceptibility to a range of parasitic and infectious diseases (Blössner and de Onis, 2005). In the developing world, starvation is known to increase susceptibility to a range of diseases (Chandra, 1997), and in athletes a number of immune parameters are suppressed during intense periods of energy-depleting activity (MacKinnon, 2000). Moreover, there is good evidence that at least some aspects of immune defense are energy-demanding. For example, when larvae of the cabbage white butterfly (*Pieris brassicae*) were experimentally manipulated to mount an encapsulation response, their standard metabolic rate increased by nearly 8% (Freitak et al., 2003), and in house sparrows (*Passer domesticus*) injection of a non-pathological immune stimulant (phytohaemagglutinin, PHA) resulted in an upregulation of cell-mediated immune

responses and caused a substantial increase in resting metabolic rate (Martin et al., 2003).

Carbohydrates and lipids also appear to play a role in immune function in some species. In Mormon crickets (*Anabrus simplex*), a diet enriched in carbohydrates resulted in an enhanced cellular encapsulation response, as well as increased lytic activity against bacteria (Srygley and Lorch, 2011). Evidence from mosquitoes (*Aedes aegypti*), showing upregulation of genes associated with lipid metabolism following bacterial infection, suggests a role for lipids in antibacterial immune function (Cheon et al., 2006, but see Adamo et al., 2008). In vertebrates, there is good evidence that protein is the important macronutrient for immune defence and survival following infection. For example, in laboratory mice, survival following inoculation with the bacterium *Salmonella typhimurium* was highest on isocaloric diets with a higher ratio of protein-to-carbohydrate, P:C (Peck et al., 1992); a study of lambs showed that individuals on a high-protein diet developed better resistance to the nematode *Trichostrongylus colubriformis* (Kambara et al., 1993); and in birds, a lack of dietary protein had a detrimental effect on the development of immune function in northern bobwhite (*Colinus virginianus*) chicks (Lochmiller et al., 1993). Arguably the clearest empirical examples showing dietary protein to be a central nutritional component for immune function and disease resistance are those carried out in insects, and in particular experiments on lepidopteran larvae. For example, in the African armyworm (*Spodoptera exempta*), larvae fed isocaloric diets with high P:C ratios had significantly higher survival following infection with either the generalist bacterium *Bacillus subtilis* (Povey et al., 2009) or a host-specific baculovirus, SpexNPV (Povey et al., 2014), and

this was associated with elevated levels of some immune parameters on high P:C diets.

In most of these experiments, it is often difficult to interpret which specific dietary trait is driving changes in immune function or survival following infection. In the bumblebee study above (Moret and Schmid-Hempel, 2000), for example, the costs of immune defense were offset when the bees were provided with *ad libitum* sugar solution. It is impossible to establish, however, whether this was because the immune response required carbohydrates, energy, water, or a combination of all three, or indeed whether starvation resulted in the breakdown of fats and proteins for energy metabolism that could otherwise have been used for the immune response. Likewise, most studies of lepidopteran larvae show that both immune function and post-infection survival are protein-dependent, but because they generally vary only in P:C ratio and not calorie density (i.e. they use isocaloric diets), it is impossible to determine whether this is due to positive effects of dietary protein or the negative effects of dietary carbohydrate or the specific balance of macronutrients, or indeed whether calorie effects far outweigh any macronutrient effects (but see Cotter et al., 2011). To tease these relationships apart requires experimental designs that carefully decouple the various co-varying nutritional traits.

Here, we apply the GF approach to disentangle the effects of macronutrient balance and calorie intake on the outcome of bacterial infections in insects, using as a model host-pathogen system *Spodoptera littoralis* (a generalist leaf-feeding caterpillar) and *Xenorhabdus nematophila* (an extracellular gram-negative bacterium). In the wild, *X. nematophila* has a mutualistic association with the entomopathogenic nematode *Steinernema carpocapsae*, which serves as the vector for *X. nematophila* (Georgis et al.,

2006; Herbert and Goodrich-Blair, 2007). However, the bacterium is capable of killing insects without its nematode host when *X. nematophila* cells are injected directly into the insect haemocoel in the laboratory (Herbert and Goodrich-Blair, 2007), so providing a tractable system for studying the effects of host diet on the host-pathogen interaction. Most previous studies of this kind, including our own, have focused on quantifying the effects on host survival and/or immune function of varying either the energy value of the host diet or its macronutrient balance (Lee et al., 2006; Moret and Schmid-Hempel, 2000; Povey et al., 2014, 2009). In contrast, here we quantify *in vivo* bacterial growth rates and age-dependent survivorship for larvae exposed to a range of doses of *X. nematophila* and fed chemically-defined diets that differ in their P:C ratio and/or calorie content (lipids comprise only a small proportion of the calorie intake of lepidopteran larvae and so are not varied here). Since protein and carbohydrate have similar caloric densities (*c.* 4.1 kcal/g or 17 kJ/g; Merrill and Watt, 1955), different P:C ratios are near isocaloric, which allows the *independent and interactive effects* of calorie content and macronutrient composition to be statistically quantified. We do this using an information theoretic approach (Burnham and Anderson, 2002; Whittingham et al., 2006) in which we define multiple plausible hypotheses (candidate models) to explain the effects of dietary attributes (absolute amounts of protein and/or carbohydrates, their interactions and their ratios) on various aspects of the host-pathogen interaction. In so doing, we aim to determine whether a single dietary attribute has pre-eminence in explaining this variation.

2.2 MATERIALS AND METHODS

2.2.1 Host: Spodoptera littoralis

The *S. littoralis* culture was established from eggs collected near Alexandria in Egypt in 2011 and has since been maintained using single pair matings of non-relatives for *c.* 40 generations, with around 150 pairs each generation to reduce inbreeding. Larvae were reared individually from the 2nd larval instar on a semi-artificial wheatgerm-based diet (**Table S2.1**) in 25 ml polypots. *S. littoralis* spend approximately two weeks in the larval stage, about seven days of which are spent in the 5th and 6th instars. Insects were maintained at 25 °C under a 12:12 light: dark photo regime.

2.2.2 Pathogen: Xenorhabdus nematophila F1D3

2.2.2.1 Storage and retrieval of bacterial stocks

Pure *X. nematophila* F1D3 (henceforth *Xenorhabdus*) stocks were stored at -20 °C in 1.5 ml microtubes (500 µl of *Xenorhabdus* in nutrient broth with 500 µl of glycerol). Vortexing ensured that all *Xenorhabdus* cells were coated in glycerol. To revive the stocks for use, 100 µl was added to 10 ml nutrient broth, and incubated at 28 °C for up to 48 h (generally stocks had grown sufficiently after 24 h).

2.2.2.2 Bacterial quantification and colony forming unit (CFU) bioassay

On the day of experimental bacterial challenge, the stock was sub-cultured, with 1 ml of the original stock added to 10 ml of nutrient broth and placed in a shaker-incubator for approximately 4 h. This ensured that the bacteria were in the exponential phase prior to challenge. Following the sub-culture, a 1 ml sample was first checked for purity and then used to produce a serial dilution in nutrient broth, from which the total cell count

was determined with fluorescence microscopy, using a haemocytometer with improved Neubauer ruling. The remaining culture was diluted with nutrient broth to the appropriate concentration required for the bacterial challenge.

The NBTL agar plates described below were made by autoclaving nutrient agar (28 g/L) and adding 25 mg/L bromothymol blue and 40 mg/L of triphenyltetrazolium chloride (TTC) before shaking vigorously. Bromothymol blue is a pH indicator and, indirectly, an aerobic indicator. Acid byproducts result in many bacteria producing yellow or red colonies on these plates. *X. nematophila* F1D3 produce deep blue colonies on these plates, presumably because these bacteria do not produce acids by fermentation. For a random sample, the identity of these bacteria was verified using PCR. Following the incubation period at 28 °C, the CFUs were counted for each sample, and using the dilution factor at which colonies could be reliably counted, the CFU/ml haemolymph were determined.

2.2.3 Experimental design

The aim of the experiments was to tease apart the importance of relative and absolute nutrient effects. Therefore, larvae were fed on one of six chemically-defined diets (A–F; **Table 2.1;** based on Bryce et al., 2005; Simpson and Abisgold, 1985) that varied in both the P:C ratio and calorie density. This comprised three P:C ratios (5:1, 1:1, 1:5) and two calorie densities (326 and 1112 kJ/100g diet; the remainder of the diet comprising indigestible cellulose). Thus, the six diets could be described with respect to the absolute amount of protein or carbohydrates (2.8, 8.4, 10.5, 14.0, 31.5 and 52.5 g/100g diet), by their sum (calorie density), by their ratio (P:C), by their interaction (P*C) or by

their individual diet characteristics (A-F). In so doing, it is possible to define at least 10 alternative models for describing the relationship between the trait of interest (bacterial growth rate, larval survivorship, etc.), and host diet (**Table 2.1**) (for simplicity, non-linear relationships were not explored). These can then be compared using an information theoretic approach by comparing AIC_c values and other model metrics (Burnham and Anderson, 2002; Whittingham et al., 2006).

A total of 468 larvae were first reared to the start of final larval instar on a semi-artificial wheat germ-based diet (Abisgold and Simpson, 1988). Within 24 h of moulting, the larvae were divided into six groups (n = 78 per group) and placed onto one of the six chemically-defined diets (A–F; **Table 2.1**). Approximately 1.5 g of the chemically-defined diets was placed in 90 mm diameter Petri dishes. Within each diet, 24 larvae were allocated to the control group (no bacterial challenge) and 54 were assigned to the bacteria-challenged group (see below). Following 24 h feeding on the assigned diets (at time, t = 0 h), each of the 324 bacteria-challenged larvae was injected with 5 µl of one of three bacterial solutions (averaging 1975, 5089 and 123300 *Xenorhabdus* cells per ml nutrient broth) using a microinjector (Pump 11 Elite Nanomite) fitted with a Hamilton syringe (gauge = 0.5mm). The syringe was sterilised in ethanol prior to use and the challenge was applied to the left anterior proleg. Injecting the 324 challenged larvae took approximately 3 h and time of injection was recorded but did not influence any of the metrics reported here. Survivorship does not differ between larvae injected with heat-killed bacteria and larvae that are handled but not injected (**Figure S2.1**), and so for logistical reasons the control larvae were handled at this time but not injected.

Table 2.1: Nutritional composition of the six chemically-defined diets and model explanatory terms relating to diet. Asterisks indicate interactions between terms (e.g. Model 5 includes the interaction between protein and carbohydrate). *P:C* = ratio of soluble protein to digestible carbohydrate (P:C = 1:5, 1:1 or 5:1). *Ratio* = relative percentage of protein in the digestible component of the diet (17%, 50% or 83%); the remainder is carbohydrate. *Cal* = energy value of digestible nutrients in the diet (326 or 1112 kJ / 100g diet); the remainder being non-digestible cellulose. *Protein* = amount of protein in the diet (g/100g total diet ingredients, both digestible and non-digestible), comprising peptone, albumen and casein in the ratio 1:1:3. *Carbs* = amount of digestible carbohydrates in the diet (g/100g total diet ingredients), in the form of sucrose. *Cellulose* = amount of non-digestible cellulose in the diet (g/100g total diet ingredients). All estimates are based on the dry mass of the diet ingredients, and all other diet ingredients (linoleic acid, cholesterol, chloroform, wesson salts, ascorbate and vitamin mix) are invariant across diets.

Model	***Diet***	***Protein*** (g/100g diet)		***Carbs*** (g/100g diet)	***Cellulose*** (g/100g diet)	***Cal*** *(kJ/100g diet)*		***Ratio*** (%)	***P:C***
	A	2.8		14.0	79.2	326		17	1 : 5
	B	8.4		8.4	79.2	326		50	1 : 1
	C	14.0		2.8	79.2	326		83	5 : 1
	D	10.5		52.5	33.0	1112		17	1 : 5
	E	31.5		31.5	33.0	1112		50	1 : 1
	F	52.5		10.5	33.0	1112		83	5 : 1
Model 0 (*Null* model)	.	.		.	.	.		.	.
Model 1 (*Diet* model)	X	.		.	.	.		.	.
Model 2 (*Protein*, P)	**.**	X		.	.	.		.	.
Model 3 (*Carb*, C)	**.**	.		X	.	.		.	.
Model 4 (P+C)	**.**	X		X	.	.		.	.
Model 5 (P*C)	**.**	X	*	X	.	.		.	.
Model 6 (*Cal*)	.	.		.	.	X		.	.
Model 7 (*Ratio*)	.	.		.	.	.		X	.
Model 8 (*Cal + Ratio*)	.	.		.	.	X		X	.
Model 9 (*Cal * Ratio*)	.	.		.	.	X	*	X	.

Within each diet treatment group, nine of the challenged larvae were assigned to each of the following times for haemolymph sampling: 12, 16, 20, 24, 28 or 36 h post-challenge (t = 0 h); in the control group, twelve larvae from each diet were sampled after either 20 h or 36 h (none of these died of *Xenorhabdus* infection). Haemolymph samples were obtained by piercing the cuticle next to the left anterior proleg with a sterile needle and allowing released haemolymph to bleed directly into a microtube. Immediately following sampling, each sample was diluted in pH 7.4 phosphate buffered saline, PBS (10 µl of haemolymph in 90 µl of PBS), and a dilution series produced down to 10^{-7} in intervals of 10^{-1}. The dilution series was plated onto NBTL agar plates (20 µl per 1/4 agar plate), incubated at 28 °C and checked after 24 h for bacterial colony quantification.

Larvae were weighed at the start of the experiment, prior to placement on the chemically-defined diet, and then every 24 h up to 96 h (72 h post-challenge). Larvae were also weighed immediately before haemolymph sampling and diet was replaced every 24 h up to 72 h (48 h post-challenge). Ninety-six hours after moulting into L6, the larvae had either pupated or were placed on standard semi-artificial diets until death or pupation. All larvae were monitored for death every hour throughout the duration of the sampling period (12 – 36 h) and as frequently as possible thereafter. The date and time of death was recorded, as well as the larval weight at death. None of the weight metrics gathered proved to be significant predictors of mortality risk and so are not discussed further.

Where logistically possible, within an hour of death, haemolymph samples were taken and serially-diluted in PBS buffer (pH 7.4) down to 10^{-10} in intervals of 10^{-1}. The dilution series was plated from 10^{-3} to 10^{-10} onto NBTL agar plates (20 µl per 1/4 agar plate). The plates were then incubated at 28 °C and checked regularly for CFU, as above. The dates of pupation and eclosion as moths were recorded, as well as weight of pupae and death date if occurring during these stages.

2.2.4 Statistical analysis

All statistical analyses were conducted using the *R* statistical package (v3.2.2; R Core Team, 2014). As the focus of this paper was to determine which of several attributes of larval diet impacts most on resistance to bacterial infection, an information theoretic approach was taken (Burnham and Anderson, 2002; Whittingham et al., 2006). Thus, rather than using a model simplification procedure to identify a single minimal adequate model to explain the effects of a key dietary attribute on host/pathogen traits, we compared multiple candidate models with different structures and establish the relative weight of evidence in favour of each. A strength of this approach is that rather than being constrained to identify a single 'best' model, it allows for multiple models to be described (e.g. with different dietary attributes) that may equally well describe the data (Burnham and Anderson, 2002; Whittingham et al., 2006). Exploratory data analysis was conducted using *Diet* (a factor with six levels) as the main nutritional metric, to determine an appropriate model structure for comparing across diet metrics (analyses not shown). This was then followed by a comparison of ten candidate models (**Table 2.1**) using AIC values corrected for finite sample sizes (AIC_c) to establish the most parsimonious models including likely nutritional attributes driving the observed data.

AIC_c values and *Akaike weights* were estimated using the *MuMIn* package (v1.15; Bartoń, 2018) in *R*. The relative weight of evidence in favour of one model over another (evidence ratio) is determined by dividing the *Akaike weight* of one model by another (Burnham and Anderson, 2002). Thus, an evidence ratio of 2 would indicate that there was twice as much evidence in favour of the best model than the second best. Because we were interested in the effects of larval diet on both bacteria-challenged and non-challenged larvae, both were included in the statistical analyses that follow, with bacterial dose included as a log_{10}-transformed covariate with the control insects given a challenge dose of zero. Subsequent analyses indicated that similar qualitative trends are apparent if the control insects are excluded from the analyses.

2.2.4.1 Survivorship in relation to diet and bacterial dose

Cox's proportional hazards models were used to establish the effects of diet, bacterial dose (log_{10}-transformed) and their interaction on survivorship post-challenge until death (in the larval, pupal or moth stage), using the *coxph* function in the *survival* library (v2.41; Therneau, 2018) of *R*. Nine individuals were excluded from the analysis because their timing of death could not be accurately established, leaving 459 individuals (318 bacteria-challenged and 141 non-challenged control larvae). The predicted values from the model are visualised using thin-plate spline plots created using the *fields* package (v9.6; Nychka, 2016) in R. These heat maps depict the risk or odds of dying (relative to 1), such that a risk score above 1 is higher risk than the average in the population and below 1 is lower risk than the average in the population.

2.2.4.2 In vivo bacterial growth rate in relation to diet and challenge dose

A subset of larvae were sampled at 12, 16 and 20 h post-challenge to estimate bacterial growth rate, reducing the sample size to 230 larvae (159 bacteria-challenged and 71 non-challenged controls). Inspection of the frequency distribution of bacterial counts revealed that they conformed to a zero-inflated negative binomial model. In other words, the distribution was heavily skewed and conformed to a negative binomial distribution but with additional zeros. Therefore, the effects of diet, bacterial dose (log_{10}-transfomed) and their interaction, plus associated covariates (i.e. sample dilution factor, sampling time) were analysed using the *zeroinfl* function in the *pscl* library (v1.5.2; Jackman et al., 2017) of *R*. This model provides separate estimates for the negative binomial component (i.e. mostly positive bacterial counts) and the zero-inflated component (zero counts over and above those estimated by the best fit negative binomial distribution).

2.2.4.3 Bacterial loads at death in relation to diet and challenge dose

For a sub-set of bacteria-challenged larvae, it was possible to estimate their bacterial load at death (none of the larvae in the control group died of bacterial infection and so were not included in this analysis). The CFU count multiplied by the serial dilution factor exhibited a negative binomial distribution, and so these data were modelled using the *glm.nb* function in the *MASS* library (v7.3; Ripley et al., 2018) of *R*. Model convergence was possible only when two outliers ($>10^{10}$ CFU/µl) were excluded from the analysis, giving a sample size of 206 larvae for which the relationships between bacterial dose (log_{10}-transfomed), diet, and bacterial load at death could be established. In a secondary analysis, the relationship between bacterial growth rate (i.e. bacterial

load at live sampling) and bacterial load at death was explored, and this reduced the sample size to 126 larvae for which both counts were available.

2.2.4.4 Correlation between survivorship and bacterial growth rates

In this Cox's proportional hazards model both bacterial load at sampling (a correlate of *in vivo* bacterial growth rate) and larval diet attributes were included as potential explanatory terms. This allowed us to consider whether larval diet had any effects on survivorship over and above those it may have on bacterial replication rate. The magnitude of challenge dose and time of sampling were also included in the model, as well as the interaction between sampling time and bacterial load at sampling (preliminary analyses indicated that other two-way interactions did not explain a significant amount of variation in survivorship).

2.3 RESULTS

2.3.1 Mortality rates in relation to diet and bacterial dose

Overall mortality in the larval stage was 84.9% (n = 270/318) in the bacterial-challenge groups and 3.6% (n = 5/141) in the non-challenged control group (none of which died due to infection by *X. nematophila*). Challenged larvae that succumbed to infection did so after approximately two days, whereas those that either survived infection or were in the non-challenged control group, lived for a further nine days on average and generally pupated successfully (median time to death post-challenge ± IQR: casualties = 26.0 ± 15.0 h, N = 270; survivors: 266.5 ± 166.3 h, N = 48; controls: 338.0 ± 168.0 h, N = 141).

The effect of larval diet differed between challenged and control insects, with the speed of mortality declining with the amount of protein in the diet for bacteria-challenged larvae but being constant across diets for larvae in the control group (**Figure 2.1a, Figure 2.2a**). A survivorship model that included just the interaction between the protein-content of the diet (*Protein*) and the magnitude of the challenge dose ($\log_{10}$*Dose*) was better (based on AIC_c) than all alternative models (0–9 in **Table 2.1**), and it explained a similar amount of variation as the full *Diet* model (*Protein*: r^2 = 0.434, *Diet*: r^2 = 0.440; **Tables 2.2**, **2.3**). Inspection of the predicted values for this model (and **Figure 2.2b**) revealed that the amount of protein in the diet had little effect on the hazard function of non-challenged (control) larvae: the odds ratios across diets varied between 0.289 (± 0.061 SEM) and 0.388 (± 0.107). In contrast, the odds of the bacteria-challenged larvae dying *increased* with the magnitude of the challenge-dose and *decreased* with the amount of protein in the diet, such that when larvae were

exposed to the largest bacterial challenge the odds ratio fell from 4.027 (± 0.194) for larvae on the most protein-poor diet (diet A – 2.8% protein) to just 1.085 (± 0.157) for those on the most protein-rich (diet F – 52.5% protein). The evidence ratio in favour of the *Protein* model relative to the second-best model (Model 4: *Protein* + *Carb*) was relatively low (2.4), indicating that survivorship may also be influenced to some degree by the amount of carbohydrate in the larval diet, though carbohydrates alone explained little variation in survivorship (**Table 2.2**, Model 3. *Carb*: ΔAIC_c = 36.31; **Figure S2.2a**). These two models were substantially better than any of the alternatives (evidence ratios ≥ 12.3; **Table 2.2**).

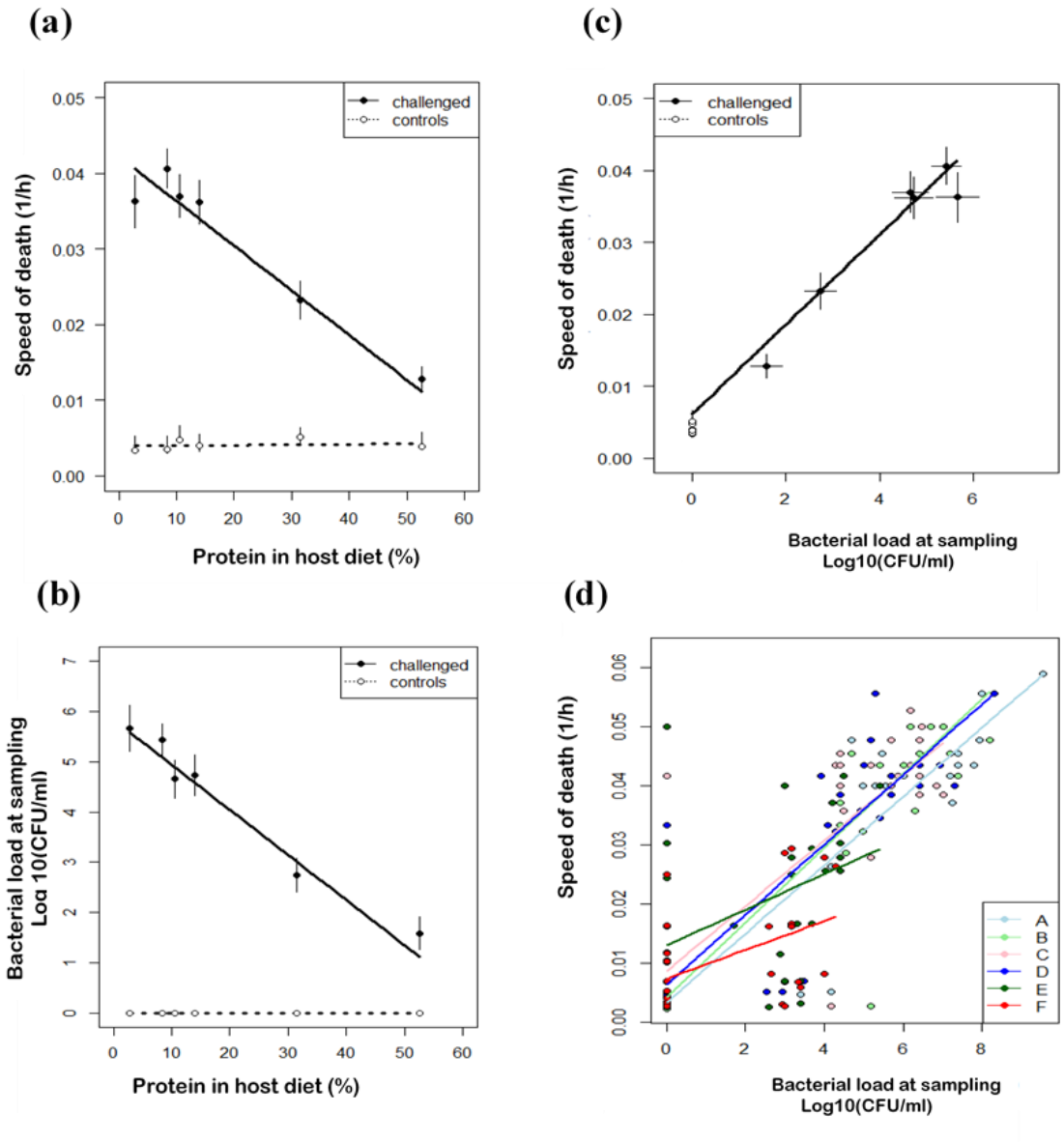
(a)
challenged
controls
Speed of death (1/h)
Protein in host diet (%)
(c)
challenged
controls
Speed of death (1/h)
Bacterial load at sampling
Log10(CFU/ml)
(b)
challenged
controls
Bacterial load at sampling
Log 10(CFU/ml)
Protein in host diet (%)
(d)
Speed of death (1/h)
A
B
C
D
E
F
Bacterial load at sampling
Log10(CFU/ml)

Figure 2.1: Relationships between the protein content of the six larval diets, bacterial load at sampling and speed of death in bacteria-challenged and non-challenged control insects. (a) The relationship between the amount of dietary protein and the mean (+ SEM) speed of death (1/time to death in hours); for a plot of speed of death versus the amount of carbohydrates in the diet, see Figure S2.2a. (b) The relationship between the amount of dietary protein and the mean (+ SEM) bacterial load at sampling; for a plot of speed of death versus the amount of carbohydrates in the diet, see Figure S2.2b. (c) The relationship between bacterial load at sampling (means + SEM) and speed of death (means + SEM) across the six diets for both challenged and control larvae. For (a)-(c), the closed symbols = bacteria-challenged larvae and the open symbols = control larvae; solid and dashed lines are the fitted regression lines through the respective raw data. (d) The relationship between bacterial load at sampling and speed of death within each of the six diets A-F; the lines are the respective within-diet regression lines. A linear regression model indicates that there is a significant interaction between diet and bacterial load at sampling (Linear model: bacterial load: $F_{1,199} = 603.43$, $P < 0.0001$; Diet: $F_{5,199} = 1.42$, $P = 0.22$; bacterial load*diet interaction: $F_{5,199} = 4.52$, $P = 0.0006$).

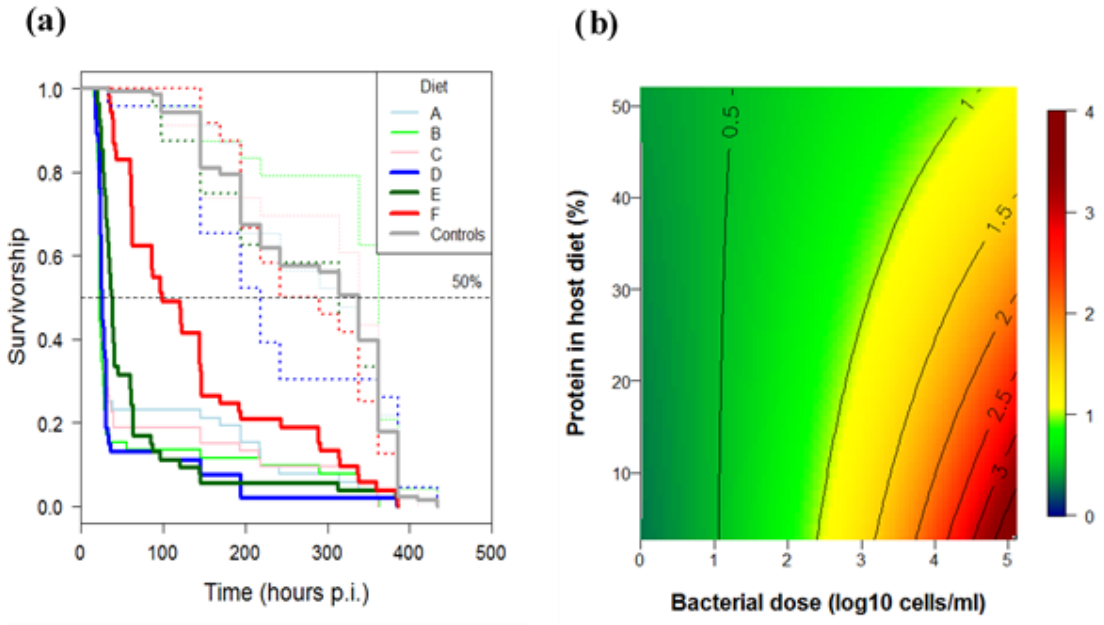

Figure 2.2: Effects of larval diet and bacterial challenge dose on survivorship and mortality risk. (a) Kaplan-Meier survivorship curves for bacteria-challenged larvae (solid colored lines) and non-challenged control larvae (dotted lines and solid gray line). For the bacteria-challenged larvae, survivorship is averaged across the three bacterial doses; for the control larvae, data are for each of the six individual diets (dotted lines) and averaged across the six diets (solid gray line), the latter is included because survival does not vary across diets for control larvae. (b) Heatmap showing the interactive effects of bacterial challenge dose and amount of protein in the larval diet on predicted relative mortality risk (see Table 2.3). The interaction is reflected in the non-linear risk isoclines: at zero-low bacterial doses, relative mortality risk is low (<1) and independent of diet, whereas at higher challenge doses mortality risk increases (>1) and diet becomes increasingly important as the amount of protein in the diet reduces (risk >>1).

Table 2.2: Table of candidate Cox's proportional hazards models explaining survivorship in relation to the nutritional attributes of their diet. All models also include $\log_{10}$(bacterial dose) and its interaction with the terms listed in the model below. K = number of parameters, AIC_c = corrected Akaike Information Criteria values; Δ AIC_c = difference in AIC_c values between the best model (lowest AIC_c) and the current model; w = Akaike weights; r^2 = adjusted r^2 for the model. The shaded models are those in which either no diet attributes are included (model 0) or diet is included as a 6-level factor (model 1), so capturing all diet-related attributes.

Model/hypothesis	***k***	***AIC$_c$***	***Δ AIC$_c$***	***w***	***r^2***
2. *Protein*	3	4461.0	0.00	0.641	0.434
4. *Protein + Carb*	5	4462.8	1.73	0.269	0.437
9. *Cal * Ratio*	7	4466.1	5.02	0.052	0.438
5. *Protein * Carb*	7	4466.8	5.79	0.035	0.437
1. *Diet*	11	4472.7	11.62	0.001	0.440
8. *Cal + Ratio*	5	4474.7	13.67	0.000	0.422
7. *Ratio*	3	4479.8	18.78	0.000	0.411
6. *Cal*	3	4488.8	27.72	0.000	0.399
3. *Carb*	3	4497.3	36.31	0.000	0.388
0. No diet attributes	1	4499.3	38.32	0.000	0.380

Table 2.3: Summary of Cox's proportional hazards model of survivorship in relation to $\log_{10}$(bacterial dose), the amount of protein in the diet and the interaction between the two. Full model likelihood ratio test: $\chi^2_3 = 261.5$, $P < 0.0001$.

Term	***b***	***exp(b)***	***SE(b)***	***z***	***P***
$\log_{10}$*Dose*	0.5347	1.7069	0.03980	13.419	< 0.0001
Protein	0.0059	1.0059	0.00480	1.221	0.2220
$\log_{10}$*Dose: Protein*	-0.0063	0.9937	0.00140	-4.456	< 0.0001

2.3.2 *In vivo* bacterial growth rate in relation to diet and challenge dose

Low levels of dietary protein resulted in increased haemolymph bacterial loads in challenged larvae (**Figure 2.1b**); and this was especially true at the highest challenge doses where the predicted bacterial loads differed by an order of magnitude across diets (**Figure 2.3a**). A model containing an interaction between protein and bacterial dose had the lowest AIC_c, explaining a similar level of variation in bacterial load as the full *Diet* model (*Protein*: r^2 = 0.119, *Diet*: r^2 = 0.121; **Tables 2.4**, **2.5**). The second-best model included protein and carbohydrate (Model 4, **Table 2.1**), but the evidence ratio for this and other models was large ($\geq$16.8), and the carbohydrate effect was again weak (**Figure S2.2b**), indicating that the *Protein* model was substantially better than the alternatives.

Bacterial load appeared to be determined by a two-step process. First, as indicated by the *zero-inflated* component of the model, the probability of the bacterium successfully establishing in the host (i.e. yielding a non-zero CFU count when sampled), increased with the size of the challenge dose and decreased with the amount of protein in the diet (and the interaction between the two; **Figure 2.3b**, **Table 2.5**). Second, as indicated by the *count* component of the model, the rate at which the bacterial population grew once established (i.e. the magnitude of the CFU count at sampling) was negatively correlated with the amount of protein in the larval diet and was independent of the size of the challenge-dose (**Figure 2.3c**, **Table 2.5**).

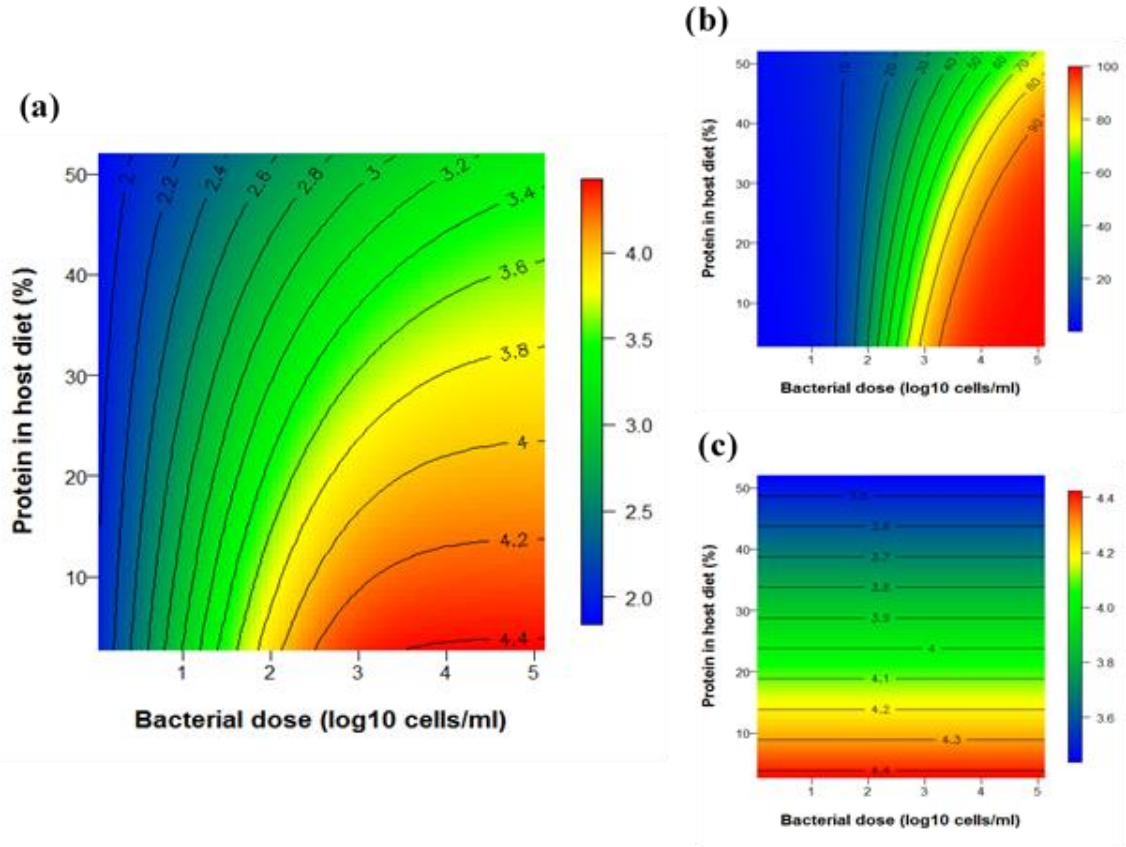

Figure 2.3: Heatmaps showing the interactive effects of bacterial challenge dose and amount of protein in the larval diet on the predicted haemolymph bacterial load and prevalence at 20 hours post-challenge (a proxy for bacterial growth rate). Figures are based on predicted from the model described in Table 2.5. (a) The predicted bacterial load at sampling is an interactive function of the size of the challenge dose and the amount of protein in the larval diet. At zero-low bacterial doses, predicted bacterial load is low and independent of diet, whereas diet becomes increasingly important as the bacterial dose increases. This is due to the combined effects of (b) the size of the challenge dose and larval diet on the probability of infection establishment (i.e. bacterial prevalence), and (d) the effects of dietary protein content on *in vivo* bacterial growth rate (i.e. bacterial count of infected larvae).

Table 2.4: Table of candidate zero-inflated negative binomial models for haemolymph bacterial counts at live sampling in relation to challenge-dose and diet. K = number of parameters, AIC_c = corrected Akaike Information Criteria values; Δ AIC_c = difference in AIC_c values between the best model (lowest AIC_c) and the current model; w = Akaike weights; r^2 = pseudo-r^2 for the model. The ten alternative Diet attributes listed in the first column are described in Table 2.1. The dependent variable in these models is the haemolymph bacterial count at sampling. All models take the following form: Count component = Dilution factor + Sampling time + Diet attribute; Zero-inflation component = log_{10}Dose * Diet attribute (except for model 1, where the model was over-parameterised and the interaction term of the zero-inflation component was omitted). The count component is assumed to take a negative binomial distribution, modelled with a log link function, and the zero-inflation component assumes a binary distribution with logit link. The shaded models are those in which either no diet attributes are included (model 0) or diet is included as a 6-level factor (model 1), so

capturing all diet-related attributes.

Model. Diet attributes	***k***	AIC_c	$\Delta\ AIC_c$	***w***	r^2
2. *Protein*	9	1557.1	0.00	0.924	0.119
4. *Protein + Carb*	12	1562.7	5.63	0.055	0.119
9. *Cal * Ratio*	15	1565.3	8.20	0.015	0.121
5. *Protein * Carb*	15	1568.3	11.23	0.003	0.120
1. *Diet*	16	1569.6	12.47	0.002	0.121
8. *Cal + Ratio*	12	1571.7	14.59	0.001	0.114
6. *Cal*	9	1585.4	28.25	0.000	0.102
7. *Ratio*	9	1591.8	34.65	0.000	0.099
0. No diet attributes	6	1599.0	41.93	0.000	0.091
3. *Carb*	9	1603.8	46.67	0.000	0.092

Table 2.5: Summary of zero-inflated negative binomial model for bacterial counts at live sampling in relation to the interaction between bacterial dose and the protein content of the larval diet. The dependent variable in the model is the haemolymph bacterial count at sampling. Dilution = haemolymph dilution factor prior to counting (numeric: 0 - 7); Sampling.time = the number of hours post-challenge that haemolymph was sampled for counting bacteria (numeric: 12, 16 or 20 h); Protein = the amount of protein in the larval diet (numeric: 2.8% - 52.5%); Theta = degree of overdispersion of the negative binomial distribution (numeric); $\log_{10}$Dose = log10(bacterial challenge dose +1) (numeric: 0 - 5.091).

Count component of model (negative binomial with log link)	***b***	***SE***	***z***	***P***
intercept	4.0289	0.6481	6.216	< 0.0001
Dilution	-0.4118	0.0972	-4.235	< 0.0001
Sampling.time	0.1483	0.0366	4.048	0.0002
Protein	-0.0462	0.0093	-4.947	< 0.0001
log(*Theta*)	-0.3615	0.1373	-2.632	0.0085
Zero-inflation component of model (binomial with logit link)	***b***	***SE***	***z***	***P***
intercept	5.7563	2.5476	2.260	0.0239
$\log_{10}$*Dose*	-2.5027	0.7675	-3.261	0.0011
Protein	-0.0406	0.0598	-0.679	0.4974
$\log_{10}$*Dose:Protein*	0.0307	0.0173	1.773	0.0763

Note that if the marginally non-significant $\log_{10}$*Dose:Protein* interaction term is omitted from this model, the following zero-inflation terms result:

Zero-inflation component of model (binomial with logit link)	***b***	***SE***	***z***	***P***
intercept	3.2993	0.9826	3.358	0.0008
$\log_{10}$*Dose*	-1.7399	0.3144	-5.533	< 0.0001
Protein	0.0643	0.0157	4.086	< 0.0001

2.3.3 Bacterial loads at death in relation to diet and challenge dose

At the point of death, the bacterial load of challenged larvae was a function of both the larval diet and the magnitude of the challenge dose, but the marginally best model (Model 2: *Protein*) explained less than 6% of the variation in bacterial load at death (r^2 = 0.055; **Tables 2.6, 2.7**). The full *Diet* model explained twice as much variation (r^2 = 0.103; evidence ratio = 1.3; **Table 2.6**), however it contains a much larger number of parameters, making it the second-best model.

As expected, bacterial loads of larvae at death were significantly higher than those of the same larvae at sampling (log_{10}mean $\pm$ SD: at death = 6.01 $\pm$ 1.82; at sampling = 3.85 $\pm$ 1.74). This is consistent with larvae dying when their bacterial loads exceed some critical threshold, at around 10^6 CFU/ml **(Figure 2.4**). Of the 126 challenged larvae for which bacterial loads were quantified both as live larvae and soon after death, only nine (7%) had counts at death less than 40,000 CFU/µl, and all but one of these had a count lower than the detection limit (the other was 1,000 CFU/ml). Of those larvae that did *not* harbour culturable bacteria at death, just two also had no bacteria at sampling, consistent with them not having received a sufficiently large bacterial challenge to establish an infection (or with the rapid elimination of injected bacteria). The remaining seven larvae (5.6% of those challenged) had an actively-replicating bacterial infection at 16-20 h post-challenge (1,000 – 300,000 CFU/ml), which they were subsequently able to eliminate. Despite resisting infection (i.e. reducing bacterial loads to near-zero), these insects still died in the larval stage; interestingly, 6 out of 7 of these larvae were reared on diet A, the least protein-rich of the six diets at 2.8% w/w (**Figure 2.4**). Bacterial loads were not quantified in the pupal or moth stages, but these results do suggest most

of the 15% of challenged larvae that successfully pupated probably did so because they were able to limit the growth of the nascent bacterial population.

Using the restricted dataset in which bacterial counts were available both prior to and at death, the marginally best model explaining bacterial load at death was again one in which the larval diet attributes were represented by the amount of *Protein* (r^2 = 0.102; **Tables 2.8, 2.9**). The second-best model was the full *Diet* model, which explained a similar level of variation (r^2 = 0.199; evidence ratio = 1.0; **Table 2.8**), with the *Protein +/* Carb* models explaining marginally less (Models 4 and 5, **Table 2.8**; $r^2 \leq 0.138$; evidence ratios ≥ 3.1). As reflected in **Figure 2.4**, the *Protein* model revealed that the magnitude of the bacterial load at death was not significantly correlated with the rate at which the haemolymph bacterial population grew, after controlling for sampling time, diet and challenge dose (z = 1.415, P = 0.16; **Table 2.9**).

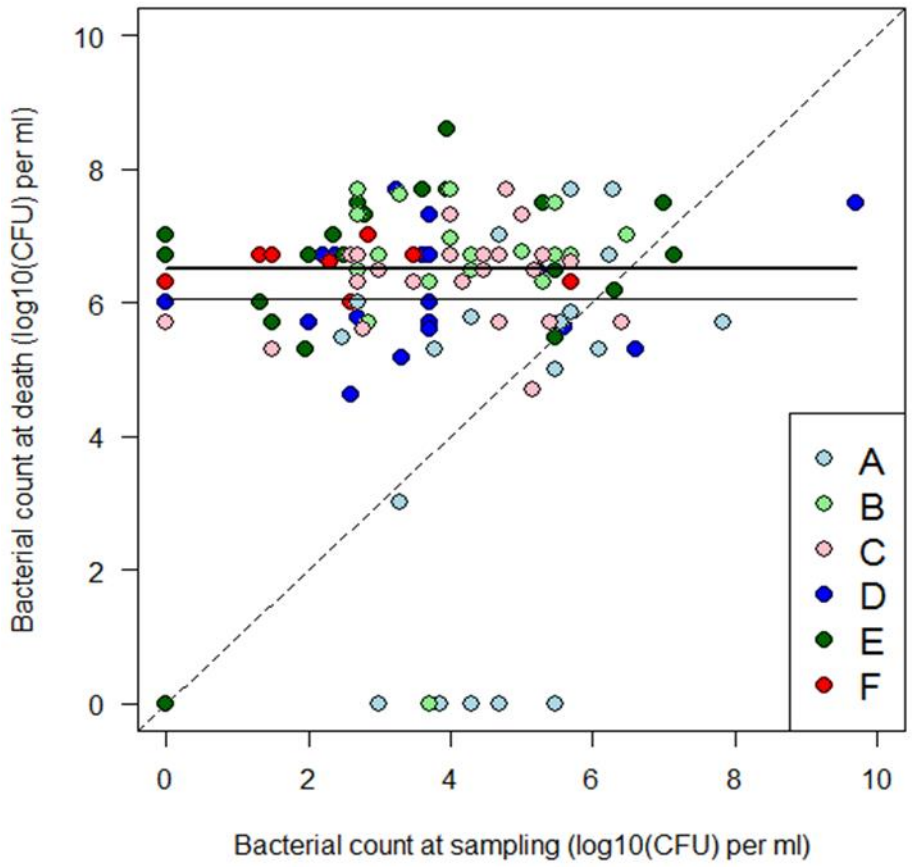

Figure 2.4: Relationship between bacterial load at sampling and bacterial load at death. Different colored symbols refer to the six different diets (A – F, Table 2.1). The dashed diagonal line is the line of parity (1:1) for bacterial counts at sampling and at death. The thin horizontal line is the mean bacterial count at death, across all diets, when the nine very low counts ($<10^1$) are included; the thick line is the mean when these are excluded.

Table 2.6: Table of candidate GLMs explaining bacterial load at death in relation to the interaction between the nutritional attributes of their diet and the magnitude of the bacterial challenge dose. Each model assumes negative binomial errors and a log link function. K = number of parameters, AIC_c = corrected Akaike Information Criteria values; ΔAIC_c = difference in AIC_c values between the best model (lowest AIC_c) and the given model; w = Akaike weights; r^2 = pseudo-r^2 for the model. The ten alternative Diet attributes listed in the first column are described in Table 2.1. The dependent variable in these models is the haemolymph bacterial count at death. Analysis was restricted to those larvae that were challenged with bacteria as larvae (non-challenged controls are not included). The shaded models are those in which either no diet attributes are included (model 0) or diet is included as a 6-level factor (model 1), so capturing all diet-related attributes.

Model/hypothesis	***k***	AIC_c	$\Delta\ AIC_c$	***w***	r^2
2. *Protein*	5	6656.6	0.00	0.369	0.055
1. *Diet*	13	6657.3	0.64	0.293	0.103
5. *Protein * Carb*	9	6658.5	1.88	0.150	0.069
4. *Protein + Carb*	7	6659.4	2.75	0.096	0.051
8. *Cal + Ratio*	7	6660.3	3.70	0.059	0.047
9. *Cal * Ratio*	9	6663.2	6.55	0.015	0.052
7. *Ratio*	5	6664.9	8.22	0.006	0.016
6. *Cal*	5	6665.0	8.39	0.006	0.016
0. No diet attributes	3	6665.2	8.60	0.005	0.000
3. *Carb*	5	6668.6	11.92	0.001	0.003

Table 2.7: Summary of the GLM with negative binomial errors and log link explaining bacterial load at death in relation to the interaction between the amount of protein in the larval diet and the magnitude of the challenge dose. Theta ± SE = 0.2840 ± 0.0231. Residual deviance (df) = 274.94 (202).

Term	***b***	***SE***	***z***	***P***
intercept	13.3962	1.1025	12.150	<0.0001
$\log_{10}$*Dose*	0.4913	0.2587	1.899	0.0576
Protein	0.1837	0.0609	3.019	0.0025
$\log_{10}$*Dose* * *Protein*	-0.0343	0.0135	-2.534	0.0113

Table 2.8: Table of candidate GLMs explaining bacterial load at death in relation to the interaction between the nutritional attributes of their diet and the magnitude of the bacterial challenge dose, as well as the bacterial load of larvae at live sampling. Each model assumes negative binomial errors and a log link function. K = number of parameters, AIC_c = corrected Akaike Information Criteria values; ΔAIC_c = difference in AIC_c values between the best model (lowest AIC_c) and the given model; w = Akaike weights; r^2 = pseudo-r^2 for the model. The ten alternative Diet attributes listed in the first column are described in Table 2.1. The dependent variable in these models is the haemolymph bacterial count at death. Analysis was restricted to those larvae that were challenged with bacteria as larvae (non-challenged controls are not included) and were sampled both at death and during live sampling). The shaded models are those in which either no diet attributes are included (model 0) or diet is included as a 6-level factor (model 1), so capturing all diet-related attributes.

Model/hypothesis	***k***	***AIC$_c$***	***Δ AIC$_c$***	***w***	***r^2***
2. *Protein*	7	4086.8	0.00	0.386	0.102
1. *Diet*	15	4087.2	0.40	0.374	0.199
5. *Protein * Carb*	11	4089.2	2.39	0.126	0.138
4. *Protein + Carb*	9	4090.2	3.40	0.073	0.108
8. *Cal + Ratio*	9	4093.5	6.68	0.014	0.090
0. No diet attributes	5	4094.6	7.79	0.008	0.034
7. *Ratio*	7	4094.6	7.82	0.008	0.059
9. *Cal * Ratio*	11	4095.0	8.15	0.007	0.108
6. *Cal*	7	4096.5	9.72	0.003	0.048
3. *Carb*	7	4098.9	12.11	0.001	0.035

Table 2.9: Summary of the GLM with negative binomial errors and log link explaining bacterial load at death in relation to the interaction between the amount of protein in the larval diet and the magnitude of the challenge dose, and the bacterial load at live sampling. Theta ± SE = 0.2931 ± 0.0305. Residual deviance (df) = 167.87 (120).

Term	***b***	***SE***	***z***	***P***
intercept	10.3461	1.4908	6.940	<0.0001
$\log_{10}$*Dose*	1.1142	0.3497	3.186	0.0014
Protein	0.3037	0.0702	4.328	<0.0001
Sampling time	-0.0103	0.0326	-0.317	0.7509
Bacterial load at sampling	0.1671	0.1181	1.415	0.1572
$\log_{10}$*Dose * Protein*	-0.0628	0.0155	-4.048	<0.0001

2.3.4 Correlation between mortality rates and bacterial growth rates

Bacterial growth rate was a highly significant predictor of mortality rate, both *across* and *within* diet treatments (**Figure 2.1c,d**). To explore the interaction between diet, bacterial growth rate and mortality further, the survival analysis was repeated with bacterial load at sampling (plus time of sampling and their interaction) included as a potential explanatory variable, along with the magnitude of the challenge dose and a range of alternative dietary attributes. The best model (lowest AIC_c) was one in which diet was represented by the interaction between the calorie density and P:C ratio of the diet (Model 9: r^2 = 0.734; **Tables 2.10, 2.11a**). In the second best model, diet was represented by *Protein* alone and this explained a similar level of variation in survivorship (Model 2: r^2 = 0.721; **Tables 2.10, 2.11b**). In fact, each of the top five diet models explained more than 70% of the variation in survivorship. In each case, bacterial load at sampling was a highly significant predictor of mortality risk, but larval diet explained additional variation *over and above* that explained by its effects on *in vivo* bacterial growth rate (**Tables 2.11a,b**). Specifically, as the (relative or absolute) amount of protein in the diet increased, so the mortality risk declined. Thus, even after accounting for (diet-induced variation in) the *in vivo* bacterial growth rate, larvae feeding on a higher protein diet lived longer on average, with the magnitude of the effect being modulated by the size of the challenge dose (**Figure 2.5**).

The importance of diet (and especially protein) in explaining variation in mortality risk is illustrated by a comparison of the AIC_c and r^2 values for models containing specific components of the full Model 2 (**Table 2.12**). All of the models that include *Protein* or bacterial count at sampling (*Count*) as an explanatory term explain in excess of 56% of

the variation in mortality risk, whereas all of those that do not include either *Protein* or *Count* (but do include $\log_{10}$*Dose*) explain less than 7% of the variation. *Protein* and *Count* are to some extent interchangeable, as models that include one or the other, but nothing else, explain similar amounts of variation (c. 57%). The addition of $\log_{10}$*Dose* to the model improves the explanatory power still further, with all three of the top models containing *Protein*, *Count* and $\log_{10}$*Dose*, with evidence ratios $\leq$10, whereas those models that do not include all three have evidence ratios in excess of 800.

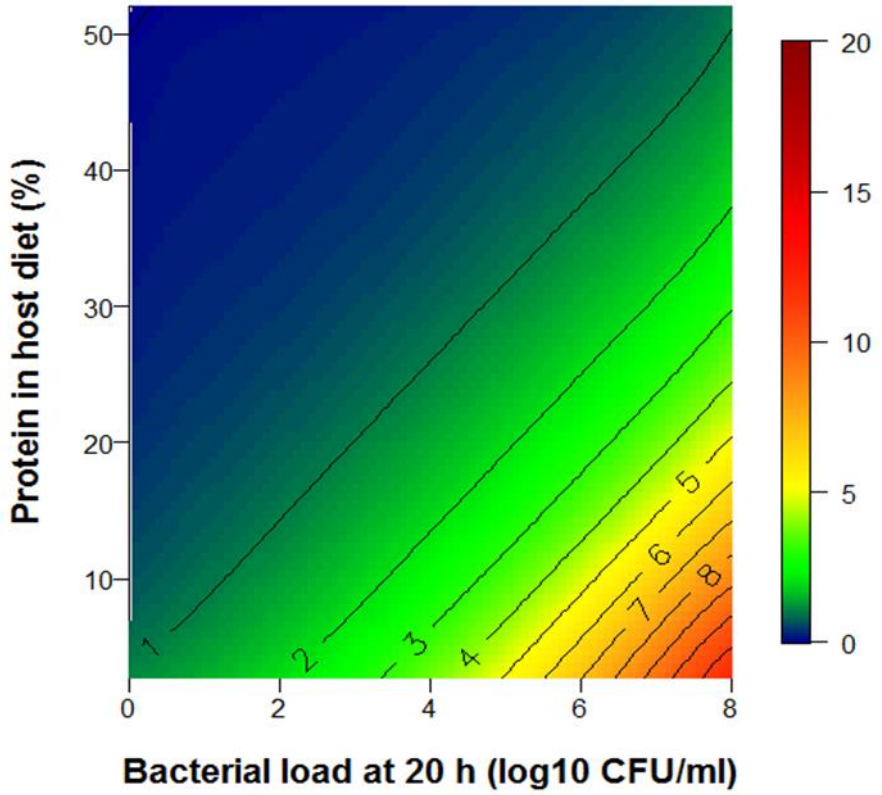

Figure 2.5: Heatmap showing the combined effects of bacterial load at 20 h post-challenge and amount of protein in the larval diet on predicted relative mortality risk. Figures are based on predicted from the model described in Table 2.11b. For illustrative purposes, predictions are shown for a high challenge dose (≥ 1000 bacterial cells/ml); for lower challenge doses, the figure is qualitatively identical but the magnitudes of the risks are reduced (and heatmap colours would be cooler). Mortality risk increases with the magnitude of the bacterial load at sampling and decreases as the amount of dietary protein increases.

Table 2.10: Table of candidate Cox's proportional hazards models explaining survivorship in relation to the nutritional attributes of their diet. All models also include bacterial challenge dose, sampling time, bacterial load at sampling and the interaction between sampling time and bacterial load at sampling. K = number of parameters, AIC_c = corrected Akaike Information Criteria values; Δ AIC_c = difference in AIC_c values between the best model (lowest AIC_c) and the current model; w = Akaike weights; r^2 = pseudo-r^2 for the model. The ten alternative Diet attributes listed in the first column are described in Table 2.1. The dependent variable in these models is the time of death (h). Analysis was restricted to those larvae that were sampled both at death and during live sampling. The shaded models are those in which either no diet attributes are included (model 0) or diet is included as a 6-level factor (model 1), so capturing all diet-related attributes.

Model/hypothesis	***k***	***AIC$_c$***	***Δ AIC$_c$***	***w***	***r^2***
9. *Cal * Ratio*	7	821.6	0.00	0.496	0.734
2. *Protein*	5	823.2	1.53	0.231	0.721
1. *Diet*	9	823.9	2.21	0.164	0.739
4. *Protein + Carb*	6	825.3	3.64	0.080	0.721
5. *Protein * Carb*	7	827.3	5.70	0.029	0.721
8. *Cal + Ratio*	6	844.8	23.14	0.000	0.674
6. *Cal*	5	849.6	27.99	0.000	0.656
7. *Ratio*	5	854.1	32.41	0.000	0.643
0. No diet attributes	4	855.5	33.81	0.000	0.633
3. *Carb*	5	856.8	35.19	0.000	0.635

Table 2.11: Summary of Cox's proportional hazards model for larval mortality in relation to $\log_{10}$(bacterial dose), bacterial load at sampling, time of sampling. (a) the two-way interaction between the amount of protein and carbohydrate in the larval diet or (b) the amount of protein in the diet. Full model likelihood ratio test: (a) χ^2_7 = 166.7, P < 0.0001. (b) χ^2_5 = 160.8, P < 0.0001.

(a)					
Term	***b***	***exp(b)***	***SE(b)***	***z***	***P***
$\log_{10}$*Dose*	0.5028	1.6533	0.1227	4.096	< 0.0001
Sampling time	0.0962	1.1010	0.0522	1.842	0.0655
Bacterial load at sampling	1.2169	3.3767	0.2749	4.426	< 0.0001
Cal	0.0138	1.0138	0.0087	1.586	0.1128
Ratio	1.6399	5.1551	0.6748	2.430	0.0151
Cal:Ratio	-0.0895	0.9144	0.0182	-4.909	< 0.0001
Sampling time: Bacterial load at sampling	-0.0448	0.9562	0.0156	-2.878	0.0040

(b)					
Term	***b***	***exp(b)***	***SE(b)***	***z***	***P***
$\log_{10}$*Dose*	0.4715	1.6025	0.1217	3.873	0.0001
Sampling time	0.0777	1.0809	0.0512	1.518	0.1289
Bacterial load at sampling	1.1511	3.1618	0.2754	4.180	< 0.0001
Protein	-0.0556	0.9459	0.0099	-5.629	< 0.0001
Sampling time: Bacterial load at sampling	-0.0416	0.9593	0.0156	-2.653	0.0080

Table 2.12: Table of candidate Cox's proportional hazards models explaining larval mortality in relation to the nutritional attributes of their diet. The 'full' model here is model 2 in Table 2.11. K = number of parameters, AIC_c = corrected Akaike Information Criteria values; Δ AIC_c = difference in AIC_c values between the best model (lowest AIC_c) and the current model; w = Akaike weights; r^2 = pseudo-r^2 for the model. Time = time of live sampling (12 – 20 h post-challenge); Count = bacterial count at live sampling; Time:Count = the interaction between Time and Count; Dose = log10(bacterial challenge dose); Protein = amount of protein in the larval diet (g w/w). The dependent variable in these models is the time of death (h). Analysis was restricted to those larvae that were sampled both at death and during live sampling.

Model/hypothesis	***k***	***AIC$_c$***	***Δ AIC$_c$***	***w***	***r^2***
2. *Time*+*Count*+*Dose*+*Protein*+*Time*:*Count*	5	823.2	0.00	0.800	0.721
Count+*Dose*+*Protein*	3	827.0	3.88	0.115	0.702
Time+*Count*+*Dose*+*Protein*	4	827.7	4.53	0.083	0.706
Time+*Count* +*Protein*+*Time*:*Count*	4	835.9	12.71	0.001	0.686
Dose+*Protein*	2	848.4	25.24	0.000	0.641
Time +*Dose*+*Protein*	3	850.5	27.32	0.000	0.641
Time+*Count*+*Dose* +*Time*:*Count*	4	855.5	32.28	0.000	0.633
Time+*Count* +*Time*:*Count*	3	858.0	34.80	0.000	0.619
Time+*Count*+Dose	3	859.6	36.43	0.000	0.614
Time+*Count*	2	861.8	38.60	0.000	0.601
Count+*Dose*	2	863.1	39.89	0.000	0.597
Count	1	866.4	43.23	0.000	0.579
Protein	1	869.9	46.76	0.000	0.567
Dose	1	967.5	144.31	0.000	0.061
Time +*Dose*	2	969.3	146.10	0.000	0.063
Intercept only	0	973.4	150.25	0.000	-
Time	1	974.0	150.84	0.000	0.011

2.4 DISCUSSION

Here, through experimental manipulation of both the calorie content and macronutrient composition of the larval diet, we have shown the central role that protein plays in determining the outcome of an insect host-pathogen interaction. In contrast to previous studies in this field (e.g. Cotter et al., 2011; Lee et al., 2006; Povey et al., 2009), most of which have focused on host survival and immune function under different dietary regimes, here we explored the effects of diet from the perspectives of both the host and the pathogen. This revealed that the *in vivo* replication rate of the bacteria declined as a linear function of the amount of protein in the larval diet, and that this was correlated to a parallel reduction in the bacteria-induced larval mortality rate, most likely because high bacterial loads precipitate larval mortality.

For all the metrics studied (survivorship, bacterial replication rate and, to a lesser extent, bacterial load at death), protein consistently emerged as the pre-eminent nutritional attribute determining the outcome of the host-pathogen interaction. In contrast, dietary carbohydrate appeared to have a negligible effect on host or pathogen fitness, usually explaining a minimal amount of variation (and, in some cases, models that included carbohydrate performed worse than models with no nutritional attributes at all). Protein also consistently out-performed the calorie content of the diet, indicating that it is the nutritional source of those calories that is the prime determinant of host and pathogen performance.

The present study is one of the few to quantify *in vivo* pathogen performance in relation to host diet (but see Frost et al., 2008; Kambara et al., 1993; Narr and Krist, 2015; Sakkas et al., 2011). It clearly demonstrates that the bacterial replication rate (as

estimated by bacterial load sampled after 16 – 20 h post-challenge) declines as a linear function of the amount of protein in the larval diet, with larvae on the lowest-protein diet (2.8g / 100g diet) harbouring bacterial loads that were on average 3.6 orders of magnitude higher than those of larvae on the highest-protein diet (52.5g / 100g diet). If the relationship between dietary protein and bacterial load is log-linear across all protein concentrations (**Figure 2.1b**), it is predicted that larvae would be virtually bacteria-free, on average, if they were fed diets exceeding 69g protein per 100g diet.

It appears that protein effects on bacterial load are manifested in at least two ways. The first is via the probability that a bacterial infection establishes post-challenge. Across all challenge doses, the prevalence of bacterial infection at sampling declined from greater than 90% on the low-protein diets to less than 50% on the highest-protein diet. In addition, a larger challenge dose was more likely to establish, especially on the low-protein diets (**Figure 2.3b**), probably because high initial bacterial numbers are better able to overcome host constitutive defences (Haine et al., 2008a). *Xenorhabdus* can destroy host haemocytes (Cho and Kim, 2004) and may inhibit nodulation (Park et al., 2003), phenoloxidase activity (da Silva et al., 2000) and antimicrobial peptides (Ji and Kim, 2004; Park et al., 2006); a larger founding population will likely allow these mechanisms to act against the host immune system more quickly and effectively.

The second mechanism by which protein influences bacterial load is via its effects on proliferation of established bacterial infections, with replication rates declining as a linear function of the protein content of the host diet and being independent of the size of the initial challenge dose (**Figure 2.3c**). This lower proliferation rate may be because the bacteria are being suppressed by a host immune system that mostly relies on

protein-dependent immune effectors (i.e. top-down regulation; Haydon et al., 2003). Previous work on this system suggests that whilst many immune effector systems are up-regulated on protein-rich diets, others appear to be either carbohydrate-dependent or relatively independent of diet (Cotter et al., 2011; Lee et al., 2006; K. P Lee et al., 2008; Ponton et al., 2011b; Povey et al., 2009, 2014). When *S. littoralis* larvae feed on high-protein diets, their haemolymph becomes rich in proteins (Cotter et al., 2011), thus another possible explanation for the lower proliferation rate on high-protein diets is that resource utilization by the bacteria is constrained in protein-rich environments (i.e. bottom-up regulation; Haydon et al., 2003). This could then be viewed a resource competition problem (Tilman, 1982). Whilst host-pathogen interactions have previously been considered within this framework theoretically (Cressler et al., 2014; Smith and Holt, 1996), empirical tests are largely lacking because of the difficulty of disentangling the independent resource requirements of hosts and their pathogens, which would require dissociating the two. Whilst we have a rudimentary understanding of the nutritional demands of the *S. littoralis* immune system (Cotter et al., 2011), we currently know little about the nutritional ecology of *X. nematophila* other than that it is capable of utilising glucose as a carbon source *in vitro* (Kooliyottil et al., 2014). Characterising the resource requirements of *X. nematophila* is a priority for future research.

Host survival was also affected by dietary protein. Specifically, protein had little impact on survivorship for larvae in the control group, but it became increasingly important as the magnitude of the challenge dose increased. On average there was a 3-fold difference in the rate at which bacteria-challenged insects died, with those on the highest-protein diet living for an average of 78 h compared to just 27 h for those on the lowest-protein

diet (**Figure 2.1a**). There was some indication that dietary carbohydrate may also play a small role in determining differential survivorship, but very little suggestion (based on evidence ratios) that other dietary attributes are important.

Bacterial loads at death were usually higher than at sampling, indicating that bacterial replication continued beyond the sampling point. However bacterial loads at death were relatively invariant and largely independent of diet (**Figure 2.4**), with the amount of protein in the larval diet explaining less than 6% of the variation in mortality. Thus it appears that dietary protein sets the *rate* at which bacteria replicate within host haemolymph, and that the insect dies when and if the bacterial density exceeds some critical threshold (at around 10^6 CFU per ml haemolymph), possibly because the concentration of bacteria-produced toxins causes lethal host tissue degradation and/or because there are simply too few resources remaining for the operation of essential host processes (Herbert and Goodrich-Blair, 2007). Across all bacterial doses, including the non-challenged controls, there was a strong log-linear relationship between bacterial load at <20h and the average speed at which insects died (**Figure 2.1c,d**). Inclusion of bacterial load at sampling in the survivorship model improved its explanatory power, with >70% of the variation in survivorship being explained by a combination of challenge dose, relative bacterial load and diet. In particular, the mortality risk associated with high bacterial replication rates was reduced on a high-protein diet, especially when larvae had been exposed to a high challenge dose (**Figure 2.5**).

The fact that larval diet explained variation in survivorship over and above that explained by bacterial load indicates that the beneficial effects of protein extend beyond

its role in limiting the bacterial proliferation rate (i.e. *resistance*; Ayres and Schneider, 2008) to also include limiting the health impacts of a given bacterial load (i.e. *tolerance*; Ayres and Schneider, 2008). This might be achieved by, for example, aiding processes such as repairing tissue damage caused by replicating bacteria. Evidence that dietary protein may improve tolerance is provided by **Figure 2.1d** (and legend), which reveals that the speed of host death is determined by the interaction between diet and bacterial load. This is manifested in the slope of the reaction norms being shallower for larvae feeding on the two highest protein diets (E and F, **Table 2.1**), indicating that, for a given bacterial load, the speed of death is slower on these diets. If data from these two treatment groups are excluded, the remaining reaction norms all have a similar slope, suggesting similar tolerances.

Fully resolving the relative importance of resistance and tolerance in this system will require a wider array of diets than we have used here. Indeed the present study has focused on just six diets representing relatively extreme P:C ratios (1:5 to 5:1) and calorie densities (326 and 1112 kJ/100g), though these do encompass the nutritional landscape likely to be experienced by lepidopteran insects in the wild (Waldbauer et al., 1984). Being a generalist feeder, *S. littoralis* has a wide host-plant range, encompassing 40 known species including strawberry, cotton, and maize (Novoselov et al., 2015). The nutritional landscape of lepidoptera such as *S. littoralis* is determined through to a mixed diet containing diverse host plants, and foliage of different ages that vary in their P:C ratio (Waldbauer et al., 1984). It is likely that additional complexity will emerge when further 'slices' through nutrient space are included (see e.g. Cotter et al., 2011), but the key role that protein appears to play in this system is striking. How general is

this finding? Our results are entirely consistent with previous work on this host species using other pathogens (Lee et al., 2006; K. P Lee et al., 2008), and other lepidopteran host-pathogen systems involving both bacteria and baculoviruses (Povey et al., 2014, 2009), most of which have documented that host survival is enhanced on protein-biased isocaloric diets. They are also consistent with the limited number of previous studies that have addressed this question in vertebrate host-pathogen systems. For example, Peck *et al.* (1992) observed that mortality in lab mice infected with *Salmonella typhimurium* decreased from 100% on protein-poor (carbohydrate-rich) diets to just 40% on protein-rich (carbohydrate-poor) diets. Although this response was observed in mice fed both normal and calorie-restricted diets, it is difficult to disentangle the relative importance of dietary protein, carbohydrate and P:C ratio in this study because there was insufficient variation in mortality generated by the two calorie levels. Our findings are also not at odds with studies that have observed a positive effect of calorie intake on parasite resistance (Anstead et al., 2001; Kristan, 2007; Moret and Schmid-Hempel, 2000), since high-calorie diets will also contain high levels of protein. Indeed, much of the human literature has focused on the exacerbating effects of 'protein-energy malnutrition' on infectious diseases, especially in children (Blössner and de Onis, 2005; Bryce et al., 2005; World Health Organization, 2004), though as far as we are aware there have been no clinical trials comparing the effects of macronutrient dietary manipulations on infectious disease mortality similar to the one presented here, for obvious ethical reasons. Thus, it is possible that the positive effects of protein on survival following infection is a widespread phenomenon, but it is only by making comparisons in different host-pathogen systems across a range of diets that span

sufficiently large regions of the organism's nutritional landscape that such generalities will emerge.

One clear and contrary example to those presented above is a recent study in which the Australian plague locust (*Chortoicetes terminifera*) was challenged with a fungal pathogen (*Metarhizium acridum*) after feeding on various isocaloric diets differing in P:C ratio (Graham et al., 2014). While immune function peaked on high-protein diets, this did not dictate the outcome of the interaction. Locusts restricted to the high P:C diets were more likely to die from infection, and it was speculated that this was because the fungus was better than its host at exploiting the protein in the locust's haemolymph, allowing enhanced fungal growth as well as protein depletion from the host's immune system. This supports previous work demonstrating the importance of protein for some aspects of immune function, but also highlights again the complexity of these interactions and the need to focus on the requirements of both parties (host and pathogen) in order to predict the outcome of the interactions in the context of possible resource competition.

In summary, this study provides initial insights into the effect of host diet on the dynamics of the host-pathogen interaction from the perspective of both the pathogen and its host. We have quantified pathogen growth under different host dietary regimes and have shown how *in vivo* pathogen growth rate varies with host diet and predicts host survivorship. We are beginning to get an appreciation of the range of diet-driven mechanisms that interact to determine the outcome of the host-pathogen interaction, including pathogen establishment and proliferation and host immune function and damage repair. Disentangling the nutrient requirements of both host and parasite, and

how they compete for these resources will inspire further research, with potential implications for animal and human health.

2.5 SUPPLEMENTARY MATERIAL

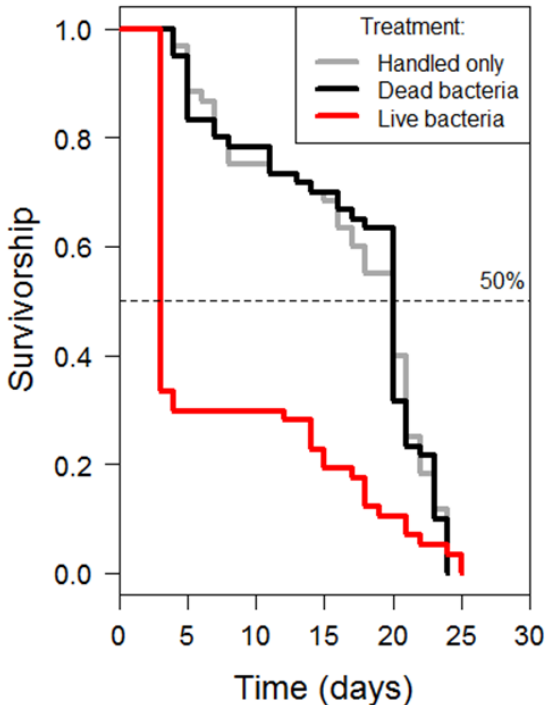

Figure S2.1: Kaplan-Meier survivorship curves of S. littoralis injected with either live bacteria or dead bacteria or not injected (handled only). Survivorship differed between the three treatment groups ($\chi^2_2 = 25.169$, $P < 0.0001$), but did not differ between the two control groups (handled only vs injected with heat-killed bacteria: b $\pm$ SE = 0.01617 $\pm$ 0.18271; z = 0.088, P = 0.929). Survivorship curves are based on 180 larvae equally divided between the three treatment groups, and reared following protocols identical to those used in the experiment reported in the main text. Larvae injected with live bacteria received 5 µl x 593 bacterial cells/ml; those injected with dead bacteria received a similar dose of autoclaved bacteria.

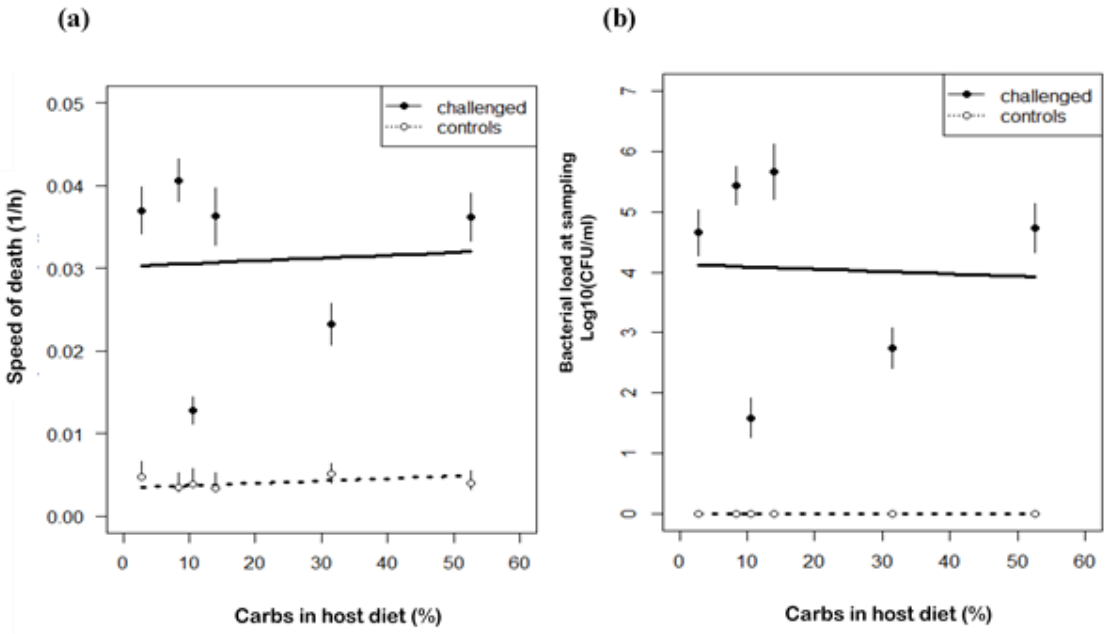

Figure S2.3: Relationships between the amount of dietary carbohydrates in the larval diet and (a) speed of death and (b) bacterial load at sampling. Means ± SE are shown for control (open symbols) and bacteria-challenged larvae (closed symbols). The lines are regression lines fitted to the raw data.

Table S2.1: Recipe for wheatgerm based semi-artificial diet. Larvae we reared on this diet from hatching till the fifth instar.

Ingredient	Quantity (g/100g)	Ingredient	Quantity (g/100g)
Wheat germ	42.41631614	Streptomycin	0.651561745
Casein	19.44081157	L-Ascorbic acid	2.606246981
Sugar	17.23162843	Nicotinic acid	0.033509322
Yeast	8.394895903	Pantothenic acid	0.033509322
Wesson's salt	5.520012254	Riboflavin	0.016754661
Sorbic acid	0.883673253	Thiamine	0.008377331
Cholesterol	0.547877417	Pyridoxine	0.008377331
P-hydroxybenzoic acid	0.547877417	Folic acid	0.008377331
Linseed oil	1.101645989	D-Biotin	0.000670186
Choline	0.547877417		

3 Diet mediates infection of *Spodoptera* caterpillars by controlling pathogen proliferation and host resilience

Acknowledgments:

Experiments were carried out by Robert Holdbrook, Catherine Reavey & Yamini Tummala. The data were analysed by Robert Holdbrook. The manuscript was written by Robert Holdbrook with input from Kenneth Wilson.

ABSTRACT

Recent nutritional immunological findings highlight the importance of protein for host immune defence. Identifying the preference of lepidopterans for diets richer in protein than other macronutrients, investigations applied the geometric framework for nutrition to uncover the influence of diet on life-history. However, restricted by the complexity of the geometric framework, research in this field remained limited to a narrow range of diets, focusing investigations on host effects.

Using *Spodoptera littoralis* caterpillars and the bacterial pathogen, *Xenorhabdus nematophila*, this study builds on findings that highlighted the equal importance of nutrient ratios and caloric densities in host-parasite interactions. By varying both nutrient ratios and concentrations in a single experiment, a direct contrast was made between the two dietary properties. Furthermore, a pathogen-focused perspective was employed to understand the bottom-up effects of nutrition influencing this system. *X. nematophila* is a haemolymph obligate parasite that depends on the nutrient pool of its hosts to proliferate. It was predicted that the growth rate of this pathogen would vary depending on the macronutrients ingested by *S. littoralis*.

Primarily, we confirmed the host's ability to modulate dietary intake after detecting infection. However, our findings show that the haemolymph nutritional content at the time of infection may be more important than diet alterations over the course of infection in influencing pathogen fitness. Aside from a confirmation of the positive protein effects on host mortality observed in previous studies, our results reveal a crucial role of carbohydrate in increasing host tolerance to infection. Based on the positive effects of carbohydrate, which simultaneously increased host tolerance and pathogen fitness, we hypothesise possible competition for this resource.

3.1 INTRODUCTION

Recent advances in ecology emphasise the integrated nature of community interactions (Weathers et al., 2016). Multidisciplinary approaches aiming to accurately depict these intricate connections focus on the drivers and processes acting across the different levels of biological systems (Lihoreau et al., 2015; Pastor, 2017). Energy fluxes are one such focal point for the study of interactions between individuals, communities and their abiotic environment (Schowalter, 2016), providing a bridge between biotic and abiotic factors (Rodríguez et al., 2018). Research is slowly revealing the central role of the microbial environment in the control of foraging behaviour (Bernardo and Singer, 2017; Simpson and Raubenheimer, 2012), directly associating microbial community composition and activity with the energetic demands of complex organisms. Attempting to increase the depth of understanding in these key focal points, the emerging field of nutritional immunology places nutrition, a key ecological driver and source of energy at the core of competitive interactions between hosts and their parasites (Ponton et al., 2013). More precisely, this field explores the role of nutrient availability in the equilibriums achieved between a host, its microbiota (Pernice et al., 2014), and pathogens (Ponton et al., 2013; Povey et al., 2014).

Parasitic colonization-extinction dynamics are determined by host physical attributes such as immunity (Ayres and Schneider, 2012; Louie et al., 2016), abiotic factors (Rynkiewicz et al., 2015; Zhang and Buckling, 2016), and interactions with host symbionts (Johnson et al., 2015; Nielsen-LeRoux et al., 2012). Pathogens feed off their hosts (Bernardo and Singer, 2017) depleting key host resources, and subsequently compelling trade-offs in life-history traits (Cotter et al., 2011; Kwang Pum Lee et al., 2008). Hosts are faced with further nutrient depletion due to the metabolic demands of mounting an immune response (Rahnamaeian et al., 2015) combined with cellular repair

of physical or chemical damage carried out by pathogen virulent factors or immune by-products (Miller and Cotter, 2017). Understanding nutritional variability in infection contexts may therefore improve the accuracy of host-pathogen dynamics models. Insects, commonly used for host-parasite modelling provide a lower cost analogue to mammalian models whilst maintaining a complex and diverse equivalent to the mammalian innate immune system (Ramarao et al., 2012). The caveat of these model systems is a host-focused perspective, with a limited view of pathogen activity; the primary driver of this being the destructive nature of pathogen sampling methods, resulting in a preference for indirect measures of pathogen activity through host fitness. *In vitro* growth assays aim to address this deficiency but remain restricted in their capture of the variability pathogens would experience *in vivo* (Aryani et al., 2015), creating uncertainty in the relationship between these findings and pathogen behaviour *in vivo*. Knowledge gaps, such as the pathogen exploitation of host nutrients (Steeb et al., 2013), must be addressed through a more directed emphasis on pathogen performance both *in vivo* and *in vitro*.

A host's resilience, or its ability to survive an infection, is a combination of vigour, tolerance and resistance (Ayres and Schneider, 2012; Louie et al., 2016). Vigour, a host's health status in the absence of infection, and resistance, the ability of a host to clear an infection, are well characterised. Tolerance, a host's reduction of fitness costs for a given parasite burden, is a relatively new concept in animal biology (Clough et al., 2016) and entomology (Miller and Cotter, 2017), although it has been studied extensively in plants (Ayres and Schneider, 2012; Louie et al., 2016). The conventional view of immunity generally focusses on resistance, since the immune system actively depletes pathogen load and provides direct measures of fitness. Although there are a plethora of immune strategies (Schmid-Hempel, 2005), it is well established that

maintaining an immune system is costly for a host, which may justify the demand for alternative strategies such as tolerance (although see Medzhitov et al., 2012). A study of laboratory mice infected by the intestinal nematode *Heligmosomoides polygyrus* found tolerance to be due to an interaction between genetic variation and diet (Clough et al., 2016). So far there is very limited research quantifying the role of nutrition in host tolerance. The complexity of measuring tolerance requires a systematic approach towards nutrition to produce interpretable results.

The geometric framework is a state-space approach towards nutrition gaining traction across multiple scientific disciplines due to its integration of nutrient ratios and caloric dietary concentrations (Raubenheimer et al., 2009; Raubenheimer and Boggs, 2009; Simpson and Raubenheimer, 2012). Investigations using this approach successfully simplify complex nutritional interactions into quantifiable stoichiometric values (Raubenheimer et al., 2009). Utilising the geometric framework, studies investigating macronutrient relationships have found hosts to alter their dietary intake to compensate for the costs of infection (Lee et al., 2006; Povey et al., 2014). For example, during choice experiments, the Egyptian cotton leafworm *Spodoptera littoralis*, alters its dietary intake from a diet rich in carbohydrates to one containing a higher proportion of protein (Lee et al., 2006).

A range of studies have attempted to explain host nutrient acquisition and allocation applying the geometric framework (Simpson and Raubenheimer, 2012). The literature investigating the complex influence of nutrition on life-history traits is dominated by research aiming to provide clarity through a focus on areas of the nutritional space, be it nutrient ratios (Graham et al., 2014; Thompson et al., 2001) or concentrations (Adamo et al., 2010; Ignell et al., 2010; Stabler et al., 2015), with fewer investigations successfully combining the two (Cotter et al., 2011; Kwang Pum Lee et al., 2008;

Solon-Biet et al., 2014). So far, the three major macronutrients, lipids (Solon-Biet et al., 2014), carbohydrates (DeGrandi-Hoffman and Chen, 2015; Graham et al., 2014; Kwang Pum Lee et al., 2008) and proteins (Graham et al., 2014) have been identified in different organisms to be essential for various life-history traits. The limited coverage of the host-nutrient space acts to further exacerbate our restricted knowledge of pathogen behaviour as a function of host nutrition, creating a knowledge gap to be filled. So far, experiments using lepidopteran hosts tend to fall into the group emphasising the importance of nutrient ratios (Lee et al., 2006; Povey et al., 2014, 2009). Most of these studies identify protein as the key limiting nutrient for immunity, irrespective of the pathogen type.

The preceding chapter attempted to build on the findings of Lee et al., (2006) by altering nutrient ratios and caloric content in the same experiment. Quantifying pathogen load also provided a measure of direct host diet effects acting on the pathogen. The desire to identify any temporal dynamics in dietary effects on the pathogen, limited the range of diets explored, due to experimental logistics. A timepoint was identified (~20 h post-infection) at which bacteria were in the exponential growth phase, but numbers were high enough for a reliable count to be made through sampling. Simultaneously, hosts were still alive, and actively expressing an immune response, whilst future mortality could be predicted by a bacterial count above a threshold value. Using this information, this chapter focuses on nutritional effects on the system, by increasing the coverage of the geometric nutritional space, through the provision of a broader range of diets.

Xenorhabdus and *Photorhabdus* are related genera of entomopathogenic gram-negative bacteria that are endosymbionts of nematode worms (Nielsen-LeRoux et al., 2012). Lacking a free-living stage maintains a dependence of the pathogens on either their

nematode hosts, or the lepidopteran caterpillars that they infect together with the nematode. This limits their nutritional sources, making them ideal for the study of parasite nutrient burdens placed on a host, as well as the nutrient requirements of pathogens *in vivo*. *In vitro* studies have found high performance of these pathogens in carbohydrate-rich environments (Bowen et al., 2012; Kooliyottil et al., 2014); however it is yet to be determined whether this remains true during infection.

Building on the work of Cotter et al., (2011), 20 diets were explored across multiple protein-to- carbohydrate (P:C) ratios and concentrations with the primary aims of quantifying pathogen fitness during infection, as well as investigating the role of dietary macronutrients in host immune investment strategies. Final instar *S. littoralis* caterpillars were infected with the entomopathogen *X. nematophila*, and parasite burden and host fitness were quantified. As with the previous chapter, bacterial load was measured by plating haemolymph samples from infected individuals onto agar, in conjunction with quantifying host fitness metrics such as larval mass. Based on previous findings, it was predicted that hosts on a higher dietary protein intake would outperform hosts restricted to carbohydrate-rich diets. It was also predicted that this P:C dependence would be stronger on energy-dense diets based on findings of Chapter 2 indicating effects of dietary nutrient ratios are stronger at higher caloric densities.

3.2 METHODS

3.2.1 Spodoptera littoralis colony maintenance

The *Spodoptera littoralis* culture was established from eggs collected near Alexandria in Egypt in 2011 and maintained using pedigree-controlled mating to minimize inbreeding. The colony has been reared to date using single pair matings for 40 generations, with around 150 pairs established each generation. Following mating of unrelated adult moths; eggs were laid within around 2 days with larvae hatching after a further 3 days. *S. littoralis* spend around 2 weeks at the larval stage and about half of this time is spent in the 5th and 6th instars, at which point maximum growth occurs. Larvae were reared from the 2nd instar on a semi-artificial wheat germ-based diet in 25 ml polypots until the final larval instar (L6), thinning the number of individuals per pot over time, to prevent overcrowding. Insects were maintained at 25°C under a 12:12 light: dark photo regime.

3.2.2 Xenorhabdus nematophila F1D3

3.2.2.1 Storage and retrieval of bacterial stocks

Green fluorescent protein labelled *Xenorhabdus nematophila* strain F1D3 were originally supplied by the laboratory of Givaudan and colleagues (Montpellier University, France; see Sicard et al., 2004). Pure *X. nematophila* F1D3 stocks were stored at -20°C in 1.5 ml Eppendorf tubes (500 µl of *X. nematophila* F1D3 in nutrient broth with 500 µl of glycerol). Vortexing ensured that all *X. nematophila* F1D3 cells were coated in glycerol. To revive the stocks for use, 100 µl was added to 10 ml nutrient broth, and incubated at 28°C for up to 48 h (generally stocks could be used after 24 h).

3.2.2.2 Bacterial quantification and colony forming unit (CFU) bioassay

On the day of experimental bacterial challenge, the stock was sub-cultured, with 1 ml of the original stock added to 10 ml of nutrient broth and placed in a shaker-incubator for approximately 4 hours. This ensured that the bacteria were in log phase prior to challenge. Following the sub-culture, a 1 ml sample was firstly checked for purity and then the concentration of bacterial cells was quantified using a fluorescence microscope. Quantification involved carrying out a serial dilution in nutrient broth and then counting the number of cells in a 10 µl sample using a haemocytometer with improved Neubauer ruling. The remaining culture was further diluted with nutrient broth to the appropriate concentration required for the bacterial challenge.

To make the NBTL agar plates described below, 25 mg/L bromothymol blue and 40 mg/L of triphenyltetrazolium chloride (TTC) were added to hot autoclaved nutrient agar (28 g/L) and the mixture was shaken vigorously. Bromothymol blue is a pH indicator and indirectly, an aerobic indicator, allowing the identification of *X. nematophila* F1D3. Acid by-products result in many bacteria producing yellow or red colonies on these plates, but *X. nematophila* F1D3 produce deep blue colonies on these plates, presumably because these bacteria do not produce acids by fermentation (Akhurst, 1980). Following the incubation period at 28°C, the CFUs were counted for each sample, and then the CFU/ml haemolymph were determined based on the dilution factor at which colonies could be reliably counted.

3.2.3 Experimental design

400 larvae were reared to the start of L6 on a semi-artificial wheat germ-based diet. Within 24 hours of moulting into L6, the larvae were divided into 20 groups (n=20) and placed onto one of twenty diets differing in dietary attributes (**Table S3.1**). Larvae from

each of 16 families used were distributed across the treatment groups. 1.8-2.1 g of the chemically defined diets were placed in 90 mm diameter Petri dishes and the larvae were housed in this manner throughout the experiment (with the diet replaced every 24 h). Within each diet, 10 caterpillars were allocated to a 'live bacteria challenged' group (henceforth live-infected), 5 caterpillars were assigned to a 'dead bacteria challenged' group (henceforth dead-infected) and 5 caterpillars were allocated to a 'sham challenged' group (henceforth sham-injected). For the live challenged caterpillars, the bacterial dose used was 1,272 F1D3 cells/ml. This dose was established from pilot experiments to determine the LD_{50} (unpublished data). The same dose (1,272 F1D3 cells/ml) was used for the heat-killed challenge, albeit the challenge would consist of cell debris as a result of autoclaving. The sham challenged caterpillars were injected with autoclaved nutrient broth (both live and dead challenges were suspended in nutrient broth).

Following 24 hours on the assigned diets, each of the 400 caterpillars was injected with the appropriate treatment; 5 µl of live *X. nematophila* (LD_{50} of 1,272 F1D3 cells/ml), 5 µl of heat-killed *X. nematophila* (LD_{50} of 1,272 F1D3 cells/ml) or 5 µl of autoclaved nutrient broth. Injections were carried out using a Hamilton Syringe in a micro-injector. The syringe was sterilized in ethanol before each injection and the challenge was applied to the left proleg nearest to the head. The caterpillars were held such that pressure was not placed on the challenged area to prevent haemolymph loss and to ensure that the bacterial challenge was entering the system. Time of injection was recorded due to the need to control for the length of time between injection of the first and last individuals (4.5 h).

Following challenge, haemolymph samples were obtained from all caterpillars at roughly 20 h post-infection. Haemolymph samples were obtained by piercing the cuticle

next to the first proleg near the head with a sterile needle and allowing released haemolymph to bleed directly into an eppendorf tube. Haemolymph samples from all the live-infected caterpillars were plated out to determine bacterial growth (n = 200). 1 of each of the 5 caterpillars for both the dead-infected and sham-injected caterpillars within each dietary treatment were plated out to ensure no bacterial contamination had occurred (n = 40). Immediately following obtaining the haemolymph, the relevant samples were diluted in pH 7.4 phosphate buffered saline (PBS; 10 µl of haemolymph placed in 90 µl of PBS and so on through the dilution series) down to 10^{-7} in intervals of 10^{-1}. The dilution series was plated onto NBTL agar plates (20 µl per 1/4 agar plate) and incubated at 28°C. Colonies were counted after 24 h and then again after 48 h. Although most of the colonies were visible at 24 h, there were some slow growing colonies that were not visible at 48 h, however by this point the fastest growing colonies had begun to merge, hence the necessity to count twice. All haemolymph samples; both the excess from those used for bacterial plating, as well as all samples from the dead and sham challenged caterpillars, were then stored at -80°C.

Larvae were weighed at the start of the experiment, prior to placement on the chemically defined diet, and were then weighed daily up to 96 hours (72 h post infection). They were also weighed immediately before haemolymph sampling. Fresh diet was provided in clean 90 mm diameter Petri dishes every 24 h up to 72 h (48 h post infection). 96 h after moulting into L6, the larvae had either pupated or were placed in semi-artificial diet polypots until death or pupation. All caterpillars were monitored for death throughout the day of sampling and every day after until pupation or death. Date of pupation and eclosion were recorded as well as date of death if occurring during the pupae or moth stage.

The amount of food eaten each day was determined by weighing the wet mass of the chemically defined diet provided each day to the caterpillars, as well as weighing uneaten control diets each day (3 control diets per diet). The unused diet and control diet were then dried to a constant mass (for approx. 72 h), allowing the consumption per larva to be estimated.

3.2.4 Statistical analysis

Statistical analysis was carried out using the R statistical software (v3.4.0; R Core Team, 2014). Aside from the initial survival analysis testing the effect of treatment on survival, which was performed using the Survival package (v2.41; Therneau, 2018), general additive models (GAM) in the mgcv package (v1.8; Wood, 2006) were used to fit Cox Proportional Hazards models to test the effects of diet and bacterial load on survival. All other analyses were carried out using GAM. Models consisted of a mixture of parametric coefficients, that were modelled using an analysis of variance and non-parametric smoothed effects, modelled through regression analysis that utilize the sum of iterative estimates to calculate a smoothing function. To aid interpretation of dietary effects, spline plots produced by the the *fields* package (v9.6; Nychka, 2016) in R were used to show complex interactions following Cotter et al., (2011).

An information theoretic approach was taken to analyse the data (Whittingham et al., 2006). This approach allows the selection of multiple candidate models accounting for how much variation each explains based on the Akaike information criterion (AIC; Burnham and Anderson, 2004). AIC analysis was carried out using the *MuMIn* package (v1.15; Bartoń, 2018). The constituent models varied, however all models contained a *Null* model, which provided a baseline measure of the variation within a variable, and a

Diet model, consisting of 20 factors. Applied to GAMs, the MuMIn package ranks models based on the degrees of freedom used to create the smoothed curve.

The full dataset was used when exploring dietary effects on the host. There was a group of individuals that died within the first 48 h of infection, which falls within the usual timeframe it takes for *X. nematophila* to kill this host, however there were no detectable CFUs on plates. This made it difficult to distinguish whether infected individuals with no CFUs had cleared infection or whether our investigation had failed to detect the presence of the pathogen. Consequently, individuals infected with live bacteria for which no CFUs could be detected (n = 61) were removed from any analysis investigating pathogen activity. Models investigating pathogen activity were also controlled for bleeding time, which varied between 18 and 31 h post-challenge. There were a number of individuals (n = 30) that survived infection but were removed from the dataset as part of the samples for which no CFU counts were obtained. After these individuals were removed, the effects of diet intake and bacterial load on survival could no longer be examined due to a low sample size (n = 9).

3.3 RESULTS

3.3.1 Host mortality

The live-infection group showed significantly higher mortality compared to the two control groups (χ^2_2 = 291.48, P < 0.001). There was 71% mortality in this treatment, compared to 2% mortality in individuals injected with heat-killed bacteria (dead-infected controls) and 5% mortality in the nutrient broth-injected group (sham-injected controls; **Figure 3.1**). No *X. nematophila* were detected in the dead-infection or sham-injected control groups (**Table S3.2a**), attributing the higher mortality in the live-infected group to pathogen activity.

Individuals died faster with increasing bacterial count at 20 h post infection (**Table 3.1**; P < 0.001, R^2 = 0.594; **Figure 3.2a**). Despite the significant effects on mortality, bacterial growth rate had a negligible effect on weight gain over the infection period (**Table 3.1**; P = 0.096, R^2 = 0.0224; **Figure 3.2b**).

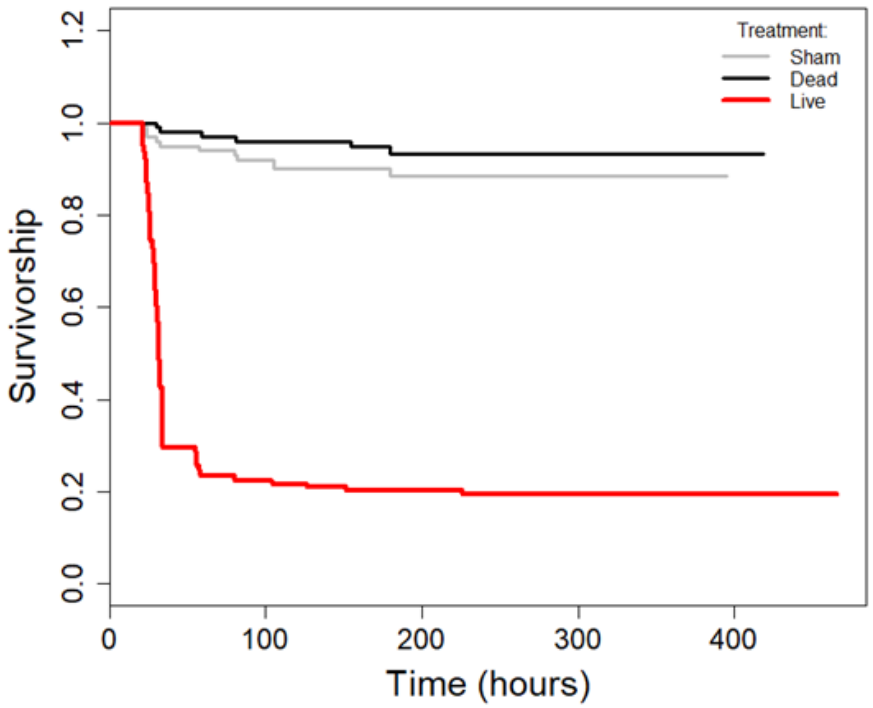

Figure 3.1: Survivorship curve and bacterial load for the treatment groups. (a) Survival plot describing larval survival across different treatments. There was a similar survival rate between the sham-injected and dead-infected treatments groups (>80%), but survival in the live-infected treatment group decreased to 20%.

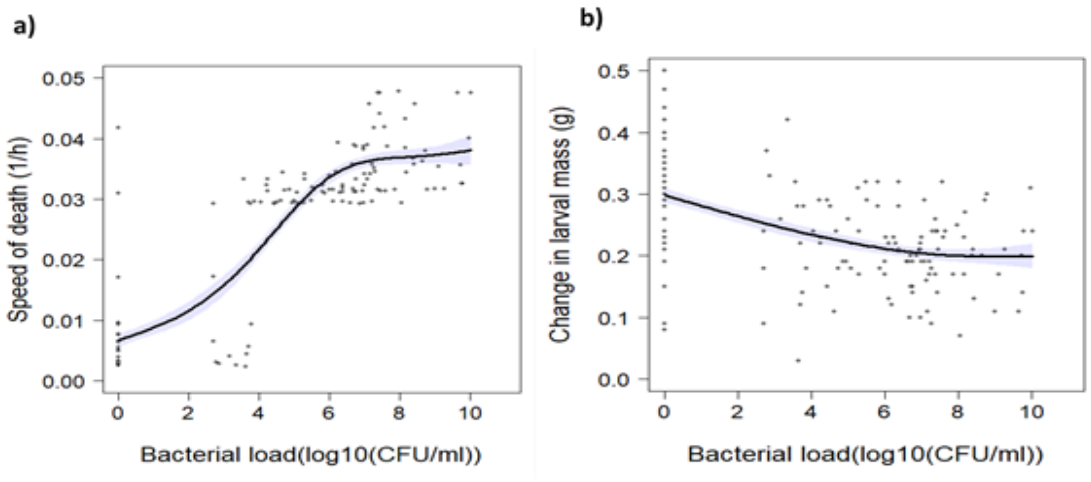

Figure 3.2: GAM model output showing the effect of bacterial load at sampling on host fitness measure. (a) Speed of death. Speed of death increased non-linearly (edf = 3.311) with increasing pathogen growth rate. (b)Change in larval mass. There was no relationship between larval weight gain and pathogen growth rate.

Table 3.1: Effect of bacterial load on host fitness measures (speed of death and change in mass). Each fitness measure was tested independently and so this the information represented in this summary table represents 3 separate models. K represents the number of terms in the model. The edf provides information about the shape of the curve, relating to the basis dimensions used by the model to fit the curve; for example, an edf close to 1 represents a linear effect, whilst an edf close to 2 represents a quadratic effect.

Term	k	edf	F-value	P-value	R^2
Speed of Death	2	3.311	37.018	<0.001	0.594
Change in larval mass	2	0.989	0.590	0.097	0.022

3.3.2 Host dietary intake

The previous section indicates a difference in host fitness (survival and speed of death) depending on whether a host is challenged with non-virulent materials (sham-injected and dead-infected control groups), or with a virulent pathogen (live-infected group). The next section investigates whether the type of challenge alters food intake behaviour in a host.

GAM models allow the combination of an analysis of variance (parametric effects), that makes a comparison between treatment groups, with smoothed effects (a regression) in a single model. This allowed the effect of food intake depending on food presented to be compared within and between the treatment groups simultaneously. The *Null* models in this case contained just the parametric effects and so compared whether there was a difference in food intake between the treatment groups. Effects of diet presented were then added in subsequent models to determine whether diet macronutrient content explained any variation on top of the variation explained by the *Null* model. There was a poor model fit for the live-infected group due to a difference in food intake between individuals that subsequently died from infection and individuals that survived infection. This was resolved by dividing this group into two sets based on the likely outcome of infection; surviving individuals and dying individuals.

Although the top model in the AIC analysis was the joint protein and carbohydrate model (m3; **Table 3.2a,b**; **Figure 3.3a,b**), the evidence ratio for this model was low (1.8) relative to the *Interaction* model (m4; ΔAIC_c = 1.180). The extra variation explained by the *Interaction* model was due to an interaction between the protein and carbohydrate intake in the uninfected controls (P = 0.035; **Table 3.2b**). The interaction was further investigated by replacing diet concentration with proportion of dietary protein as the explanatory variable. This model (**Figure 3.3c**) revealed that whilst

uninfected individuals increased ingestion with increasing proportions of dietary protein (P = 0.009; **Table 3.2c**), individuals harbouring a high bacterial load decreased food intake when presented with higher proportions of dietary protein (P = 0.002; **Table 3.2c**). Additionally, both relationships were linear (edf = 0.855 and 0.894 respectively).

Investigating the relationship between diet presented and diet eaten further, sham-injected controls ate more on the first day post-challenge than they had pre-challenge (P < 0.001; **Table 3.2b**), when presented with diet containing less than 30% protein (**Figure 3.3a**). Challenge, in the form of heat-killed or live bacteria, correlated with a change in host feeding behaviour (**Figure 3.3a; Table 3.2b**), indicating possible diet regulation in response to an immune threat. Furthermore, individuals that later died of infection, showed a significant reduction in their overall intake of food post-infection (Parametric P < 0.001; **Table 3.2a; Figure 3.3**). In contrast, infected individuals that survived infection maintained an overall food intake comparable to controls (Parametric P > 0.08; **Table 3.2a).** Unlike protein intake, which stayed consistent between dying and surviving individuals irrespective of dietary concentration, those individuals that died of infection abandoned carbohydrate regulation. For these individuals, there was a positive linear relationship (edf = 0.954; **Figure 3.3b**) between diet eaten and carbohydrate presented in the diet (P < 0.001; **Table 3.2b**). The individuals that died of infection also had a higher bacterial count at 20 h (mean: $5.3x10^8$ CFU/ml; **Table S3.2b**), than the individuals that survived infection (mean bacterial load: $2.6x10^3$ CFU/ml). As a result, there may be a relationship between bacterial load and carbohydrate intake; individuals carrying fast-growing bacteria are more likely to alter feeding in response to variation in the levels of carbohydrate in the diet (**Figure 3.3b**).

In summary, in the absence of infection (sham-injected and dead-infected controls), *S. littoralis* increases food intake slightly when presented with diets containing increasing

proportions of dietary protein. During infection, individuals harbouring a slow-growing population of bacteria (i.e. future survivors) regulate food intake irrespective of dietary protein content, whereas individuals carrying a fast-growing bacterial population (i.e. future mortalities) decrease their food intake overall, especially when their diet is relatively poor in carbohydrate.

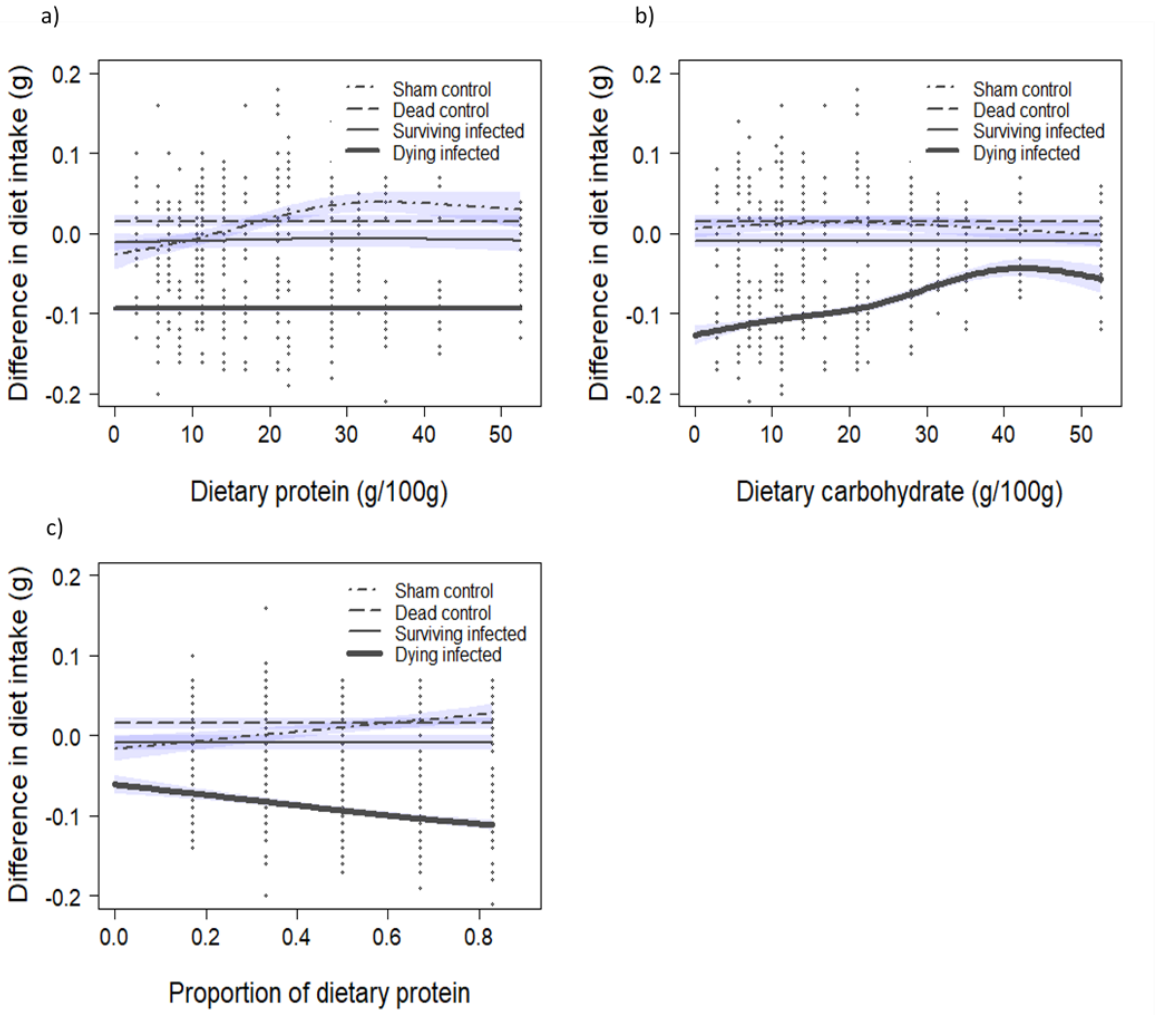
a)
b)
c)
Sham control
Dead control
Surviving infected
Dying infected
Difference in diet intake (g)
Dietary protein (g/100g)
Dietary carbohydrate (g/100g)
Proportion of dietary protein

Figure 3.3: Difference between the quantity of food eaten post-infection compared to pre-infection, depending on the dietary macronutrient content and treatment group. The live-infection group was separated into the individuals that survived infection and those that died from infection. (a) Change in dietary intake in relation to the protein content of the diet presented to larvae. Sham-injected controls increased their dietary intake over the course of the infection period in response to the concentration of protein in the diet. Dietary protein produced no effect on any other treatment group. The individuals that died later from infection ate less food post-infection than they had pre-infection. (b) Change in dietary intake in relation to the carbohydrate content of the diet presented to larvae. Aside from the group of individuals that later died from infection, dietary carbohydrate content had no effect on the difference in food intake post-infection compared to pre-infection. This group reduced their carbohydrate intake after infection, however individuals presented diets with a high concentration of carbohydrates were more likely to eat a similar amount post-infection to the amount they ate pre-infection. (c). Change in dietary intake in relation to the proportion of protein in the diet presented to larvae. Sham controls increased their dietary intake linearly with increasing proportions of dietary protein. Dead-infected and live-infected individuals that survived infection ate similar amounts of diet post-infection compared to pre-infection. Live-infected individuals that died from infection ate less post-infection compared to pre-infection. There was also a linear (edf = 0.894) decrease in the relative amount of diet eaten post-infection with increasing proportions of dietary protein.

Table 3.2: Relationship between dietary macronutrient content and the change in host diet intake in reaction to infection model summary tables. (a) AIC comparison table for models containing diet macronutrient concentration as explanatory variables. m0 (Null) is a model containing the parametric terms (treatment groups), providing a baseline measure of variation. m1 (Protein) is a model containing the concentration of protein in the diet presented to the host. m2 (Carbs) is a containing the concentration of carbohydrate in the diet presented to the host. m3 (Protein + Carbs) is a model containing both diet protein and carbohydrate content. m4 (Protein * Carbs) is a model that includes an interaction term (represented by asterisk) between diet protein and carbohydrate content. m5 (diet) is a model containing diet as a factoral variable. df is the degrees of freedom used by the model to produce a fit and not the degrees of freedom based on the number of explanatory variables. k is the number terms in the model. AICc is the model Aikake values. Delta represents the difference between a model and the model explaining the most variation. Weight is determined by the amount of variation a model explains penalized for the degrees of freedom used by the model. The parametric p-value reports the results of parametric terms in the model. Parametric effects are tested by an analysis of variance, and results indicate differences between treatments, in this case the outcome of infection depending on treatment group. (b) Summary information for each model in the AIC comparison table. The edf provides information about the shape of the curve, relating to the basis dimensions used by the model to fit the curve; for example, an edf close to 1 represents a linear effect, whilst an edf close to 2 represents a quadratic effect. (c) Independent model replacing diet protein and carbohydrate concentrations with the proportion of dietary protein as the explanatory variable in the change in diet intake by the host.

(a) Model AICs: Diet presented and change in food eaten										
Model	**df**	**k**	**AICc**	**delta**	**weight**	**R^2**	**Parametric p-values**			
							Sham (intercept)	**Dead Controls**	**Surviving Individuals**	**Dying Individuals**
m3 *Protein+Carbs*	10	2	-1128.1	0.000	0.642	0.463	0.080	0.512	0.082	<0.001
m4 *Protein*Carbs*	12	3	-1126.9	1.180	0.356	0.466	0.079	0.510	0.107	<0.001
m2 *Carbs*	7	1	-1115.8	12.320	0.001	0.442	0.086	0.520	0.088	<0.001
m1 *Protein*	7	1	-1109.4	18.670	0.000	0.432	0.089	0.523	0.091	<0.001
m0 *Null*	5	1	-1096.8	31.340	0.000	0.409	0.095	0.531	0.097	<0.001
m5 *Diet*	24	1	-1092.2	35.880	0.000	0.434	0.522	0.522	0.315	<0.001

(b) Diet presented and change in food eaten model summaries												
Model	**Sham Controls**			**Dead Controls**			**Surviving Individuals**			**Dying Individuals**		
	edf	**F-value**	**P-value**	**edf**	**F-value**	**P-value**	**edf**	**F-value**	**P-value**	**edf**	**F-value**	**P-value**
m1 *Protein*	2.037	3.968	<0.001	0.000	0.000	1.000	0.000	0.000	0.403	0.000	0.000	1.000
m2 *Carbs*	1.361	0.800	0.094	0.000	0.000	0.428	0.000	0.000	1.000	0.953	4.937	<0.001
m3 *Protein +*	2.077	4.055	<0.001	0.000	0.000	1.000	0.000	0.000	0.404	0.000	0.000	0.371
Carbs	1.023	0.415	0.193	0.000	0.000	0.416	0.000	0.000	1.000	0.954	5.138	<0.001
m4 *Protein +*	1.282	1.746	0.001	0.000	0.000	1.000	0.000	0.000	0.442	0.001	0.000	0.398
Carbs +	0.000	0.000	0.340	0.000	0.000	0.422	0.000	0.000	1.000	0.954	5.174	<0.001
*Protein * Carbs*	2.843	0.750	0.035	0.000	0.000	0.891	0.498	0.158	0.277	0.000	0.000	0.808

(c) Effect of proportion of protein in host diet on diet eaten; $R^2 = 0.430$							
Sham Controls				**Dead Controls**			
Parametric P-value	**edf**	**F-value**	**P-value**	**Parametric P-value**	**edf**	**F-value**	**P-value**
0.089	0.855	1.478	0.009	0.524	0.000	0.000	1.000
Surviving Individuals				**Dying Individuals**			
Parametric P-value	**edf**	**F-value**	**P-value**	**Parametric P-value**	**edf**	**F-value**	**P-value**
0.092	0.000	0.000	0.686	<0.001	0.894	2.104	0.002

3.3.3 Effects of host diet on host and pathogen fitness

Having established that there was a difference in food intake depending on the type of challenge, the next step is to investigate whether diet macronutrients eaten can alter host or pathogen fitness. It was important to distinguish whether diet eaten pre-infection, which determines the pathogen establishment rate, or diet eaten post-infection, which determines the pathogen proliferation rate, was a better predictor of pathogen or host success. Both diet intake metrics produced similar relationships in their explanation of host and pathogen fitness (diet eaten post-infection data not shown), and so were compared directly to determine which metric explained more variation (**Table S3a-c**). Diet intake pre-infection was chosen as the explanatory variable to investigate diet effects on pathogen growth rate, speed of host death, and host weight gain due to models containing macronutrient intake pre-infection generally explaining more variation in both the direct comparison and individual analyses.

Because the live-infected individuals were the only group carrying actively replicating bacteria, only this group was used to test the effects of diet on pathogen fitness. GAM models with mixed parametric and smoothed effects were used again to measure the effects of diet on host fitness. In this case, models compared the effect of diet intake on fitness within and between the treatment groups. The *Null* models, containing just the parametric effects, compared whether there was a difference in fitness between the treatment groups, and diet effects were added in subsequent models. As in section 3.2, the live-infected group was divided based on the outcome of infection for models evaluating the effects of diet on speed of death and change in larval mass.

3.3.3.1 Pathogen growth rate

Dietary carbohydrate availability was the key nutrient determining bacterial growth rate ($P < 0.001$; $R^2 = 0.113$; **Table 3.3**). Moreover, this increase in bacterial growth rate was linear (edf = 0.928; **Figure 3.4**) and showed no sign of plateau.

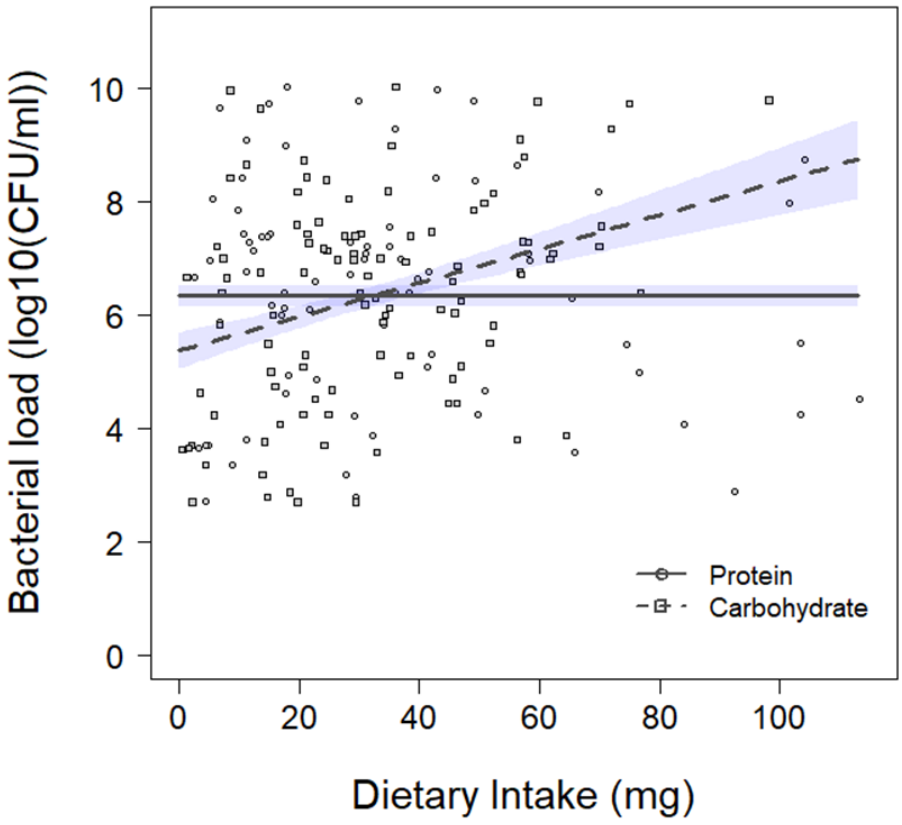

Figure 3.4: Effect of diet intake pre-infection on bacterial load at sampling. Bacterial load at sampling (~ 20 h post-infection), increased linearly (edf = 0.928) with increasing carbohydrate intake pre-infection. There was no effect on protein intake pre-infection on bacterial load at sampling.

Table 3.3: Effect of host diet intake pre-infection on bacterial load model summary tables. (a) AIC comparison table for models containing host macronutrient intake pre-infection as explanatory variables. m0 (Null) is a model with no explanatory terms included, providing a baseline measure of variation. m1 (Protein) is a model containing the amount of protein eaten by the host. m2 (Carbs) is a model containing the amount of carbohydrate eaten by the host. m3 (Protein + Carbs) is a model containing both protein and carbohydrate intake. m4 (Protein * Carbs) is a model that includes an interaction term (represented by asterisk) between protein and carbohydrate eaten. m5 (diet) is a model containing diet as a factoral variable. df is the degrees of freedom used by the model to produce a fit and not the degrees of freedom based on the number of explanatory variables. k is the number terms in the model. AICc is the model Aikake values. Delta represents the difference between a model and the model explaining the most variation. Weight is determined by the amount of variation a model explains penalized for the degrees of freedom used by the model. (b) Summary information for each model in the AIC comparison table. The edf provides information about the shape of the curve, relating to the basis dimensions used by the model to fit the curve; for example, an edf close to 1 represents a linear effect, whilst an edf close to 2 represents a quadratic effect.

(a) Model AICs: Diet and bacterial load

Model	df	k	AICc	delta	weight	R^2
m2 *Carbs*	3	4	417.1	0.00	0.332	0.113
m3 *Protein + Carbs*	3	3	417.1	0.00	0.332	0.113
m4 *Protein * Carbs*	3	2	417.1	0.00	0.332	0.113
m0 *Null*	2	1	427.9	10.76	0.002	0.000
m1 *Protein*	2	2	427.9	10.76	0.002	0.000
m5 *Diet*	20	1	431.2	14.12	0.000	0.211

(b) Diet and bacterial load model summaries

Model	edf	F-value	P-value
m1			
Protein	0.000	0.000	0.461
m2			
Carbs	0.928	3.237	<0.001
m3			
Protein +	0.000	0.000	0.573
Carbs	0.928	3.237	<0.001
m4			
Protein +	0.000	0.000	0.512
Carbs +	0.928	3.237	<0.001
*Protein * Carbs*	0.000	0.000	0.508

3.3.3.2 Speed of death

The identity of the diet eaten explained little variation in the speed of host death (**Table 3.4**) once the *Null* model ($R^2 = 0.775$), including infection outcome, was accounted for (top model $R^2 = 0.025$). Those that overcame the infection had a similar ($P = 0.1$; **Table 3.4b**) speed of death to the controls (< 0.01 h^{-1}; **Figure 3.5b,c**), whilst those that died from infection died at a significantly ($P < 0.001$; **Table 3.4b**) faster speed (0.03 - 0.04 h^{-1}; **Figure 3.5a,b**). In this group, speed of death increased with increasing carbohydrate intake and reduced with increasing protein intake. Oddly, the *Interaction* model (top model; **Table 3.4a**) produced a different result from the other models; models 1 and 3 showed a significant protein effect in reducing the speed of death of individuals with a high bacterial load ($P < 0.001$; **Table 3.4b**), whilst model 4 attributed this protein effect to an interaction with carbohydrate intake (protein $P = 0.285$; protein * carbs $P < 0.001$). Although the evidence ratio for the top model was high (38.92), models 3 and 4 explained a similar amount of variation ($R^2 = 0.800$ and 0.806 respectively). Consistent with pathogen nutrient requirements (Section 3.3.1), a higher carbohydrate intake corresponded with an increased speed of death ($P < 0.001$ in all models). This was, however, a quadratic effect (edf > 2.075; **Table 3.4b**) and so above 40mg ingested carbohydrate, speed of death plateaued. In other words, speed of death increased when hosts ate a low amount of carbohydrate but was unaffected once hosts ate in excess of 40 mg of carbohydrate.

Overall, these results show that hosts with a high pathogen burden could slow down their speed of death by eating more protein, whilst eating more carbohydrate increased their speed of death.

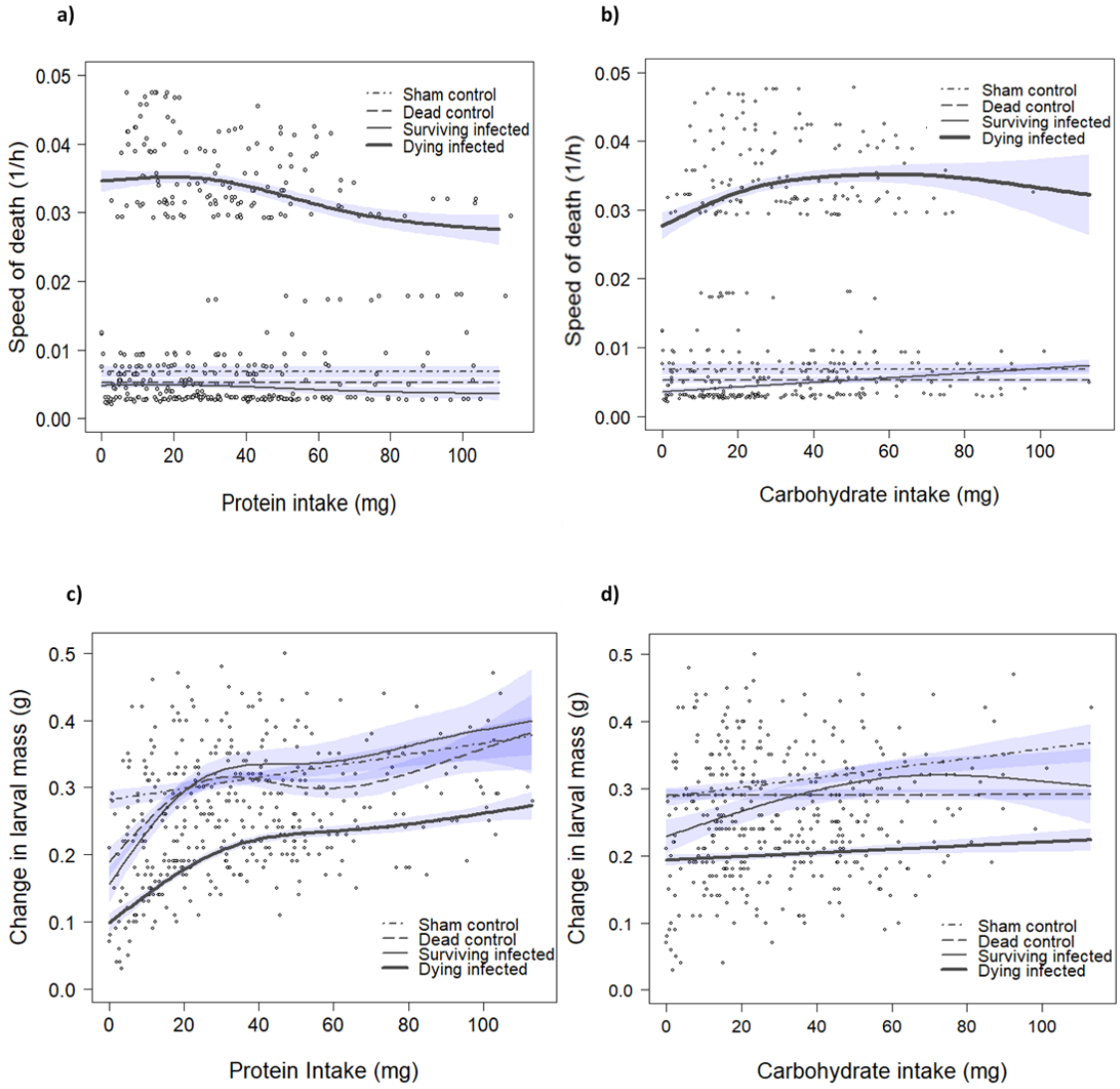
a)
b)
c)
d)
Speed of death (1/h)
Protein intake (mg)
Carbohydrate intake (mg)
Change in larval mass (g)
Protein Intake (mg)
Carbohydrate intake (mg)
Sham control
Dead control
Surviving infected
Dying infected

Figure 3.5: Effect of diet pre-infection on host fitness measures. (a) Speed of death depending on protein intake pre-infection for different treatment groups. Speed of death was higher for individuals that died from infection than those that survived infection. This latter group had a similar speed of death to controls (sham-injected or dead-infected). Protein intake had no significant effect on speed of death of control individuals and the group that survived infection. Individuals that died from infection died slower with increasing protein intake pre-infection. (b) Speed of death depending on carbohydrate intake pre-infection for different treatment groups. Speed of death was higher for individuals that died from infection than those that survived infection. This latter group had a similar speed of death to controls (sham-injected or dead-infected). Carbohydrate intake had no significant effect on speed of death of control individuals and the group that survived infection. Individuals that died from infection died faster with increasing carbohydrate intake pre-infection. (c) Change in larval mass depending on protein intake pre-infection for different treatment groups. Larval mass increased with increasing protein intake pre-infection across all treatment groups. However, individuals that later died from infection had a significantly lower weight gain than all other individuals. (d) Change in larval mass depending on carbohydrate intake pre-infection for different treatment groups. Sham-injected and live-infected individuals that survived infection had a higher weight gain with higher carbohydrate intake pre-infection. There was no significant effect of carbohydrate intake pre-infection on the weight gain in dead-injected controls or individuals that died from infection.

Table 3.4: Effect of diet intake pre-infection on the speed of host death model summary tables. (a) AIC comparison table for models containing host macronutrient intake pre-infection as explanatory variables. m0 (Null) is a model containing the parametric terms (treatment groups), providing a baseline measure of variation. m1 (Protein) is a model containing the amount of protein eaten by the host. m2 (Carbs) is a model containing the amount of carbohydrate eaten by the host. m3 (Protein + Carbs) is a model containing both protein and carbohydrate intake. m4 (Protein * Carbs) is a model that includes an interaction term (represented by asterisk) between protein and carbohydrate eaten. m5 (diet) is a model containing diet as a factoral variable. df is the degrees of freedom used by the model to produce a fit and not the degrees of freedom based on the number of explanatory variables. k is the number terms in the model. AICc is the model Aikake values. Delta represents the difference between a model and the model explaining the most variation. Weight is determined by the amount of variation a model explains penalized for the degrees of freedom used by the model. The parametric p-value reports the results of parametric terms in the model. Parametric effects are tested by an analysis of variance, and results indicate differences between treatments, in this case the outcome of infection depending on treatment group. (b) Summary information for each model in the AIC comparison table. The edf provides information about the shape of the curve, relating to the basis dimensions used by the model to fit the curve; for example, an edf close to 1 represents a linear effect, whilst an edf close to 2 represents a quadratic effect.

(a) Model AICs: Diet and speed of host death

Model	df	k	AICc	delta	weight	R^2	Parametric p-values			
							Sham (intercept)	Dead Controls	Surviving Individuals	Dying Individuals
m4 *Protein * Carbs*	14	3	-2849.9	0.00	0.973	0.806	<0.001	0.114	0.091	<0.001
m3 *Protein + Carbs*	9	2	-2842.6	7.30	0.025	0.800	<0.001	0.120	0.096	<0.001
m5 *Diet*	24	1	-2837.2	12.71	0.002	0.805	<0.001	0.115	0.061	<0.001
m1 *Protein*	7	1	-2821.4	28.50	0.000	0.787	<0.001	0.131	0.107	<0.001
m2 *Carbs*	8	1	-2817.6	32.28	0.000	0.786	<0.001	0.132	0.108	<0.001
m0 *Null*	5	1	-2802.6	47.33	0.000	0.775	<0.001	0.142	0.116	<0.001

(b) Diet and speed of host death model summaries

Model	Sham Controls			Dead Controls			Surviving Individuals			Dying Individuals		
	edf	F-value	P-value	edf	F-value	P-value	edf	F-value	P-value	edf	F-value	P-value
m1 *Protein*	0.001	0.000	0.588	0.000	0.000	1.000	0.000	0.000	0.755	1.918	5.450	<0.001
m2 *Carbs*	0.001	0.000	0.428	0.000	0.000	0.674	0.002	0.001	0.358	2.729	4.832	<0.001
m3 *Protein +*	0.000	0.000	0.594	0.000	0.000	1.000	0.000	0.000	0.786	0.963	6.160	<0.001
Carbs	0.001	0.000	0.413	0.000	0.000	0.677	0.002	0.000	0.338	3.185	6.797	<0.001
m4 *Protein +*	0.000	0.000	0.576	0.000	0.000	1.000	0.000	0.000	0.767	0.002	0.000	0.285
Carbs +	0.000	0.000	0.383	0.000	0.000	0.654	0.006	0.001	0.318	2.075	3.456	<0.001
*Protein * Carbs*	0.000	0.000	0.509	0.000	0.000	1.000	0.000	0.000	0.840	5.697	5.118	<0.001

3.3.3.3 Change in host mass

Individuals that fail to decrease their food intake in response to infection are more likely to survive (Section 3.2). The positive correlation between food intake and mass indicates heavier individuals may have a higher survival rate due to greater resource availability. Consistent with this hypothesis, hosts that showed the greatest increase in mass despite infection also showed a significantly lower bacterial load ($P < 0.001$; **Table S3.4; Figure S3.1**).

Diet explained a much larger amount of variation in change in larval mass (22%) than it had in speed of death (Section 3.3.2 - 3%) once the infection dynamics had been accounted for. Similar to the speed of host death, the top model was the *Interaction* model (evidence ratio: 2.5), although the variation in this model was driven by an interaction in the sham-injected control group rather than diseased individuals (**Table 3.5**). There appeared to be a marginally significant difference in the change in mass between the individuals that were injected with dead bacteria and the sham-injected controls, but the effect was inconsistent in the various models (**Table 3.5b**). Similarly, a significant difference between individuals that survived infection and the sham controls in the *Null* model ($P = 0.019$; **Table 3.5a**), disappeared once dietary terms were introduced. There was a more notable difference between the individuals with a high parasite burden and the other 3 groups ($P < 0.001$; **Table 3.5a**). In other words, there was a less notable difference between the treatment groups when analysing change in larval mass than had been observed for host survival and host speed of death. Only the group that succumbed to infection gained significantly lower change in mass during the infection period (**Figure 3.5c,d**).

The relationship between diet and larval mass was driven by protein intake, with the top 3 models (models 4, 3 and 1) all showing a significant effect of protein intake but not

carbohydrate. In the top model (*Interaction* model), larval mass increased linearly (edf = 0.923, P < 0.001; **Table 3.5b**) with carbohydrate intake for the sham controls, and there was also a significant interaction between protein and carbohydrate intake (P = 0.022) in this group. Another difference between the sham treatment and the (live and dead) bacterial treatment groups was the linear increase in protein intake (edf = 0.828) in this group, in contrast to the quadratic increase in mass with increasing protein intake (edf > 2.00; **Table 3.5b**) seen in the other treatments. Individuals infected with live and dead bacteria showed a greater increase in mass upon a protein intake of less than 30 mg in 24 hours, after which point there was a slower increase (**Figure 3.5c**). Altogether it appears that irrespective of treatment, larval mass increased primarily due to protein intake.

To summarise the effects of host macronutrient intake on host and pathogen fitness, bacterial growth rate was higher in individuals that had eaten more carbohydrate pre-infection. Individuals that had eaten more carbohydrate before challenge also died faster, whilst individuals that had eaten more protein died slower. Finally, there was a strong positive correlation between protein intake pre-infection and larval weight gain.

Table 3.5: Effect of diet intake pre-infection on the change in host mass over the course of the experiment model summary tables. (a) AIC comparison table for models containing host macronutrient intake pre-infection as explanatory variables. m0 (Null) is a model containing the parametric terms (treatment groups), providing a baseline measure of variation. m1 (Protein) is a model containing the amount of protein eaten by the host. m2 (Carbs) is a model containing the amount of carbohydrate eaten by the host. m3 (Protein + Carbs) is a model containing both protein and carbohydrate intake. m4 (Protein * Carbs) is a model that includes an interaction term (represented by asterisk) between protein and carbohydrate eaten. m5 (diet) is a model containing diet as a factoral variable. df is the degrees of freedom used by the model to produce a fit and not the degrees of freedom based on the number of explanatory variables. k is the number terms in the model. AICc is the model Aikake values. Delta represents the difference between a model and the model explaining the most variation. Weight is determined by the amount of variation a model explains penalized for the degrees of freedom used by the model. The parametric p-value reports the results of parametric terms in the model. Parametric effects are tested by an analysis of variance, and results indicate differences between treatments, in this case the outcome of infection depending on treatment group. (b) Summary information for each model in the AIC comparison table. The edf provides information about the shape of the curve, relating to the basis dimensions used by the model to fit the curve; for example, an edf close to 1 represents a linear effect, whilst an edf close to 2 represents a quadratic effect.

(a) Model AICs: Diet and change in larval mass										
Model	**df**	**k**	**AICc**	**delta**	**weight**	**R^2**	**Parametric p-values**			
							Sham (intercept)	**Dead Controls**	**Surviving Individuals**	**Dying Individuals**
m4 *Protein * Carbs*	23	3	-1014.6	0.00	0.705	0.486	<0.001	0.035	0.459	<0.001
m3 *Protein + Carbs*	19	2	-1012.8	1.81	0.286	0.477	<0.001	0.030	0.431	<0.001
m1 *Protein*	17	1	-1005.9	8.68	0.009	0.464	<0.001	0.041	0.491	<0.001
m5 *Diet*	23	1	-907.5	107.11	0.000	0.323	<0.001	0.131	0.107	<0.001
m2 *Carbs*	8	1	-905.9	108.73	0.000	0.292	<0.001	0.076	0.056	<0.001
m0 *Null*	5	1	-893.3	121.26	0.000	0.260	<0.001	0.090	0.019	<0.001

(b) Diet and change in larval mass model summaries												
Model	**Sham Controls**			**Dead Controls**			**Surviving Individuals**			**Dying Individuals**		
	edf	**F-value**	**P-value**	**edf**	**F-value**	**P-value**	**edf**	**F-value**	**P-value**	**edf**	**F-value**	**P-value**
m1 *Protein*	2.151	3.490	<0.001	3.265	8.071	<0.001	2.936	11.038	<0.001	2.617	15.024	<0.001
m2 *Carbs*	0.860	1.531	0.008	0.003	0.001	0.326	1.716	2.659	0.002	0.485	0.236	0.164
m3 *Protein +*	0.923	2.971	<0.001	3.282	8.304	<0.001	2.810	9.704	<0.001	2.501	15.310	<0.001
Carbs	1.541	2.813	<0.001	0.000	0.000	0.905	0.717	0.338	0.146	0.656	0.477	0.087
m4 *Protein+*	0.828	1.205	0.003	3.294	8.476	<0.001	2.827	9.891	<0.001	2.517	15.607	<0.001
Carbs +	0.923	3.011	<0.001	0.000	0.000	0.999	0.723	0.343	0.144	0.661	0.487	0.085
*Protein * Carbs*	3.131	0.936	0.022	0.000	0.000	0.994	0.000	0.000	0.263	0.000	0.000	0.771

3.3.4 Tolerance at a dietary level

Inverse pathogen load is a measure of a host's ability to resist infection which is one of two physiological mechanisms involved in host resilience, the ability of a host to survive infection (Ayres and Schneider, 2012). We can assume that any variation within our dataset that can be explained by diet, above the variation explained by resistance, indicates the use of diet by the host to tolerate infection. Disease tolerance, the other physiological mechanism involved in resilience, measures the change in health/fitness for a given pathogen load. The more traits used to describe tolerance the better of an understanding that can be created (Louie et al., 2016). We chose to represent tolerance with the fitness measures explored so far; speed of death and change in mass. Individuals were aggregated by diet to produce a mean health status and pathogen load for each of the 20 diets; this allowed the investigation of the general relationship between resistance and tolerance across experimental diets. Although the effects of bacterial growth rate and diet on survival could not be investigated at an individual level, it was possible to investigate tolerance due to the use of aggregated data. All models, including the *Null* model contained resistance (inverse bacterial load) to provide a baseline measure of variation against which dietary effects could be compared.

There was a significant positive correlation between survival and resistance (**Figure 3.6a**). Diet plays a notable role in host tolerance (as measured by survival) since the top models explained more than 25% of the variation unaccounted for by host resistance (bacterial load) alone (*Null* model; $R^2 = 0.644$; **Table 3.6a**). Furthermore, host resilience was also increased by dietary carbohydrate intake ($P < 0.001$; **Table 3.6b**; **Figure 3.6d**) and the top model also indicated an interaction between dietary protein

and dietary carbohydrate (m4; P = 0.01; **Table 3.6b; Figure 3.6e**). Supporting this, the second-best model was the carbohydrate model, although this explained 3% less variation than the *Interaction* model; the evidence ratio for these models was 4.6, indicating that most of the variation in the *Interaction* model could be attributed to dietary carbohydrate. Diet nutrient ratio and the concentration of the diet ingested explained some variation, but the evidence ratio for these models compared to the top model (*Interaction* model) was 405.5, meaning they explained much less variation within the dataset. Protein intake explained a negligible amount of variation and was worse than the *Null* model.

Due to the positive correlation between bacterial growth rate and host speed of death (**Figure 3.2a; Table 3.1**), the *Null* model, which includes resistance (inverse bacterial load), explained a large amount of variation in speed of death (R^2 = 0.742; **Table 3.7a**). Having accounted for this, speed of death was significantly faster for individuals maintained on diets containing a higher proportion of protein (m6; P = 0.015; **Table 3.7c; Figure 3.7a-c**). This supports the findings in section 3.2 examining the host dietary intake, however the evidence ratio for this effect was low compared to the *Null* model (1.4), attributing most of the variation to resistance.

Consistent with the findings in section 3.1, bacterial load was unable to explain any variation in host mass, however, host mass significantly increased when an individual was kept on diets containing a higher proportion of protein (R^2 = 0.608; **Table 3.8a**; **Figure 3.8a-c**). This model explained 61% of the variation within this dataset, 10% more than the variation explained by the second-best model (*Diet* model; evidence ratio: 1.8).

In summary, there appears to be an effect of diet in increasing host resilience above the effects explainable by host resistance alone. Whilst the effect was primarily due to carbohydrate intake when tolerance was measured through host survival, it was due to protein intake when tolerance was measured through change in larval mass. There appeared to be a decrease in tolerance (as measured by speed of host death) with an increasing proportion of dietary protein. Altogether, the results don't produce a consistent pattern and so further investigation is necessary.

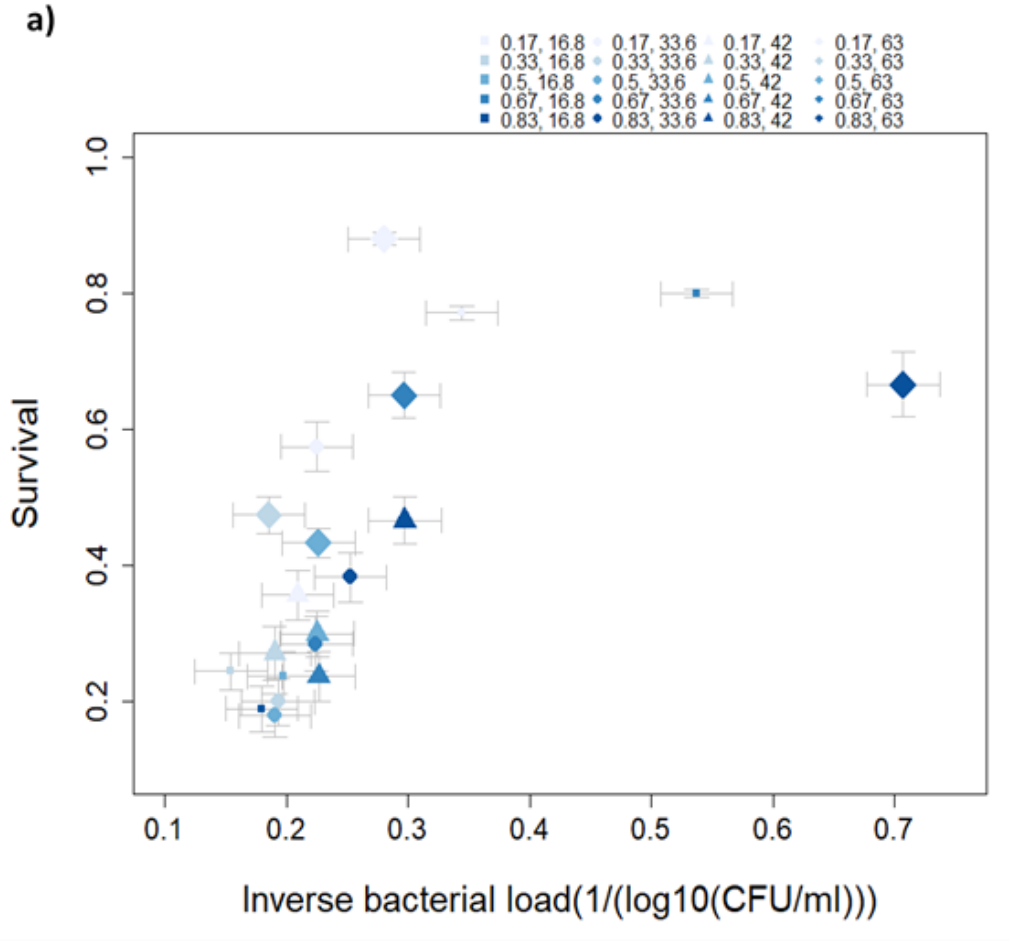
a)
0.17, 16.8
0.17, 33.6
0.17, 42
0.17, 63
0.33, 16.8
0.33, 33.6
0.33, 42
0.33, 63
0.5, 16.8
0.5, 33.6
0.5, 42
0.5, 63
0.67, 16.8
0.67, 33.6
0.67, 42
0.67, 63
0.83, 16.8
0.83, 33.6
0.83, 42
0.83, 63
Survival
0.2
0.4
0.6
0.8
1.0
0.1
0.2
0.3
0.4
0.5
0.6
0.7
Inverse bacterial load(1/(log10(CFU/ml)))

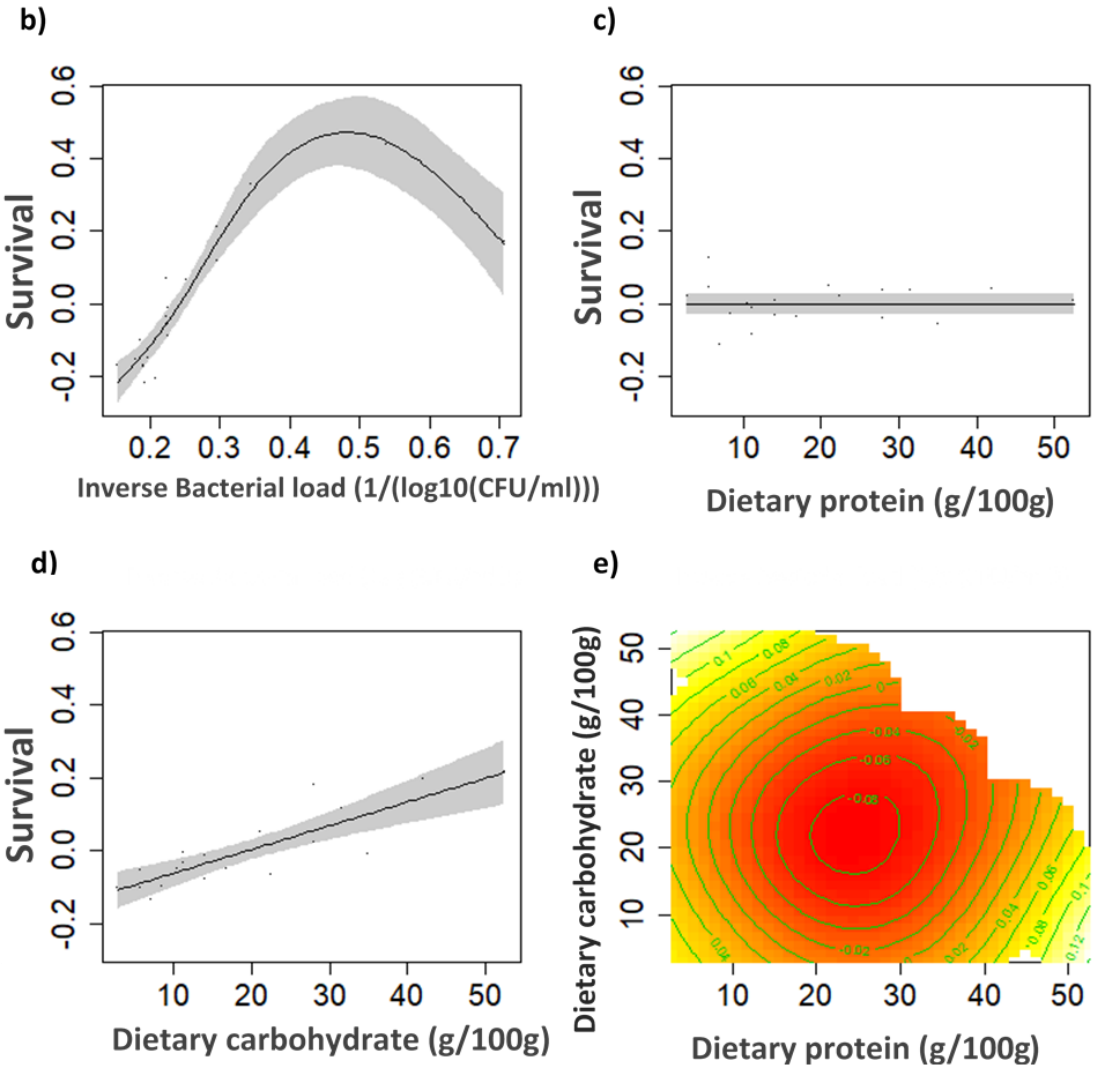
b)
Survival
-0.2
0.0
0.2
0.4
0.6
0.2
0.3
0.4
0.5
0.6
0.7
Inverse Bacterial load (1/(log10(CFU/ml)))
c)
Survival
-0.2
0.0
0.2
0.4
0.6
10
20
30
40
50
Dietary protein (g/100g)
d)
Survival
-0.2
0.0
0.2
0.4
0.6
10
20
30
40
50
Dietary carbohydrate (g/100g)
e)
Dietary carbohydrate (g/100g)
10
20
30
40
50
10
20
30
40
50
Dietary protein (g/100g)

Figure 3.6: Mean survival and inverse bacterial load across the 20 experimental diets. Inverse bacterial load is a measure of resistance, an animal's ability to clear an infection. An increase in a fitness trait (e.g. survival) for a given pathogen load is a measure of an animal's ability to tolerate infection. (a) Plot showing distribution of diets depending on survival and mean inverse pathogen load. The depth of symbol colour and symbol size represent the proportion of protein in the diet; diets with higher proportions of protein are coloured a deeper shade of blue and are bigger. Symbol shape represents diet concentration. The vertical dispersion of the symbols indicates a difference in tolerance at high pathogen loads (low resistance levels) in relation to diet. (b-e) GAM model output for the top model testing for variation in survival explained by diet above the variation explained by resistance alone. (b) Model shows that survival increases with increasing resistance. (c) Protein is unable to explain any variation above this effect. (d) Survival increases with increasing dietary carbohydrate concentration. (e) There is also an interaction between dietary protein and carbohydrate in explaining further variation above the variation explained by resistance alone.

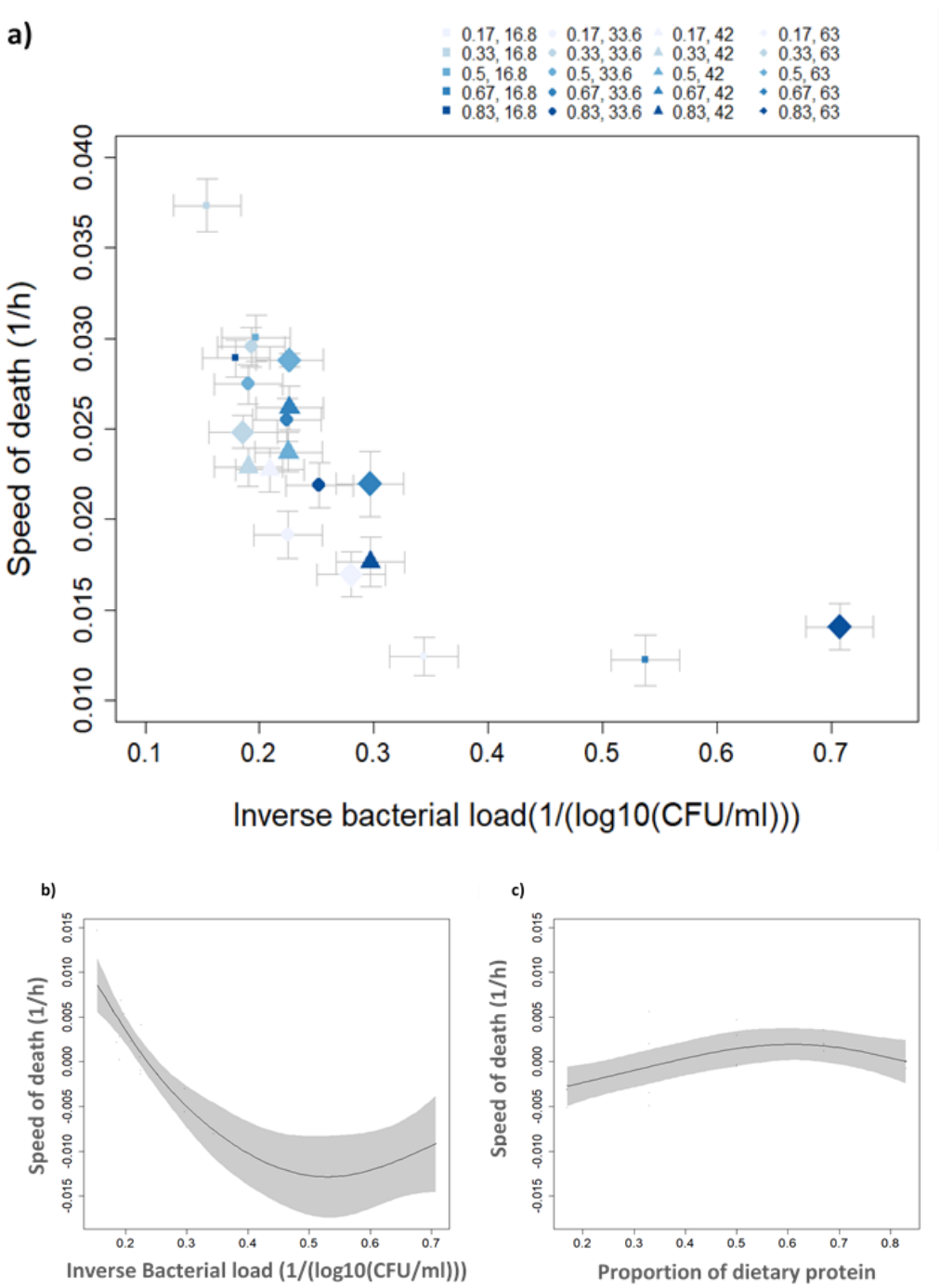
a)
0.17, 16.8
0.17, 33.6
0.17, 42
0.17, 63
0.33, 16.8
0.33, 33.6
0.33, 42
0.33, 63
0.5, 16.8
0.5, 33.6
0.5, 42
0.5, 63
0.67, 16.8
0.67, 33.6
0.67, 42
0.67, 63
0.83, 16.8
0.83, 33.6
0.83, 42
0.83, 63
Speed of death (1/h)
0.010
0.015
0.020
0.025
0.030
0.035
0.040
0.1
0.2
0.3
0.4
0.5
0.6
0.7
Inverse bacterial load(1/(log10(CFU/ml)))
b)
Speed of death (1/h)
Inverse Bacterial load (1/(log10(CFU/ml)))
c)
Speed of death (1/h)
Proportion of dietary protein

Figure 3.7: Mean speed of death and inverse bacterial load across the 20 experimental diets. Inverse bacterial load is a measure of resistance, an animal's ability to clear an infection. An increase in a fitness trait (e.g. speed of death) for a given pathogen load is a measure of an animal's ability to tolerate infection. (a) Plot showing distribution of diets depending on mean speed of death and mean inverse pathogen load. The depth of symbol colour and symbol size represent the proportion of protein in the diet; diets with higher proportions of protein are coloured a deeper shade of blue and are bigger. Symbol shape represents diet concentration. The vertical dispersion of the symbols indicates a difference in tolerance at high pathogen loads (low resistance levels) in relation to diet. (b-c) GAM model output for the top model testing for variation in speed of death explained by diet above the variation explained by resistance alone. (b) Model shows that speed of death decreases with increasing resistance. (c) Speed of death also increases with an increasing proportion of dietary protein, once variation explained by resistance is accounted for.

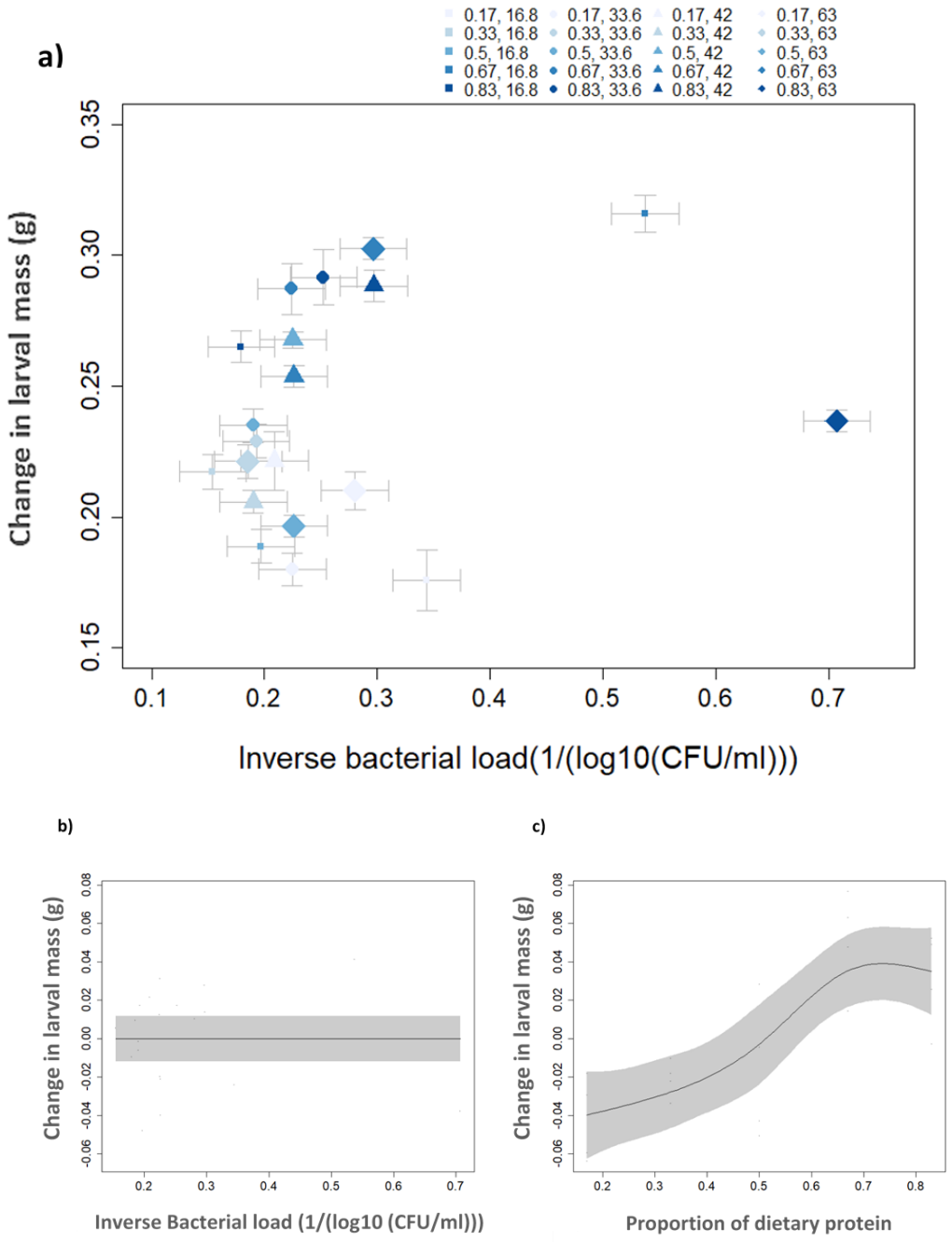
a)
0.17, 16.8
0.17, 33.6
0.17, 42
0.17, 63
0.33, 16.8
0.33, 33.6
0.33, 42
0.33, 63
0.5, 16.8
0.5, 33.6
0.5, 42
0.5, 63
0.67, 16.8
0.67, 33.6
0.67, 42
0.67, 63
0.83, 16.8
0.83, 33.6
0.83, 42
0.83, 63
Change in larval mass (g)
0.15
0.20
0.25
0.30
0.35
0.1
0.2
0.3
0.4
0.5
0.6
0.7
Inverse bacterial load(1/(log10(CFU/ml)))
b)
Change in larval mass (g)
-0.06
-0.04
-0.02
0.00
0.02
0.04
0.06
0.08
0.2
0.3
0.4
0.5
0.6
0.7
Inverse Bacterial load (1/(log10 (CFU/ml)))
c)
Change in larval mass (g)
-0.06
-0.04
-0.02
0.00
0.02
0.04
0.06
0.08
0.2
0.3
0.4
0.5
0.6
0.7
0.8
Proportion of dietary protein

Figure 3.8: Mean change in larval mass and inverse bacterial load across the 20 experimental diets. Inverse bacterial load is a measure of resistance, an animal's ability to clear an infection. An increase in a fitness trait (e.g. change in mass) for a given pathogen load is a measure of an animal's ability to tolerate infection. (a) Plot showing distribution of diets depending on mean change in mass and mean inverse pathogen load. The depth of symbol colour and symbol size represent the proportion of protein in the diet; diets with higher proportions of protein are coloured a deeper shade of blue and are bigger. Symbol shape represents diet concentration. The vertical dispersion of the symbols indicates a difference in tolerance at high pathogen loads (low resistance levels) in relation to diet. (b-c) GAM model output for the top model testing for variation in change in mass explained by diet above the variation explained by resistance alone. (b) Model shows that resistance has no effect on the change in larval mass. (c) Change in mass is higher with increasing proportions of dietary protein.

Table 3.6: Diet-level tolerance models exploring the amount of variation in survival explained by diet above the variation explained by host resistance alone. Data were aggregated by diet to create a dataset of 20 variables containing the mean survival and mean resistance for each diet. Resistance, the ability of a host to clear an infection is measured by inverse bacterial load. (a) AIC model comparison. m0 (Null) is a model containing resistance (1/log10(CFU/ml))), providing a measure of baseline variation. m1 (Protein) is a model containing the concentration of protein in the diet presented to the host. m2 (Carbs) is a model containing the concentration of carbohydrate in the diet presented to the host. m3 (Protein + Carbs) is a model containing both diet protein and carbohydrate concentrations. m4 (Protein * Carbs) is a model that includes an interaction term (represented by asterisk) between diet protein and carbohydrate concentration. m5 (Conc) is a model containing the concentration of macronutrients in the host diet. m6 (Ratio) is a model containing the ratio of protein to carbohydrate in the host diet. m7 (Conc + Ratio) is a model containing both the concentration of dietary macronutrients and the ratio of protein to carbohydrate in the diet presented to the host. m8 (Conc * Ratio) is a model that includes an interaction between diet macronutrient concentration and the ratio of dietary protein. m9 (diet) is a model containing resistance and diet as a factoral variable. df is the degrees of freedom used by the model to produce a fit and not the degrees of freedom based on the number of explanatory variables. k is the number terms in the model. AICc is the model Aikake values. Delta represents the difference between a model and the model explaining the most variation. Weight is determined by the amount of variation a model explains penalized for the df. (b-c) Summary information for each model in the AIC comparison table. The edf provides information about the shape of the curve, relating to the basis dimensions used by the model to fit the curve; for example, an edf close to 1 represents a linear effect, whilst an edf close to 2 represents a quadratic effect.

(a) Model AICs: Mean survival and resistance						
Model	**df**	**k**	**AICc**	**delta**	**weight**	**R^2**
m4 *Protein * Carbs*	7	4	-34.7	0.00	0.810	0.922
m2 *Carbs*	6	2	-31.6	3.06	0.175	0.894
m3 *Protein + Carbs*	9	3	-24.6	10.07	0.005	0.914
m7 *Conc + Ratio*	10	3	-24.3	10.41	0.004	0.940
m9 *Diet*	6	1	-23.3	11.32	0.003	0.817
m8 *Conc * Ratio*	10	4	-22.6	12.09	0.002	0.943
m6 *Ratio*	6	2	-19.8	14.86	0.000	0.798
m5 *Conc*	6	2	-17.0	17.72	0.000	0.767
m0 *Null*	4	1	-14.3	20.33	0.000	0.644
m1 *Protein*	5	2	-12.5	22.13	0.000	0.666

(b) Mean survival and resistance model summaries

Model	edf	F-value	P-value
m0			
Null (Resistance)	2.305	8.579	<0.001
m1			
Resistance +	2.349	8.608	<0.001
Protein	0.602	0.240	0.194
m2			
Resistance +	2.661	33.711	<0.001
Carbs	1.611	9.389	<0.001
m3			
Resistance +	2.456	27.955	<0.001
Protein +	1.614	1.111	0.078
Carbs	1.981	11.014	<0.001
m4			
Resistance +	2.500	30.934	<0.001
Protein +	0.000	0.000	0.548
Carbs +	0.963	6.563	<0.001
*Protein * Carbs*	1.716	5.025	0.012

(c) Mean survival and resistance model summaries

Model	edf	F-value	P-value
m5			
Resistance +	2.212	10.445	<0.001
Conc	1.714	3.182	0.013
m6			
Resistance +	2.633	17.013	<0.001
Ratio	1.166	3.131	0.002
m7			
Resistance +	2.499	31.364	<0.001
Conc +	2.285	13.421	<0.001
Ratio	2.298	10.204	<0.001
m8			
Resistance +	2.514	33.144	<0.001
Conc +	0.954	6.841	<0.001
Ratio +	2.316	10.746	<0.001
*Conc * Ratio*	1.639	9.381	0.001
m9			
Resistance + Diet	2.696	20.377	<0.001

Table 3.7: Diet-level tolerance models exploring the amount of variation in speed of host death explained by diet above the variation explained by host resistance alone. Data were aggregated by diet to create a dataset of 20 variables containing the mean speed of death and mean resistance for each diet. Resistance, the ability of a host to clear an infection is measured by inverse bacterial load. (a) AIC model comparison. m0 (Null) is a model containing resistance (1/log10(CFU/ml))), providing a measure of baseline variation. m1 (Protein) is a model containing the concentration of protein in the diet presented to the host. m2 (Carbs) is a model containing the concentration of carbohydrate in the host diet. m3 (Protein + Carbs) is a model containing both diet protein and carbohydrate concentrations. m4 (Protein * Carbs) is a model that includes an interaction term (represented by asterisk) between diet protein and carbohydrate concentration. m5 (Conc) is a model containing the concentration of macronutrients in the host diet. m6 (Ratio) is a model containing the ratio of protein to carbohydrate in the host diet. m7 (Conc + Ratio) is a model containing both the concentration of dietary macronutrients and the ratio of protein to carbohydrate in the diet presented to the host. m8 (Conc * Ratio) is a model that includes an interaction between diet macronutrient concentration and the ratio of dietary protein. m9 (diet) is a model containing resistance and diet as a factoral variable. df is the degrees of freedom used by the model to produce a fit and not the degrees of freedom based on the number of explanatory variables. k is the number terms in the model. AICc is the model Aikake values. Delta represents the difference between a model and the model explaining the most variation. Weight is determined by the amount of variation a model explains penalized for the df. (b-c) Summary information for each model in the AIC comparison table. The edf provides information about the shape of the curve, relating to the basis dimensions used by the model to fit the curve; for example, an edf close to 1 represents a linear effect, whilst an edf close to 2 represents a quadratic effect.

(a) Speed of death						
Model	**df**	**k**	**AICc**	**delta**	**weight**	**R^2**
m6 *Ratio*	7	2	-162.1	0.00	0.199	0.834
m9 *Diet*	6	1	-161.9	0.19	0.181	0.784
m0 *Null*	5	1	-161.4	0.69	0.141	0.742
m2 *Carbs*	5	2	-161.1	0.94	0.124	0.776
m1 *Protein*	5	2	-161.0	1.08	0.116	0.770
m3 *Protein + Carbs*	6	3	-160.1	2.00	0.073	0.792
m4 *Protein * Carbs*	6	4	-160.1	2.00	0.073	0.792
m5 *Conc*	5	2	-159.4	2.65	0.053	0.751
m8 *Conc * Ratio*	8	4	-157.5	4.53	0.021	0.857
m7 *Conc + Ratio*	8	3	-157.3	4.79	0.018	0.858

(b) Speed of death model summaries			
Model	**edf**	**F-value**	**P-value**
m0			
Null (Resistance)	2.534	13.677	<0.001
m1			
Resistance +	2.617	15.460	<0.001
Protein	0.582	0.348	0.118
m2			
Resistance +	2.570	16.412	<0.001
Carbs	0.725	0.658	0.073
m3			
Resistance +	2.593	17.544	<0.001
Protein +	0.482	0.233	0.154
Carbs	0.707	0.602	0.080
m4			
Resistance +	2.593	17.544	<0.001
Protein +	0.482	0.233	0.154
Carbs +	0.707	0.602	0.080
*Protein * Carbs*	0.000	0.000	0.759

(c) Speed of death model summaries			
Model	**edf**	**F-value**	**P-value**
m5			
Resistance +	2.509	14.073	<0.001
Conc	0.494	0.215	0.271
m6			
Resistance +	2.736	17.147	<0.001
Ratio	1.672	2.185	0.015
m7			
Resistance +	2.639	19.651	<0.001
Conc +	1.211	0.984	0.102
Ratio	1.750	2.714	0.009
m8			
Resistance +	2.700	19.890	<0.001
Conc +	0.000	0.000	0.233
Ratio +	1.732	2.651	0.009
*Conc * Ratio*	1.037	1.379	0.095
m9			
Resistance + Diet	2.696	20.377	<0.001

Table 3.8: Diet-level tolerance models exploring the amount of variation in change in larval mass explained by diet above the variation explained by host resistance alone. Data were aggregated by diet to create a dataset of 20 variables containing the mean change in mass and mean resistance for each diet. Resistance, the ability of a host to clear an infection is measured by inverse bacterial load. (a) AIC model comparison. m0 (Null) is a model containing resistance (1/log10(CFU/ml))), providing a measure of baseline variation. m1 (Protein) is a model containing the concentration of protein in the diet presented to the host. m2 (Carbs) is a model containing the concentration of host diet carbohydrate. m3 (Protein + Carbs) is a model containing both diet protein and carbohydrate concentrations. m4 (Protein * Carbs) is a model that includes an interaction term (represented by asterisk) between diet protein and carbohydrate concentration. m5 (Conc) is a model containing the concentration of macronutrients in the host diet. m6 (Ratio) is a model containing the ratio of protein to carbohydrate in the host diet. m7 (Conc + Ratio) is a model containing both the concentration of dietary macronutrients and the ratio of protein to carbohydrate in the diet. m8 (Conc * Ratio) is a model that includes an interaction between diet macronutrient concentration and the ratio of dietary protein. m9 (diet) is a model containing resistance and diet as a factoral variable. df is the degrees of freedom used by the model to produce a fit and not the degrees of freedom based on the number of explanatory variables. k is the number terms in the model. AICc is the model Aikake values. Delta represents the difference between a model and the model explaining the most variation. Weight is determined by the amount of variation a model explains penalized for the degrees of freedom used by the model. (b-c) Summary information for each model in the AIC comparison table. The edf provides information about the shape of the curve, relating to the basis dimensions used by the model to fit the curve; for example, an edf close to 1 represents a linear effect, whilst an edf close to 2 represents a quadratic effect.

(a) Change in larval mass						
Model	**df**	**k**	**AICc**	**delta**	**weight**	**R^2**
m6 *Ratio*	4	3	-79.7	0.00	0.277	0.608
m7 *Conc + Ratio*	4	2	-79.7	0.00	0.277	0.608
m8 *Conc * Ratio*	4	4	-79.7	0.00	0.277	0.608
m9 *Diet*	3	1	-78.5	1.21	0.151	0.509
m4 *Protein * Carbs*	5	4	-73.8	5.92	0.014	0.533
m2 *Carbs*	2	2	-68.0	11.68	0.001	0.176
m3 *Protein + Carbs*	6	3	-67.9	11.83	0.001	0.522
m1 *Protein*	5	2	-66.9	12.80	0.000	0.400
m0 *Null*	2	1	-64.9	14.86	0.000	0.035
m5 *Conc*	2	2	-64.9	14.86	0.000	0.035

(b) Change in larval mass model summaries

Model	edf	F-value	P-value
m0			
Null (Resistance)	0.493	0.171	0.261
m1			
Resistance +	1.179	0.844	0.075
Protein	1.736	2.472	0.010
m2			
Resistance +	0.000	0.000	0.387
Carbs	0.803	1.016	0.037
m3			
Resistance +	1.122	0.719	0.097
Protein +	1.837	2.821	0.007
Carbs	0.814	1.096	0.033
m4			
Resistance +	0.989	0.592	0.108
Protein +	0.000	0.000	0.332
Carbs +	0.000	0.000	0.328
*Protein * Carbs*	1.399	9.366	<0.001

(c) Change in larval mass model summaries

Model	edf	F-value	P-value
m5			
Resistance +	0.493	0.171	0.261
Conc	0.000	0.000	0.743
m6			
Resistance +	0.000	0.000	0.567
Ratio	2.081	7.375	<0.001
m7			
Resistance +	0.000	0.000	0.597
Conc +	0.000	0.000	0.650
Ratio	2.081	7.375	<0.001
m8			
Resistance +	0.000	0.000	0.600
Conc +	0.000	0.000	0.646
Ratio +	2.081	7.375	<0.001
*Conc * Ratio*	0.000	0.000	0.367
m9			
Resistance + Diet	0.000	0.000	0.437

3.3.5 Tolerance due to host macronutrient intake

Tolerance is also described by the slope of the reaction norm, but can only be compared between groups and not between individuals (Ayres and Schneider, 2012). Dividing our dataset into groups based on diet eaten would therefore allow the confirmation of whether the variation in resilience explained by diet is due to tolerance. The data were split into thirds by the amount of diet eaten in the 24 h pre-infection; those that ate a low level of protein/carbohydrate (<25 mg), a medium level (25 – 50 mg), or a high level (>50 mg). The slope of fitness for a given bacterial load was then compared between the groups. Once again, the effect of diet intake on survival could not be investigated due to a low sample size.

Consistent with dietary level investigations (Section 2.4), diet was unable to explain any more variation in host speed of death once bacterial load was accounted for. This was reflected by the top model in the AIC comparison being the *Null* model (**Table 3.9; Figure 3.9a,b**).

Hosts that had ingested a higher level of protein showed a greater increase in mass for a given bacterial load (R^2 = 0.461; **Table 3.10a; Figure 3.9c**). However, because the slopes of the change in larval mass due to infection were similar for the different protein-intake groups, the overall effect was due to an increased vigour (fitness in the absence of infection), rather than tolerance. The carbohydrate model, which was the third worst model, explained almost half (1.8 times) the amount of variation explained by any model containing protein, indicating there was no effect of carbohydrate intake in the relationship between bacterial load and change in larval mass (**Figure 3.9d**).

The effect of diet intake on host vigour (shown by points with error bars on **Figure 3.9**), was consistent; host resistance was reduced for individuals that ate less than 30 mg of

food, irrespective of its macronutrient composition. These individuals had an average bacterial load of 1 x 10^4 CFU/ml compared to 0 for the individuals that ate over 30 mg of food.

In summary, these results are consistent with the notion that diet macronutrient intake increased host resilience through mechanisms other than resistance. However, rather than a tolerance effect, a high protein intake increased a host's vigour (measured by change in mass).

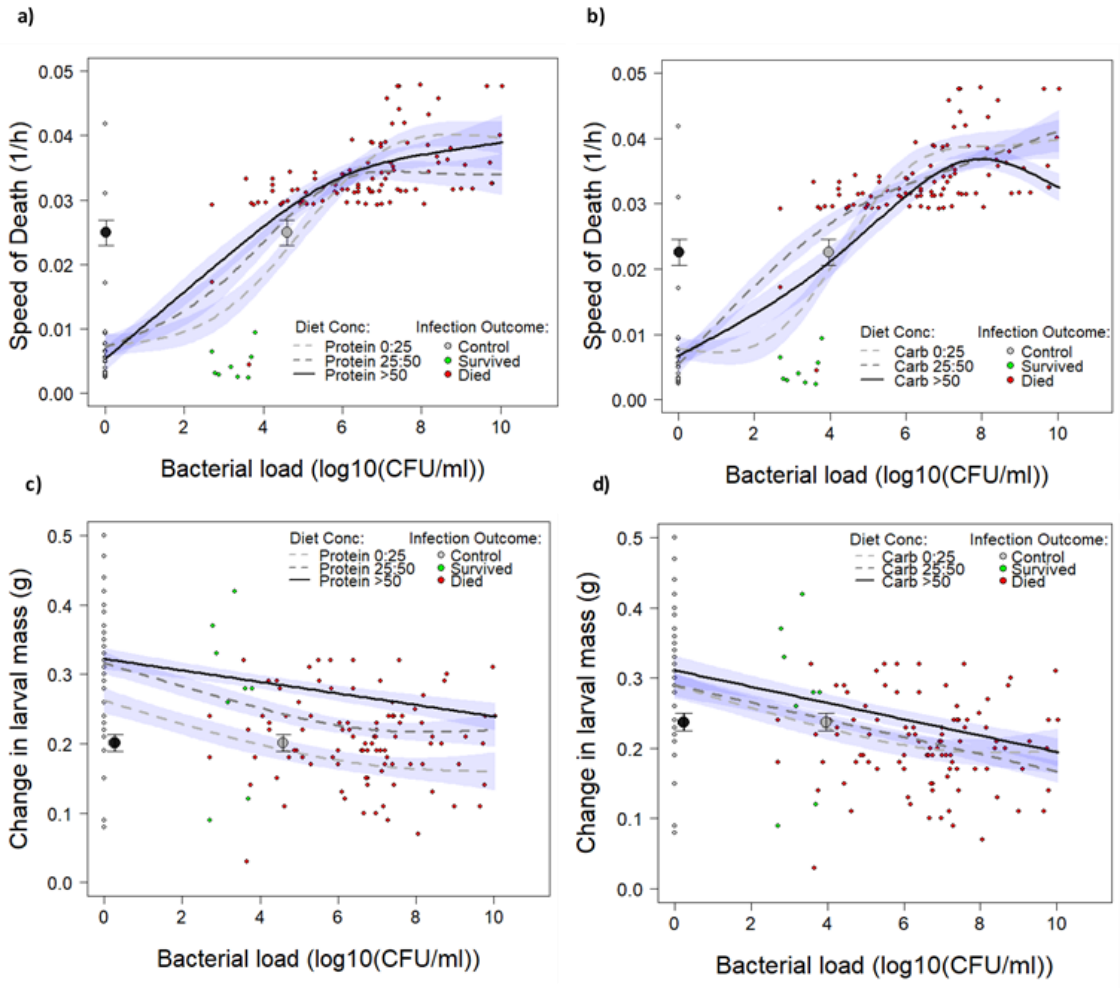
a)
b)
c)
d)
Speed of Death (1/h)
Change in larval mass (g)
Bacterial load (log10(CFU/ml))
Diet Conc:
Protein 0:25
Protein 25:50
Protein >50
Carb 0:25
Carb 25:50
Carb >50
Infection Outcome:
Control
Survived
Died

Figure 3.9: Models testing for a change in tolerance for a given pathogen load due to protein or carbohydrate intake. An increase in a fitness trait (e.g. survival) for a given pathogen load is a measure of an animal's ability to tolerate infection. Data was aggregated into groups of three depending on diet intake; low macronutrient intake (<25 mg), mid-macronutrient intake (25-50 mg), high macronutrient intake (>50 mg). Mean fitness per diet (large symbols with error bars) was also plotted for each trait to indicate an organism's vigour (health status in the absence of infection). There was no difference in vigour between the mid- and high macronutrient intake groups, which had a negligible bacterial load at sampling. The low macronutrient intake group had a bacterial load of ~ 1 x 10^4 CFU/ml at sampling. The raw data (small symbols) were coloured to show the distribution of individuals in relation to their bacteria load. Controls (grey) had no experimental bacteria at sampling. Individuals that survived infection (green) had a bacterial load of <1 x 10^4 CFU/ml, and individuals that died of infection had a bacterial load of between 1 x 10^3 and 1 x 10^9 CFU/ml at the time of sampling. (a) Difference in speed of death for a given bacterial load depending on protein intake. Protein intake had no effect on the speed of death above the effect of increasing bacterial load alone. (b) Difference in speed of death for a given bacterial load depending on carbohydrate intake. Carbohydrate intake had no effect on the speed of death above the effect of increasing bacterial load alone. (c) Difference in change in larval mass for a given bacterial load depending on protein intake. Individuals gained less weight with increasing bacterial load. There was a difference in change in mass for a given pathogen load depending on protein intake; individuals eating more protein gained more weight than counterparts with the same bacterial load who ate less protein. (d) Difference in change in larval mass for a given bacterial load depending on carbohydrate intake. There was no effect of carbohydrate intake on larval weight gain above the effects of increasing pathogen load alone.

Table 3.9: Tolerance models exploring the relationship between speed of host death and bacterial load at sampling depending on macronutrient intake. (a) AIC model comparison. m0 (Bact) is a model containing bacterial load, providing a baseline against which other models could be compared. P0 refers to the amount of protein eaten by the host pre-infection. C0 refers to the amount of carbohydrate eaten by the host pre-infection. P1 refers to the amount of protein eaten by the host on the first day post-infection. C1 refers to the amount of carbohydrate eaten by the host on the first day post-infection. P0:C0 refers to the inclusion of an interaction between protein and carbohydrate pre-infection in a model. m9 (diet) is a model containing bacterial load and diet as a factoral variable. df is the degrees of freedom used by the model to produce a fit and not the degrees of freedom based on the number of explanatory variables. k is the number terms in the model. AICc is the model Aikake values. Delta represents the difference between a model and the model explaining the most variation. Weight is determined by the amount of variation a model explains penalized for the degrees of freedom used by the model. (b-c) Summary information for each model in the AIC comparison table. The edf provides information about the shape of the curve, relating to the basis dimensions used by the model to fit the curve; for example, an edf close to 1 represents a linear effect, whilst an edf close to 2 represents a quadratic effect.

(a) Model AICs: Bacterial load, diet eaten and speed of death								
Model	**Terms**	**df**	**k**	**AICc**	**delta**	**weight**	**R^2**	**Significant Terms**
m0	Bact	6	3	-1016.4	0.00	0.106	0.776	Bact
m2	Bact+C0	6	3	-1016.4	0.00	0.106	0.776	Bact
m8	Bact+P0+C0+Bact:P0+P0:C0	6	6	-1016.4	0.02	0.105	0.776	Bact
m3	Bact+P0+C0	6	4	-1016.4	0.02	0.105	0.776	Bact
m1	Bact+P0	6	3	-1016.4	0.02	0.105	0.776	Bact
m4	Bact+P0+C0+Bact:P0	6	5	-1016.4	0.03	0.104	0.776	Bact
m6	Bact+P0+C0+P0:C0	6	5	-1016.4	0.03	0.104	0.776	Bact
m10	Bact+P0+C0+Bact:P0+Bact:C0+P0+C0	7	7	-1015.7	0.73	0.073	0.778	Bact
m7	Bact+P0+C0+Bact:P0+Bact:C0	7	6	-1015.7	0.74	0.073	0.778	Bact
m5	Bact+P0+C0+Bact:C0	8	5	-1015.3	1.17	0.059	0.779	Bact
m9	Bact+P0+C0+Bact:C0+P0:C0	8	6	-1015.3	1.18	0.059	0.779	Bact
m11	Bact+Diet	24	3	-994.6	21.88	0.000	0.782	Bact

(b) Bacterial load, diet eaten and speed of death model summaries

Model	edf	F-value	P-value
m0			
Null (Bact)	0.810	1.067	0.023
m1			
Bact +	3.274	105.869	<0.001
Protein	0.010	0.003	0.325
m2			
Bact +	3.274	105.868	<0.001
Carbs	0.000	0.000	0.419
m3			
Bact +	3.274	105.867	<0.001
Protein +	0.009	0.002	0.328
Carbs	0.001	0.000	0.388
m4			
Bact +	3.274	105.865	<0.001
Protein +	0.012	0.003	0.326
Carbs +	0.001	0.000	0.397
*Bact * Protein*	0.000	0.000	0.965
m5			
Bact +	3.291	102.220	<0.001
Protein +	0.000	0.000	0.426
Carbs +	0.000	0.000	0.453
*Bact * Carbs*	0.982	0.171	0.229
m6			
Bact +	3.274	105.865	<0.001
Protein +	0.014	0.003	0.326
Carbs +	0.001	0.000	0.388
*Protein * Carbs*	0.000	0.000	0.738

(c) Bacterial load, diet eaten and speed of death model summaries

Model	edf	F-value	P-value
m7			
Bact +	3.286	105.299	<0.001
Protein +	0.001	0.000	0.353
Carbs +	0.000	0.000	0.511
*Bact * Protein +*	0.000	0.000	0.978
*Bact * Carbs*	0.491	0.084	0.230
m8			
Bact +	3.274	105.866	<0.001
Protein +	0.007	0.002	0.326
Carbs +	0.001	0.000	0.387
*Bact * Protein +*	0.000	0.000	0.964
*Protein * Carbs*	0.000	0.000	0.739
m9			
Bact +	3.291	102.241	<0.001
Protein +	0.000	0.000	0.412
Carbs +	0.000	0.000	0.480
*Bact * Carbs +*	0.980	0.171	0.229
*Protein * Carbs*	0.000	0.000	0.859
m10			
Bact +	3.286	105.326	<0.001
Protein +	0.003	0.001	0.345
Carbs +	0.000	0.000	0.442
*Bact * Protein +*	0.000	0.000	0.978
*Bact * Carbs +*	0.487	0.083	0.230
*Protein * Carbs*	0.000	0.000	0.842
m11			
Bact + Diet	3.107	102.311	<0.001

Table 3.10: Tolerance models exploring the relationship between change in larval mass and bacterial load at sampling depending on macronutrient intake. (a) AIC model comparison. m0 (Bact) is a model containing bacterial load, providing a baseline against which other models could be compared. P0 refers to the amount of protein eaten by the host pre-infection. C0 refers to the amount of carbohydrate eaten by the host pre-infection. P1 refers to the amount of protein eaten by the host on the first day post-infection. C1 refers to the amount of carbohydrate eaten by the host on the first day post-infection. P0:C0 refers to the inclusion of an interaction between protein and carbohydrate pre-infection in a model. m9 (diet) is a model containing bacterial load and diet as a factoral variable. df is the degrees of freedom used by the model to produce a fit and not the degrees of freedom based on the number of explanatory variables. k is the number terms in the model. AICc is the model Aikake values. Delta represents the difference between a model and the model explaining the most variation. Weight is determined by the amount of variation a model explains penalized for the degrees of freedom used by the model. (b-c) Summary information for each model in the AIC comparison table. The edf provides information about the shape of the curve, relating to the basis dimensions used by the model to fit the curve; for example, an edf close to 1 represents a linear effect, whilst an edf close to 2 represents a quadratic effect.

(a) Model AICs: Bacterial load, diet eaten and change in mass								
Model	**Terms**	**df**	**k**	**AICc**	**delta**	**weight**	**R^2**	**Significant Terms**
m10	Bact+P0+C0+Bact:P0+Bact:C0+P0+C0	10	7	-369.3	0.00	0.117	0.461	Bact, P0
m3	Bact+P0+C0	10	4	-369.3	0.00	0.117	0.461	Bact, P0
m8	Bact+P0+C0+Bact:P0+P0:C0	10	6	-369.3	0.00	0.117	0.461	Bact, P0
m5	Bact+P0+C0+Bact:C0	10	5	-369.3	0.00	0.117	0.461	Bact, P0
m7	Bact+P0+C0+Bact:P0+Bact:C0	10	6	-369.3	0.00	0.117	0.461	Bact, P0
m4	Bact+P0+C0+Bact:P0	10	5	-369.3	0.00	0.117	0.461	Bact, P0
m6	Bact+P0+C0+P0:C0	10	5	-369.3	0.00	0.117	0.461	Bact, P0
m9	Bact+P0+C0+Bact:C0+P0:C0	10	6	-369.3	0.00	0.117	0.461	Bact, P0
m1	Bact+P0	9	3	-368.2	1.13	0.066	0.452	Bact, P0
m2	Bact+C0	6	3	-328.5	40.83	0.000	0.251	Bact, C0
m0	Bact	4	3	-325.5	43.80	0.000	0.228	Bact
m11	Bact+Diet	25	3	-320.7	48.66	0.000	0.350	Bact

(b) Bacterial load, diet eaten and change in mass model summaries

Model	edf	F-value	P-value
m0			
Null (Bact)	1.919	10.540	<0.001
m1			
Bact +	2.230	17.267	<0.001
Protein	2.544	13.619	<0.001
m2			
Bact +	1.819	11.441	<0.001
Carbs	0.804	1.024	0.024
m3			
Bact +	2.196	18.063	<0.001
Protein +	2.406	13.044	<0.001
Carbs	0.733	0.684	0.052
m4			
Bact +	2.196	18.063	<0.001
Protein +	2.406	13.037	<0.001
Carbs +	0.732	0.684	0.052
*Bact * Protein*	0.000	0.000	0.255
m5			
Bact +	2.196	18.063	<0.001
Protein +	2.406	13.044	<0.001
Carbs +	0.733	0.684	0.052
*Bact * Carbs*	0.000	0.000	0.800
m6			
Bact +	2.196	18.063	<0.001
Protein +	2.406	13.042	<0.001
Carbs +	0.732	0.684	0.052
*Protein * Carbs*	0.000	0.000	0.600

(c) Bacterial load, diet eaten and change in mass model summaries

Model	edf	F-value	P-value
m7			
Bact +	2.196	18.063	<0.001
Protein +	2.406	13.043	<0.001
Carbs +	0.733	0.684	0.052
*Bact * Protein +*	0.000	0.000	0.232
*Bact * Carbs*	0.000	0.000	0.800
m8			
Bact +	2.196	18.063	<0.001
Protein +	2.406	13.043	<0.001
Carbs +	0.732	0.684	0.052
*Bact * Protein +*	0.000	0.000	0.226
*Protein * Carbs*	0.000	0.000	0.606
m9			
Bact +	2.196	18.063	<0.001
Protein +	2.406	13.043	<0.001
Carbs +	0.732	0.684	0.052
*Bact * Carbs +*	0.000	0.000	0.800
*Protein * Carbs*	0.000	0.000	0.603
m10			
Bact +	2.196	18.063	<0.001
Protein +	2.406	13.044	<0.001
Carbs +	0.732	0.684	0.052
*Bact * Protein +*	0.000	0.000	0.227
*Bact * Carbs +*	0.000	0.000	0.808
*Protein * Carbs*	0.000	0.000	0.603
m11			
Bact + Diet	2.174	12.963	<0.001

3.4 DISCUSSION

The aims of this study were to determine *in vivo* pathogen fitness and host defence strategy in the context of diets that covered a broad range of the host nutrient landscape. Unexpectedly, once the whole nutritional landscape was accounted for, protein did not dominate the host-pathogen relationship as consistently as it had in immunological nutritional investigations carried out so far on *Spodoptera* caterpillars (Lee et al., 2006; Povey et al., 2014, 2009). Protein intake pre-infection determined the change in larval mass, which was an accurate predictor of the host's ability to fight infection. Speed of death seemed to be determined by the availability of both macronutrients, slowing down with protein intake but speeding up with carbohydrate intake in correspondence with carbohydrate effects on pathogen fitness. Carbohydrate availability accelerated pathogen growth rate, however diet carbohydrate content appeared to increased host tolerance, as measured by host survival.

3.4.1 Host Diet Regulation

Lepidopteran adults are predominantly nectar feeders and so acquire their essential amino acids at the larval stage (Chapman, 2012). *Spodoptera* caterpillars therefore increase protein consumption with available dietary protein, but are capable of regulating intake (Lee et al., 2002). Both aspects were seen, firstly by our sham-injected controls, which increased protein ingestion with increasing dietary protein. Then, as was observed by Lee et al., (2002), *S. littoralis* caterpillars infected with live bacteria in our experiment regulated their protein intake. Our findings indicated that the diet protein regulation was in response to high infection levels. Lee et al., (2006), found an increased survival rate in *S. littoralis* larvae infected with nucleopolyhedrovirus (NPV), when larvae ate diets containing a higher protein-to-carbohydrate ratio. We found a

similar result; larvae that did not reduce their food intake when presented with higher proportions of protein to carbohydrates were also more likely to survive the infection. Individuals carrying a high pathogen load appeared to abandon carbohydrate regulation. Further investigation is needed to clarify whether the larvae were trying to meet their protein intake target in response to this immune stress, or replace the carbohydrate being used by *X. nematophila* for proliferation.

The reduction in food intake due to infection is a possible example of illness-induced anorexia, which has been observed across multiple taxa (Adamo et al., 2010). Adamo et al., (2010) hypothesised that, due to trade-offs between immune function and metabolic pathways, eating less food during infection reduces metabolic demands, allowing more energy for immunity. We found that individuals displaying an anorexic response to infection were more likely to die and died faster. Our findings suggest that the costs of resource limitation outweigh any benefits conveyed by trade-off avoidance, possibly due to nutritional-stress impairing immune function (Graham et al., 2014). Moreover, the anorexia response was dependent on bacterial load at sampling, only appearing in individuals carrying a fast-growing bacterial population. A combination of this result with that of Povey et al., (2009), who found no difference in the feeding behaviour of *Spodoptera exempta* in response to infection with low levels of *Bacillus subtilis*, leads to the conclusion that there may be a threshold pathogen load for the activation of illness-induced anorexia in *Spodoptera*.

3.4.2 Effects of diet on host fitness

Unlike preceding experiments that presented a clear picture of protein's ability to increase survival to infection in *S. littoralis* (Lee et al., 2006), and *S. exempta* (Povey et al., 2014, 2009), our results showed a role of carbohydrate in reducing the speed of host

death. Unfortunately, were unable to test the direct effects of diet on overall survival due to a low sample size, but the reduction in speed of death with increasing protein intake aligned with previous findings (Chapter 2). It is also possible that the beneficial role of carbohydrate is revealed more clearly in the current experiment due to the increased range of diet concentrations used. Although this is the first observation of a beneficial role of carbohydrate in disease resistance in *Spodoptera*, other insects such as the Australian plague locust, *Chortoicetes terminifera* (Graham et al., 2014), have provided evidence that carbohydrate intake can enhance resistance to pathogens.

Although increase in mass is protein-dependent in this species, the generalist grasshopper *Melanoplus differentialis* shows a carbohydrate-dependent mass increase (Le Gall and Behmer, 2014). This indicates an evolutionary benefit to the preference of protein for growth in Lepidoptera, possibly related to the strong positive correlation observed between host mass and vigour. The observed correlation is an indication of the host's effective conversion of ingested protein into usable resources. Individuals with a greater mass, who have ingested more nutrients (predominantly protein), have more resources available to dedicate to immune defence. The costs of an upregulated immune defence (Sheldon and Verhulst, 1996), and of recovery from infection (Archie, 2013), have been well documented. Recently, costs of immunity even in the absence of a pathogen have been established in *Spodoptera* (Cotter et al., 2011, 2004; Povey et al., 2009). Higher protein intake provides deeper reserves that can be drawn upon during infection. As well as the increased vigour observed based on protein intake, the data revealed a negative correlation between host weight gain and bacterial load. Although we found a weak relationship between host mass and resistance, a future experiment measuring immune responses directly may be able to disentangle the dual effect of protein on host vigour and resistance.

3.4.3 Tolerance

As far as we are aware, this study is the first to present diet-mediated tolerance effects in *Spodoptera* caterpillars. There appeared to be an effect of dietary carbohydrate concentration on host survival even after the effects of resistance had been accounted for. Although, further investigation is still needed because testing the effects of carbohydrate intake pre-infection on host survival was impeded by a low sample size. It is possible that, like the effects of protein on larval weight gain, carbohydrate increased the vigour of the larvae rather than tolerance. The primary role of carbohydrate as an energy source for metabolism in cells (DeGrandi-Hoffman and Chen, 2015), means that carbohydrate may increase host tolerance by providing energy for cellular function. This indicates a role for haemolymph sugar in either neutralizing bacterial virulence factors or helping the host repair damage produced by the pathogen. The limited investigation of nutrients relating to host tolerance effects may explain the under-development of the role of carbohydrate in the host-pathogen relationship in lepidopterans.

The key mechanism through which carbohydrate can increase host tolerance may be via the phenoloxidase pathway. Cotter et al., (2011) found using the same range of diets presented here that phenoloxidase activity in *S. littoralis* is up-regulated in carbohydrate-rich nutrient space. *X. nematophila* inhibits humoral pathways such as antimicrobial peptide (AMP) production, however it uses defensive mechanisms when faced with cellular immune factors (Richards and Goodrich-Blair, 2009), providing a case for the phenoloxidase pathway as a primary form of defence employed by lepidopterans against this pathogen. The phenoloxidase pathway involves the production of melanin, which is also involved in processes such as wound healing (Stączek et al., 2017), allowing the host to simultaneously increase resistance and tolerance, leading to a higher resilience.

Changes in pathogen growth rate, host mass and speed of host death were determined by the diet ingested pre-infection. This indicates a possible futility in the host's change in feeding behaviour in response to infection, since the outcome is determined by nutritional status at the point of infection. The conditions that the pathogen experiences upon introduction into the host determine its establishment rate (number of founding individuals), which creates a differential dose response (Chapter 2). Since pathogen load is the most significant determinant of host survival and speed of death, the outcome of infection may be determined predominantly by this pathogen's establishment rate. This advocates a need for hosts to maintain conditions unsuitable for the pathogen, providing an alternative hypothesis for the development of lepidopterans on a basal diet high in protein and low in carbohydrate.

3.4.4 Effects of the pathogen on the host

Xenorhabdus nematophila showed a preference for carbohydrates, consistent with previous studies showing that this gram-negative bacterium performs best on glucose-rich media (Kooliyottil et al., 2014). It remains unclear whether the bacteria in our study uses dietary sucrose directly or once it has been broken down into its constituent monosaccharides (glucose and fructose). The linear nature of the relationship between the amount of carbohydrate ingested the caterpillars and their bacterial loads suggests that the host had not reached its carrying capacity for the bacterium. This implies an overlap between the optimal growth requirements for the bacterium and the range of carbohydrate levels experienced by it in the host haemolymph based on diet ingested. The increased speed of host death with ingested carbohydrate may build on this finding further in its revelation that the pathogen is successfully using the carbohydrate available in the host haemolymph. Further investigation may be necessary to determine whether there is direct competition between the two organisms for this macronutrient.

Given the high virulence of this pathogen (mortality occurred within 48 hours), it was surprising that the change of larval mass could not be predicted by bacterial load, although the infected larvae showed a greater variation in mass than the controls. The high pathogen virulence may mean that death occurs before larvae show obvious morbidity. Protein intake, which controls larval growth, may not be included amongst the nutrients competed for between *X. nematophila* and its host; not much is known about this pathogen's nutrient requirements (Richards and Goodrich-Blair, 2009). This would allow continuous availability of protein for the host to use. Furthermore, virulence of *X. nematophila* depends on the inhibition of immune effectors and the breakdown of cellular material, which may not affect larval mass as no larval material is recycled (Nielsen-LeRoux et al., 2012). Perhaps it is in the bacteria's interest for the larvae to gain weight since heavier larvae have more resources to be mined by *S. carpocapsae*, the host of symbiotic *Xenorhabdus*; an idea supported by the dependence on the levels of nutrients such as iron to signal host death, after which point *Xenorhabdus* prepares to recombine with its nematode carrier (Jubelin et al., 2011; Singh and Banerjee, 2008).

3.4.5 Summary

Our results build on previous findings in this species and other lepidopterans, not just indicating a role for dietary protein in delaying host mortality, but also providing a new position for dietary carbohydrates as a macronutrient aiding host survival in the form of tolerance. We show that although *S. littoralis* regulates dietary intake in response to infection, this may be fruitless since pathogen success is mainly decided by the nutritional environment at the point of infection.

It would be interesting to explore competition between the host and pathogen for carbohydrates since both the host and this pathogen require this nutrient during infection. Moreover, we nominate the phenoloxidase pathway as a possible candidate for the increased tolerance of the host in a carbohydrate-rich nutrient space. Although measuring immune responses was impeded by logistical constraints in this experiment, future research that measures *S. littoralis* immunity during *X. nematophila* infection may provide further evidence for the diet-mediated tolerance response identified by this study.

3.5 SUPPLEMENTARY MATERIAL

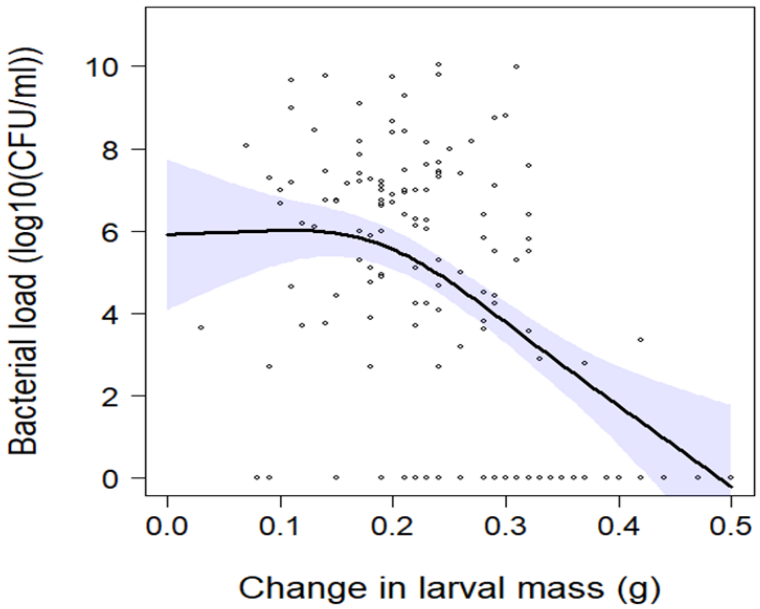

Figure S3.1: GAM model output showing variation explained by change in larval mass bacterial load at sampling. Bacterial load decreased non-linearly (edf = 1.790) with increasing weight gained by the host.

Table S3.1: Twenty diets fed to *Spodoptera littoralis* caterpillars varying in their ratios and concentrations of protein and carbohydrate.

Diet.no	P:C	P:C ratio	conc	ratio prot	%prot	%carb
1	10.5 : 52.5	1:5	63	0.17	10.5	52.5
2	7:35	1:5	42	0.17	7	35
3	5.6 : 28	1:5	33.6	0.17	5.6	28
4	2.8 :14	1:5	16.8	0.17	2.8	14
5	21:42	1:2	63	0.33	21	42
6	14:28	1:2	42	0.33	14	28
7	11.2 : 22.4	1:2	33.6	0.33	11.2	22.4
8	5.6 : 11.2	1:2	16.8	0.33	5.6	11.2
9	31.5 : 31.5	1:1	63	0.50	31.5	31.5
10	21:21	1:1	42	0.50	21	21
11	16.8 : 16.8	1:1	33.6	0.50	16.8	16.8
12	8.4 : 8.4	1:1	16.8	0.50	8.4	8.4
13	42 : 21	2:1	63	0.67	42	21
14	28:14	2:1	42	0.67	28	14
15	22.4 : 11.2	2:1	33.6	0.67	22.4	11.2
16	11.2 : 5.6	2:1	16.8	0.67	11.2	5.6
17	52.5 : 10.5	5:1	63	0.83	52.5	10.5
18	35:7	5:1	42	0.83	35	7
19	28 : 5.6	5:1	33.6	0.83	28	5.6
20	14 : 2.8	5:1	16.8	0.83	14	2.8

Table S3.2: Analysis of variance models showing the significant difference between bacterial load at sampling for live-infected individuals and control treatments. (a) Analysis of variance test performed on the bacterial counts between sham-injected, dead-infected and live-infected individuals. There were no bacteria detected in either the sham-injected or dead-infected treatments. (b) An analysis of variance test performed on the treatment groups predominantly showing the significance in the bacterial counts in the live-infected group, depending on the likelihood of surviving infection.

(a) Infection load ; $R^2 = 0.761$				
Treatment	**Estimate**	**SE**	**T-value**	**P-value**
Sham (Intercept)	-4.968E-14	0.356	0	1
Dead	6.193E-14	0.504	0	1
Live	6.337	0.389	16.280	<0.001

(b) Infection Outcome; $R^2 = 0.815$				
Treatment	**Estimate**	**SE**	**T-value**	**P-value**
Sham (Intercept)	6.446E-15	0.314	0	1
Dead	-1.592E-14	0.444	0	1
Surviving	3.251	0.587	5.538	<0.001
Dying	6.594	0.345	19.119	<0.001

Table S3.3: Model AIC tables investigating whether diet eaten pre-infection or diet eaten post infection explained more variation in bacterial load at sampling and host fitness. (a) Bacterial load at sampling. (b) Host survival. (c) Speed of host death. (d) Change in larval mass. m0 (Null) is a model with no explanatory terms included, providing a baseline measure of variation. P0 refers to the amount of protein eaten by the host pre-infection. C0 refers to the amount of carbohydrate eaten by the host pre-infection. P1 refers to the amount of protein eaten by the host on the first day post-infection. C1 refers to the amount of carbohydrate eaten by the host on the first day post-infection. P0:C0 refers to the inclusion of an interaction between protein and carbohydrate pre-infection in a model. P1:C1 refers to the inclusion of an interaction between protein and carbohydrate eaten on the first day post-infection in a model. P0:C1 refers to the inclusion of an interaction between protein eaten pre-infection and carbohydrate eaten post-infection in a model. C0:P1 refers to the inclusion of an interaction between carbohydrate eaten pre-infection and protein eaten post-infection in a model. Diet is a model containing diet as a factoral variable. df is the degrees of freedom used by the model to produce a fit and not the degrees of freedom based on the number of explanatory variables. k is the number terms in the model. AICc is the model Aikake values. Delta represents the difference between a model and the model explaining the most variation. Weight is determined by the amount of variation a model explains penalized for the degrees of freedom used by the model.

(a) Model AICs: Diet eaten and bacterial load							
Model	**Terms**	**df**	**k**	**AICc**	**delta**	**weight**	**R^2**
m2	C0	3	2	417.1	0.000	0.081	0.113
m15	P0+C0+P1+C1+P1:C1	3	6	417.1	0.000	0.081	0.113
m5	P0+C0	3	3	417.1	0.000	0.081	0.113
m14	P0+C0+P1+C1+P0:C0	3	6	417.1	0.000	0.081	0.113
m7	P0+C0+P1	3	4	417.1	0.000	0.081	0.113
m11	P0+C0+P1+C1	3	5	417.1	0.000	0.081	0.113
m18	P0+C0+P1+C1+P0:C0+P1:C1	3	7	417.1	0.000	0.081	0.113
m8	P0+C0+C1	3	4	417.1	0.000	0.081	0.113
m17	P0+C0+P1+C1+P1:C0	3	6	417.1	0.000	0.081	0.113
m16	P0+C0+P1+C1+P0:C1	3	6	417.1	0.000	0.081	0.113
m10	C0+P1+C1	3	4	417.1	0.000	0.081	0.113
m12	P0+C0+P0:C0	3	4	417.1	0.000	0.081	0.113
m9	P0+P1+C1	3	4	422.4	5.249	0.006	0.070
m6	P1+C1	3	3	422.4	5.249	0.006	0.070
m4	C1	3	2	422.4	5.250	0.006	0.070
m13	P1+C1+P1:C1	3	4	422.4	5.295	0.006	0.070
m0	*Null*	2	2	427.9	10.764	0.000	0.000
m3	P1	2	2	427.9	10.765	0.000	0.000
m1	P0	2	2	427.9	10.765	0.000	0.000
m19	*Diet*	20	2	431.2	14.116	0.000	0.211

(b) Model AICs: Diet eaten and speed of host death							
Model	**Terms**	**df**	**k**	**AICc**	**delta**	**weight**	**R^2**
m14	P0+C0+P1+C1+P0:C0	19	6	-2854.4	0.00	0.342	0.811
m18	P0+C0+P1+C1+P0:C0+P1:C1	20	7	-2854.1	0.28	0.297	0.812
m17	P0+C0+P1+C1+P1:C0	19	6	-2853.9	0.51	0.265	0.812
m16	P0+C0+P1+C1+P0:C1	18	6	-2850.6	3.80	0.051	0.809
m12	P0+C0+P0:C0	14	4	-2849.9	4.45	0.037	0.806
m11	P0+C0+P1+C1	14	5	-2843.7	10.72	0.002	0.804
m8	P0+C0+C1	10	4	-2843.6	10.78	0.002	0.801
m15	P0+C0+P1+C1+P1:C1	17	6	-2843.5	10.91	0.001	0.806
m5	P0+C0	9	3	-2842.6	11.75	0.001	0.800
m7	P0+C0+P1	14	4	-2842.0	12.40	0.001	0.803
m10	C0+P1+C1	13	4	-2841.4	13.01	0.001	0.801
m19	*Diet*	24	2	-2837.2	17.16	0.000	0.805
m9	P0+P1+C1	14	4	-2833.6	20.81	0.000	0.798
m13	P1+C1+P1:C1	15	4	-2833.0	21.35	0.000	0.799
m6	P1+C1	11	3	-2830.4	23.96	0.000	0.795
m1	P0	7	2	-2821.4	32.95	0.000	0.787
m3	P1	8	2	-2818.2	36.17	0.000	0.786
m2	C0	8	2	-2817.6	36.73	0.000	0.786
m4	C1	8	2	-2810.2	44.21	0.000	0.782
m0	*Null*	5	2	-2802.6	51.78	0.000	0.775

(c) Change in larval mass							
Model	**Terms**	**df**	**k**	**AICc**	**delta**	**weight**	**R^2**
m8	P0+C0+C1	21	4	-1016.4	0.00	0.316	0.484
m7	P0+C0+P1	23	4	-1015.7	0.70	0.223	0.487
m14	P0+C0+P1+C1+P0:C0	24	6	-1015.2	1.16	0.177	0.489
m12	P0+C0+P0:C0	23	4	-1014.6	1.79	0.129	0.486
m5	P0+C0	19	3	-1012.8	3.60	0.052	0.477
m17	P0+C0+P1+C1+P1:C0	27	6	-1012.5	3.84	0.046	0.492
m16	P0+C0+P1+C1+P0:C1	23	6	-1011.6	4.79	0.029	0.483
m18	P0+C0+P1+C1+P0:C0+P1:C1	28	7	-1010.8	5.55	0.020	0.491
m15	P0+C0+P1+C1+P1:C1	25	6	-1006.9	9.51	0.003	0.480
m9	P0+P1+C1	18	4	-1006.5	9.84	0.002	0.467
m1	P0	17	2	-1005.9	10.47	0.002	0.464
m11	P0+C0+P1+C1	22	5	-1003.2	13.13	0.000	0.470
m10	C0+P1+C1	23	4	-996.5	19.88	0.000	0.461
m13	P1+C1+P1:C1	21	4	-967.2	49.19	0.000	0.418
m3	P1	15	2	-966.2	50.13	0.000	0.403
m6	P1+C1	16	3	-965.6	50.82	0.000	0.405
m19	*Diet*	23	2	-907.5	108.90	0.000	0.323
m2	C0	8	2	-905.9	110.52	0.000	0.292
m4	C1	8	2	-901.4	115.02	0.000	0.283
m0	*Null*	5	2	-893.3	123.05	0.000	0.260

Table S3.4: Relationship between change in host mass and bacterial load at sampling with change in host mass treated as the explanatory variable. K represents the number of terms in the model. The edf provides information about the shape of the curve, relating to the basis dimensions used by the model to fit the curve; for example, an edf close to 1 represents a linear effect, whilst an edf close to 2 represents a quadratic effect.

	k	**edf**	**F-value**	**P-value**	**R^2**
Bacterial load	2	1.790	4.038	<0.001	0.253

4 The transition from diet to blood: exploring the insect haemolymph nutrient pool

Acknowledgements:

Experiments were carried out by Robert Holdbrook, Catherine Reavey, Joanna Randall & Yamini Tummala. The data were analysed by Robert Holdbrook. The manuscript was written by Robert Holdbrook with input from Kenneth Wilson.

ABSTRACT

Nutritional status is important for homeostasis and has knock-on effects on the fitness of an organism. However, research into nutrition has largely focused on diet choice, and studies exploring nutrient allocation post-ingestion remain limited to a few species and a narrow range of diets. Here we address this gap by introducing a caterpillar model to investigate haemolymph nutrient interactions resulting from variation in host diet.

Final instar *Spodoptera littoralis* caterpillars were restricted to one of 20 diets varying in protein and carbohydrate ratio and concentration, and their haemolymph macro- and micronutrients were measured 48 h later. The geometric framework for nutrition (GFN) is a multi-dimensional approach used to examine the complex effects of nutrition on the life-history and ecological interactions of an organism. So far, the use of this approach has produced significant progress in our understanding of the mechanisms behind nutrient selection. Utilising the geometric framework approach, we then placed post-digestion nutritional status in a macronutrient space.

As expected, there was a large amount of variation in the abundance of several haemolymph nutrients. Moreover, there was disparity in the amount of variation explained by diet intake within the different nutrient groups. Diet explained variation in haemolymph proteins and carbohydrates, but not lipids. Macronutrient intake played a greater role in regulating the relative proportions of the vital haemolymph nutrient groups, essential amino acids and reducing sugars, rather than their abundance. Principal component analysis revealed two key axes, which contained a mix of sugars and amino acids and varied based on protein intake. Overall, our findings suggest that the relationship between dietary macronutrients and haemolymph nutrients could be better understood from an enantiostatic perspective than a homeostatic one.

4.1 INTRODUCTION

Nutrition affects a range of life-history traits, including longevity (Couteur et al., 2016; Raubenheimer et al., 2016; Solon-Biet et al., 2015), fecundity (Jensen et al., 2015; Moatt et al., 2016), and disease resistance (Kogut and Klasing, 2009; Li et al., 2007; Ponton et al., 2013; Povey et al., 2014, 2009; Trichet, 2010). The field of nutritional ecology aims to disentangle the ecological and evolutionary relationships that impact an animal's nutrient acquisition and subsequent allocation (Raubenheimer and Boggs, 2009). Nutrition is involved in multifaceted interactions with the physiology of an organism, as well as its micro- and macro-organismal community relationships (Raubenheimer et al., 2009). A challenge in this field has been to provide a template for investigations that can capture the complexity of these nutritional interactions (Raubenheimer et al., 2009).

The geometric framework for nutrition (GFN) attempts to do this by using a state-space approach that models trait variation in reaction to changes in an organism's nutrient environment (Raubenheimer et al., 2016, 2009; Simpson and Raubenheimer, 2012). This occurs through the assignment of an optimal dietary intake to a life-history trait, referred to as an intake target, allowing exploration of the mechanisms used by an organism to achieve that target. These mechanisms involve food selection based on internal feedback loops combined with post-ingestive regulation via alterations to digestion and absorption rates in the gut (Simpson and Raubenheimer, 2012). There is a growing body of work that explores and quantifies nutrient requirements across a range of species, including humans (Simpson and Raubenheimer, 2005), non-human vertebrates (Cowieson, 2014; Simpson and Raubenheimer, 2012) and invertebrates (Graham et al., 2014; Ponton et al., 2014; Povey et al., 2014).

In-depth understanding derives from the use of synthetic chemically-defined diets, however these are currently available only for a limited range of species such as locusts, lepidopteran larvae and *Drosophila* flies (Chapman, 2012). To date, most of our knowledge on the mechanisms of post-digestive nutrient regulation in insects comes from experiments using locusts (Harrison et al., 2012; Simpson et al., 2015; Simpson and Raubenheimer, 2012). Nutrients acquired from the diet may be stored in the fat body as proteins, lipid or glycogen, or in the haemolymph (insect blood) as proteins, carbohydrates, phospholipids, sugars or amino acids (Chapman, 2012). An organism may over-ingest certain nutrients to meet their quota for other, more important, nutrients. These over-ingested nutrients are excreted as a final form of regulation (Simpson and Raubenheimer, 2012). Most arthropod studies measure nutritional status via the haemolymph since it can be a non-destructive sampling method, and the nutritional status of the haemolymph is directly influenced by environmental changes (Simpson and Raubenheimer, 1993b).

The haemolymph comprises 20-25% of an organism's water content, rising to about 50% in caterpillars. It serves important functions in physical structure, acts as a reservoir for cell hydration, provides oxygen for metabolism, and regulates pH and osmolality. Immune effectors also depend on haemolymph transportation and so can utilise immediate nutrient stores (Chapman, 2012). Furthermore, metabolised nutrients from the gut, and synthesised nutrients from the fat body, are transported into the haemolymph for use by other tissues (Chapman, 2012; Simpson and Raubenheimer, 1993b). The open circulatory system of the insect haemocoel necessitates the bathing of the internal organs in haemolymph. The nutritional content of the haemolymph must therefore be kept at a high level to provide immediate access for metabolic processes (Thompson, 2003). As a result, organisms must balance nutrient concentration with the

chemical effects of those nutrients on haemolymph fluid dynamics such as volume, osmolality and temperature (reviewed by Beyenbach, 2016). This results in a complex haemolymph nutritional profile containing certain nutrients that are regulated and others that fluctuate freely with dietary intake (Zanotto et al., 1996). Therefore, the nutritional profile of the haemolymph directly influences an organism's homeostatic capacity. However, it is not always possible for organisms to achieve their nutrient requirements (Raubenheimer et al., 2012).

One of the primary focuses of the geometric framework is to understand behavioural responses when animals are unable to meet their intake target (Raubenheimer and Simpson, 2003). By studying the compensatory responses of animals during periods of nutritional imbalance, rules of compromise can be identified. When faced with foods that contain a deficiency of important nutrients or an excess of less important ones, generalist feeders tend to practice an equal distance rule, which involves balancing foods to over-ingest less important nutrients to meet the target for an important nutrient. Specialist feeders tend to follow a closest distance rule, involving nutrient balancing to ingest less important nutrients to a point that minimises the deficiency of the desired nutrient, never actually meeting the intake target for the desired nutrient (Simpson and Raubenheimer, 2005). The notion that, in certain contexts, an organism may not be able to achieve their desired physiological balance led to the development of enantiostasis, an extension of homeostasis. In an enantiostatic system, organisms would not be expected to maintain their internal nutrient levels at a given concentration to achieve homeostasis, but would fluctuate internal nutrients to maintain metabolic and physiological functions (Raubenheimer et al., 2012). In the context of nutritional immunology, such a perturbation could occur during the intensified demands placed on host nutrient resources by an invading pathogen and/or a heightened immune system

during infection (Ponton et al., 2011b). Understanding how organisms use ingested resources could help disentangle the contexts that drive changes between homeostasis to enantiostasis. However, progress in our understanding of these compensatory responses has been hindered by our limited knowledge of nutrient allocation mechanisms, an area in need of exploration since the discovery of nutrition-based trade-offs (Cotter et al., 2011; Kwang Pum Lee et al., 2008).

The Egyptian cotton leafworm, *Spodoptera littoralis*, is a generalist noctuid moth, commonly used as a model insect in nutritional ecology. Previous studies have shown that it regulates its macronutrient intake in response to changes in diet availability (Lee et al., 2004, 2002; Simpson et al., 2004) and infection (Cotter et al., 2011; Lee et al., 2006), but there is still limited information on how dietary intake influences variation in the nutritional properties of the haemolymph in this (Boctor, 1980, 1974) and other species (Ignell et al., 2010; Stabler et al., 2015; Thompson and Redak, 2000). Here, we explore how the macro- and micronutrient composition of the haemolymph varies in response to changes in both the amount and ratio of macronutrients in the diet. Assuming perfect pre- and post-digestive homeostasis, and a single optimal haemolymph composition, we would predict that, regardless of the diets offered to the insects, the nutritional composition of the haemolymph would be invariant across all diets. Deviations from this 'target' may identify constraints on achieving nutritional homeostasis.

4.2 METHODS

4.2.1 Spodoptera caterpillars

4.2.1.1 Insect Culture

The *Spodoptera littoralis* culture was founded in 2002 from eggs collected near Alexandria in Egypt. It is maintained using single pair matings of over 150 pairs per generation. For experiments, larvae were collected in the 2nd instar and reared singly on a semi-artificial wheatgerm-based diet until the start of the final instar (6th). Larvae were kept in 25 ml polypots at 27^{o}C under a 12:12 light:dark regime.

4.2.1.2 Haemolymph collection

Within 24 h of moulting to the 6th instar, 400 larvae were transferred to Petri dishes (90 mm diameter), containing 1.5 g of a chemically-defined diet (Dadd, 1961; Simpson and Abisgold, 1985). A total of 20 diets were used (**Table S4.1**), ranging in protein and carbohydrate concentration (see Cotter et al., 2011; Lee et al., 2004), resulting in a sample size of 20 larvae per diet. After 48 h, the larvae were weighed, and haemolymph was collected using a sterile hypodermic Microlance^{TM} 3 needle into a sterile ice-cooled 1.5 ml Eppendorf tube, which was then stored at -20^{o}C. The diet was weighed to record ingestion rates and replaced daily for the first three days, after which the larvae were transferred to 36.9 ml polypots containing semi-artificial wheatgerm-based diet. All larvae were retained for further life history information.

4.2.2 Macronutrients

4.2.2.1 Protein analysis

Protein was assessed using a method previously described for *S. littoralis* haemolymph by Cotter *et al.*, (2011). Briefly, 4 µl haemolymph samples were diluted in 184 µl sodium cacodylate buffer (pH 7.4), mixed under vortex, and incubated for 1 h at 25^{o}C.

A 5 µl sample was dispensed into a sterile 96-well plate in duplicate with 200 µl Bio-Rad protein reagent. Optical density was measured in a SpectraMax Plus microtiter plate reader (Molecular Devices) at a 360 nm wavelength, and the levels of protein were determined from a standard curve of bovine serum albumin (0 – 1 mg/ml increasing in steps of 0.1) using SoftMax Pro software.

4.2.2.2 Carbohydrate and Lipids

Total levels of carbohydrates were determined using an anthrone test adapted from Kaufmann and Brown (2008). The sugar portion of the haemolymph was first separated from the lipid components. A 5 µl sample of haemolymph was dispensed into a sterile 5 ml glass sample tube containing 40 µl sodium sulphate solution and mixed under vortex. The salt preparation was diluted in 560 µl of 2:1 chloroform:methanol (Folch et al., 1957) and centrifuged at 13,000 rpm for 3 min to remove cell debris. The two layers were separated by addition of 400 µl sterile distilled H_2O and mixing under vortex. The top layer containing the sugar-water-methanol component was isolated for carbohydrate analysis by pipetting to a separate glass tube. The bottom layer containing the lipid-chloroform complex was retained for further analysis (see below). Methanol was removed by heating the glass tubes in a heating block at 100^{o}C until all liquid had evaporated, after which 1 ml of anthrone reagent was added. The anthrone-sugar solutions were heated at 100^{o}C for 17 minutes, cooled and the optical density determined at 625 nm in a SpectraMax Plus microtiter plate reader. The concentration of sugar was determined using the SoftMax Pro software using a standard series of glucose (0, 5, 10, 20, 30, 40 µl of 100 mg/100 ml glucose in sterile distilled water).

After separation from sugars, lipid samples were placed in a fume cupboard to evaporate the chloroform. Samples were then transferred to a heating block at 100^{o}C with 40 µl sulphuric acid (95%) for 10 min. 1 ml volume of vanillin reagent was added

to each tube and mixed under vortex. The tubes were allowed to cool and the optical density determined at 625 nm with a SpectraMax Plus microtiter plate reader. The lipid concentration was calculated using SoftMax Pro software with a standard lipid series (0 – 80 µl of 100 mg/ml vegetable oil in chloroform).

4.2.3 Micronutrients

Here we define micronutrients as free haemolymph sugars and amino acids.

4.2.3.1 Sugar analysis

Sugars were analysed using high performance liquid chromatography (HPLC). Haemolymph samples were diluted with nanopure water (1:10 on average). HPLC was used to measure concentrations of glucose, fructose, sucrose, sorbitol, trehalose, lactose, stachyose and maltose. Analysis was conducted by injecting 20 µl of sample via a Rheodyne valve onto a Carbopac PA-100 column (Dionex, Sunnyvale, California, USA). Sample components were eluted from the column isocratically using 100 mM NaOH flowing at 1 ml/min. The chromatographic profile was recorded using pulsed amperometric detection (ED40 electrochemical detector, Dionex). Elution profiles were analysed using the Chromeleon software package (Thermofisher Scientific). Daily reference curves were obtained for sugars by injecting calibration standards with concentrations of 10 p.p.m. for each sugar.

4.2.3.2 Amino acids

Amino acids were analysed using ultra-high performance liquid chromatography (uHPLC). To extract free amino acids, samples were diluted in 300 µl HPLC-grade methanol (Sigma-Aldrich, Dorset, UK.) and mixed for 60 s in an electrical vortex to extract free amino acids, followed by centrifugation at 13,000 rpm for 5 min. The supernatant was filtered through 0.45 µm syringe-tip filters (Whatman Puradisc 4, nylon

4 mm) to remove particulates and was then analysed for free amino acids. The pellet was analysed for protein-bound amino acids as per Stabler *et al*., (2015). Briefly, the pellet was dried down at 70°C; mixed with 30 µl ± 25 of 6 Mol.L-1 hydrochloric acid (HCl) and briefly vortexed. Sealed tubes were placed in plastic microfuge tube boxes, sealed, and placed in a domestic 900W (2450 MHz) microwave oven inside of a fume hood according to Zhong *et al*., (2005). Samples were irradiated for 15 min on full power, left to cool, and then heated at 70°C in a heat block to evaporate the acid. 300 µl of de-ionised uHPLC gradient grade water was then added to each dried sample, followed by centrifugation and filtration through 0.45 µm syringe-tip filters (Whatman Puradisc 4, nylon, 4 mm). 10 µl of each sample was then quantified by uHPLC. 21 amino acids were quantified in the samples using a Dionex Ultimate 3000 RS system fitted with a 150 x 2.1 mm Accucore RP-MS (Thermo Scientific) column as per Stabler *et al.*, (2015). AA-S-18 amino acid calibration standards supplemented with asparagine, glutamine tryptophan, and γ-aminobutyric acid (GABA), diluted to 2.5 µM using HPLC-grade water were used for comparison.

4.2.4 Data Analysis

Data analysis was performed using the R statistical software (v3.2.2; R Core Team, 2014). To account for variation in nutrient concentrations, data were standardized using the mean (µ) and standard deviation (σ) as per Cotter et al., (2011), allowing comparisons between nutrient groups; a standardized variable (Z) was produced from a nutrient variable (X) using the formula: ($Z = (X-\mu)/\sigma$). There were a large number of explanatory variables to be examined, so principal component analysis (R base) was used to reduce the number of dimensions in the dataset. The *factoextra* package (v1.0.5; Kassambara and Mundt, 2017) was used to examine the output of the analysis and the *corrplot* package (v0.77; Wei and Simko, 2016), used for correlation analysis, allowed

further investigation of the nutrient relationships found. Correlation analysis was based on a correlation matrix created using the Spearman's rank method. Subsequent analysis was carried out using generalized additive models (GAMs) in the *mgcv* package (v1.8; Wood, 2006), which were visualised using thin-plate spline plots using the *fields* package and REML smoothing (Nychka, 2016), following Cotter *et al.*, (2011).

For analysis, sugars were aggregated into reducing (glucose, fructose, lactose and maltose) and non-reducing sugars (sorbitol, stachyose, sucrose and trehalose). This was of interest because alteration of the reduced state of macromolecules, such as sugars and amino acids, plays a crucial homeostatic function in the insect haemolymph (Chapman, 2012; Rockstein, 2012; Thompson, 2003). Amino acids were also aggregated into essential and non-essential amino acids, since the essential amino acids can only be obtained from diet, but are necessary for protein synthesis in all animals, including insects (Chapman, 2012; Karowe and Martin, 1989; O'Brien et al., 2002).

4.2.4.1 GAMs

GAMs are a nonparametric form of regression analysis that utilize the sum of iterative estimates to calculate a smoothing function, rather than assuming a linear function, as in linear models (Hastie and Tibshirani, 1990). When smoothed models were compared to linear models, the former generally explained more variation (data not shown), making them the preferred choice for analysis. An information theoretic approach was taken to analyse the data (Whittingham et al., 2006), which allows the selection of multiple candidate models accounting for how much variation each explains based on the Akaike information criterion (AIC; Burnham and Anderson, 2004). Six models were compared: a 'Null' model, a protein model (P), a carbohydrate model (C), a model containing both protein and carbohydrate (P+C), a model containing protein, carbohydrate and an

interaction between the two (P*C) and a model representing diet as a 20-level factor (Diet). AIC analysis was carried out using the *MuMIn* package (v1.15; Bartoń, 2018) in R, which when combined with the *mgcv* package, ranks models based on the degrees of freedom used to create the smoothed curve.

4.3 RESULTS

4.3.1 Effect of diet eaten on haemolymph macronutrients

The amount of protein and carbohydrate consumed by *S. littoralis* larvae depended on the relative amounts of these two macronutrients in the diet (**Tables 4.1,4.2**), with protein intake peaking in a nutrient space containing a mid-to-high level of dietary protein and low level of dietary carbohydrate (**Figure 4.1a**), and carbohydrate intake peaking at mid-to-high level of dietary carbohydrate and low levels of dietary protein (**Figure 4.1b**)

Haemolymph protein levels tended to increase linearly with dietary protein intake (**Figure 4.1c; Table 4.3**). In contrast, haemolymph carbohydrate levels were much less dependent on dietary carbohydrate levels, with variation in haemolymph carbohydrate explained by a combined effect of protein and carbohydrate intake (**Table 4.4a**), with a peak in haemolymph carbohydrate at a mid-level carbohydrate intake and a low level of protein intake (**Figure 4.1d**).

Although lipid levels have been found to increase with dietary carbohydrates in *S. littoralis* (Lee et al., 2002), we found no significant relationship (**Figure S4.1**; **Table 4.5**).

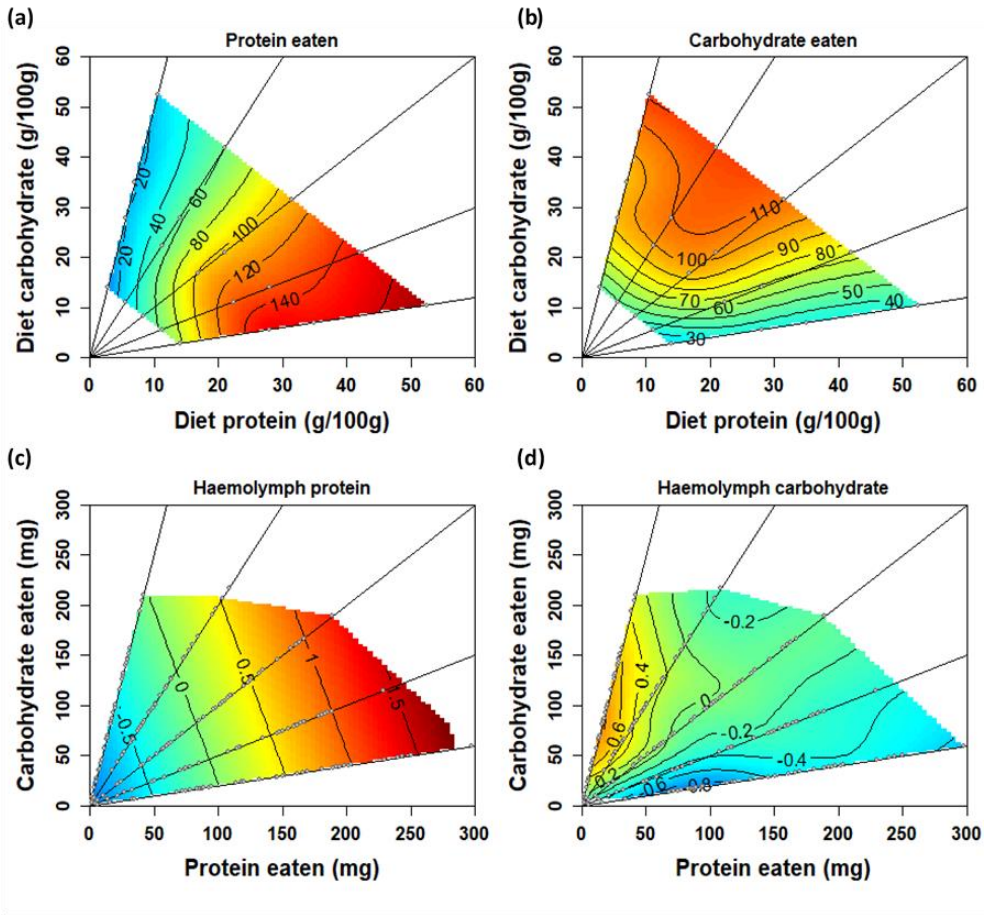

Figure 4.1: The relationship between dietary macronutrients, diet eaten and haemolymph macronutrients. 2D Contour plot comparing various variables (z) with carbohydrate eaten (y) and protein eaten (x) simultaneously. Straight lines originating at 0 represent nutrient rails with grey dots showing the nutrient space created by macronutrient intake. Contour lines represent the type of relationship between the dependent variable and the two independent variables. Colour represents the strength of effect, with blue indicating the weakest effect going up to red which represents the strongest effect. Variables: (a) Protein eaten, (b) Carbohydrate eaten, (c) Haemolymph protein, (d) Haemolymph carbohydrate.

Table 4.1: Protein eaten model summary table. (a) AIC model comparison table. m0 (Null) is a model with no explanatory terms included, providing a baseline measure of variation. m1 (Protein) is a model containing the total amount of protein in the diet (g/100g). m2 (Carbs) is a model containing the total amount of carbohydrate in the diet (g/100g). m3 (Protein + Carbs) is a model containing both protein and carbohydrate. m4 (Protein * Carbs) is a model that includes an interaction term (represented by asterisk) between dietary protein and carbohydrate. m5 (Diet) is a model containing diet as a factorial variable. df is the degrees of freedom used by the model to produce a fit and not the degrees of freedom based on the number of explanatory variables. K is the number of terms in the model. AICc is the model Aikake values. Delta represents the difference between a model and the model explaining the most variation. Weight is determined by the amount of variation a model explains penalized for the degrees of freedom used by the model. (b) Summary information for each model in the AIC comparison table. The edf provides information about the shape of the curve, relating to the basis dimensions used by the model to fit the curve; for example, an edf close to 1 represents a linear effect, whilst an edf close to 2 represents a quadratic effect.

(a) Model AICs: Protein eaten

Model	df	k	AICc	delta	weight	R^2
m3 *Protein + Carbs*	7	2	2063.3	0.000	0.685	0.598
m4 *Protein * Carbs*	9	3	2064.8	1.552	0.315	0.602
m1 *Protein*	5	1	2083.6	20.313	0.000	0.550
m5 *Diet*	21	0	2084.0	20.682	0.000	0.591
m2 *Carbs*	3	1	2218.4	155.088	0.000	0.105
m0 *Null*	2	0	2239.6	176.265	0.000	0.000

(b) Protein eaten model summaries

Model	edf	F-value	P-value
m1			
Protein	2.651	60.714	0.000
m2			
Carbs	0.960	5.861	0.000
m3			
Protein +	2.752	60.720	0.000
Carbs	1.880	5.899	0.000
m4			
Protein +	2.445	25.889	0.000
Carbs +	1.509	1.609	0.000
*Protein * Carbs*	1.831	0.388	0.060

Table 4.2: Carbohydrate eaten model summary tables. (a) AIC model comparison table. m0 (Null) is a model with no explanatory terms included, providing a baseline measure of variation. m1 (Protein) is a model containing the total amount of protein in the diet (g/100g). m2 (Carbs) is a model containing the total amount of carbohydrate in the diet (g/100g). m3 (Protein + Carbs) is a model containing both protein and carbohydrate. m4 (Protein * Carbs) is a model that includes an interaction term (represented by asterisk) between dietary protein and carbohydrate. m5 (Diet) is a model containing diet as a factorial variable. df is the degrees of freedom used by the model to produce a fit and not the degrees of freedom based on the number of explanatory variables. K is the number of terms in the model. AICc is the model Aikake values. Delta represents the difference between a model and the model explaining the most variation. Weight is determined by the amount of variation a model explains penalized for the degrees of freedom used by the model. (b) Summary information for each model in the AIC comparison table. The edf provides information about the shape of the curve, relating to the basis dimensions used by the model to fit the curve; for example, an edf close to 1 represents a linear effect, whilst an edf close to 2 represents a quadratic effect.

(a) Model AICs: Carbohydrate eaten

Model	df	k	AICc	delta	weight	R^2
m3 *Protein + Carbs*	7	2	2038.39	0.000	0.631	0.420
m4 *Protein * Carbs*	9	3	2039.55	1.160	0.353	0.423
m2 *Carbs*	5	1	2046.03	7.646	0.014	0.388
m5 *Diet*	21	0	2050.22	11.835	0.002	0.432
m1 *Protein*	4	1	2132.96	94.569	0.000	0.049
m0 *Null*	2	0	2140.24	101.853	0.000	0.000

(b) Carbohydrate eaten model summaries

Model	edf	F-value	P-value
m1			
Protein	1.014	21.115	0.003
m2			
Carbs	2.771	31.566	0.000
m3			
Protein +	1.866	2.514	0.004
Carbs	2.880	31.691	0.000
m4			
Protein +	0.002	0.000	0.189
Carbs +	2.023	15.245	0.000
*Protein * Carbs*	3.763	1.659	0.002

Table 4.3: Haemolymph protein model summary tables. (a) AIC model comparison table. m0 (Null) is a model with no explanatory terms included, providing a baseline measure of variation. m1 (Protein) is a model containing the total amount of protein eaten in 48 h (mg). m2 (Carbs) is a model containing the total amount of carbohydrate eaten in 48 h (mg). m3 (Protein + Carbs) is a model containing both protein and carbohydrate. m4 (Protein * Carbs) is a model that includes an interaction term (represented by asterisk) between protein and carbohydrate eaten. m5 (Diet) is a model containing diet as a factorial variable. df is the degrees of freedom used by the model to produce a fit and not the degrees of freedom based on the number of explanatory variables. K is the number of terms in the model. AICc is the model Aikake values. Delta represents the difference between a model and the model explaining the most variation. Weight is determined by the amount of variation a model explains penalized for the degrees of freedom used by the model. (b) Summary information for each model in the AIC comparison table. The edf provides information about the shape of the curve, relating to the basis dimensions used by the model to fit the curve; for example, an edf close to 1 represents a linear effect, whilst an edf close to 2 represents a quadratic effect.

(a) Model AICs: Protein						
Model	**df**	**k**	**AICc**	**delta**	**weight**	**R^2**
m3 *Protein + Carbs*	4	2	398.52	0.000	0.523	0.362
m4 *Protein * Carbs*	7	3	399.39	0.876	0.338	0.371
m1 *Protein*	3	1	401.17	2.655	0.139	0.341
m5 *Diet*	20	0	433.36	34.841	0.000	0.303
m2 *Carbs*	2	1	466.29	67.775	0.000	0.020
m0 *Null*	2	0	468.48	69.966	0.000	0.000

(b) Protein model summaries			
Model	**edf**	**F-value**	**P-value**
m1			
Protein	1.014	21.115	0.000
m2			
Carbs	0.773	0.849	0.038
m3			
Protein +	0.989	21.887	0.000
Carbs	1.452	1.288	0.029
m4			
Protein +	0.967	7.200	0.000
Carbs +	0.000	0.000	0.336
*Protein * Carbs*	3.105	0.942	0.028

Table 4.4: Haemolymph carbohydrate model summary tables. (a) AIC model comparison table. m0 (Null) is a model with no explanatory terms included, providing a baseline measure of variation. m1 (Protein) is a model containing the total amount of protein in the diet (g/100g). m2 (Carbs) is a model containing the total amount of carbohydrate eaten in 48 h (mg). m3 (Protein + Carbs) is a model containing both protein and carbohydrate. m4 (Protein * Carbs) is a model that includes an interaction term (represented by asterisk) between protein and carbohydrate eaten. m5 (Diet) is a model containing diet as a factorial variable. df is the degrees of freedom used by the model to produce a fit and not the degrees of freedom based on the number of explanatory variables. K is the number of terms in the model. AICc is the model Aikake values. Delta represents the difference between a model and the model explaining the most variation. Weight is determined by the amount of variation a model explains penalized for the degrees of freedom used by the model. (b) Summary information for each model in the AIC comparison table. The edf provides information about the shape of the curve, relating to the basis dimensions used by the model to fit the curve; for example, an edf close to 1 represents a linear effect, whilst an edf close to 2 represents a quadratic effect.

(a) Model AICs: Carbohydrate

Model	df	k	AICc	delta	weight	R^2
m5 *Diet*	20	0	389.43	0.000	0.841	0.337
m3 *Protein + Carbs*	8	2	392.82	3.388	0.155	0.246
m4 *Protein * Carbs*	9	3	400.20	10.771	0.004	0.217
m1 *Protein*	4	1	409.92	20.487	0.000	0.123
m2 *Carbs*	4	1	421.69	32.259	0.000	0.045
m0 *Null*	2	0	425.92	36.490	0.000	0.000

(b) Carbohydrate model summaries

Model	edf	F-value	P-value
m1			
Protein	2.184	5.181	0.000
m2			
Carbs	1.699	1.753	0.016
m3			
Protein +	2.833	8.763	0.000
Carbs	2.836	5.373	0.000
m4			
Protein +	1.005	1.001	0.014
Carbs +	0.527	0.278	0.082
*Protein * Carbs*	4.645	2.102	0.000

Table 4.5: Haemolymph lipid model summary tables. (a) AIC model comparison table. m0 (Null) is a model with no explanatory terms included, providing a baseline measure of variation. m1 (Protein) is a model containing the total amount of protein in the diet (g/100g). m2 (Carbs) is a model containing the total amount of carbohydrate eaten in 48 h (mg). m3 (Protein + Carbs) is a model containing both protein and carbohydrate. m4 (Protein * Carbs) is a model that includes an interaction term (represented by asterisk) between protein and carbohydrate eaten. m5 (Diet) is a model containing diet as a factorial variable. df is the degrees of freedom used by the model to produce a fit and not the degrees of freedom based on the number of explanatory variables. K is the number of terms in the model. AICc is the model Aikake values. Delta represents the difference between a model and the model explaining the most variation. Weight is determined by the amount of variation a model explains penalized for the degrees of freedom used by the model. (b) Summary information for each model in the AIC comparison table. The edf provides information about the shape of the curve, relating to the basis dimensions used by the model to fit the curve; for example, an edf close to 1 represents a linear effect, whilst an edf close to 2 represents a quadratic effect.

(a) Model AICs: Lipid						
Model	**df**	**k**	**AICc**	**delta**	**weight**	**R^2**
m0 *Null*	2	0	389.04	0.000	0.216	0.000
m1 *Protein*	2	1	389.04	0.001	0.216	0.000
m3 *Protein + Carbs*	2	2	389.30	0.260	0.190	0.005
m2 *Carbs*	2	1	389.30	0.260	0.190	0.005
m4 *Protein * Carbs*	2	3	389.30	0.260	0.190	0.005
m5 *Diet*	20	0	408.53	19.491	0.000	0.042

(b) Lipid model summaries			
Model	**edf**	**F-value**	**P-value**
m1 *Protein*	0.000	0.000	0.883
m2 *Carbs*	0.402	0.168	0.198
m3 *Protein + Carbs*	0.000 0.402	0.000 0.168	0.710 0.198
m4 *Protein + Carbs + Protein * Carbs*	0.000 0.402 0.000	0.000 0.168 0.000	0.715 0.198 0.666

4.3.2 Haemolymph micronutrient concentration

Lysine was the most abundant amino acid in *S. littoralis* haemolymph (34% relative abundance) **(Table 4.6a)**. This was followed by histidine (14%), serine (11%), alanine (10%) and arginine (6%), with the remaining 16 amino acids found in much lower abundances (<5%), which together comprised less than 25% of the circulating haemolymph amino acid pool. Of the ten essential amino acids (EAAs) for animals (Karowe and Martin, 1989; Rock and King, 1967), only lysine, histidine and arginine appeared amongst the most abundant amino acids. The other EAAs comprised 14.7% of the haemolymph amino acid pool, with only methionine and tryptophan present at less than a 1% concentration. This meant that more than two-thirds of the haemolymph amino acid constituents (68.7%) are EAAs obtained directly from dietary protein (Chapman, 2012; Karowe and Martin, 1989; O'Brien et al., 2002), establishing a strong link between diet and haemolymph amino acids. Overall, haemolymph EAA concentration was significantly greater than non-EAA concentration across the various diets (paired t-test, $t = -2.191$, $df = 19$, $P = 0.021$).

Although most previous studies have established trehalose to be the dominant sugar in insect haemolymph (Chapman, 2012; Saito, 1963; Thompson, 2003), we found glucose (39% relative abundance) to be the most abundant haemolymph sugar (**Table 4.6b**), with trehalose being the second most abundant sugar (27%), followed by fructose (14%) and lactose (14%). Together, the remaining sugars (sorbitol, sucrose, stachyose and maltose), comprised less than 10% of the total haemolymph sugar pool. Of these sugars, 66.8% were reducing sugars (glucose, fructose, maltose and lactose) and 33.2% were non-reducing sugars (trehalose, sucrose, sorbitol and stachyose).

Table 4.6: Mean concentrations of haemolymph micronutrients

(a) Amino acids		
Amino Acid	**Mean (±se) (nmol/ml)**	**Proportion of total abundance**
Lysine	533.03 (±66.96)	0.34
Histidine	288.64 (±34.90)	0.14
Serine	198.08 (±24.05)	0.11
Alanine	178.96 (±20.62)	0.10
Arginine	91.67 (±14.80)	0.06
Glycine	90.22 (±8.05)	0.04
Threonine	79.40 (±12.45)	0.04
Valine	61.56 (±8.84)	0.04
Leucine	53.61 (±5.92)	0.03
Cystine	46.88 (±4.93)	0.03
Proline	24.89 (±9.00)	0.01
Methionine	21.43 (±4.60)	0.01
Isoleucine	20.20 (±2.36)	0.01
Phenylalanine	15.73 (±1.81)	0.01
Aspartate	10.57 (±4.19)	0.01
Tyrosine	9.99 (±1.69)	0.00
Glutamate	4.84 (±0.53)	0.00
Glutamine	0.17 (±0.02)	0.00
Asparagine	0.02 (±0.00)	0.00
Tryptophan	0.01 (±0.00)	0.00

(b) Simple sugars		
Sugar	**Mean (±se) (nmol/ml)**	**Proportion of total abundance**
Glucose	1059.86 (±197.24)	0.39
Trehalose	738.21 (±186.82)	0.27
Fructose	395.40 (±73.91)	0.14
Lactose	375.55 (±68.36)	0.14
Sorbitol	195.30 (±36.51)	0.03
Sucrose	60.96 (±14.68)	0.02
Stachyose	35.52 (±8.29)	0.01
Maltose	21.00 (±13.11)	0.00

4.3.3 Effect of diet intake on key nutrient groups

After determining the relative abundances of the various amino acids and sugars, the next step was to establish whether physiologically important nutrients varied with the composition of diet or were regulated. Therefore, the new variables essential and non-essential amino acids, and reducing and non-reducing sugars were created by aggregating their constituent nutrients. Essential amino acids are important because they cannot be synthesised by insects and must be obtained from diet, while reducing and non-reducing sugars are important because their balance is key to haemolymph homeostasis (Chapman, 2012).

Diet intake was an extremely poor indicator of variation in haemolymph nutrient groups (**Figure 4.2**; **Tables 4.7 – 4.10**). Within the groups examined, diet intake explained only 6% variation in essential amino acids ($P = 0.024$; **Table 4.7**), with essential amino acid concentration peaking at a middling amount of protein intake (~100 mg) and decreasing when more or less protein was eaten in the same time period (**Figure 4.2a**).

Based on the importance of nutrient ratios in diet presented to *S. littoralis* larvae (Lee et al., 2002), and the notion that haemolymph homeostasis is maintained by altering the reducing state of sugars (Chapman, 2012), it was hypothesised that diet intake may also alter the proportions of nutrients within the haemolymph. To test this hypothesis, variation in the proportions of haemolymph essential amino acids and reducing sugars was analysed with respect to macronutrient intake (**Figure 4.3**; **Tables 4.11 & 4.12**). Diet explained more variation in haemolymph micronutrient ratios than it had in their absolute concentrations. The ratios of both essential amino acids and reducing sugars increased with increasing protein intake (**Figure 4.3**), although protein intake explained more variation in the proportions of essential amino acids ($R^2 = 0.189$; **Table 4.11a**)

than in the proportion of reducing sugars (R^2 = 0.137; **Table 4.12a**). In both cases, a non-significant relationship with carbohydrate intake also explained a small amount of variation (R^2 < 0.01; P < 0.05; **Tables 4.11b & 4.12b**).

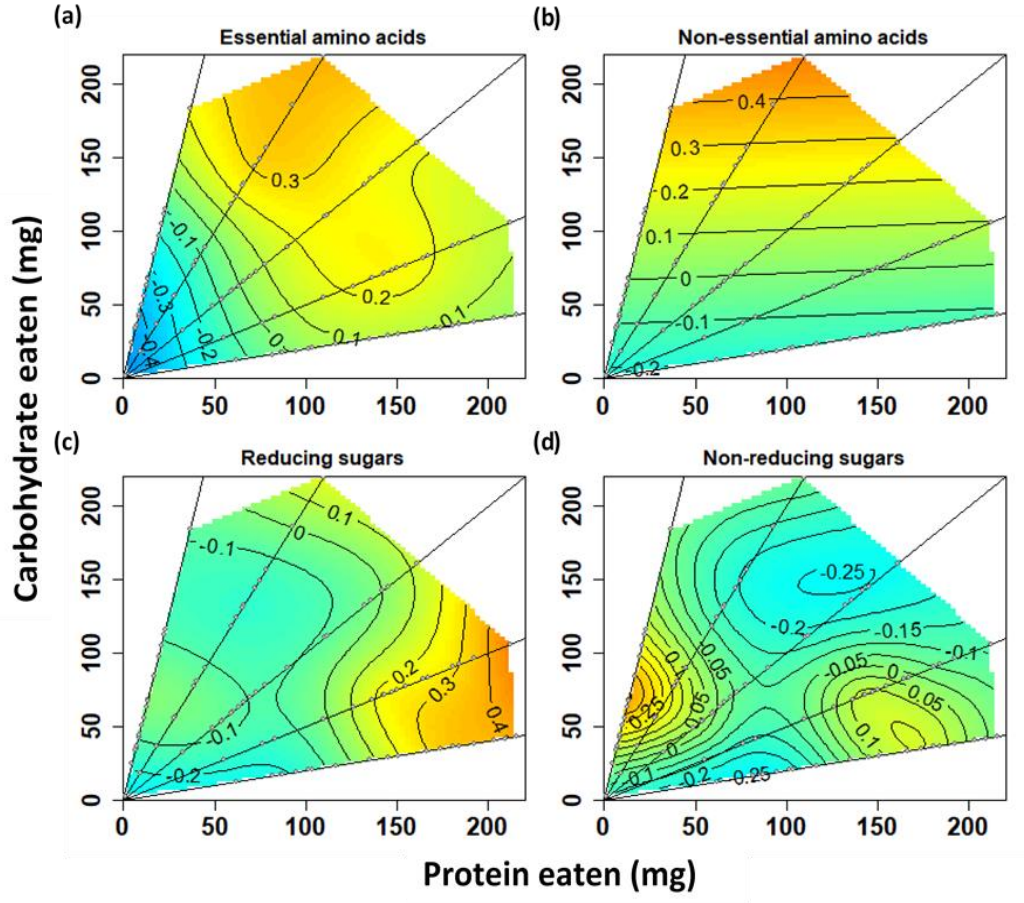

Figure 4.2: The relationship between macronutrient intake and key micronutrient groups. 2D Contour plot comparing various variables (z) with carbohydrate eaten (y) and protein eaten (x) simultaneously. Straight lines originating at 0 represent nutrient rails with grey dots showing the nutrient space created by macronutrient intake. Contour lines represent the type of relationship between the dependent variable and the two independent variables. Colour represents the strength of effect, with blue indicating the weakest effect going up to red which represents the strongest effect. Variables: (a) Essential amino acids, (b) Non-essential amino acids, (c) Reducing sugars, (d) Non-reducing sugars.

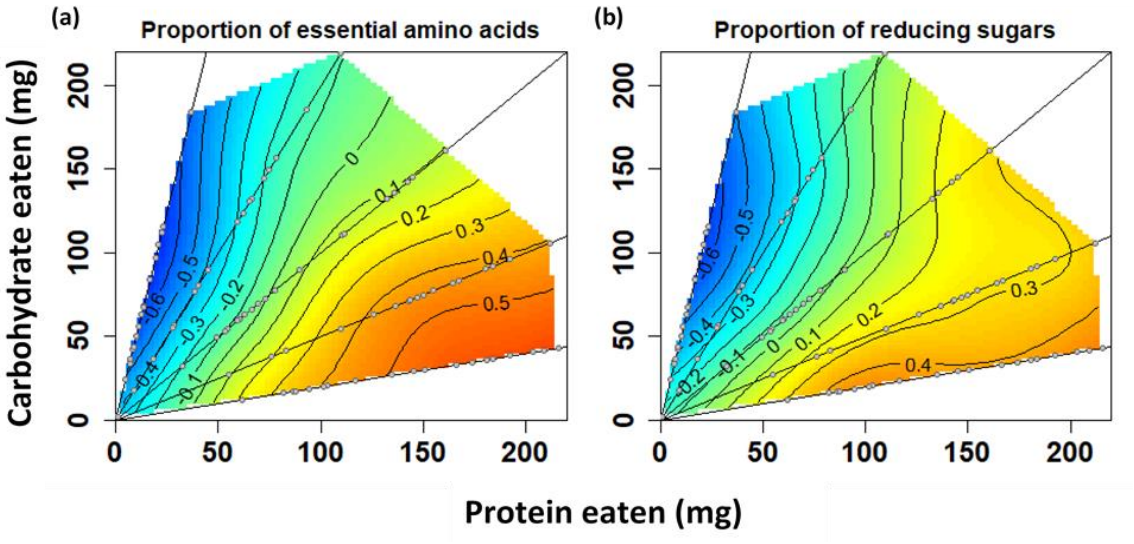

Figure 4.3: The relationship between dietary macronutrients and the proportions of key nutrient groups. 2D Contour plot comparing various variables (z) with carbohydrate eaten (y) and protein eaten (x) simultaneously. Straight lines originating at 0 represent nutrient rails with grey dots showing the nutrient space created by macronutrient intake. Contour lines represent the type of relationship between the dependent variable and the two independent variables. Colour represents the strength of effect, with blue indicating the weakest effect going up to red which represents the strongest effect. Variables: (a) Proportion of essential amino acids (b) Proportion of reducing sugars.

Table 4.7: Haemolymph essential amino acids model summary tables. (a) AIC model comparison table. m0 (Null) is a model with no explanatory terms included, providing a baseline measure of variation. m1 (Protein) is a model containing the total amount of protein in the diet (g/100g). m2 (Carbs) is a model containing the total amount of carbohydrate eaten in 48 h (mg). m3 (Protein + Carbs) is a model containing both protein and carbohydrate. m4 (Protein * Carbs) is a model that includes an interaction term (represented by asterisk) between protein and carbohydrate eaten. m5 (Diet) is a model containing diet as a factorial variable. df is the degrees of freedom used by the model to produce a fit and not the degrees of freedom based on the number of explanatory variables. K is the number of terms in the model. AICc is the model Aikake values. Delta represents the difference between a model and the model explaining the most variation. Weight is determined by the amount of variation a model explains penalized for the degrees of freedom used by the model. (b) Summary information for each model in the AIC comparison table. The edf provides information about the shape of the curve, relating to the basis dimensions used by the model to fit the curve; for example, an edf close to 1 represents a linear effect, whilst an edf close to 2 represents a quadratic effect.

(a) Model AICs: Essential amino acids

Model	df	k	AICc	delta	weight	R^2
m1 *Protein*	3	1	272.28	0.000	0.355	0.060
m3 *Protein + Carbs*	3	2	272.28	0.001	0.355	0.060
m4 *Protein * Carbs*	5	3	273.87	1.588	0.160	0.070
m0 *Null*	2	0	275.56	3.277	0.069	0.000
m2 *Carbs*	2	1	275.83	3.548	0.060	0.007
m5 *Diet*	20	0	284.96	12.679	0.001	0.184

(b) Essential amino acids model summaries

Model	edf	F-value	P-value
m1 *Protein*	1.582	1.515	0.023
m2 *Carbs*	0.409	0.173	0.196
m3 *Protein + Carbs*	1.582 0.000	1.515 0.000	0.023 0.488
m4 *Protein + Carbs + Protein * Carbs*	1.325 0.000 1.127	0.810 0.000 0.178	0.030 0.573 0.200

Table 4.8: Haemolymph non-essential amino acids model summary tables. (a) AIC model comparison table. m0 (Null) is a model with no explanatory terms included, providing a baseline measure of variation. m1 (Protein) is a model containing the total amount of protein in the diet (g/100g). m2 (Carbs) is a model containing the total amount of carbohydrate eaten in 48 h (mg). m3 (Protein + Carbs) is a model containing both protein and carbohydrate. m4 (Protein * Carbs) is a model that includes an interaction term (represented by asterisk) between protein and carbohydrate eaten. m5 (Diet) is a model containing diet as a factorial variable. df is the degrees of freedom used by the model to produce a fit and not the degrees of freedom based on the number of explanatory variables. K is the number of terms in the model. AICc is the model Aikake values. Delta represents the difference between a model and the model explaining the most variation. Weight is determined by the amount of variation a model explains penalized for the degrees of freedom used by the model. (b) Summary information for each model in the AIC comparison table. The edf provides information about the shape of the curve, relating to the basis dimensions used by the model to fit the curve; for example, an edf close to 1 represents a linear effect, whilst an edf close to 2 represents a quadratic effect.

(a) Model AICs: Non-essential amino acids

Model	df	k	AICc	delta	weight	R^2
m2 *Protein*	2	1	275.54	0.000	0.201	0.012
m3 *Protein + Carbs*	2	2	275.54	0.000	0.201	0.012
m4 *Protein * Carbs*	2	3	275.54	0.000	0.201	0.012
m0 *Null*	2	0	275.56	0.020	0.199	0.000
m1 *Protein*	2	1	275.56	0.020	0.199	0.000
m5 *Diet*	20	0	294.27	18.734	0.000	0.101

(b) Non-essential amino acids model summaries

Model	edf	F-value	P-value
m1			
Protein	0.000	0.000	0.813
m2			
Carbs	0.532	0.284	0.147
m3			
Protein +	0.000	0.000	0.927
Carbs	0.532	0.284	0.147
m4			
Protein +	0.000	0.000	0.714
Carbs +	0.532	0.284	0.147
*Protein * Carbs*	0.000	0.000	0.635

Table 4.9: Haemolymph reducing sugars model summary tables. (a) AIC model comparison table. m0 (Null) is a model with no explanatory terms included, providing a baseline measure of variation. m1 (Protein) is a model containing the total amount of protein in the diet (g/100g). m2 (Carbs) is a model containing the total amount of carbohydrate eaten in 48 h (mg). m3 (Protein + Carbs) is a model containing both protein and carbohydrate. m4 (Protein * Carbs) is a model that includes an interaction term (represented by asterisk) between protein and carbohydrate eaten. m5 (Diet) is a model containing diet as a factorial variable. df is the degrees of freedom used by the model to produce a fit and not the degrees of freedom based on the number of explanatory variables. K is the number of terms in the model. AICc is the model Aikake values. Delta represents the difference between a model and the model explaining the most variation. Weight is determined by the amount of variation a model explains penalized for the degrees of freedom used by the model. (b) Summary information for each model in the AIC comparison table. The edf provides information about the shape of the curve, relating to the basis dimensions used by the model to fit the curve; for example, an edf close to 1 represents a linear effect, whilst an edf close to 2 represents a quadratic effect.

(a) Model AICs: Reducing sugars

Model	df	k	AICc	delta	weight	R^2
m0 *Null*	2	0	275.56	0.000	0.206	0.000
m2 *Carbs*	2	1	275.56	0.000	0.206	0.000
m1 *Protein*	3	1	275.65	0.094	0.196	0.021
m3 *Protein + Carbs*	3	2	275.65	0.095	0.196	0.021
m4 *Protein * Carbs*	3	3	275.65	0.095	0.196	0.021
m5 *Diet*	21	0	302.89	27.326	0.000	0.017

(b) Reducing sugars model summaries

Model	edf	F-value	P-value
m1 *Protein*	0.989	0.514	0.130
m2 *Carbs*	0.000	0.000	0.787
m3 *Protein + Carbs*	0.989 0.000	0.514 0.000	0.130 0.738
m4 *Protein + Carbs + Protein * Carbs*	0.989 0.000 0.000	0.514 0.000 0.000	0.130 0.779 0.409

Table 4.10: Haemolymph non-reducing sugars model summary tables. (a) AIC model comparison table. m0 (Null) is a model with no explanatory terms included, providing a baseline measure of variation. m1 (Protein) is a model containing the total amount of protein in the diet (g/100g). m2 (Carbs) is a model containing the total amount of carbohydrate eaten in 48 h (mg). m3 (Protein + Carbs) is a model containing both protein and carbohydrate. m4 (Protein * Carbs) is a model that includes an interaction term (represented by asterisk) between protein and carbohydrate eaten. m5 (Diet) is a model containing diet as a factorial variable. df is the degrees of freedom used by the model to produce a fit and not the degrees of freedom based on the number of explanatory variables. K is the number of terms in the model. AICc is the model Aikake values. Delta represents the difference between a model and the model explaining the most variation. Weight is determined by the amount of variation a model explains penalized for the degrees of freedom used by the model. (b) Summary information for each model in the AIC comparison table. The edf provides information about the shape of the curve, relating to the basis dimensions used by the model to fit the curve; for example, an edf close to 1 represents a linear effect, whilst an edf close to 2 represents a quadratic effect.

(a) Model AICs: Non-reducing sugars						
Model	**df**	**k**	**AICc**	**delta**	**weight**	**R^2**
m0 *Null*	2	0	275.56	0.000	0.230	0.000
m2 *Carbs*	2	1	275.56	0.000	0.230	0.000
m1 *Protein*	2	1	275.56	0.001	0.230	0.000
m3 *Protein + Carbs*	2	2	275.56	0.002	0.230	0.000
m4 *Protein * Carbs*	5	3	277.68	2.120	0.080	0.026
m5 *Diet*	20	0	298.39	22.826	0.000	0.062

(b) Non-reducing sugars model summaries			
Model	**edf**	**F-value**	**P-value**
m1			
Protein	0.000	0.000	0.587
m2			
Carbs	0.000	0.000	0.640
m3			
Protein	0.000	0.000	0.592
Carbs	0.001	0.000	0.389
m4			
Protein	0.000	0.000	0.665
Carbs	0.000	0.000	0.631
*Protein * Carbs*	1.855	0.322	0.228

Table 4.11: Proportion of haemolymph essential amino acids model summary tables. (a) AIC model comparison table. m0 (Null) is a model with no explanatory terms included, providing a baseline measure of variation. m1 (Protein) is a model containing the total amount of protein in the diet (g/100g). m2 (Carbs) is a model containing the total amount of carbohydrate eaten in 48 h (mg). m3 (Protein + Carbs) is a model containing both protein and carbohydrate. m4 (Protein * Carbs) is a model that includes an interaction term (represented by asterisk) between protein and carbohydrate eaten. m5 (Diet) is a model containing diet as a factorial variable. df is the degrees of freedom used by the model to produce a fit and not the degrees of freedom based on the number of explanatory variables. K is the number of terms in the model. AICc is the model Aikake values. Delta represents the difference between a model and the model explaining the most variation. Weight is determined by the amount of variation a model explains penalized for the degrees of freedom used by the model. (b) Summary information for each model in the AIC comparison table. The edf provides information about the shape of the curve, relating to the basis dimensions used by the model to fit the curve; for example, an edf close to 1 represents a linear effect, whilst an edf close to 2 represents a quadratic effect.

(a) Model AICs: Proportion of essential amino acids

Model	df	k	AICc	delta	weight	R^2
m3 *Protein + Carbs*	5	2	260.99	0.000	0.475	0.189
m1 *Protein*	4	1	261.70	0.704	0.334	0.162
m4 *Protein * Carbs*	7	3	262.82	1.823	0.191	0.198
m0 *Null*	2	0	275.56	14.566	0.000	0.000
m2 *Carbs*	2	1	275.78	14.783	0.000	0.001
m5 *Diet*	21	0	278.75	17.751	0.000	0.235

(b) Proportion of essential amino acids model summaries

Model	edf	F-value	P-value
m1			
Protein	1.856	4.598	0.000
m2			
Carbs	0.109	0.029	0.315
m3			
Protein +	1.966	5.222	0.000
Carbs	1.029	0.691	0.072
m4			
Protein +	1.073	0.776	0.011
Carbs +	0.000	0.000	0.337
*Protein * Carbs*	2.969	0.791	0.038

Table 4.12: Proportion of haemolymph reducing sugars model summary tables. (a) AIC model comparison table. m0 (Null) is a model with no explanatory terms included, providing a baseline measure of variation. m1 (Protein) is a model containing the total amount of protein in the diet (g/100g). m2 (Carbs) is a model containing the total amount of carbohydrate eaten in 48 h (mg). m3 (Protein + Carbs) is a model containing both protein and carbohydrate. m4 (Protein * Carbs) is a model that includes an interaction term (represented by asterisk) between protein and carbohydrate eaten. m5 (Diet) is a model containing diet as a factorial variable. df is the degrees of freedom used by the model to produce a fit and not the degrees of freedom based on the number of explanatory variables. K is the number of terms in the model. AICc is the model Aikake values. Delta represents the difference between a model and the model explaining the most variation. Weight is determined by the amount of variation a model explains penalized for the degrees of freedom used by the model. (b) Summary information for each model in the AIC comparison table. The edf provides information about the shape of the curve, relating to the basis dimensions used by the model to fit the curve; for example, an edf close to 1 represents a linear effect, whilst an edf close to 2 represents a quadratic effect.

(a) Model AICs: Proportion of reducing sugars

Model	df	k	AICc	delta	weight	R^2
m3 *Protein + Carbs*	5	2	258.96	0.000	0.517	0.137
m1 *Protein*	4	1	260.37	1.414	0.255	0.098
m4 *Protein * Carbs*	6	3	260.76	1.803	0.210	0.138
m2 *Carbs*	3	1	267.03	8.071	0.009	0.025
m0 *Null*	2	0	267.05	8.094	0.009	0.000
m5 *Diet*	20	0	277.68	18.721	0.000	0.183

(b) Proportion of reducing sugars model summaries

Model	edf	F-value	P-value
m1			
Protein	1.628	2.486	0.003
m2			
Carbs	1.118	0.581	0.129
m3			
Protein +	1.679	2.842	0.001
Carbs	1.312	0.973	0.054
m4			
Protein +	0.719	0.640	0.014
Carbs +	0.199	0.055	0.156
*Protein * Carbs*	2.548	0.691	0.032

4.3.4 Effect of diet on correlating haemolymph micronutrients

Diet explained a limited amount of variation in nutrient groups, so the next question was whether diet explains more variation once nutrients are organized by their functional importance. Due to the large number of variables being tested, it was important to reduce the number of dimensions being examined. First, the least abundant amino acids and sugars were aggregated, creating the new variables, 'minor sugars' and 'minor amino acids'. Further reduction in the number of variables to be analysed was achieved through principal component analysis, which, being based on a covariance matrix, would aggregate nutrients that interact in the haemolymph.

Analysis revealed two principal components with an eigenvalue greater than 1, and together they captured 78% of the variation within the dataset (**Table 4.13**). The first principal component (PC1), which alone represented almost 60% of the total variation, correlated positively with the haemolymph sugars, and the amino acids histidine and alanine. Correlation analysis (**Figure 4.4; Green zone**) revealed these two amino acids to have the strongest correlations with haemolymph sugars, explaining the grouping of PC1. The second principal component (PC2), which explained 19% of the total variation, correlated negatively with the amino acids, lysine, serine and alanine, but positively with the sugars, glucose and lactose. Correlation analysis revealed strong intra-correlations between amino acids (**Figure 4.4; Yellow zone**) and even stronger intra-correlation between sugars (**Figure 4.4; Red zone**). Glucose showed the strongest correlations with amino acids (**Figure 4.4; Green zone**).

Having established the covariances within and between amino acid and sugar groups, the next step was to investigate the explanatory power of dietary intake on the variation found within the principal components. Variation in both principal components

correlated strongly with protein intake (**Figure 4.5**), which explained more variation in PC2 (R^2 = 0.215; **Table 4.15a**) than PC1 (R^2 = 0.091; **Table 4.14a**). Furthermore, PC1 increased linearly with protein intake (edf = 0.836, P = 0.017; **Table 4.14b**), whilst PC2 only increased at protein intake above 150mg, producing a non-linear relationship (edf = 2.859, P = 0.003; **Table 4.15b**). Finally, there was also a significant interaction (P = 0.038; **Table 4.15b**) between protein and carbohydrate intake, which produced a second (smaller) peak in PC2 (**Figure 4.5b**).

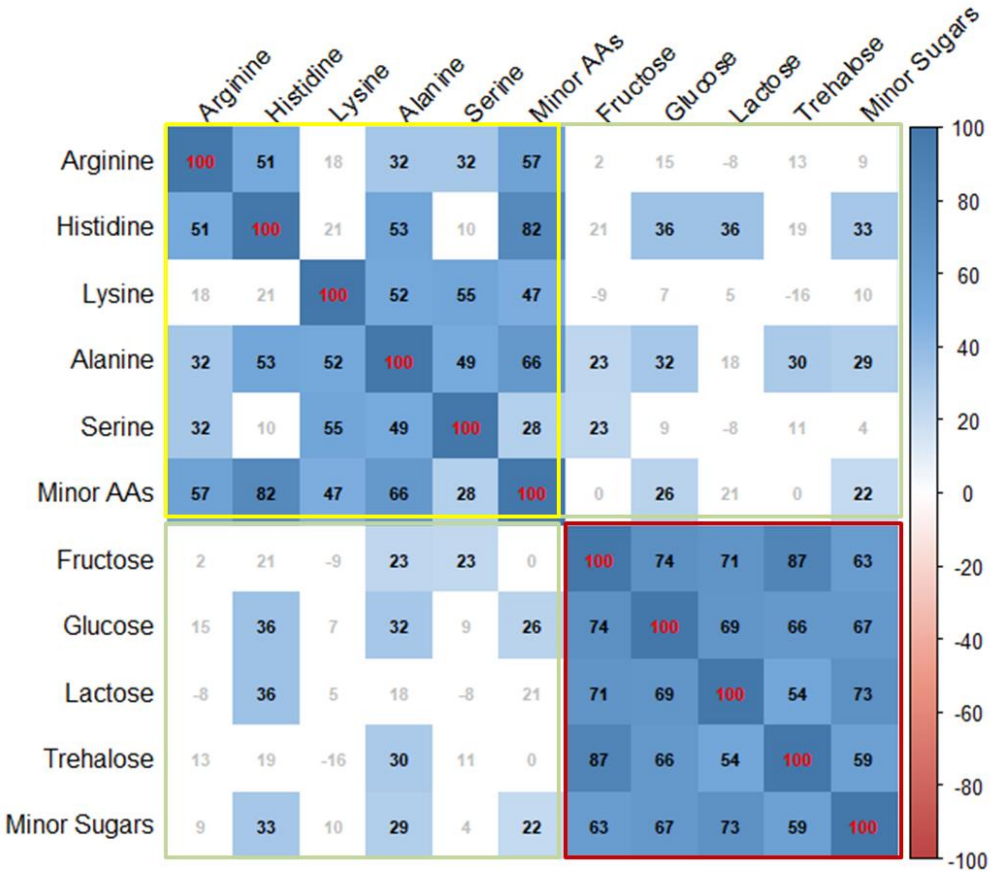

Figure 4.4: Correlation plot comparing haemolymph micronutrients. The values shown are the Spearman's rank correlations coefficients, represented as percentages. Only statistically significant correlations ($P < 0.05$) are coloured. As shown by the colour bar on the right, colour tone matches the strength of correlations. Yellow zone: amino acids. Red zone: sugars. Green zone: correlations between sugars and amino acids.

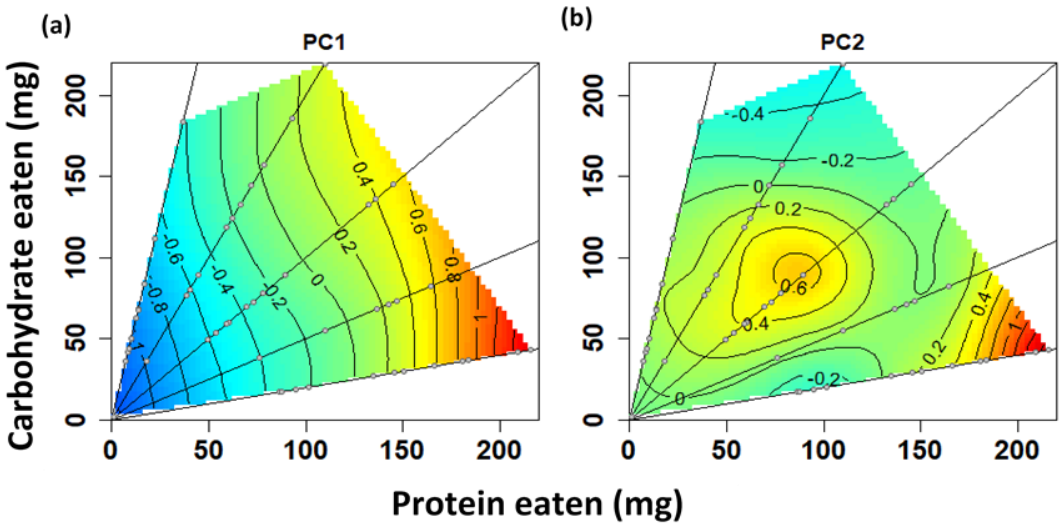

Figure 4.5: The relationship between macronutrient intake and micronutrient principal components. 2D Contour plot comparing various variables (z) with carbohydrate eaten (y) and protein eaten (x) simultaneously. Straight lines originating at 0 represent nutrient rails with grey dots showing the nutrient space created by macronutrient intake. Contour lines represent the type of relationship between the dependent variable and the two independent variables. Colour represents the strength of effect, with blue indicating the weakest effect going up to red which represents the strongest effect. Variables: (a) Principal component 1, (b) Principal component 2.

Table 4.13: Primary principal components. The two principal components that explained more variation in the overall dataset than individual micronutrient variables (eigenvalue > 1). The table shows the factor loadings of the micronutrients within each principal component. Variable loadings with a percentage contribution higher than the expected average contribution for each principal component are shown in bold. These variables are considered as important contributing variables to the principal component.

	PC1	**PC2**
Eigenvalue	*4.30*	*1.348*
% of total variance	*58.95*	*18.50*
Standard deviation	*2.07*	*1.16*
	Loading	**Loading**
Arginine	0.01	-0.07
Histidine	**0.32**	0.03
Lysine	0.20	**-0.58**
Alanine	0.25	**-0.44**
Serine	0.12	**-0.33**
Minor amino acids	0.16	-0.19
Fructose	**0.31**	0.26
Glucose	**0.40**	**0.31**
Lactose	**0.44**	0.28
Trehalose	0.19	0.19
Minor sugars	**0.51**	-0.15

Table 4.14: Principal Component 1 model summary tables. (a) AIC model comparison table. m0 (Null) is a model with no explanatory terms included, providing a baseline measure of variation. m1 (Protein) is a model containing the total amount of protein in the diet (g/100g). m2 (Carbs) is a model containing the total amount of carbohydrate eaten in 48 h (mg). m3 (Protein + Carbs) is a model containing both protein and carbohydrate. m4 (Protein * Carbs) is a model that includes an interaction term (represented by asterisk) between protein and carbohydrate eaten. m5 (Diet) is a model containing diet as a factorial variable. df is the degrees of freedom used by the model to produce a fit and not the degrees of freedom based on the number of explanatory variables. K is the number of terms in the model. AICc is the model Aikake values. Delta represents the difference between a model and the model explaining the most variation. Weight is determined by the amount of variation a model explains penalized for the degrees of freedom used by the model. (b) Summary information for each model in the AIC comparison table. The edf provides information about the shape of the curve, relating to the basis dimensions used by the model to fit the curve; for example, an edf close to 1 represents a linear effect, whilst an edf close to 2 represents a quadratic effect.

(a) Model AICs: PC1

Model	df	k	AICc	delta	weight	R^2
m1 *Protein*	2	1	211.88	0.000	0.301	0.091
m3 *Protein + Carbs*	2	2	211.88	0.000	0.301	0.091
m4 *Protein * Carbs*	2	3	211.88	0.000	0.301	0.091
m0 *Diet*	1	0	215.50	3.621	0.049	0.000
m2 *Carbs*	2	1	215.50	3.621	0.049	0.000
m5 *Null*	20	0	254.77	42.887	0.000	0.093

(b) PC1 model summaries

Model	edf	F-value	P-value
m1 *Protein*	0.836	1.275	0.017
m2 *Carbs*	0.000	0.000	0.846
m3 *Protein +* *Carbs*	0.836 0.000	1.275 0.000	0.017 0.739
m4 *Protein +* *Carbs +* *Protein * Carbs*	0.836 0.000 0.000	1.275 0.000 0.000	0.017 0.739 0.490

Table 4.15: Principal Component 2 model summary tables. (a) AIC model comparison table. m0 (Null) is a model with no explanatory terms included, providing a baseline measure of variation. m1 (Protein) is a model containing the total amount of protein in the diet (g/100g). m2 (Carbs) is a model containing the total amount of carbohydrate eaten in 48 h (mg). m3 (Protein + Carbs) is a model containing both protein and carbohydrate. m4 (Protein * Carbs) is a model that includes an interaction term (represented by asterisk) between protein and carbohydrate eaten. m5 (Diet) is a model containing diet as a factorial variable. df is the degrees of freedom used by the model to produce a fit and not the degrees of freedom based on the number of explanatory variables. K is the number of terms in the model. AICc is the model Aikake values. Delta represents the difference between a model and the model explaining the most variation. Weight is determined by the amount of variation a model explains penalized for the degrees of freedom used by the model. (b) Summary information for each model in the AIC comparison table. The edf provides information about the shape of the curve, relating to the basis dimensions used by the model to fit the curve; for example, an edf close to 1 represents a linear effect, whilst an edf close to 2 represents a quadratic effect.

(a) Model AICs: PC2

Model	df	k	AICc	delta	weight	R^2
m1 *Protein*	5	1	115.64	0.000	0.533	0.215
m3 *Protein + Carbs*	6	2	116.61	0.966	0.329	0.242
m4 *Protein * Carbs*	9	3	118.73	3.090	0.114	0.275
m0 *Diet*	1	0	123.18	7.542	0.012	0.000
m2 *Carbs*	3	1	123.22	7.580	0.012	0.048
m5 *Null*	20	0	149.38	33.737	0.000	0.294

(b) PC2 model summaries

Model	edf	F-value	P-value
m1			
Protein	2.859	3.484	0.003
m2			
Carbs	1.211	0.649	0.125
m3			
Protein +	2.842	3.331	0.004
Carbs	1.054	0.439	0.187
m4			
Protein +	1.910	2.270	0.001
Carbs +	0.000	0.000	0.227
*Protein * Carbs*	3.492	0.977	0.038

4.4 DISCUSSION

The main aim of this study was to increase our understanding of post-ingestive nutrient regulation following the consumption of diets varying in their macronutrient profiles. Our findings reflected the difficulty of addressing this issue. We identified the most abundant haemolymph amino acids and sugars across 20 diets ingested, which strongly correlated with each other. However, rather than a clear-cut image of certain nutrient groups fluctuating with diet or not, the relationship between dietary nutrients and haemolymph nutrients was more easily understood by thinking about *how* nutrients fluctuated with diet. For example, a stronger influence of diet was found on the proportions of important nutrient groups, such as EAAs vs non-EAAs and reducing vs non-reducing sugars, than on their concentrations. Exploring the idea of nutrient groups based on functionality rather than physiological importance, we identified two principal components that together captured 78% of the variation in the haemolymph micronutrient profile, both of which contained a mixture of amino acids and sugars and correlated with larval protein intake. Overall, our results indicate that although haemolymph nutrient levels respond to variation in the intake of both proteins and carbohydrates, protein appears to be the more important dietary component.

4.4.1 Proteins and other macronutrients

Our findings reflected previous studies on this species, showing that protein is regulated pre-ingestively and there is a high conversion of ingested protein into haemolymph protein resources (Cotter et al., 2011; Lee et al., 2002). It appears that haemolymph carbohydrate levels are also balanced depending on dietary protein levels, since protein intake explained more variation in this haemolymph nutrient than carbohydrate intake. Although *S. littoralis* sensilla respond to changes in both sugar and amino acid content

of the diet (Simmonds et al., 1992), they may be more sensitive to amino acids (Lee et al., 2002). Similarly, *Locusta migratoria* showed stronger compensatory feeding in response to dietary protein than to dietary carbohydrates (Simpson and Abisgold, 1985). The prioritization of amino acids can be ascribed to the insect's need to accumulate protein (Chown and Nicolson, 2004; Lee et al., 2002; O'Brien et al., 2002; Zanotto et al., 1996); *S. littoralis* adults are nectar feeders restricted to carbohydrate-dominated diets (Chapman and Boer, 2012), and so must build protein reserves at the larval stage.

Haemolymph lipids were anticipated to correlate with dietary carbohydrate in a similar way to haemolymph carbohydrates, since both nutrients are synthesised from ingested carbohydrates (Chapman 2012). Moreover, a previous study on this species found that dietary carbohydrates were converted directly into lipids in pupae (Lee et al. 2002). However, lipid levels in the haemolymph were low and not correlated with dietary properties, possibly due to the fat body being the preferred storage location. Observations of haemolymph lipid properties may require direct manipulation of dietary lipids since studies in orthopteran species such as the Texas field cricket, *Gryllus texensis* (Adamo et al., 2010), and the Australian plague locust, *Chortoicetes terminifera* (Graham et al., 2015), have found variation in lipid content attributable to diet.

4.4.2 Regulation of micronutrients

Diet could not explain variation in the grouped reducing and non-reducing sugars. This may be due to the tight regulation of micronutrient levels by insects to modulate their effects on homeostatic factors, such as haemolymph pH and osmolality (Abisgold and Simpson, 1988; Thompson, 2003; Wyatt, 1961). Reducing sugars, such as glucose, must be regulated due to their toxicity at high concentrations (Boctor 1974; Kerkut 2013).

However, trehalose (the primary non-reducing sugar) is stored in the haemolymph as a crucial carbohydrate reserve, utilised in periods of stress such as flight or starvation (Saito 1963; Thompson 2003), and is not normally regulated (Raubenheimer et al., 2012). Since the haemolymph macronutrients were strongly correlated with diet, this may suggest that the regulation of individual nutrients does not extend to complexes. Dietary carbohydrates are initially converted to glycogen and lipids, before the breakdown and manufacture of sugars (Chapman, 2012). Correspondingly, diet explained more variation in complex carbohydrates than in simple sugars. The fact that protein intake increased the proportion of reducing sugars implies that the breakdown of complex carbohydrates to simple sugars and vice versa may be used to balance changes in haemolymph EAA levels. At high dietary protein, more reducing sugars may be produced to balance excess amino acids, whereas low protein intake and the consequent lower amino acid levels may cause homeostatic imbalances, which the organism corrects by producing non-reducing sugars.

Although micronutrients are abundant in insect haemolymph, their profile varies depending on species and diet (Pant and Agrawal, 1964; Wyatt, 1961). Consequently, it was of interest to determine which nutrients were dominant across the range of diets we explored and how tightly these were regulated. Our results differ from previous studies on *S. littoralis*, which measured the levels of sugars (Boctor, 1974) and amino acids (Boctor, 1980) in the haemolymph of insects reared on castor oil leaves. Boctor (1980) found asparagine to be the most abundant amino acid whilst our study identified this to be lysine, and the primary sugar identified by Boctor (1974) was trehalose, rather than glucose (our primary haemolymph sugar). Although the results of Boctor (1974) correspond with the general view of trehalose as the principal insect sugar (Thompson, 2003), the study only considered a single diet. Whilst haemolymph trehalose levels were higher than glucose

levels on a number of our diets, the broad range of diets explored here makes a strong case for glucose being the principal haemolymph sugar in this species. However, our findings may be due to our choice of sucrose as the primary source of dietary carbohydrates; sucrose is broken down into glucose and fructose. Furthermore, a study by Wyatt *et al.* (1956) failed to identify the presence of trehalose in their examination of *Bombyx mori* haemolymph, highlighting variation of haemolymph sugar content in this insect order (Wyatt, 1961). The implication of these results is a move away from envisioning a single maximum nutrient that is homeostatically maintained, towards dynamic nutrient levels that vary with nutrient availability in the diet. However, our studies and those of Boctor, do not consider the role of feeding intervals, which is important since nutrient concentrations change depending on the time since the last meal (Abisgold and Simpson, 1987).

4.4.3 Towards an enantiostatic profile

The haemolymph nutrient profile is determined through a combination of environmental conditions such as diet availability and temperature, and internal conditions such as physiological state and metabolic demands (Thompson and Redak, 2000). The resulting profile forms part of a feedback loop that regulates feeding behaviour, including nutrient selection (Simpson et al., 2015; Thompson and Redak, 2000; Waldbauer and Friedman, 1991). The number of factors influencing internal nutrient state and the importance of acquired nutrients for physiological activity results in a dynamic picture of haemolymph nutrients (Simpson et al., 2015; Thompson and Redak, 2000), which is poorly reflected in models investigating homeostasis. Homeostasis prioritises the maintenance of an internal physical state, and so homeostatic models provide a binary picture of how regulation or non-regulation of nutrients contribute to maintaining

internal balance (Raubenheimer et al., 2012). Enantiostatic models capture the variation in haemolymph nutrients better than a traditional homeostatic perspective, by considering the importance in nutrient fluctuations in achieving overall physiological stability (Thompson and Redak, 2000). Hence, enantiostatic theory dictates that there is an importance in considering how nutrient variation might contribute to homeostasis at a higher behavioural level based on the functions of the nutrients within the system (Raubenheimer et al., 2012; Thompson and Redak, 2000).

Correlation analysis, which provided an idea of nutrient co-variation across the nutrient space investigated, presented a distinction between sugars and amino acids. Sugars generally showed stronger intra-correlations than amino acids, possibly due to the origins of the latter creating disparities within its subgroups; the EAAs are derived entirely from dietary protein, whereas the non-EAAs are derived from various sources, including sugars (O'Brien et al., 2002). For example, serine, can be synthesised in the fat body using glucose or glycogen (Chapman, 2012; Karowe and Martin, 1989; O'Brien et al., 2002). This might explain why diet intake corresponded to a significant amount of variation in EAA concentration, but not the concentration of non-EAAs. The positive correlation observed between EAAs and protein ingested was not surprising, since the haemolymph amino acid pool is crucial for protein synthesis (Kerkut, 2013). Moreover, certain individual EAAs perform important roles in feeding regulation. Simpson et al., (1991) identified 8 amino acids that inhibit excess feeding in protein-deprived locusts. Amongst these were lysine and serine, our most abundant haemolymph EAA and non-EAA. Out of the haemolymph sugars, glucose exhibited the greatest number of correlations with amino acids, possibly due to glucose production from amino acids via gluconeogenesis (Le Gall and Behmer, 2014; Thompson, 2000). The shared function of amino acids and sugars in homeostatic roles, such as

osmoregulation (Chapman, 2012; Rockstein, 2012; Thompson, 2003), provides the possibility for interactions between these macromolecules in the haemolymph.

The groupings of micronutrients within each of our principal components supports the idea that sugars covary positively with amino acids when more protein is ingested. Arginine was the only haemolymph amino acid not correlated with either of the primary principal components. The role of this EAA in infection (Kraaijeveld et al., 2011) may result in control of its variability in the haemolymph. The first principal component consisted of the primary reducing sugars, and the amino acids histidine and alanine. The proportion of these reducing sugars (relative to non-reducing sugars) also increased with protein intake. The second principal component (PC2) also showed a positive increase at high levels of dietary protein, however this axis negatively correlated with the amino acids, lysine, alanine and serine. This implies that along this axis, excess intake of protein leads to a reduction in the levels of these amino acids. This is not the first study to identify a negative relationship between amino acid levels and excess protein intake: Zanotto et al., (1994) found that locusts maintained on a high-protein, low-carbohydrate diet selectively excreted large amounts of EAAs, especially lysine, which was the most abundant EAA in the locust frass. Excreting these amino acids inhibits the feeling of satiation, allowing the locusts to continue eating to gain limiting carbohydrate. Serine was one of the 8 key amino acids identified by Simpson et al. (1991) for dietary regulation. It may have evolved to play its key role due to the ability of animals to synthesise this non-EAA from both proteins and carbohydrates (Chapman, 2012). This aligns it with alanine, another amino acid that has already been determined to be crucial in gluconeogenic pathways (Thompson et al., 2001; Zanotto et al., 1996). Altogether, an insect's ability to synthesise non-EAAs from various sources might produce the significant interaction found between proteins and carbohydrates in explaining variation

in PC2. By measuring the amino acid profile of larval frass on the various diets, it may be possible to determine whether the excess EAAs are eliminated by excretion (Simpson et al., 1991; Zanotto et al., 1994).

Overall, our results show that more variation in micronutrient levels could be explained by diet intake when the functional similarities of nutrients were analysed based on natural covariation, than when the nutrients were grouped by homeostatic importance. A clear example of this was the added variation explained when the *proportions* of reducing and non-reducing sugars were analysed rather than their *concentrations*. The idea of diet explaining more variation from the perspective of enantiostasis rather than homeostasis could be explored further by investigating the identified nutrient effects in the context of starvation or an infection.

4.4.4 Conclusion

In summary, this study emphasises the role of diet in modulating the balance of key haemolymph nutrients. The use of a large range of diets allowed comparisons to be made between haemolymph nutrients, and the role of diet in explaining variation in nutrient groupings. Overall, this investigation combined the depth and breadth provided by various studies to develop our understanding of how dietary regulation affects haemolymph nutrient availability. One issue to be addressed in future studies is the lack of variation observed in haemolymph lipids. Since the importance of this nutrient has been established in other insect species, a more directed approach may provide further insights into nutrient regulation in lepidopteran larvae. Further direct manipulation of the nutrients identified to covary may also reveal how individual nutrients are regulated (statically or dynamically), in response to diet availability.

4.5 SUPPLEMENTARY MATERIAL

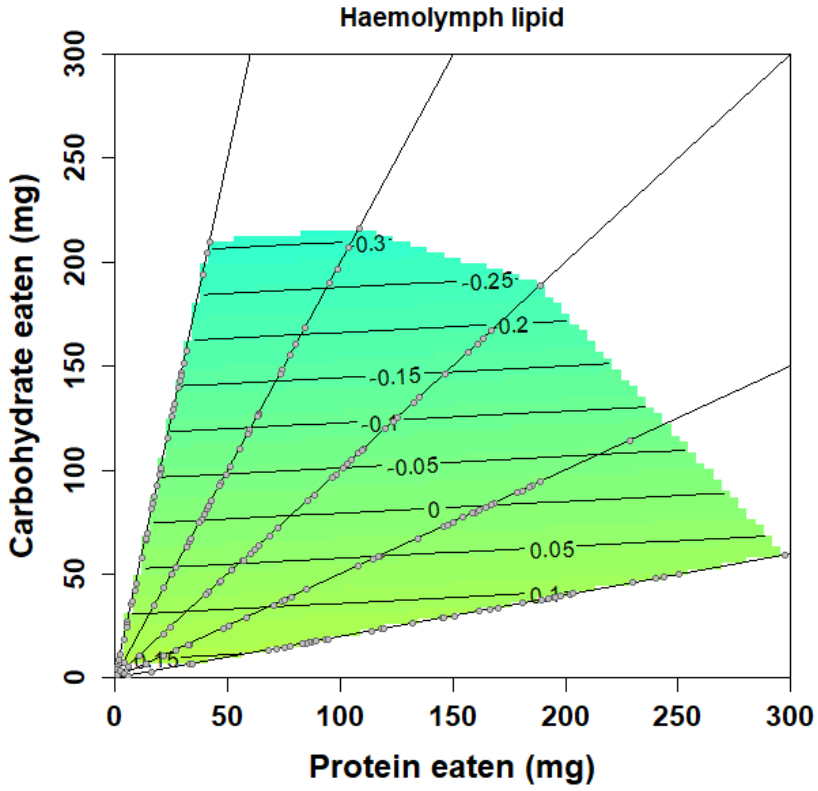

Figure S4.1: The relationship between dietary macronutrients and haemolymph lipid. 2D Contour plot comparing haemolymph lipid (z) with carbohydrate eaten (y) and protein eaten (x) simultaneously. Straight lines originating at 0 represent nutrient rails with grey dots showing the nutrient space created by macronutrient intake. Contour lines represent the type of relationship between the dependent variable and the two independent variables. Colour represents the strength of effect, with blue indicating the weakest effect going up to red which represents the strongest effect. The yellow, green range of colours in the figure indicates there are no significant effects.

Table S4.1: Twenty diets fed to *Spodoptera littoralis* caterpillars varying in their ratios and concentrations of protein and carbohydrate.

Diet.no	P:C		P:C ratio	conc	ratio prot	%prot	%carb
1	10.5 : 52.5		1:5	63	0.17	10.5	52.5
2	7:35		1:5	42	0.17	7	35
3	5.6 : 28		1:5	33.6	0.17	5.6	28
4	2.8 :14		1:5	16.8	0.17	2.8	14
5	21:42		1:2	63	0.33	21	42
6	14:28		1:2	42	0.33	14	28
7	11.2 : 22.4		1:2	33.6	0.33	11.2	22.4
8	5.6 : 11.2		1:2	16.8	0.33	5.6	11.2
9	31.5 : 31.5		1:1	63	0.50	31.5	31.5
10	21:21		1:1	42	0.50	21	21
11	16.8 : 16.8		1:1	33.6	0.50	16.8	16.8
12	8.4 : 8.4		1:1	16.8	0.50	8.4	8.4
13	42 : 21		2:1	63	0.67	42	21
14	28:14		2:1	42	0.67	28	14
15	22.4 : 11.2		2:1	33.6	0.67	22.4	11.2
16	11.2 : 5.6		2:1	16.8	0.67	11.2	5.6
17	52.5 : 10.5		5:1	63	0.83	52.5	10.5
18	35:7		5:1	42	0.83	35	7
19	28 : 5.6		5:1	33.6	0.83	28	5.6
20	14 : 2.8		5:1	16.8	0.83	14	2.8

5 *Xenorhabdus nematophila*: a model for pathogen growth in an *in vitro* host environment

Acknowledgments:

Experiments were carried out and the data were analysed by Robert Holdbrook. The manuscript was written by Robert Holdbrook with input from Kenneth Wilson.

ABSTRACT

Resource availability shapes the outcome of host-pathogen interactions. Increasingly, diet composition is seen as more significant in determining host fitness than total calorie content alone. Whilst the availability of resources has known impacts on pathogen growth *in vitro*, studies lack comparability with *in vivo* systems due to limitations in approach. It is therefore essential to our understanding of the nutritional constraints on host-pathogen interactions that pathogen growth is examined in representative host scenarios *in vitro* and *in vivo*.

Here, we present a model insect-bacteria system to examine growth of a pathogen (*Xenorhabdus nematophila*) in synthetic host blood resources, and a method for tractable bacterial growth in an insect host, the cotton leafworm *Spodoptera littoralis*. First, *S. littoralis* haemolymph nutrient levels were determined from hosts reared on a series of 20 chemically-defined diets ranging in their protein-carbohydrate (P:C) ratio and caloric density. Next, haemolymph nutrient levels were replicated in a series of synthetic haemolymphs to determine the performance of bacteria across the measured host nutrient range.

Bacterial fitness peaked in nutrient space dominated by carbohydrates, and protein concentration negatively impacted bacterial carrying capacity. By examining the resources available to the pathogen within the host, we have established a tractable model system for examining the role that nutrition plays in the host-pathogen interaction. In future work, this model host-pathogen system can be used to test a range of nutritionally-driven processes, including competition during co-infection and interactions with the host microbiome.

5.1 INTRODUCTION

Nutritional immunology explores the role of nutrient availability in the delicate balance between hosts and their commensal and pathogenic microbiota (Pernice et al., 2014; Ponton et al., 2013; Povey et al., 2014). Linking biotic interactions such as parasitism, mutualism and competition with the abiotic environment allows encapsulation of ecological network properties and, by extension, species interactions (Chagnon et al., 2016; Mills and Marchant-Forde, 2010). Studying resource variation allows the isolation and quantification of these 'bottom up' effects on population densities from the 'top down' effects, such as predation and competition, that have classically been viewed as primary ecosystem drivers (Letnic and Dickman, 2010). As a result, there has been a lot of research focusing on behavioural, physiological and ecological changes that equip organisms to adapt to variation in resource availability (Kussell and Leibler, 2005). Investigating nutrient acquisition behaviours, such as foraging, that affect population dynamics (Lafferty et al., 2015) has revealed a central function of the microbial environment in regulating the energetic requirements of complex organisms (Bernardo and Singer, 2017; Simpson and Raubenheimer, 2012).

Nutritional immunological research has revealed a therapeutic response in insects, whereby hosts make dietary alterations in response to infection to increase fitness (Adamo, 2008; Poissonnier et al., 2018; Singer et al., 2014). Symbiotic microbes rely on their host environment for nutrient acquisition (Bernardo and Singer, 2017), making them susceptible to variation in the within-host nutritional profile, and compelling the use of adaptation mechanisms for survival (Chubukov and Sauer, 2014). The short generation time of microbes makes them an ideal model for the study of trait variation in fluctuating environments (Litchman et al., 2015; New et al., 2014). Furthermore, microbes show high plasticity and rapid adaptation to environmental stresses (Kussell

and Leibler, 2005). For example, the model bacterium *Escherichia coli* senses fluxes in the nutrient environment through the Pta-AckA pathway (Richards and Goodrich-Blair, 2009), allowing the expression of different phenotypes during nutrient limitation (Chubukov et al., 2014; Chubukov and Sauer, 2014). Measuring population attributes, such as growth rate and carrying capacity, from the microbial perspective can therefore provide information on the variability of the host environment (Begon et al., 2005), clarifying how this shapes host-parasite relationships.

Nutritional Geometry (NG) is a state-space nutritional approach towards the analysis of organismal nutritional requirements. A highlight of this approach is the identification of an 'intake target' representing a nutrient balance that maximises fitness (Raubenheimer et al., 2016; Simpson and Raubenheimer, 2012). The Geometric Framework (GF) approach differs from the parallel nutrition investigative framework, Environmental Stoichiometry (ES) due to its focus on the energetic/non-energetic components of food (mainly macromolecules such as proteins and vitamins) rather than simple elements (such as Nitrogen and Carbon) (Sperfeld et al., 2016). NG has so far been applied to vertebrates and invertebrates of various taxa, revealing the role of the macronutrients protein, lipids and carbohydrates in the optimisation of various fitness traits such as immunity and fecundity (reviewed by Simpson and Raubenheimer, 2012). Conversely, the strength of the ES approach in revealing nutrient flows in varying environments (Sperfeld et al., 2016) has made it the *a priori* choice for microbial investigations. Microbes adapted to a certain resource environment may show poor performance on alternative resources (Litchman et al., 2015; Pulkkinen et al., 2018), hence microbes can also express intake targets. Although identification of nutrient optima is important for *in vitro* mass culture, studies investigating microbial nutrient-use usually involve batch cultures with generic media containing multiple nutrients that are varied simultaneously

(e.g. Pulkkinen et al., 2018) or modification of a single dietary component (Bowen et al., 2012; Kooliyottil et al., 2014).

The genera *Xenorhabdus* and *Photorhabdus* comprise gram-negative bacteria belonging to the family enterobacteriaceae that have symbiotic relationships with entomopathogenic nematodes of the families *Steinernematidae* and *Heterorhabditidae* (Boemare et al., 1993). These bacteria are widely used as models due to their dual role as commensals and pathogens, a variable range of host species, and their importance for biological pest control (Nielsen-LeRoux et al., 2012; Richards and Goodrich-Blair, 2009; Stilwell et al., 2018). Infective juvenile (IJ) nematodes carrying the bacteria either in special intestinal formation called the receptacle (Steinernematidae; Snyder et al., 2007), or throughout the intestinal tract (Heterorhadbitidae), actively seek out and infiltrate lepidopteran larvae through cavities such as the mouth and anus (Akhurst, 1980; Boemare et al., 1993). The nematodes protect the bacteria during the early stages of infection by inhibiting antimicrobial peptide production by the host until the bacteria are released into the haemolymph (Gotz et al., 1981; Nielsen-LeRoux et al., 2012). Haemolymph entry triggers the bacterial production of virulence factors that suppress both the cellular and humoral immune responses (Park et al., 2006). *Xenorhabdus nematophilus*, one of the most studied species in these genera, has been shown to suppress host phenoloxidase activity (Dunphy and Webster, 1991), nodulation (Ji and Kim, 2004; Park et al., 2003), and antimicrobial peptide production (da Silva et al., 2000; Ji and Kim, 2004). Pathogenicity, the first of three infection phases, is followed by host disintegration (Richards and Goodrich-Blair, 2009). During the latter stages of host mortality, an increase in environmental iron levels causes up-regulation of the fliZ gene, a part of the FLiAZ operon, that encodes flagellar motility and virulence genes (Lanois et al., 2008). These genes code for lipases, proteases and haemolysins that break down the insect cadaver into a nutrient-rich resource, as well as antibiotics to reduce

competition from other microbes (Jubelin et al., 2011; Lanois et al., 2008). The final infection stage involves re-association with its nematode host (Richards and Goodrich-Blair, 2009).

X. nematophila is an ideal microbe for the study of pathogen resource utilization due to its intimacy with its host environment. Lacking an external environmental phase limits the genetic adaptation that might occur were it to be exposed to environments highly variable in their resource availability (New et al., 2014). Moreover, nutrition plays a key role in the transition of the bacterial-nematode complex from mutualistic to pathogenic. A low haemolymph iron level is the primary signal for the *Steinernerma* to defaecate *Xenorhabdus*, which enters the exponential growth phase associated with increased virulence (Nielsen-LeRoux et al., 2012). The infective juveniles that had entered the host begin maturation during a high nutrient environment created by the bacterium and depletion of nutrients combined with increased density signals the formation of pre-IJ nematodes that take-up their bacterial symbionts before exiting the host (Chaston et al., 2013; Stilwell et al., 2018).

Invertebrate nutritional self-medication, such as the beetle *Tenebrio molitor* increasing their carbohydrate intake when infected with the rat tapeworm *Hymnolepis diminuta* (Ponton et al., 2011a), has been characterized in several nutritional immunological studies. This host response alters the nutritional environment in favour, or to the detriment, of pathogen fitness. Higher host protein diets increased sporulation in the microsporidian *Nosama apis* during infection of the honey bee *Apis mellifera* (Rinderer and Dell Elliott, 1977; Tritschler et al., 2017), and allowed it to out-compete a viral competitor deformed wing virus (DWV) (Tritschler et al., 2017). In contrast, higher protein diets decreased the lethal effects of the gram-positive opportunist bacterium *Bacillus subtilis* on the African armyworm *Spodoptera exempta*. So far there has been a

limited number of studies investigating host diet effects on *X. nematophila* pathogenicity (Chapter 2 and Chapter 3), and no studies directly investigating the outcome of host internal-environment nutrient variation on this pathogen's fitness.

Chapter 4 characterized the host haemolymph nutrients on 20 diets varying in their protein-to-carbohydrate ratio. Cotter et al., (2011) showed, using the same 20 diets, that *S. littoralis* immune expression is heightened in a high-protein environment. *Spodoptera* caterpillars can use dietary protein to increase their resistance to the bacterium (Chapter 2), and may use dietary carbohydrate to increase their tolerance (Chapter 3), demonstrating the potential for top-down (immunological) effects. On the other hand, *Xenorhabdus* performance peaked in a nutrient-space rich in carbohydrate and low in protein (Chapters 2 and 3). To disentangle direct (nutritional) and indirect (host-mediated) bottom-up effects on *Xenorhabdus* performance, we need to isolate the bacterium from its host and other potential microbes. One way of doing this is to characterise bacterial performance in synthetic haemolymphs that have similar nutritional properties to the natural haemolymphs generated when hosts feed on different diets. Several previous studies have attempted to do this for a single host diet/haemolymph, with some degree of success (Dunphy and Webster, 1989; Gotz et al., 1981; Maranga et al., 2003; Yoo et al., 2000), but we are not aware of any previous studies that have synthesised multiple haemolymphs.

This chapter aims to characterise the population dynamics of *Xenorhabdus* grown in nutritional environments (synthetic haemolymphs) based on a nutritional analysis of *Spodoptera littoralis* haemolymph for larvae fed on 20 diets varying in their protein-to-carbohydrate ratios and concentrations (Chapter 4). The haemolymph nutrient variation was modelled statistically to produce 20 variable nutrient environments that the pathogen would experience based on those 20 host diets. First, pathogen nutrient

requirements were determined using a growth solution containing fixed nutrients, apart from one nutrient group (protein, carbohydrates, or amino acids), which was varied within the range observed in the host. Pathogen growth was then measured over 30 hours in nutrient growth solutions matching the 20 model environments produced. The resulting growth rates were used to calculate growth kinetics with the aim of identifying the optimal nutrient environment for pathogen maximum growth rate (*r*) and carrying capacity (*K*). The former was chosen due to the exponential replication phase being the period at which pathogen nutrient-demand is highest, and the latter was chosen for its importance as a measure of the maximum population density a nutrient environment can support. We predicted that pathogen performance would be maximised in a carbohydrate-rich environment, based on our *in vivo* findings (Chapters 2 & 3) and the fact that bacteria-infected hosts survive better, and show a preference for, protein-rich diets (Cotter et al., 2008; Lee et al., 2006; Povey et al., 2014, 2009).

5.2 METHODS

5.2.1 Cultures

5.2.1.1 Insect culture

The *Spodoptera littoralis* culture was founded in 2002 from eggs collected near Alexandria in Egypt. It was maintained using single-pair matings of over 150 pairs per generation to reduce in-breeding. For experiments, larvae were collected in the 2nd instar and reared singly on a semi-artificial wheatgerm-based diet until the start of the final instar (6th). Larvae were kept in 25 mL polypots at 27^{o}C under a 12:12 light:dark regime.

5.2.1.2 Bacteria

Bacteria were originally supplied by the laboratory of Givaudan and colleagues (Montpellier University, France; *X. nematophila* F1D3 GFP labelled). All species were maintained on nutrient agar at 4°C and stored in liquid culture at -80°C (1:1 nutrient broth culture:glycerol). To maintain virulence, bacteria were used to infect 6th instar *S. littoralis* larvae. Harvested single colonies grown from haemolymph smeared NBTA agar plates (Sicard et al., 2004) were then grown in sterile nutrient broth for 24 h at 28°C shaking at 150 rpm. Stocks were made by mixing 500 µl of liquid culture with glycerol at a 1:1 ratio and stored again at -80°C. Prior to experiments, bacteria were revived from the frozen stores: 100 µl of frozen culture was added to 10 mL nutrient broth, which was then incubated for 16 h at 28°C shaking at 150 rpm.

5.2.2 Synthetic haemolymph design

5.2.2.1 Nutrient sources

All nutrients used were obtained from Sigma Aldrich. The protein source used was bovine serum albumen (BSA, A7906), the carbohydrate source used was glycogen (G8751), and all amino acids used were L-amino acids (A09416). The following sugars

were used: Glucose (G8270), Fructose (F0127), Lactose (L3750), Sucrose (S9378), Trehalose (T9531).

5.2.2.2 Haemolymph collection

Within 24 h of moulting to the 6th instar, 400 larvae were transferred to Petri dishes (90mm diameter), containing 1.5 g of a chemically-defined diet (Dadd, 1961; Simpson and Abisgold, 1985). A total of 20 diets were used, ranging in protein and carbohydrate concentration (**Table S5.1**; see Cotter et al., 2011; Lee et al., 2004), resulting in a sample size of 20 larvae per diet. After 48 h, the larvae were weighed, and haemolymph was collected using a sterile hypodermic Microlance^{TM} 3 needle into a sterile ice-cooled 1.5 mL Eppendorf tube, which was then stored at -20°C. The diet was weighed to record ingestion rates and replaced daily for the first three days, after which the larvae were transferred to 36.9 mL polypots containing semi-artificial wheatgerm-based diet. All larvae were retained for further life history information.

Haemolymph nutrients were analysed through HPLC and lab nutrient assays (for details refer to Chapter 4), and modelled using GLMs in R (v3.2.2; (R Core Team, 2014). The model equation was then used to produce a new set of variables for each of the 20 diets (**Tables S5.2 & S5.3**). Mean values were used for nutrients that showed no variation according to the proportion of dietary protein or diet concentration. The 5 sugars, trehalose, glucose, fructose, lactose and sucrose were chosen to represent all sugars since these made up more than 95% of the haemolymph sugar content and sugars did not vary with diet (Chapter 4).

5.2.2.3 Synthetic haemolymphs (SH)

All synthetic haemolymph (SH) media prepared for growth experiments were based on the saline and vitamin content of Sigma Grace's insect medium (SGIM, Sigma Aldrich,

G8142). A basic salt solution (SGIM-saline) was prepared in sterile distilled water (**Table S5.2**: inorganic salts), the pH was adjusted to 4.5 with HCl and NaOH to dissolve the salts, and the solution was stored at 4°C. The first step in making the 20 SH solutions was to make concentrated micronutrient solutions: the SGIM-saline was filter-sterilized using 0.2 µM Corning sterile syringe filter and vitamins, sugars and amino acids were added from concentrated stock solutions to 10x the desired final concentrations (**Tables S5.2 & S5.3**). The sugar and amino acid values were based on the linear model fitted values of the HPLC outputs from the haemolymph nutrient analysis (data not shown). The solutions were made to a final volume of 10 mL by adding the micronutrients to 9 mL of SGIM-saline solution, adjusting the pH to 6.4 and making up the final volume to 10 mL using SGIM-saline. These solutions were then filter-sterilized and divided into 1 mL aliquots in Eppendorf tubes and stored at -80°C. To make the final synthetic haemolymph solution, a 1 mL micronutrient solution was diluted to 9 mL with SGIM-saline, protein (bovine serum albumin, BSA; Sigma Aldrich, A7906) and carbohydrate (glycogen from oyster; Sigma Aldrich, G8751) were added to the final concentration (**Table S5.4**). The pH was adjusted to 6.4 with HCL and NaOH to match the pH of lepidopteran haemolymph (Wyatt et al., 1956), and the final volume was made up to 9.8 mL with SGIM-saline. The solution was filter-sterilized with 0.2 µm cellulose acetate membrane filters (Sigma Aldrich, WHA69012502), and stored in 980 µL aliquots in Eppendorf tubes at -80°C. The volume was made up to 1 mL with the addition of 20 µL of a filter-sterilised 0.05 g/mL lipid stock solution once the tubes were retrieved from storage prior to use in assays.

5.2.2.4 Single-variable haemolymphs (SVHs)

To isolate the effect of each nutrient group on bacterial growth, the other nutrient groups in solution were fixed at their mean value, whilst the nutrient of interest was increased in concentration. A set of 24 single-variable haemolymphs (SVHs) were

designed based on the variable nutrients in the 20 SH solutions (**Table S5.6**). Each series included 6 increments, ranging from 0% of that nutrient to 100%. The 100% value was the maximum value plus 2 standard deviations from the SH concentrations (**Table S5.5**). This range was chosen as it covers the full range of variation a pathogen would experience in the nutrient environment in the host haemolymph. The numbers were all based on the model fitted values from the host haemolymph nutrient measurements (Section 5.2.2.2), except for the lipid series which used the raw haemolymph measurements. The final solutions were made up as per Section 5.2.2.3.

5.2.3 *In vitro* growth experiments

5.2.3.1 Preparation of bacterial cell culture for growth experiments

Bacteria were revived from frozen liquid stores (see Section 5.2.1.2) after which time 2 ml was sub-cultured into 8 ml of nutrient broth and incubated for a further 4 h to reach log phase. The bacterial cells were washed to avoid the transfer of nutrients from nutrient broth into the growth media, following Crawford et al., (2012). Briefly, 1 mL of sample was centrifuged for 6 min at 3000 g twice, removing the supernatant each time. Filter-sterilized SGIM-saline was used to re-suspend the cells in between the centrifugation steps. A 1 mL sample was subsequently used to produce a dilution series in SGIM-saline from which the total cell count was determined using a compound microscope (Zeiss Axioskop40) under fluorescence microscopy using a haemocytometer with improved Neubauer ruling. The remaining culture was diluted to 1 x 10^7 cells/mL in the SGIM-saline solution, making the final starting concentration in each treatment 1 x 10^6 cells/mL since 20 μL of bacterial cells were added to 180 μL of growth media.

5.2.3.2 Bacterial growth assays

Cell growth was determined at 28°C in Corning 96-well plates (Sigma Aldrich, CLS3595) using a SpectraMax Plus microtiter plate reader with SoftMax Pro software (Molecular Devices™). The wells of the plate contained 180 µL of one of the 24 SVHs (Experiment 1) or 20 SHs (Experiment 2) in quadruplets. SGIM-saline and SGIM were used as the negative and positive controls respectively. Twenty µL of bacterial culture was added to half of the wells (duplicates) and 20 µL of SGIM-saline was added to the other half as blank controls. The turbidity at 600 nm was determined every 10 min for 30 h and the plate was shaken for 30 s before each measurement. The experiment was repeated for three plates for each experiment (making a total of 6 plates), with each plate containing all growth solutions and controls.

5.2.4 Data analysis

Due to varying optical densities (OD) produced by lipids in the SHs and SVHs, the minimum OD in each solution were variable. Prior to analysis, data were corrected by first subtracting a growth series from its corresponding blank series (to which no bacteria had been added). Then, the mean of the minimum 10 values in a series was subtracted from all the values in the series, producing a new zero-point. The adjustments removed the variation in OD caused by nutrients, maintaining only variation due to bacterial growth.

Data analysis was performed using the R statistical software (v3.2.2; R Core Team, 2014). To account for variation in haemolymph nutrient concentrations, data were standardized using the mean (µ) and standard deviation (σ), as per Cotter et al., (2011), allowing comparisons between nutrient groups; a standardized variable (Z) was produced from a nutrient variable (X) using the formula: ($Z = (X-\mu)/\sigma$). Firstly, bacterial growth kinetics were calculated using the *Growthcurver* package (v0.3.0;

Sprouffske and Wagner, 2016). Growth statistics were then analysed using generalized additive models (GAM) in the *mgcv* package (v1.8; Wood, 2006) in conjunction with spline plots, following Cotter *et al.*, (2011). Where appropriate, an information theoretic approach was taken for analysis (Whittingham et al., 2006). This approach allows the selection of multiple candidate models accounting for how much variation each explains based on the Akaike information criterion (AIC; Burnham and Anderson, 2004). AIC analysis was carried out using the *MuMIn* package (v1.15; Bartoń, 2018) in R, which when combined with the *mgcv* package, ranks models based on the degrees of freedom used to create the smoothed curve. Where appropriate model selection was carried out using evidence ratios which provides the ratio of the model weights: an evidence ratio for the best model against model *X* is calculated by the Akaike weight of the best model/the Akaike weight of model *X*. The specific analyses varied, however they all included a '*Null* model', which provided a baseline measure of variation, and a '*Full* model', consisting of a factor with 20 levels, one for each of the 20 diets. Some models consisted of a mixture of parametric coefficients, that were modelled using an analysis of variance and non-parametric smoothed effects, modelled through regression analysis that utilize the sum of iterative estimates to calculate a smoothing function.

5.2.4.1 Growth kinetics

From the growth kinetic data produced by the *Growthcurver* package, starting population size (N_0), maximum growth rate (*r*), and carrying capacity (*K*) were the statistics directly related to the shape of the growth curve. Being an *in vitro* system, it is unclear whether bacterial growth was dynamic or static at the time of measurement, meaning *K* could be more accurately described as the maximum population size. The N_0 was treated as a constant since the same quantity of bacteria had been added in each solution, leaving *K* and *r* for analysis against the variable SH nutrients. Because there

was no variation in the haemolymph sugars, all haemolymph carbohydrates were analysed as an aggregate of glycogen and the sum of sugars. Similarly, although all amino acids were included in the aggregate variables (sum of amino acids, essential amino acids and non-essential amino acids), only the amino acids whose haemolymph quantities had varied with host diet were analysed individually.

5.2.4.2 Figures

Data were visualized through the use of scatterplots produced by the *mgcv* package, as well as via thin-plate regression splines created using the *fields* package (v9.6; Nychka, 2016). To complement the GAM analysis, the thin-plate regression splines were produced using the REML method for smoothing.

5.3 RESULTS

5.3.1 Single-variable haemolymph (SVH) experiment

Bacterial nutrient requirements were investigated using single variable haemolymphs (SVHs) in which the levels of all the nutrients, but one, was fixed at their mean values. A single nutrient or nutrient group, specifically BSA (protein), glycogen (carbohydrate) and amino acids, was varied across a broad range of concentrations. The concentration-range was centred around the mean haemolymph value for that nutrient group, to replicate the variation the pathogen would experience *in vivo*, but extended by up to approximately 2 standard deviations above the observed haemolymph range. GAMs allow the combination of an analysis of variance (parametric effects), that makes a comparison between treatment groups, with smoothed effects (non-linear regression) in a single model. As such, the effects of nutrients (BSA, glycogen or amino acids) on bacterial maximum growth rate per hour, *r*, and carrying capacity, *K*, could be compared with each other in the same model that tested the effect of each nutrient on bacterial growth.

Visualising the parametric effects (**Figure 5.1**), *r* was lowest when SVH protein levels were varied (mean $r = 0.13$), followed by amino acids (mean $r = 0.16$), and was highest when carbohydrate levels were varied (mean $r = 0.18$). The growth rate did not increase significantly with an increasing concentration of amino acids in the SVH ($P = 0.697$; **Table 5.1**), however there was a quadratic increase in *r* with increasing protein concentration (edf = 2.980, $P < 0.001$) and increasing carbohydrate concentration (edf = 2.002, $P = 0.001$). The quadratic relationship between *r* and protein/carbohydrate is because *r* increased at values below the mean nutrient concentration, after which it plateaued and there was no further increase.

Although there were significant differences between the nutrient groups in both *r* and *K* (Parametric P < 0.001; **Table 5.1**), nutrients explained more variation in *K* (R^2 = 0.797) than they did in *r* (R^2 = 0.417). There was no significant difference (Tukey HSD: P = 0.982) in the average carrying capacity between the amino acid (mean *K* = 0.086) and carbohydrate series (mean *K* = 0.083), but *K* was significantly lower, on average, in the protein series (mean *K* = 0.060).

There was a significant linear increase in *K* with increasing carbohydrate concentration (edf = 0.972, P < 0.001), and both protein and amino acids exhibited significant non-linear changes in *K* with increasing nutrient concentration (amino acids: edf = 2.719, P < 0.001; protein: edf = 3.747, P < 0.001). Adding a low concentration of protein to the solution increased *K*, but any further protein additions caused *K* to decrease, with the bacterial carrying capacity being lowest at the highest protein concentration, lower even than when there was no protein at all in solution. On the other hand, there was a linear increase in *K* with increasing amino acid concentration until, at the highest concentration of amino acids, *K* decreased slightly.

In summary, bacterial maximum growth rate, *r*, increased with increasing concentrations of protein and carbohydrate but not amino acids. However mean *r* was highest in a nutrient environment variable in carbohydrate and lowest in a nutrient environment variable in protein. Carrying capacity, *K*, was similar in SVHs varying in carbohydrate and amino acid concentrations, however it was lower in SVHs varying in protein concentration. Whilst *K* increased linearly with increasing carbohydrate concentration, it increased non-linearly with increasing amino acid concentration. *K* decreased at the highest concentrations of amino acids, however it decreased across most of the protein range.

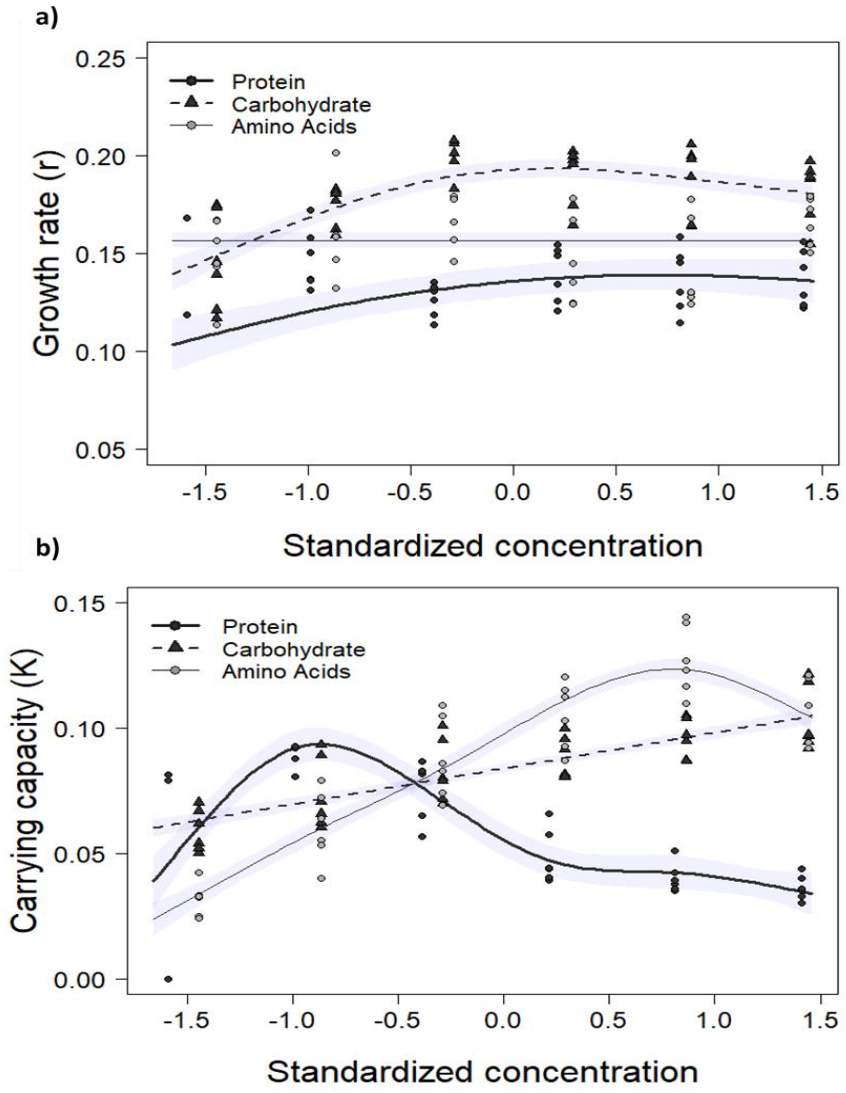

Figure 5.1: Model fits for bacterial growth rate and carrying capacity measured in single-variable haemolymph (SVH). All nutrients were fixed in the SVH apart from one. Nutrient concentrations were standardized for analysis to allow comparison. (a) Bacterial growth rate (*r*), measured by change in absorbance per hour; *r* increased with increasing concentrations of protein and carbohydrate but not amino acids. (b) Bacterial carrying capacity (*K*), measured by maximum absorbance; *K* increased with increasing concentrations of glycogen and amino acids but decreased with increasing concentrations of protein.

Table 5.1: Single-variable haemolymph (SVH) experiment model summary tables. The left-hand side of the table contains the summary information from a model testing the effect of nutrients in the SVH on bacterial growth rate (*r*). The right-hand side of the table contains the summary information produced by a separate model testing the effect of nutrients in the SVH on bacterial carrying capacity (*K*). The parametric p-value reports the results of parametric terms in the model, tested by an analysis of variance, and results indicate differences between treatments, in this case nutrients. The edf provides information about the shape of the curve, relating to the basic dimensions used by the model to fit the curve; for example, an edf close to 1 represents a linear effect, whilst an edf close to 2 represents a quadratic effect.

Nutrient	***r***				***K***			
	Parametric P-value	**edf**	**F-value**	**P-value**	**Parametric P-value**	**edf**	**F-value**	**P-value**
Protein (Intercept)	<0.001	2.980	4.570	<0.001	<0.001	3.747	19.683	<0.001
Carbohydrate	<0.001	2.002	3.156	0.001	<0.001	0.972	8.403	<0.001
Amino Acids	<0.001	0.000	0.000	0.697	<0.001	2.719	40.924	<0.001

5.3.2 Macronutrients

To provide comparison with the *in vivo* growth data collected for this pathogen-host pairing (Chapter 2 & Chapter 3), variation in haemolymph nutrients of hosts maintained on diets varying in their macronutrient composition was replicated (Section 5.2.2.2). Pathogen growth kinetics (*r* and *K*) were measured in the 20 synthetic haemolymphs (SHs), which varied in their contents of both macro- and micronutrients. The SHs differ from the SVHs (Section 5.3.1) in that the SHs contain nutrients (BSA, glycogen and amino acids) that vary simultaneously. As such, more nutrient interactions could be explored using the SHs. One major difference was in the amino acids, which were treated as a single group in the SVH media, whilst individual amino acids were varied in the SH media.

In all the analyses discussed below, the model that included a separate level for each of the 20 SHs (the '*Full*' model) tended to explain most of the variation in *r* and *K*. As this yields limited insights into the species nutritional constraints on bacterial growth, the analyses were re-run without the *Full* model and these are the results that are reported here.

5.3.2.1 Host diet macronutrients

Before investigating the effects of the SHs on bacterial growth, the growth rate, *r*, and carrying capacity, *K*, were modelled against the nutrient variation in the diet fed to the hosts to produce the nutrient environments on which the SHs were modelled. In this way, a direct comparison could be made with *in vivo* data collected for this host and pathogen (Chapter 3). Models containing absolute quantities of dietary protein and carbohydrate presented to the host explained more variation in both bacterial *r* and *K* than models containing dietary nutrient ratios and caloric content (**Table 5.2a**). Diet

explained very little variation in *r*, with the top models (m2, m3 and m4) explaining only 1% of the variation (R^2 = 0.013); all three models include dietary carbohydrate (**Table 5.2a**). The low explanatory power of host diet can be observed by the flat surface produced when the model is visualised in a thin-plate spline plot (**Figure 5.2a**).

In contrast, relatively large amounts of variation in *K* was associated with host diet attributes (R^2 = 0.589; **Table 5.2a**), with *K* decreasing linearly with increasing dietary protein (edf = 0.922, P < 0.001; m4; **Table 5.2b**). This model (m4) attributes host dietary effects on *K* to an interaction between host dietary protein and carbohydrate intake (P < 0.001), rather than to an additive effect between P and C, explaining 10% more variation. Upon visualisation, *K* appears to peak in nutrient space containing low concentrations of dietary protein and a mid-level of dietary carbohydrate (**Figure 5.1b**).

5.3.2.2 Solution macronutrients

SH macronutrients were better at explaining variation in *r* than diet presented to the host (***cf* Table 5.2 and Table 5.3**). The top model (m4) explained 23% variation (**Table 5.3a**) and indicated that *r* increased significantly through an interaction between protein and carbohydrate (P < 0.001; **Table 5.3b**). There were no significant effects of either protein or carbohydrate concentrations, independently or in combination, and so all other models were weighted lower than the *Null* model (m0) in the AIC Table (**Table 5.3a**). Model visualisation indicates a relatively flat response surface (**Figure 5.2c**).

Carrying capacity, *K*, (**Table 5.3a**) decreased with increasing protein (P = 0.022) and increased with increasing carbohydrate in the SH (P < 0.001; m3, **Table 5.3b**). Reflecting this, the bacterial carrying capacity peaked in a nutrient space low in protein and high in carbohydrate (**Figure 5.2d**). Both effects were approximately linear (protein edf = 0.806; carbohydrate edf = 0.927) and the overall model explained 31% variation in *K* (R^2 = 0.308). An evidence ratio for this model against the carbohydrate model of

2.76, compared to the protein model of 65 (**Table 5.3a**), suggests that a larger proportion of the variation explained by this model is due to SH carbohydrate levels.

The proportion of protein in the SH (relative to the amount of carbohydrates) had no significant effect on *r* ($P = 0.226$; $R^2 = 0.001$; **Table 5.3c; Figure S5.1**), but *K* decreased significantly with an increasing proportion of SH protein ($P < 0.001$; $R^2 = 0.306$). Due to the non-linear nature of this relationship (edf = 1.861), the decrease in *K* is slow at first then the negative slope becomes linear with increasing proportion protein.

In summary, although the macronutrient content of the host diet was poor at explaining variation in *r*, the top models all contained dietary carbohydrate. Bacterial carrying capacity, in contrast, peaked in an area of nutrient space containing diets with low concentrations of protein and mid-levels of carbohydrate. The macronutrients in the SH media were also relatively poor at explaining variation in *r*, attributing observed variation to an interaction between carbohydrate and protein. Carrying capacity was highest when SHs contained a low concentration of protein and a high concentration of carbohydrate. This was a combined effect rather than an interaction, implying that *K* decreased with increasing SH protein concentration and increased with increasing SH carbohydrate concentration.

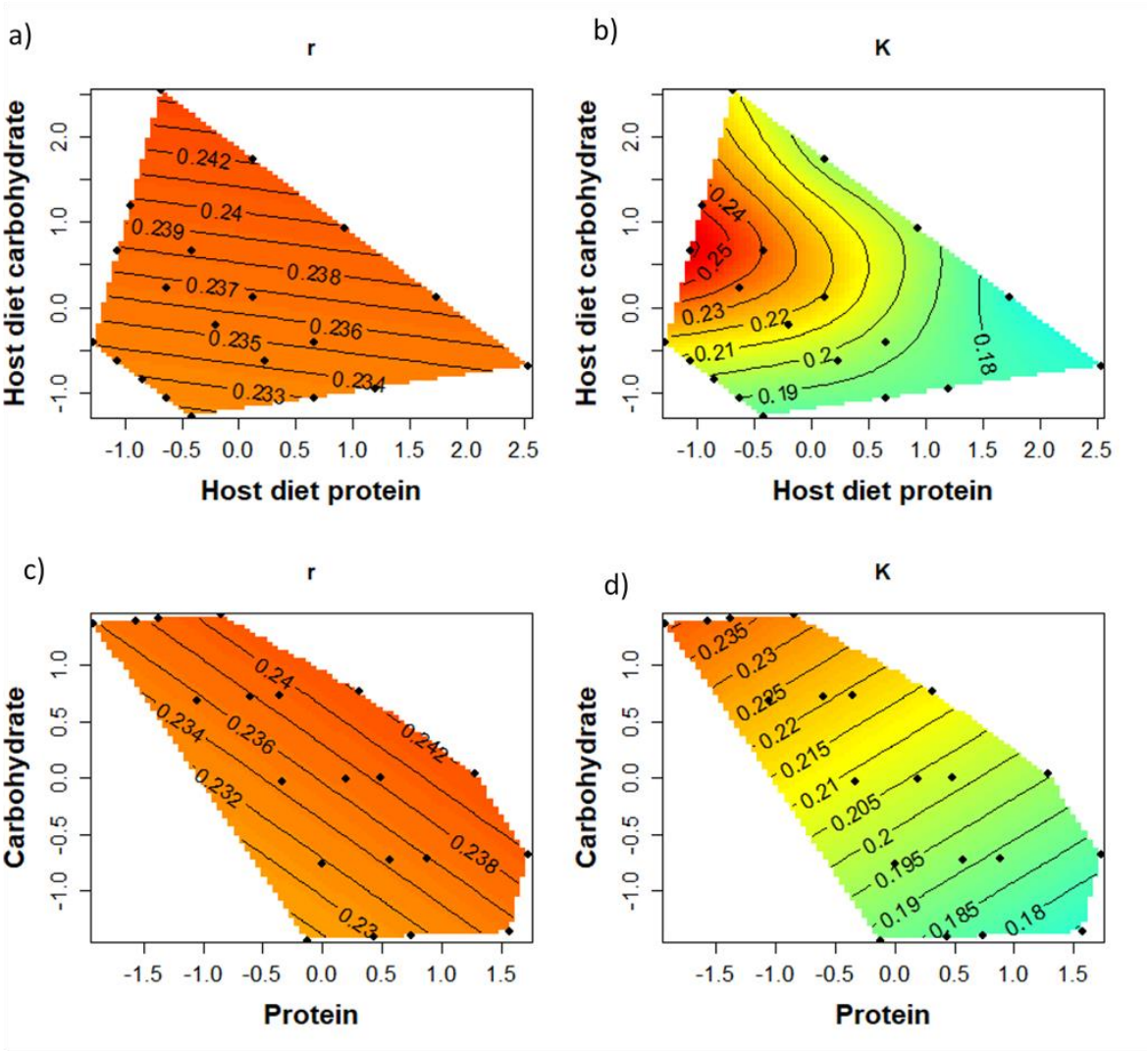
a)
r
Host diet carbohydrate
Host diet protein
0.242
0.24
0.239
0.238
0.237
0.236
0.235
0.234
0.233
b)
K
Host diet carbohydrate
Host diet protein
0.24
0.25
0.23
0.22
0.21
0.2
0.19
0.18
c)
r
Carbohydrate
Protein
0.24
0.242
0.234
0.236
0.232
0.238
0.23
d)
K
Carbohydrate
Protein
0.235
0.23
0.225
0.22
0.215
0.21
0.205
0.2
0.195
0.19
0.185
0.18

Figure 5.2: Effect of macronutrient content of diet presented to the host and the concentration of protein and carbohydrate in synthetic haemolymphs (SH) on bacterial growth rate (*r*) and carrying capacity (*K*). 2D contour plots compare a dependent variable (*r* or *K*) on the z-axis with two independent variables (e.g. proteins (x-axis) and carbohydrate (y-axis)) simultaneously. Contour lines represent the type of relationship between the dependent variable and the two independent variables. Colour represents the strength of effect, with blue indicating the weakest effect going up to red which represents the strongest effect. Nutrient concentrations were standardized for analysis to allow comparison. (a) Effect of macronutrients presented to the host on *r*. There was no significant effect of either protein or carbohydrates presented to the host on *r*. (b) Effect of macronutrients presented to the host on *K*. *K* peaked in a nutrient space containing a mid-level of dietary carbohydrates and a low concentration of dietary protein. (c) Effect of SH macronutrient concentration on *r*. Although, a model containing an interaction between SH carbohydrate and protein concentration explained significant variation in r (R^2= 0.226), this was not captured by the contour plot. (d) Effect of SH macronutrient concentration on *K*. *K* peaked in a nutrient space containing a low concentration of SH protein and a high concentration of SH carbohydrate.

Table 5.2: Host diet model summary tables. The left-hand side of the tables contain the summary information from models testing the effects of macronutrients in the diet fed to the host on bacterial growth rate (*r*). The right-hand side of the tables contain the summary information produced by separate models testing the effects of macronutrients in the diet fed to the host on bacterial carrying capacity (*K*). (a) AIC comparison table for models containing attributes of diet presented to the host. m0 (Null) is a model with no explanatory terms included, providing a baseline measure of variation. m1 (Protein) is a model containing the total amount of protein in the diet. m2 (Carbs) is a model containing the total amount of carbohydrate in the diet. m3 (Protein + Carbs) is a model containing both protein and carbohydrate. m4 (Protein * Carbs) is a model that includes an interaction term (represented by asterisk) between dietary protein and carbohydrate. m5 (Conc) is a model containing the concentration of macronutrients in the diet. m6 (Ratio) is a model containing the ratio of protein to carbohydrate in the diet. m7 (Conc + Ratio) is a model containing both the concentration of macronutrients in the diet and the ratio of protein to carbohydrate in the diet. m8 (Conc * Ratio) is a model that includes an interaction term between diet macronutrient concentration and diet protein to carbohydrate ratio. df is the degrees of freedom used by the model to produce a fit and not the degrees of freedom based on the number of explanatory variables. K is the number terms in the model. AICc is the model Aikake values. Delta represents the difference between a model and the model explaining the most variation. Weight is determined by the amount of variation a model explains penalized for the degrees of freedom used by the model. (b) Summary information for each model in the AIC comparison table. The edf provides information about the shape of the curve, relating to the basis dimensions used by the model to fit the curve; for example, an edf close to 1 represents a linear effect, whilst an edf close to 2 represents a quadratic effect.

(a) Model AICs: Host-diet protein and carbohydrate

r							***K***						
Model	**df**	**k**	**AICc**	**delta**	**weight**	**R^2**	**Model**	**df**	**k**	**AICc**	**delta**	**weight**	**R^2**
m2 *Carbs*	2	1	-568.6	0.00	0.139	0.013	m4 *Protein * Carbs*	9	3	-546.2	0.00	0.998	0.589
m3 *Protein + Carbs*	2	2	-568.6	0.00	0.139	0.013	m8 *Conc * Ratio*	10	3	-534.1	12.16	0.002	0.555
m4 *Protein * Carbs*	2	3	-568.6	0.00	0.139	0.013	m7 *Conc + Ratio*	4	2	-522.0	24.24	0.000	0.472
m0 *Null*	1	0	-568.2	0.40	0.113	0.000	m3 *Protein + Carbs*	7	2	-521.8	24.41	0.000	0.487
m1 *Protein*	2	1	-568.2	0.41	0.113	0.000	m5 *Conc*	3	1	-489.3	56.99	0.000	0.292
m5 *Conc*	2	1	-567.9	0.72	0.097	0.005	m2 *Carbs*	4	1	-485.4	60.82	0.000	0.284
m6 *Ratio*	2	1	-567.9	0.72	0.097	0.004	m1 *Protein*	3	1	-473.8	72.42	0.000	0.198
m8 *Conc * Ratio*	3	3	-567.5	1.05	0.082	0.009	m6 *Ratio*	3	1	-469.4	76.87	0.000	0.173
m7 *Conc + Ratio*	3	2	-567.5	1.05	0.082	0.009	m0 *Null*	2	0	-448.9	97.33	0.000	0.000

(b) Host-diet protein and carbohydrate model summaries						
Model	***r***			***K***		
	edf	**F-value**	**P-value**	**edf**	**F-value**	**P-value**
m1						
Protein	0.000	0.000	1.000	1.108	7.341	<0.001
m2						
Carbs	0.611	0.392	0.112	2.714	11.773	<0.001
m3						
Protein +	0.000	0.000	1.000	2.539	11.130	<0.001
Carbs	0.611	0.392	0.112	2.824	16.334	<0.001
m4						
Protein +	0.000	0.000	1.000	0.922	2.962	<0.001
Carbs +	0.611	0.392	0.112	0.000	0.000	0.694
*Protein * Carbs*	0.000	0.000	0.734	6.236	14.104	<0.001
m5						
Conc	0.348	0.177	0.218	1.839	8.303	<0.001
m6						
Ratio	0.355	0.138	0.216	0.980	12.275	<0.001
m7						
Conc +	0.351	0.180	0.217	1.897	13.367	<0.001
Ratio	0.358	0.139	0.215	0.986	16.531	<0.001
m8						
Conc +	0.350	0.180	0.217	1.596	2.187	<0.001
Ratio +	0.357	0.139	0.215	2.537	2.489	<0.001
*Conc * Ratio*	0.000	0.000	0.935	3.497	2.316	<0.001

Table 5.3: Synthetic haemolymph (SH) macronutrient model summary tables. The left-hand side of the tables contain the summary information from models testing the effect of macronutrients in the SH on bacterial growth rate (*r*). The right-hand side of the tables contain the summary information produced by a separate model testing the effect of macronutrients in the SH on bacterial carrying capacity (*K*). (a) AIC comparison table for models containing macronutrients in the SH as explanatory variables. m0 (Null) is a model with no explanatory terms included, providing a baseline measure of variation. m1 (Protein) is a model containing standardized variation in SH protein concentration. m2 (Carbs) is a model containing standardized variation in SH carbohydrate concentration. m3 (Protein + Carbs) is a model containing both SH protein and carbohydrate. m4 (Protein * Carbs) is a model that includes an interaction term (represented by asterisk) between SH protein and carbohydrate. df is the degrees of freedom used by the model to produce a fit and not the degrees of freedom based on the number of explanatory variables. K is the number terms in the model. AICc is the model Aikake values. Delta represents the difference between a model and the model explaining the most variation. Weight is determined by the amount of variation a model explains penalized for the degrees of freedom used by the model. (b) Summary information for each model in the AIC comparison table. The edf provides information about the shape of the curve, relating to the basis dimensions used by the model to fit the curve; for example, an edf close to 1 represents a linear effect, whilst an edf close to 2 represents a quadratic effect. (c) Summary information from models testing the effect of proportion of dietary protein on *r* and *K*.

(a) Model AICs: SH protein and carbohydrate													
r							***K***						
Model	**df**	**k**	**AICc**	**delta**	**weight**	**R^2**	**Model**	**df**	**k**	**AICc**	**delta**	**weight**	**R^2**
m4 *Protein * Carbs*	10	3	-587.4	0.00	1.000	0.226	m3 *Protein + Carbs*	3	2	-490.7	0.00	0.420	0.308
m0 *Null*	1	0	-568.2	19.27	0.000	0.000	m4 *Protein * Carbs*	3	3	-490.6	0.00	0.419	0.308
m1 *Protein*	2	1	-568.2	19.27	0.000	0.000	m2 *Carbs*	3	1	-488.6	2.03	0.152	0.288
m2 *Carbs*	2	1	-567.9	19.56	0.000	0.005	m1 *Protein*	2	1	-482.8	7.82	0.008	0.253
m3 *Protein + Carbs*	2	2	-567.9	19.56	0.000	0.005	m0 *Null*	2	0	-448.9	41.74	0.000	0.000

(b) SH protein and carbohydrate model summaries						
Model	***r***			***K***		
	edf	**F-value**	**P-value**	**edf**	**F-value**	**P-value**
m1						
Protein	0.000	0.000	0.831	0.976	10.086	<0.001
m2						
Carbs	0.390	0.159	0.203	0.980	12.056	<0.001
m3						
Protein +	0.000	0.000	0.765	0.806	1.039	0.022
Carbs	0.389	0.159	0.203	0.927	3.170	<0.001
m4						
Protein +	0.618	0.403	0.091	0.806	1.039	0.022
Carbs +	0.000	0.000	0.819	0.927	3.169	<0.001
*Protein * Carbs*	6.833	0.435	<0.001	0.001	0.000	0.466

(c) Proportion of SH protein model summaries								
Nutrient	***r***				***K***			
	R^2	**edf**	**F-value**	**P-value**	**R^2**	**edf**	**F-value**	**P-value**
Proportion Protein	0.007	0.596	0.218	0.226	0.306	1.861	13.119	<0.001

5.3.3 Aggregate amino acids

5.3.3.1 Sum of all amino acids

Consistent with the macronutrient effects (Section 5.3.2), a variable containing the additive effects of the free amino acids in solution (**Table 5.4a**) appeared to have a stronger effect on *K* ($R^2 = 0.171$) than on *r* ($R^2 = 0.005$); the latter being non-significant ($P = 0.210$). The effect of amino acids on *K* was quadratic (edf = 2.016; $P < 0.001$), with the carrying capacity increasing at low concentrations of amino acids, peaking at an interim concentration, and then decreasing at concentrations of amino acids above the mean (**Figure 5.3a**).

5.3.3.2 Essential and non-essential amino acids

Reflecting the macronutrients (Section 5.3.2), there was no significant effect of either essential (EAA) or non-essential amino acids (non-EAA) on *r*. The evidence ratio for the top model for *r* (m2; **Table 5.4b**) against the *Null* model (m0) was low (1.31), matching the marginal variation explained by this model ($R^2 = 0.014$), and this is reflected in a flat heatmap surface (**Figure 5.3b**).

Although the carrying capacity, *K*, decreased non-linearly (edf = 2.155) with increasing EAA concentration ($P < 0.001$) and increased non-linearly (edf = 1.889) with increasing non-EAA concentration ($P < 0.001$), these effects were non-significant once the interaction term was introduced (m4, **Table 5.4c**). However, the evidence ratio for this model (m4) against the additive effect model (m3) was relatively low (7.76) since it only explained 3% more variation (m4, $R^2 = 0.276$, m3, $R^2 = 0.245$; **Table 5.4b**). Thus, *K* peaked in a nutrient space that contained medium concentrations of non-EAA and a low concentration of EAA (**Figure 5.3c**).

The proportion of EAA reflected these findings: there was no effect of increasing EAA proportion on *r* ($P = 0.146$; $R^2 = 0.01$; **Table 5.4a**), but there was a non-linear (edf = 1.987) decrease in *K* ($P < 0.001$; $R^2 = 0.201$; **Figure 5.3d**).

These results show that the aggregated amino acid variables were consistently poor at explaining variation in *r*, as had been observed with SH macronutrients. The quadratic relationship between *K* and a variable containing total amino acids in solution was consistent with the findings of bacterial amino acid requirements using the SVHs (Section 5.3.1), however *K* peaked at a lower concentration of amino acids in the SHs than it had in the SVHs. Variation in *K* was due to an interaction between SH EAA and non-EAA contents; *K* peaked in a nutrient space containing a low concentration of EAA and a mid- to high concentration of non-EAA. Reflecting this, *K* decreased with increasing proportions of EAA in the SH media.

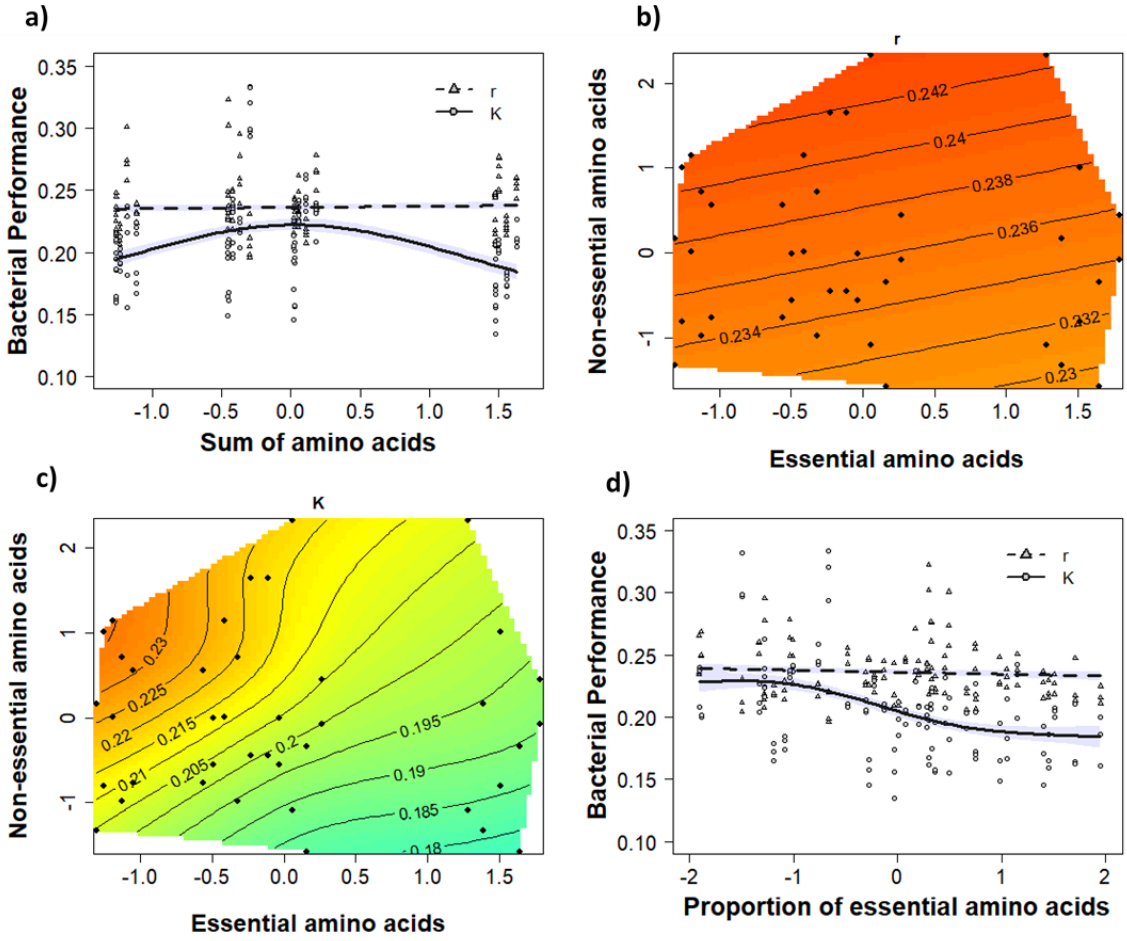
a)
Bacterial Performance
Sum of amino acids
r
K
b)
Non-essential amino acids
Essential amino acids
0.242
0.24
0.238
0.236
0.234
0.232
0.23
c)
Non-essential amino acids
Essential amino acids
0.23
0.225
0.22
0.215
0.21
0.205
0.2
0.195
0.19
0.185
0.18
d)
Bacterial Performance
Proportion of essential amino acids

Figure 5.3: Effect of amino acid groups in synthetic haemolymphs (SH) on bacterial growth rate (r) and carrying capacity (K). Amino acids in the SH were aggregated into groups for analysis; sum of all amino acids, essential amino acids (EAA), non-essential amino acids (non-EAA). Nutrient concentrations were standardized for analysis to allow comparison. 2D contour plots (b and c) compare a dependent variable (r or K) on the z-axis with two independent variables (e.g. EAA (x-axis) and non-EAA (y-axis)) simultaneously. Contour lines represent the type of relationship between the dependent variable and the two independent variables. Colour represents the strength of effect, with blue indicating the weakest effect going up to red which represents the strongest effect. (a) GAM model representing the effect of an aggregate variable containing all the amino acids in SH on r and K. The sum of the amino acids in SH could not explain variation in r. The effect of the sum of amino acids on K was quadratic (edf = 2.016), peaking at a mean concentration of amino acids. (b) Effect of aggregated EAA and aggregated non-EAA in SH on r. There was no significant effect of either EAA or non-EAA on r. (c) Effect of aggregated EAA and aggregated non-EAA in SH on K. K peaked in a nutrient space containing a mid-to-high concentration of non-EAA and a low concentration of EAA. (d) GAM model representing the effect of the proportion of EAA in SH on r and K. There was no effect of increasing the proportion of EAA in SH on r. K decreased non-linearly (edf = 1.987) with an increasing proportion of EAA.

Table 5.4: Aggregated synthetic haemolymph (SH) amino acids model summary tables. The left-hand side of the tables contain the summary information from models testing the effect of amino acid groups in the SH on bacterial growth rate (*r*). The right-hand side of the table contains the summary information produced by separate models testing the effect of amino acid groups in the SH on bacterial carrying capacity (*K*). (a) Summary information from models testing the effects of an aggregate variable containing all the amino acids in the SH on *r* and *K*, and models testing the effect of the proportion of essential amino acids on *r* and *K*. Each section of the table contains information from a separate model, so this table presents information from 4 independent models. The edf provides information about the shape of the curve, relating to the basis dimensions used by the model to fit the curve; for example, an edf close to 1 represents a linear effect, whilst an edf close to 2 represents a quadratic effect. (b) AIC comparison table for models containing total essential amino acids (EAA) and total non-essential amino acids (non-EAA) in the SH as explanatory variables. m0 (Null) is a model with no explanatory terms included, providing a baseline measure of variation. m1 (EAA) is a model containing standardized variation in SH EAA concentration. m2 (non-EAA) is a model containing standardized variation in SH non-EAA concentration. m3 (EAA + non-EAA) is a model containing both SH EAA and non-EAA. m4 (EAA * non-EAA) is a model that includes an interaction term (represented by asterisk) between SH EAA and non-EAA. df is the degrees of freedom used by the model to produce a fit and not the degrees of freedom based on the number of explanatory variables. K is the number terms in the model. AICc is the model Aikake values. Delta represents the difference between a model and the model explaining the most variation. Weight is determined by the amount of variation a model explains penalized for the degrees of freedom used by the model. (c) Summary information for each model in the AIC comparison table.

(a) Sum of SH amino acids and proportion of SH EAA model summaries								
Nutrient	***r***				***K***			
	R^2	**edf**	**F-value**	**P-value**	**R^2**	**edf**	**F-value**	**P-value**
Sum of amino acids	0.005	0.370	0.147	0.210	0.171	2.016	6.157	<0.001
Prop. of essential amino acids	0.009	0.533	0.285	0.146	0.201	1.987	7.487	<0.001

(b) Model AICs: EAA and non-EAA													
r							***K***						
Model	**df**	**k**	**AICc**	**delta**	**weight**	**R^2**	**Model**	**df**	**k**	**AICc**	**delta**	**weight**	**R^2**
m2 *Non-EAA*	2	1	-568.7	0.00	0.243	0.014	m4 *EAA * Non-EAA*	7	3	-480.7	0.00	0.885	0.276
m3 *EAA + Non-EAA*	2	2	-568.7	0.00	0.243	0.014	m3 *EAA + Non-EAA*	6	2	-476.6	4.10	0.114	0.245
m0 *Null*	1	0	-568.2	0.55	0.185	0.000	m2 *Non-EAA*	4	1	-464.3	16.38	0.000	0.140
m1 *EAA*	2	1	-568.2	0.55	0.185	0.000	m1 *EAA*	4	1	-464.1	16.59	0.000	0.141
m4 *EAA * Non-EAA*	5	3	-567.7	1.06	0.143	0.039	m0 *Null*	2	0	-448.9	31.77	0.000	0.000

(c) EAA and non-EAA model summaries						
Model	***r***			***K***		
	edf	**F-value**	**P-value**	**edf**	**F-value**	**P-value**
m1 *EAA*	0.000	0.000	0.643	2.147	4.867	<0.001
m2 *Non-EAA*	0.633	0.431	0.102	1.938	4.858	<0.001
m3 *EAA +*	0.000	0.000	0.906	2.155	4.157	<0.001
Non-EAA	0.633	0.431	0.102	1.889	4.075	<0.001
m4 *EAA +*	0.000	0.000	1.000	0.000	0.000	0.247
Non-EAA	0.774	0.855	0.012	0.000	0.000	0.467
*EAA * Non-EAA*	1.617	0.307	0.163	5.329	5.663	<0.001

5.3.4 Variable free amino acids

Having established the effect of macronutrients and groups of amino acids on bacterial growth kinetics, the following section reports models containing individual amino acid effects. There was a difference in bacterial growth (r and K) depending on whether all the free amino acids were increased simultaneously (**Figure 5.1a**), or in a more disjointed fashion (**Figure 5.3a**). This indicates that individual amino acids had varying effects on r and K, which will be investigated in the following section. Not all haemolymph amino acids varied due to host dietary intake (Chapter 4), and so only the amino acids that were variable in host haemolymph due to variation in protein and carbohydrate intake are represented. In our SH design (Section 5.2.2.3), concentrations of these amino acids were varied, whilst all other amino acids were added in the mean values measured in the host haemolymph.

5.3.4.1 Non-essential amino acids

The variable non-EAA in the SH did not influence the bacterial growth rate, *r* (R^2 < 0.02; **Table 5.5a**) but produced variable effects on the carrying capacity, *K* (**Figure 5.4**); *K* decreased non-linearly (edf = 1.952) with increasing aspartic acid concentration (P < 0.001; R^2 = 0.301; **Figure 5.4a**), and linearly (edf = 1.477) with increasing cysteine concentration (P < 0.001; R^2 = 0.290; **Figure 5.4b**). In contrast, there was a non-linear increase in *K* with increasing levels of both glutamic acid (edf = 2.024; P < 0.001; R^2 = 0.167; **Figure 5.4c**) and serine (edf = 1.968; P < 0.001; R^2 = 0.170; **Figure 5.4d**), the primary difference being an earlier plateau in carrying capacity for the former.

5.3.4.2 Essential amino acids

Much like the variable non-EAA, altering EAA concentration was also poor at explaining variation in growth rate, *r* (R^2 < 0.01; **Table 5.5b**), but consistent in

explaining variation in carrying capacity, *K* (R^2 between 0.16 and 0.19), which decreased in a Sigmoidal fashion (**Figures 5.5a-c**) with increasing concentrations of isoleucine (edf = 1.970; P < 0.001), leucine (edf = 2.019; P < 0.001) and phenylalanine (edf = 1.973; P < 0.001). *K* decreased linearly with increasing concentration of tryptophan (edf = 0.963; P < 0.001; **Figure 5.5d**), but increased non-linearly with arginine (edf = 1.804; P < 0.001), lysine (edf = 1.814; P < 0.001) and valine (edf = 1.804; P < 0.001), peaking at mean amino acid concentrations (**Figures 5.5e-g**). The primary difference between the three EAA (arginine, lysine, and valine) and the other EAA was in the design of the SH: variation in the haemolymph concentrations of these three amino acids had been due to diet concentration rather than diet macronutrient content.

In summary, there appeared to be mixed effects of varying amino acid concentrations in the SHs on bacterial carrying capacity, *K*. There was no consistency depending on whether the amino acids were essential or not to the host. Serine was the only amino acid for which *K* was high at high concentrations. *K* increased with increasing concentrations of glutamic acid, arginine, lysine and valine, but decreased when these amino acids were added at concentrations above the mean. *K* decreased with increasing concentrations of all the other variable amino acids in the SH solution. All the amino acids were poor at explaining variation in bacterial growth rate, *r*.

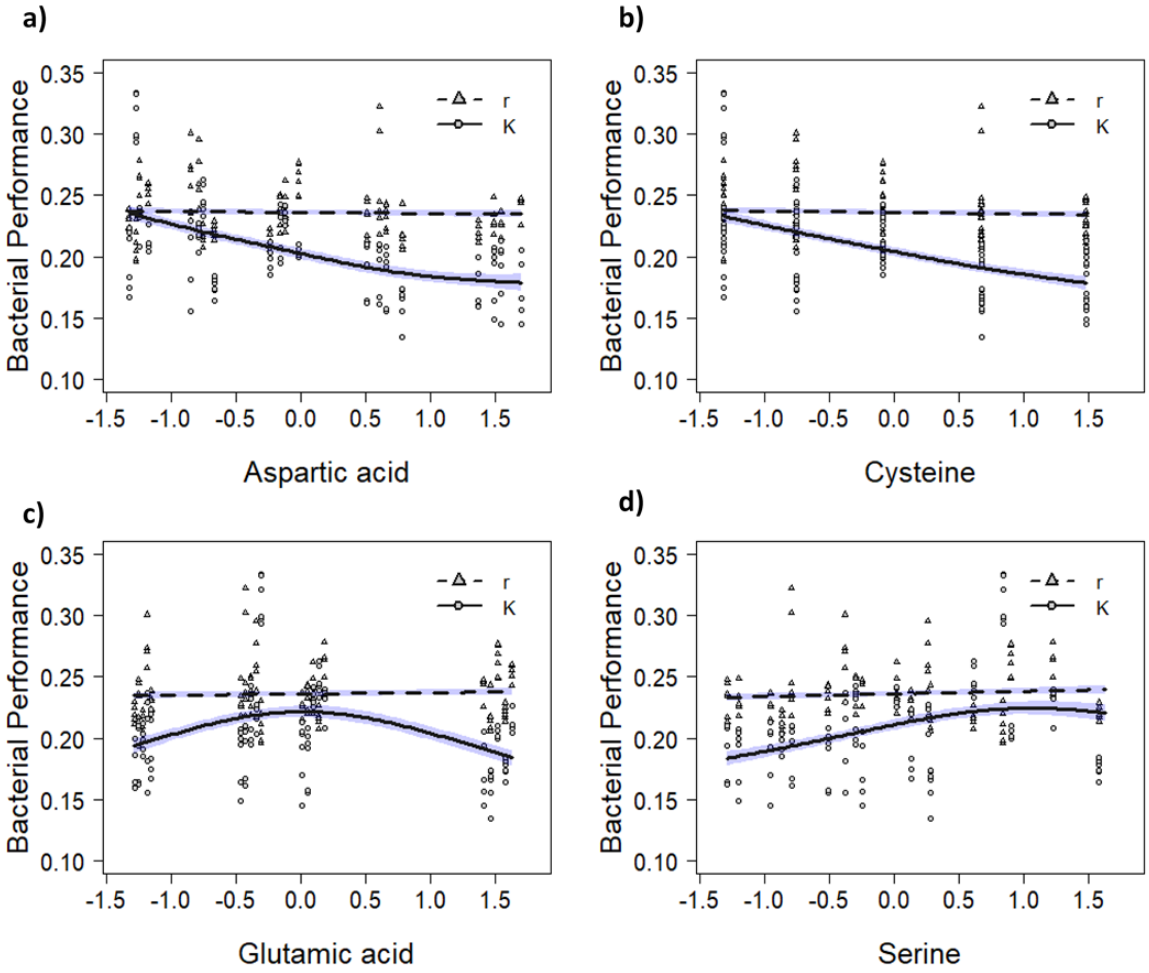
a)
b)
c)
d)
Bacterial Performance
0.35
0.30
0.25
0.20
0.15
0.10
-1.5
-1.0
-0.5
0.0
0.5
1.0
1.5
r
K
Aspartic acid
Cysteine
Glutamic acid
Serine

Figure 5.4: Effect of variable non-essential amino acids in synthetic haemolymphs (SH) on bacterial growth rate (*r*) and carrying capacity (*K*). Nutrient concentrations were standardized for analysis to allow comparison. (a) GAM model representing the effect of increasing aspartic acid concentration on *r* and *K*. There was no significant effect of increasing aspartic acid concentration on *r*. *K* decreased non-linearly (edf = 1.952) with increasing aspartic acid concentration in the SH. (b) GAM model representing the effect of increasing cysteine concentration on *r* and *K*. There was no significant effect of increasing cysteine concentration on *r*. *K* decreased linearly (edf = 1.477) with increasing cysteine concentration in the SH. (c) GAM model representing the effect of increasing glutamic acid concentration on *r* and *K*. There was no significant effect of increasing glutamic acid concentration on *r*. *K* increased quadratically (edf = 2.024) with an increasing concentration of glutamic acid in the SH, peaking at a mean glutamic acid concentration. (d) GAM model representing the effect of serine concentration on *r* and *K*. There was no effect of increasing serine concentration on *r*. *K* increased non-linearly (edf = 1.968) with increasing serine concentration in the SH.

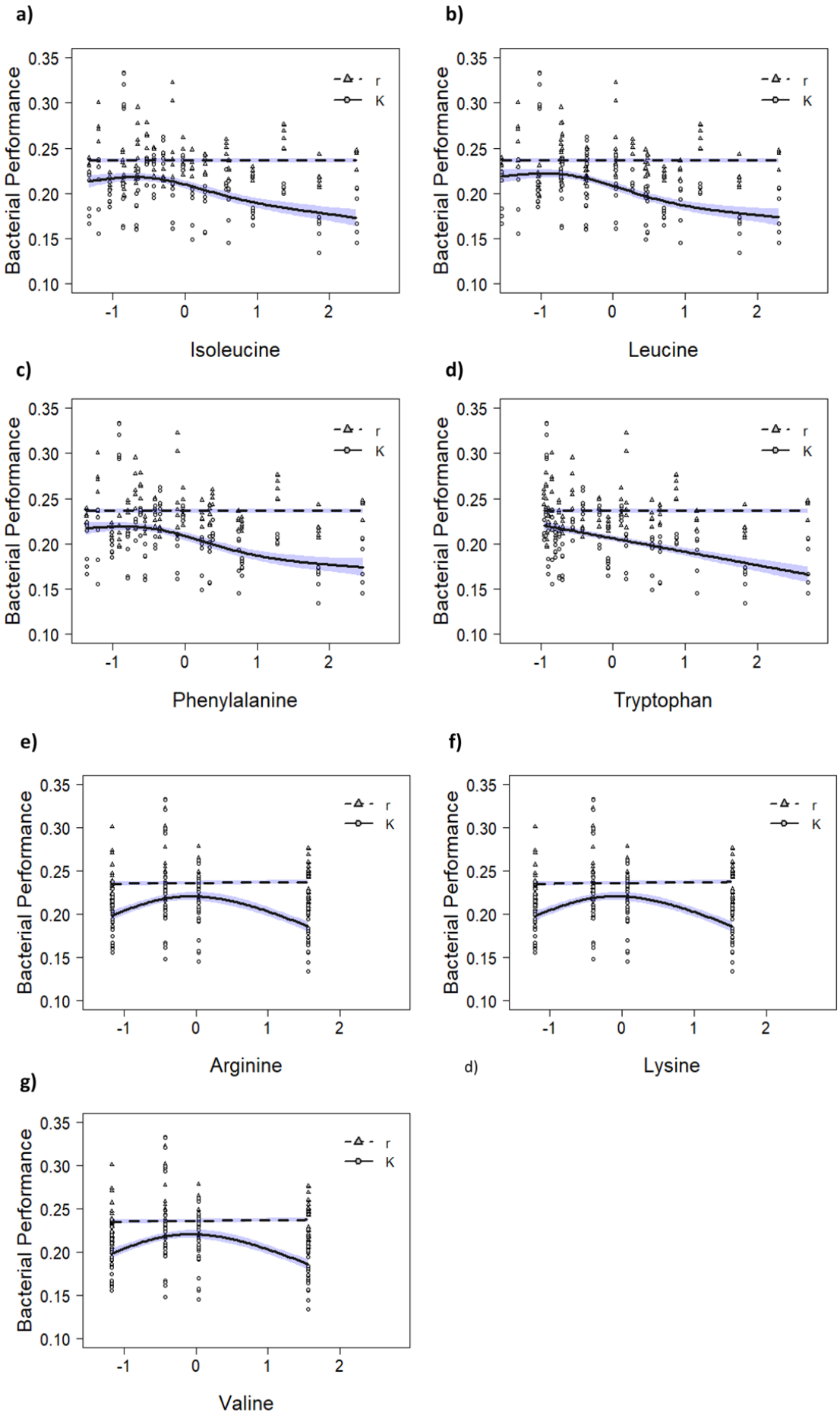
a)
b)
c)
d)
e)
f)
g)
Bacterial Performance
0.10
0.15
0.20
0.25
0.30
0.35
-1
0
1
2
r
K
Isoleucine
Leucine
Phenylalanine
Tryptophan
Arginine
Lysine
Valine
d)

Figure 5.5: Effect of variable essential amino acids in synthetic haemolymphs (SH) on bacterial growth rate (*r*) and carrying capacity (*K*). Nutrient concentrations were standardized for analysis to allow comparison. (a) GAM model representing the effect of increasing isoleucine concentration on *r* and *K*. There was no significant effect of increasing isoleucine concentration on *r*. *K* decreased non-linearly (edf = 1.970) with increasing isoleucine concentration in the SH. (b) GAM model representing the effect of increasing leucine concentration on *r* and *K*. There was no significant effect of increasing leucine concentration on *r*. *K* decreased non-linearly (edf = 2.019) with increasing leucine concentration in the SH. (c) GAM model representing the effect of increasing phenylalanine concentration on *r* and *K*. There was no significant effect of increasing phenylalanine concentration on *r*. *K* decreased non-linearly (edf = 1.973) with an increasing concentration of phenylalanine in the SH. (d) GAM model representing the effect of tryptophan concentration on *r* and *K*. There was no effect of increasing tryptophan concentration on *r*. *K* decreased linearly (edf = 0.963) with increasing tryptophan concentration in the SH. (e) GAM model representing the effect of increasing arginine concentration on *r* and *K*. There was no significant effect of increasing arginine concentration on *r*. *K* increased quadratically (edf = 1.804) with an increasing concentration of arginine in the SH, peaking at a mean arginine concentration. (f) GAM model representing the effect of increasing lysine concentration on *r* and *K*. There was no significant effect of increasing lysine concentration on *r*. *K* increased quadratically (edf = 1.814) with an increasing concentration of lysine in the SH, peaking at a mean lysine concentration. (g) GAM model representing the effect of increasing valine concentration on *r* and *K*. There was no significant effect of increasing valine concentration on *r*. *K* increased quadratically (edf = 1.804) with an increasing concentration of valine in the SH, peaking at a mean valine concentration.

Table 5.5: Individual synthetic haemolymph (SH) amino acids model summary tables. The left-hand side of the tables contains the summary information from models testing the effect of individual amino acids in the SH on bacterial growth rate (*r*). The right-hand side of the table contains the summary information produced by separate models testing the effect of individual amino acids in the SH on bacterial carrying capacity (*K*). Only the amino acids with varying concentrations in different SH were tested statistically. Each amino acid was analysed independently as an explanatory variable. Amino acids were also analysed in separate models for variation in *r* and variation in *K*. The edf provides information about the shape of the curve, relating to the basis dimensions used by the model to fit the curve; for example, an edf close to 1 represents a linear effect, whilst an edf close to 2 represents a quadratic effect. (a) Summary information from models testing the effects of the non-essential amino acids that varied in the SH on *r* and *K*. (b) Summary information from models testing the effects of the essential amino acids that varied in the SH on *r* and *K*.

(a) Non-essential amino acid model summaries								
Nutrient	***r***				***K***			
	R^2	**edf**	**F-value**	**P-value**	**R^2**	**edf**	**F-value**	**P-value**
Aspartic acid	0.004	0.331	0.123	0.224	0.301	1.952	12.833	<0.001
Cysteine	0.006	0.416	0.177	0.194	0.290	1.477	12.156	<0.001
Glutamic acid	0.005	0.396	0.164	0.201	0.167	2.024	5.964	<0.001
Serine	0.015	0.640	0.445	0.098	0.170	1.968	6.085	<0.001

(b) Essential amino acid model summaries								
Nutrient	***r***				***K***			
	R^2	**edf**	**F-value**	**P-value**	**R^2**	**edf**	**F-value**	**P-value**
Isoleucine	0.000	0.000	0.000	0.644	0.160	1.970	5.680	<0.001
Leucine	0.000	0.000	0.000	0.955	0.199	2.019	7.410	<0.001
Phenylalanine	0.000	0.000	0.000	0.785	0.174	1.973	6.282	<0.001
Tryptophan	0.000	0.000	0.000	1.000	0.169	0.963	6.058	<0.001
Arginine	0.004	0.305	0.146	0.233	0.163	1.804	7.702	<0.001
Lysine	0.004	0.317	0.154	0.229	0.166	1.814	7.874	<0.001
Valine	0.004	0.305	0.146	0.233	0.163	1.804	7.710	<0.001

5.3.5 Amino acid interactions

The preceding section explained the effects of each amino acid that had been varied in the SH design on *K*. Although modelling the effect of each amino acid independently provides some clarity, it is a poor reflection of the environment that the pathogen would experience *in vivo*. There are further interactions between amino acids as they vary simultaneously in the insect haemolymph. This section explores the cumulative effects of all the amino acids and then, presents models that investigated pair-wise interactions between amino acids. Pair-wise interactions were used to ease interpretation of model outcomes. Since the amino acids were poor at explaining variation in bacterial growth rate, *r*, these interactive effects are explored only for variation in the bacterial carrying capacity, *K*.

5.3.5.1 Comparing variation explained by amino acids

An information theoretic approach was used to compare the proportion of variation in *K* explained by each amino acid independently (**Table 5.6a**). This model attributed the variation in *K* solely to asparagine ($R^2 = 0.301$) and cysteine ($R^2 = 0.290$), both of which explained 10% more variation in *K* than leucine ($R^2 = 0.199$), the third 'best' amino acid. Oddly, the variation explained by these two amino acids became negligible once variation in other amino acids was accounted for in a single model (**Table 5.6b**). This single model attributed variation in *K* to glutamic acid ($P = 0.001$), arginine ($P = 0.015$), serine ($P < 0.001$), lysine ($P < 0.001$), tryptophan ($P = 0.004$) and valine ($P = 0.009$).

The six amino acids that explained variation in *K* in a single model were chosen for subsequent analysis exploring interaction effects between amino acids. Models containing interaction terms between arginine, lysine and valine did not converge, due to a positive correlation between the concentrations of these amino acids in the SH

media. As such, lysine was chosen to represent the three amino acids since it explained marginally more variation in *K* (**Table S5.7**). The data for arginine and valine are not shown because they produced identical relationships to lysine.

5.3.5.2 Amino acid interactions

5.3.5.2.1 Lysine and tryptophan

Variation in *K* was entirely explained by a model containing an interaction between lysine and tryptophan (m4; **Table 5.7a**). This model (R^2 = 0.539) explained 8% more variation than a model containing the combined effect of the two amino acids (m3; R^2 = 0.460). When visualised (**Figure 5.6**), *K* peaked in a nutrient space containing a mid-to-low concentration of lysine and low concentration of tryptophan.

5.3.5.2.2 Lysine and glutamic acid

Although there was a significant interaction between lysine and glutamic acid ($P < 0.001$; **Table 5.8b**), a model containing this effect (m4) was only the second-best model in the AIC comparison. The AIC result attributed variation in *K* entirely to an additive model (m3; **Table 5.8b**), that explained 30% more variation. This model indicated that *K* decreased non-linearly (edf = 2.338, $P < 0.001$) with increasing lysine concentration and increased non-linearly (edf = 1.953, $P < 0.001$) with increasing glutamic acid concentration (**Figure 5.7**).

5.3.5.2.3 Lysine and serine

A model containing an interaction between lysine and serine (m4; R^2 = 0.548) explained 4% more variation in *K* than a model containing only additive effects (m3; R^2 = 0.504). This was reflected in the AIC table (**Table 5.9a**), which attributed most of the variation in *K* to m4, with an evidence ratio of 22.8 against m3. Visualisation of the interaction between these two amino acids (**Figure 5.8**) indicated that *K* peaked in a nutrient space

containing a mid-to-low concentration of lysine and a mid-to-high concentration of serine.

5.3.5.2.4 Tryptophan and glutamic acid

8% more variation in *K* was explained by the model containing an interaction between tryptophan and glutamic acid (m4; R^2 = 0.569) than the model containing additive effects (m3; R^2 = 0.487) of these two amino acids (**Table 5.10a**). The AIC comparison attributed variation in *K* entirely to m4, and visualization by a thin-plate spline plot (**Figure 5.9**) indicated that *K* peaked in a nutrient space containing a mean concentration of glutamic acid and a low concentration of tryptophan.

5.3.5.2.5 Tryptophan and serine

When combined with tryptophan, variation in *K* explained by serine is entirely due to an interaction effect (**Table 5.11b**). The effect of serine on *K*, which is significant in the individual model (m2; P < 0.001) and the additive model (m3; P < 0.001) is non-significant in the *Interaction* model (m4; P = 0.236). The *Interaction* model (R^2 = 0.525) was the top model in the AIC comparison (**Table 5.11a**) and explained 16% more variation than the second-best model (m3; R^2 = 0.364). Visualisation by thin-plate regression (**Figure 5.10**) indicated that *K* peaked in a nutrient space high in serine concentration and low in tryptophan concentration.

5.3.5.2.6 Glutamic acid and serine

6% more variation in *K* was explained by the model containing an interaction between glutamic acid and serine (m4; R^2 = 0.560; **Table 5.12a**) than the model containing solely additive effects (m3; R^2 = 0.500). As such the evidence ratio for m4, the best model in the AIC comparison table (**Table 5.12a**), against m3 (the second-best model)

was 141.9. When visualised, *K* peaked in a nutrient space containing a mid-to-low concentration of glutamic acid and a mid-to-high concentration of serine (**Figure 5.11**).

5.3.5.2.7 Summary

As expected, there were multiple interactions between pairs of amino acids in the SH media, leading to variable effects on bacterial carrying capacity, *K*. The non-EAA (glutamic acid and serine) increased *K* when combined with EAA (lysine, and tryptophan), however, models containing both non-EAA indicated that increasing SH glutamic acid concentration produced a predominantly negative effect on *K* in the presence of serine. Similarly, lysine, produced predominantly negative effects on *K* with increasing concentration, but *K* increased at low concentrations of lysine in the presence of the other EAA, tryptophan. The only pair-wise relationship explored for which variation in *K* was better explained by additive effects than an interaction was lysine and glutamic acid.

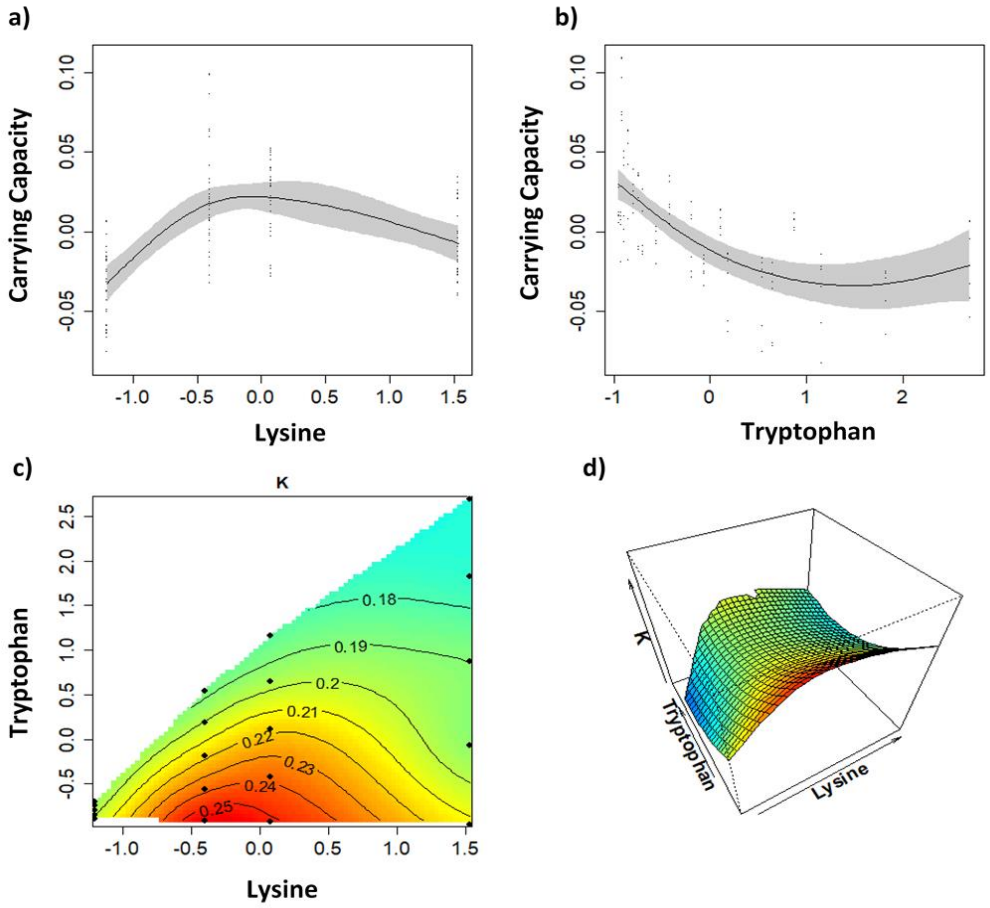

Figure 5.6: Interactive effects between lysine and tryptophan in synthetic haemolymphs (SH) on bacterial carrying capacity (*K*). Nutrient concentrations were standardized for analysis to allow comparison. (a) GAM model representing the effect of lysine concentration in SH on *K*. The effect of increasing SH lysine concentration on *K* was quadratic (edf = 2.615), peaking at a mean concentration of lysine. (b) GAM model representing the effect of tryptophan concentration in SH on *K*. *K* decreased non-linearly (edf = 2.404) with increasing tryptophan concentration. (c) 2D contour plot comparing *K* (z-axis) with lysine (x-axis) and tryptophan (y-axis) simultaneously. Contour lines represent the type of relationship between the dependent variable and the two independent variables. Colour represents the strength of effect, with blue indicating the weakest effect going up to red which represents the strongest effect. *K* peaked in a nutrient space containing a mid-level of lysine and a low concentration of tryptophan. (d) 3D representation of contour plot.

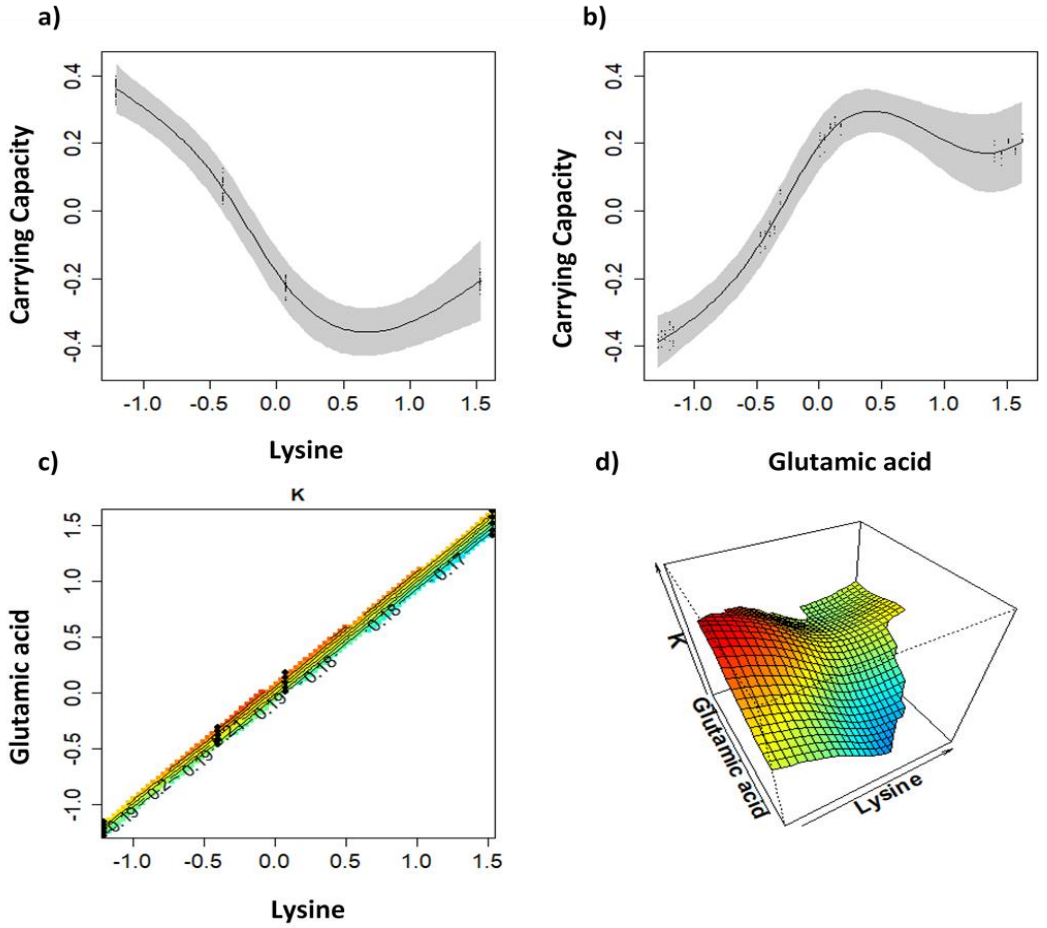

Figure 5.7: Interactive effects between lysine and glutamic acid in synthetic haemolymphs (SH) on bacterial carrying capacity (*K*). Nutrient concentrations were standardized for analysis to allow comparison. (a) GAM model representing the effect of lysine concentration in SH on *K*. *K* decreased non-linearly (edf = 2.338) with increasing lysine concentration. (b) GAM model representing the effect of glutamic acid concentration in SH on *K*. *K* increased non-linearly (edf = 1.953) with increasing glutamic acid concentration. (c) 2D contour plot comparing *K* (z-axis) with lysine (x-axis) and glutamic acid (y-axis) simultaneously. Contour lines represent the type of relationship between the dependent variable and the two independent variables. Colour represents the strength of effect, with blue indicating the weakest effect going up to red which represents the strongest effect. *K* peaked in a nutrient space containing a low concentration of lysine and a high concentration of glutamic acid. (d) 3D representation of contour plot.

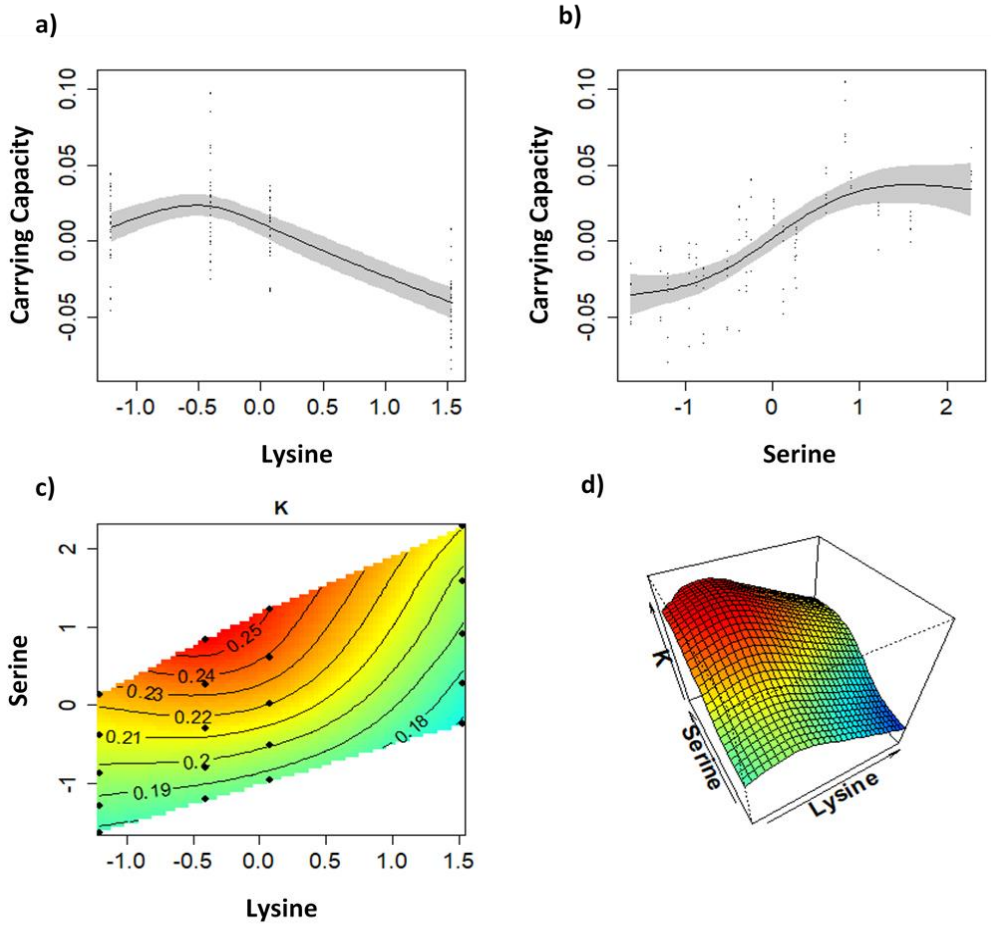

Figure 5.8: Interactive effects between lysine and serine in synthetic haemolymphs (SH) on bacterial carrying capacity (*K*). Nutrient concentrations were standardized for analysis to allow comparison. (a) GAM model representing the effect of lysine concentration in SH on *K*. *K* decreased non-linearly (edf = 1.936) with increasing lysine concentration. (b) GAM model representing the effect of serine concentration in SH on *K*. *K* increased non-linearly (edf = 1.930) with increasing serine concentration. (c) 2D contour plot comparing *K* (z-axis) with lysine (x-axis) and serine (y-axis) simultaneously. Contour lines represent the type of relationship between the dependent variable and the two independent variables. Colour represents the strength of effect, with blue indicating the weakest effect going up to red which represents the strongest effect. *K* peaked in a nutrient space containing a mid-to-low concentration of lysine and a mid-to-high concentration of serine. (d) 3D representation of contour plot.

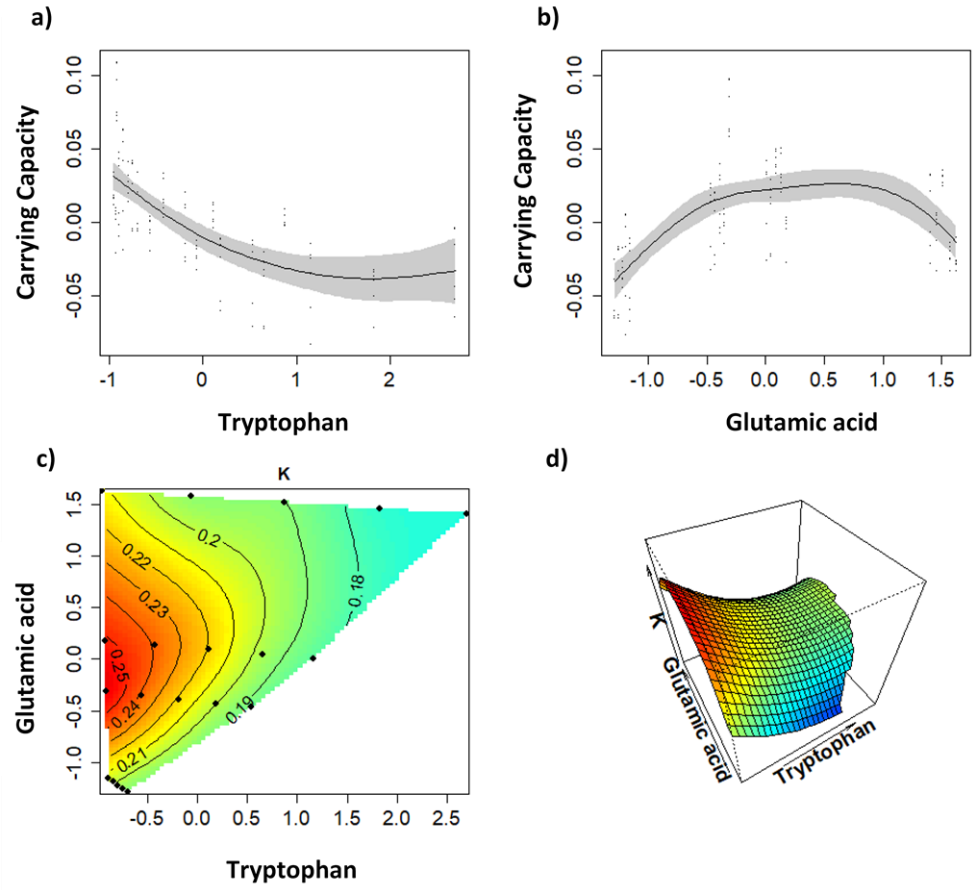

Figure 5.9: Interactive effects between tryptophan and glutamic acid in synthetic haemolymphs (SH) on bacterial carrying capacity (*K*). Nutrient concentrations were standardized for analysis to allow comparison. (a) GAM model representing the effect of tryptophan concentration in SH on *K*. *K* decreased non-linearly (edf = 2.617) with increasing tryptophan concentration. (b) GAM model representing the effect of glutamic acid concentration in SH on *K*. The effect of SH glutamic acid concentration on *K* was quadratic (edf = 2.574), peaking at a mean concentration of glutamic acid. (c) 2D contour plot comparing *K* (z-axis) with tryptophan (x-axis) and glutamic acid (y-axis) simultaneously. Contour lines represent the type of relationship between the dependent variable and the two independent variables. Colour represents the strength of effect, with blue indicating the weakest effect going up to red which represents the strongest effect. *K* peaked in a nutrient space containing a low concentration of tryptophan and a mid-level of glutamic acid. (d) 3D representation of contour plot.

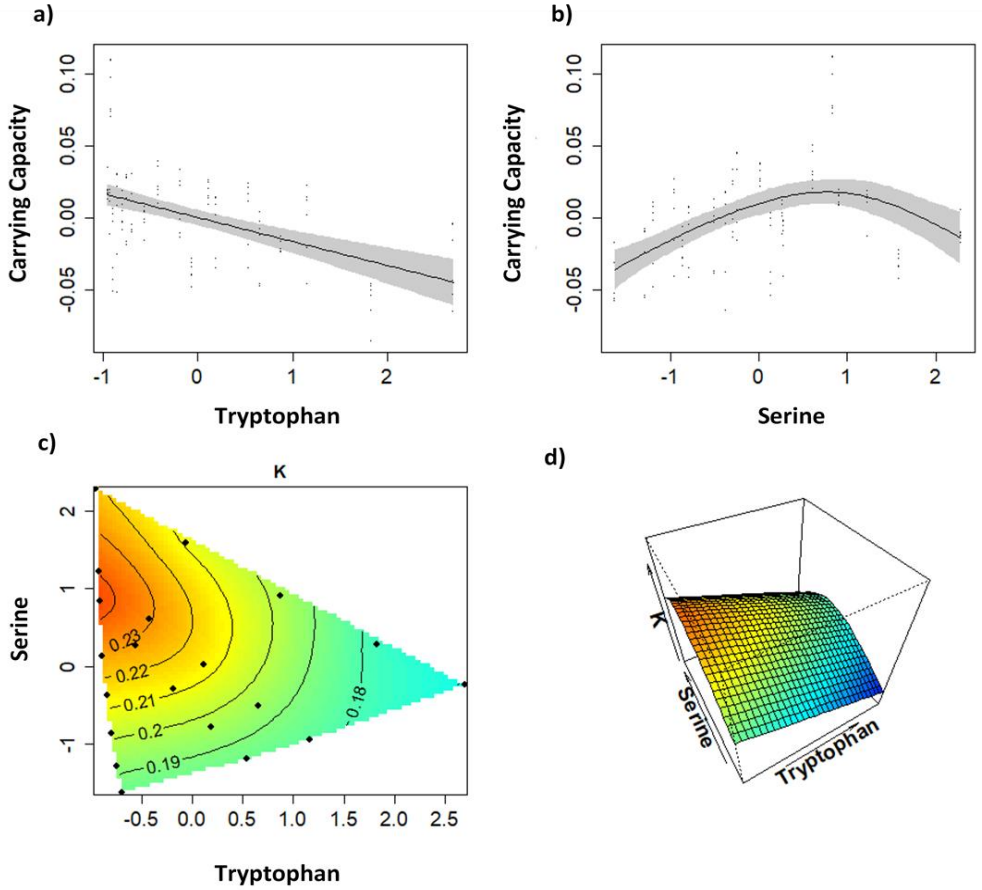

Figure 5.10: Interactive effects between tryptophan and serine in synthetic haemolymphs (SH) on bacterial carrying capacity (*K*). Nutrient concentrations were standardized for analysis to allow comparison. (a) GAM model representing the effect of tryptophan concentration in SH on *K*. *K* decreased linearly (edf = 0.819) with increasing tryptophan concentration. (b) GAM model representing the effect of serine concentration in SH on *K*. The effect of SH serine concentration on *K* was quadratic (edf = 2.194); *K* peaked at a high concentration of serine. (c) 2D contour plot comparing *K* (z-axis) with tryptophan (x-axis) and serine (y-axis) simultaneously. Contour lines represent the type of relationship between the dependent variable and the two independent variables. Colour represents the strength of effect, with blue indicating the weakest effect going up to red which represents the strongest effect. *K* peaked in a nutrient space containing a low concentration of tryptophan and a high concentration of serine. (d) 3D representation of contour plot.

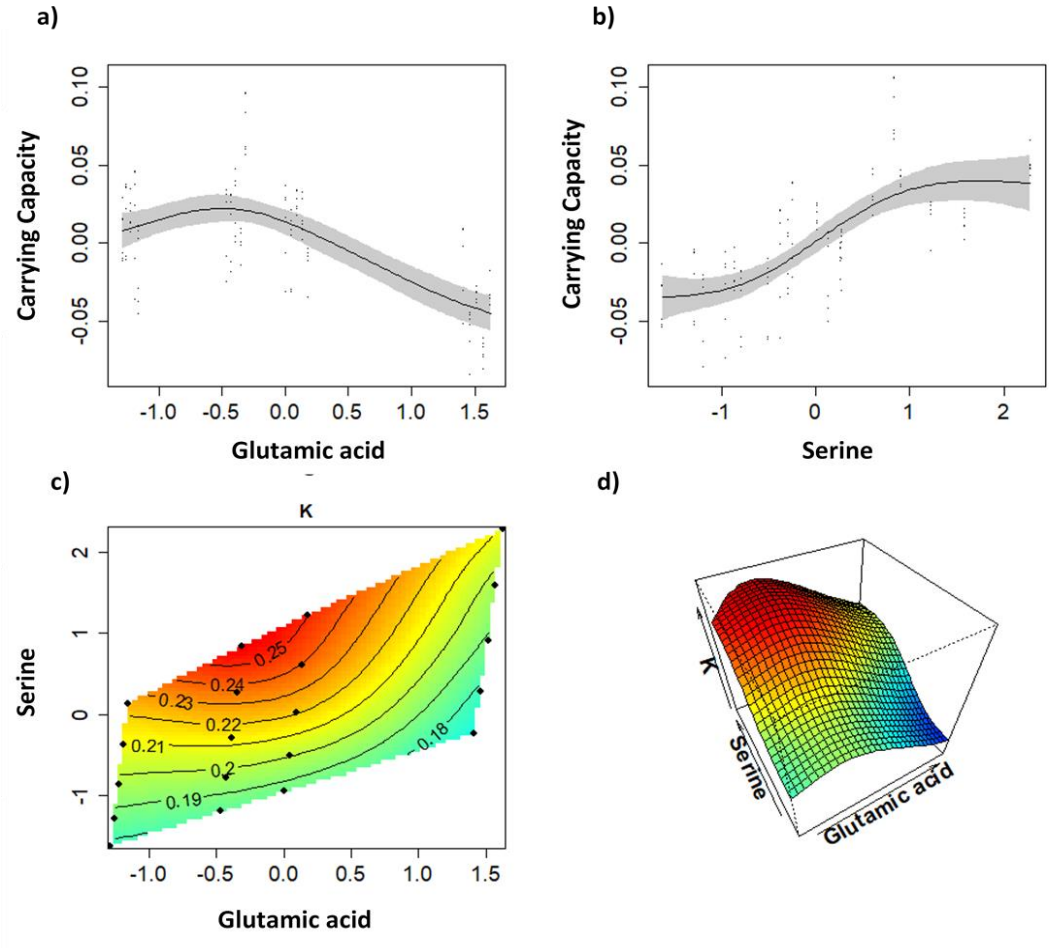

Figure 5.11: Interactive effects between glutamic acid and serine in synthetic haemolymphs (SH) on bacterial carrying capacity (*K*). Nutrient concentrations were standardized for analysis to allow comparison. (a) GAM model representing the effect of glutamic acid concentration in SH on *K*. *K* decreased non-linearly (edf = 2.272) with increasing glutamic acid concentration. (b) GAM model representing the effect of serine concentration in SH on *K*. *K* increased non-linearly (edf = 2.359) with increasing serine concentration. (c) 2D contour plot comparing *K* (z-axis) with glutamic acid (x-axis) and serine (y-axis) simultaneously. Contour lines represent the type of relationship between the dependent variable and the two independent variables. Colour represents the strength of effect, with blue indicating the weakest effect going up to red which represents the strongest effect. *K* peaked in a nutrient space containing a mid-to-low concentration of glutamic acid and a mid-to-high concentration of serine. (d) 3D representation of contour plot.

Table 5.6: Variation in bacterial carrying capacity (K) explained by the amino acids in the synthetic haemolymph (SH) model summary tables. (a) AIC comparison table for models containing each of the amino acids in the SH as explanatory variables. df is the degrees of freedom used by the model to produce a fit and not the degrees of freedom based on the number of explanatory variables. K is the number terms in the model. AICc is the model Aikake values. Delta represents the difference between a model and the model explaining the most variation. Weight is determined by the amount of variation a model explains penalized for the degrees of freedom used by the model. The edf provides information about the shape of the curve, relating to the basis dimensions used by the model to fit the curve; for example, an edf close to 1 represents a linear effect, whilst an edf close to 2 represents a quadratic effect. (b) Summary information from a single model testing the variation in *K* explained by all the variable amino acids in the SH together.

(a) Model AICs: Independent amino acid models for *K*									
Model	**df**	**k**	**AICc**	**delta**	**weight**	**edf**	**F-value**	**P-value**	**R^2**
m1 *Aspartic acid*	4	1	-488.8	0.00	0.642	1.952	12.833	<0.001	0.301
m3 *Cysteine*	3	1	-487.7	1.17	0.358	1.477	12.156	<0.001	0.290
m7 *Leucine*	4	1	-472.8	16.00	0.000	2.019	7.410	<0.001	0.199
m10 *Tryptophan*	3	1	-470.0	18.81	0.000	0.963	6.058	<0.001	0.169
m9 *Phenylalanine*	4	1	-469.1	19.70	0.000	1.973	6.282	<0.001	0.174
m4 *Serine*	4	1	-468.6	20.26	0.000	1.968	6.085	<0.001	0.170
m8 *Lysine*	3	1	-468.3	20.54	0.000	1.814	7.874	<0.001	0.166
m2 *Glutamic acid*	4	1	-468.1	20.72	0.000	2.024	5.964	<0.001	0.167
m11 *Valine*	3	1	-467.9	20.96	0.000	1.804	7.710	<0.001	0.163
m5 *Arginine*	3	1	-467.8	20.98	0.000	1.804	7.702	<0.001	0.163
m6 *Isoleucine*	4	1	-467.0	21.82	0.000	1.970	5.680	<0.001	0.160
m0 *Null*	2	0	-448.9	39.91	0.000				0.000

(b) Single model with all amino acids; R^2= 0.53			
Model Term	**edf**	**F-value**	**P-value**
Aspartic acid	0.000	0.000	0.695
Glutamic acid	0.003	0.001	0.001
Cysteine	0.000	0.000	0.734
Arginine	0.000	0.000	0.015
Serine	1.856	11.717	<0.001
Isoleucine	0.000	0.000	0.693
Leucine	0.000	0.000	0.655
Lysine	1.839	14.509	<0.001
Phenylalanine	0.000	0.000	0.590
Tryptophan	1.531	2.685	0.004
Valine	0.000	0.000	0.009

Table 5.7: Variation in bacterial carrying capacity (*K*) by synthetic haemolymph (SH) lysine and tryptophan model summary tables. (a) AIC comparison table for models containing SH lysine and tryptophan as explanatory variables. m0 (Null) is a model with no explanatory terms included, providing a baseline measure of variation. m1 (Lysine) is a model containing standardized variation in SH lysine concentration. m2 (Tryptophan) is a model containing standardized variation in SH tryptophan concentration. m3 (Lysine + Tryptophan) is a model containing both SH lysine and tryptophan. m4 (Lysine * Tryptophan) is a model that includes an interaction term (represented by asterisk) between SH lysine and tryptophan. df is the degrees of freedom used by the model to produce a fit and not the degrees of freedom based on the number of explanatory variables. k is the number terms in the model. AICc is the model Aikake values. Delta represents the difference between a model and the model explaining the most variation. Weight is determined by the amount of variation a model explains penalized for the degrees of freedom used by the model. (b) Summary information for each model in the AIC comparison table. The edf provides information about the shape of the curve, relating to the basis dimensions used by the model to fit the curve; for example, an edf close to 1 represents a linear effect, whilst an edf close to 2 represents a quadratic effect.

(a) Model AICs: Lysine and tryptophan

Model	df	k	AICc	delta	weight	R^2
m4 *Lysine * Tryptophan*	10	3	-530.6	0.00	0.999	0.539
m3 *Lysine + Tryptophan*	7	2	-515.8	14.76	0.001	0.460
m2 *Tryptophan*	3	1	-470.0	60.55	0.000	0.169
m1 *Lysine*	3	1	-468.3	62.28	0.000	0.166
m0 *Null*	2	0	-448.9	81.65	0.000	0.000

(b) Lysine and tryptophan model summaries

Model	edf	F-value	P-value
m1			
Lysine	1.814	7.874	<0.001
m2			
Tryptophan	0.961	8.076	<0.001
m3			
Lysine +	2.615	20.512	<0.001
Tryptophan	2.404	20.267	<0.001
m4			
Lysine +	0.902	3.053	0.001
Tryptophan +	0.804	1.360	0.018
*Lysine * Tryptophan*	6.073	11.639	<0.001

Table 5.8: Variation in bacterial carrying capacity (*K*) by synthetic haemolymph (SH) lysine and glutamic acid model summary tables. (a) AIC comparison table for models containing SH lysine and glutamic acid as explanatory variables. m0 (Null) is a model with no explanatory terms included, providing a baseline measure of variation. m1 (Lysine) is a model containing standardized variation in SH lysine concentration. m2 (Glutamic acid) is a model containing standardized variation in SH glutamic acid concentration. m3 (Lysine + Glutamic acid) is a model containing both SH lysine and glutamic acid. m4 (Lysine * Glutamic acid) is a model that includes an interaction term (represented by asterisk) between SH lysine and glutamic acid. df is the degrees of freedom used by the model to produce a fit and not the degrees of freedom based on the number of explanatory variables. k is the number terms in the model. AICc is the model Aikake values. Delta represents the difference between a model and the model explaining the most variation. Weight is determined by the amount of variation a model explains penalized for the degrees of freedom used by the model. (b) Summary information for each model in the AIC comparison table. The edf provides information about the shape of the curve, relating to the basis dimensions used by the model to fit the curve; for example, an edf close to 1 represents a linear effect, whilst an edf close to 2 represents a quadratic effect.

(a) Model AICs: Lysine and glutamic acid

Model	df	k	AICc	delta	weight	R^2
m3 *Lysine + Glutamic acid*	6	2	-522.1	0.00	1.000	0.481
m4 *Lysine * Glutamic acid*	5	3	-469.3	52.80	0.000	0.184
m2 *Glutamic acid*	3	1	-468.7	53.40	0.000	0.168
m1 *Lysine*	3	1	-468.3	53.80	0.000	0.166
m0 *Null*	2	0	-448.9	73.17	0.000	0.000

(b) Lysine and glutamic acid model summaries

Model	edf	F-value	P-value
m1			
Lysine	1.814	7.874	<0.001
m2			
Glutamic acid	1.846	8.027	<0.001
m3			
Lysine +	2.338	22.869	<0.001
Glutamic acid	1.953	22.690	<0.001
m4			
Lysine +	0.432	0.201	0.015
Glutamic acid +	0.000	0.000	0.137
*Lysine * Glutamic acid*	2.075	0.963	<0.001

Table 5.9: Variation in bacterial carrying capacity (*K*) by synthetic haemolymph (SH) lysine and serine model summary tables. (a) AIC comparison table for models containing SH lysine and serine as explanatory variables. m0 (Null) is a model with no explanatory terms included, providing a baseline measure of variation. m1 (Lysine) is a model containing standardized variation in SH lysine concentration. m2 (Serine) is a model containing standardized variation in SH serine concentration. m3 (Lysine + Serine) is a model containing both SH lysine and serine. m4 (Lysine * Serine) is a model that includes an interaction term (represented by asterisk) between SH lysine and serine. df is the degrees of freedom used by the model to produce a fit and not the degrees of freedom based on the number of explanatory variables. k is the number terms in the model. AICc is the model Aikake values. Delta represents the difference between a model and the model explaining the most variation. Weight is determined by the amount of variation a model explains penalized for the degrees of freedom used by the model. (b) Summary information for each model in the AIC comparison table. The edf provides information about the shape of the curve, relating to the basis dimensions used by the model to fit the curve; for example, an edf close to 1 represents a linear effect, whilst an edf close to 2 represents a quadratic effect.

(a) Model AICs: Lysine and serine						
Model	**df**	**k**	**AICc**	**delta**	**weight**	**R^2**
m4 *Lysine * Serine*	9	3	-534.6	0.00	0.958	0.548
m3 *Lysine + Serine*	5	2	-528.3	6.25	0.042	0.504
m2 *Serine*	3	1	-469.1	65.52	0.000	0.171
m1 *Lysine*	3	1	-468.3	66.31	0.000	0.166
m0 *Null*	2	0	-448.9	85.68	0.000	0.000

(b) Lysine and serine model summaries			
Model	**edf**	**F-value**	**P-value**
m1			
Lysine	1.814	7.874	<0.001
m2			
Serine	1.801	8.190	<0.001
m3			
Lysine +	1.936	25.782	<0.001
Serine	1.930	26.190	<0.001
m4			
Lysine +	1.824	7.591	<0.001
Serine +	0.934	4.698	<0.001
*Lysine * Serine*	4.005	2.582	<0.001

Table 5.10: Variation in bacterial carrying capacity (*K*) by synthetic haemolymph (SH) tryptophan and glutamic acid model summary tables. (a) AIC comparison table for models containing SH tryptophan and glutamic acid as explanatory variables. m0 (Null) is a model with no explanatory terms included, providing a baseline measure of variation. m1 (Tryptophan) is a model containing standardized variation in SH tryptophan concentration. m2 (Glutamic acid) is a model containing standardized variation in SH glutamic acid concentration. m3 (Tryptophan + Glutamic acid) is a model containing both SH tryptophan and glutamic acid. m4 (Tryptophan * Glutamic acid) is a model that includes an interaction term (represented by asterisk) between SH tryptophan and glutamic acid. df is the degrees of freedom used by the model to produce a fit and not the degrees of freedom based on the number of explanatory variables. k is the number terms in the model. AICc is the model Aikake values. Delta represents the difference between a model and the model explaining the most variation. Weight is determined by the amount of variation a model explains penalized for the degrees of freedom used by the model. (b) Summary information for each model in the AIC comparison table. The edf provides information about the shape of the curve, relating to the basis dimensions used by the model to fit the curve; for example, an edf close to 1 represents a linear effect, whilst an edf close to 2 represents a quadratic effect.

(a) Model AICs: Tryptophan and glutamic acid

Model	df	k	AICc	delta	weight	R^2
m4 *Tryptophan * Glutamic acid*	10	3	-538.6	0.00	1.000	0.569
m3 *Tryptophan + Glutamic acid*	7	2	-521.3	17.32	0.000	0.487
m1 *Tryptophan*	3	1	-470.0	68.63	0.000	0.169
m2 *Glutamic acid*	4	1	-468.1	70.55	0.000	0.167
m0 *Null*	2	0	-448.9	89.73	0.000	0.000

(b) Tryptophan and glutamic acid model summaries

Model	edf	F-value	P-value
m1 *Tryptophan*	0.963	6.058	<0.001
m2 *Glutamic acid*	2.024	5.964	<0.001
m3 *Tryptophan +*	2.617	17.806	<0.001
Glutamic acid	2.574	17.630	<0.001
m4 *Tryptophan +*	0.857	1.494	0.006
Glutamic acid +	0.923	2.987	<0.001
*Tryptophan * Glutamic acid*	6.184	13.158	<0.001

Table 5.11: Variation in bacterial carrying capacity (*K*) by synthetic haemolymph (SH) tryptophan and serine model summary tables. (a) AIC comparison table for models containing SH tryptophan and serine as explanatory variables. m0 (Null) is a model with no explanatory terms included, providing a baseline measure of variation. m1 (Tryptophan) is a model containing standardized variation in SH tryptophan concentration. m2 (Serine) is a model containing standardized variation in SH serine concentration. m3 (Tryptophan + Serine) is a model containing both SH tryptophan and serine. m4 (Tryptophan * Serine) is a model that includes an interaction term (represented by asterisk) between SH tryptophan and serine. df is the degrees of freedom used by the model to produce a fit and not the degrees of freedom based on the number of explanatory variables. k is the number terms in the model. AICc is the model Aikake values. Delta represents the difference between a model and the model explaining the most variation. Weight is determined by the amount of variation a model explains penalized for the degrees of freedom used by the model. (b) Summary information for each model in the AIC comparison table. The edf provides information about the shape of the curve, relating to the basis dimensions used by the model to fit the curve; for example, an edf close to 1 represents a linear effect, whilst an edf close to 2 represents a quadratic effect.

(a) Model AICs: Tryptophan and serine

Model	df	k	AICc	delta	weight	R^2
m4 *Tryptophan * Serine*	10	3	-527.5	0.00	1.000	0.525
m3 *Tryptophan + Serine*	5	2	-499.0	28.50	0.000	0.364
m1 *Tryptophan*	3	1	-470.0	57.49	0.000	0.169
m2 *Serine*	4	1	-468.6	58.94	0.000	0.170
m0 *Null*	2	0	-448.9	78.59	0.000	0.000

(b) Tryptophan and serine model summaries

Model	edf	F-value	P-value
m1			
Tryptophan	0.963	6.058	<0.001
m2			
Serine	1.968	6.085	<0.001
m3			
Tryptophan +	0.972	8.716	<0.001
Serine	2.194	8.973	<0.001
m4			
Tryptophan +	0.819	1.131	0.014
Serine +	0.237	0.078	0.236
*Tryptophan * Serine*	6.187	9.972	<0.001

Table 5.12: Variation in bacterial carrying capacity (*K*) by synthetic haemolymph (SH) glutamic acid and serine model summary tables. (a) AIC comparison table for models containing SH glutamic acid and serine as explanatory variables. m0 (Null) is a model with no explanatory terms included, providing a baseline measure of variation. m1 (Glutamic acid) is a model containing standardized variation in SH glutamic acid concentration. m2 (Serine) is a model containing standardized variation in SH serine concentration. m3 (Glutamic acid + Serine) is a model containing both SH glutamic acid and serine. m4 (Glutamic acid * Serine) is a model that includes an interaction term (represented by asterisk) between SH glutamic acid and serine. df is the degrees of freedom used by the model to produce a fit and not the degrees of freedom based on the number of explanatory variables. k is the number terms in the model. AICc is the model Aikake values. Delta represents the difference between a model and the model explaining the most variation. Weight is determined by the amount of variation a model explains penalized for the degrees of freedom used by the model. (b) Summary information for each model in the AIC comparison table. The edf provides information about the shape of the curve, relating to the basis dimensions used by the model to fit the curve; for example, an edf close to 1 represents a linear effect, whilst an edf close to 2 represents a quadratic effect.

(a) Model AICs: Glutamic acid and serine

Model	df	k	AICc	delta	weight	R^2
m4 *Glutamic acid * Serine*	10	3	-536.1	0.00	0.993	0.560
m3 *Glutamic acid + Serine*	6	2	-526.2	9.94	0.007	0.500
m2 *Serine*	4	1	-468.6	67.56	0.000	0.170
m1 *Glutamic acid*	4	1	-468.1	68.03	0.000	0.167
m0 *Null*	2	0	-448.9	87.22	0.000	0.000

(b) Glutamic acid and serine model summaries

Model	edf	F-value	P-value
m1 *Glutamic acid*	2.024	5.964	<0.001
m2 *Serine*	1.968	6.085	<0.001
m3 *Glutamic acid +* *Serine*	2.272 2.359	18.949 19.202	<0.001 <0.001
m4 *Glutamic acid +* *Serine +* *Glutamic acid * Serine*	1.984 0.940 4.700	4.405 3.840 3.213	<0.001 <0.001 <0.001

5.4 DISCUSSION

This study aimed to investigate *Xenorhabdus nematophila* maximum growth rate (*r*) and carrying capacity (*K*) in the range of nutritional environments it is likely to experience in the haemolymph of its host *Spodoptera littoralis*. Building on previous *in vivo* findings that showed an increased pathogen performance in a host nutrient space rich in carbohydrate and poor in protein, we took an *in vitro* approach to understanding the nutritional ecology of the bacterium in the absence of its host. Our results revealed the primary effects of host nutrition to be on the carrying capacity of the bacterium rather than its growth rate (**Figure S5.2**). In nutritional media that was constant in all respects apart from a focal nutrient group, pathogen growth rate, *r*, tended to increase with nutrient-concentration but the pattern of growth differed across nutrient groups. Overall, the mean bacterial growth rates were highest in carbohydrate-rich mediums and lowest for protein-rich ones. Bacterial carrying capacity, *K*, tended to be highest in a carbohydrate-rich environment (or one that was dominated by the non-EAA, serine) and to be lowest in environments rich in protein or EAA. Rather than additive effects of the various amino acids, *K* appeared to be determined by interactions between various amino acids.

5.4.1 Difference in growth rate and carrying capacity.

Our synthetic host environment showed a negligible effect of host diet on *r*, which was influenced only by the interaction between haemolymph protein and carbohydrate concentrations. This indicates that *X. nematophila* invests equally in its growth rate irrespective of fluctuations in its nutrient environment. Similarly, virulent strains of *Flavobacterium columnare*, a pathogen of freshwater fish, consistently outcompeted non-virulent strains in high and low nutritional environments due to predetermined

differences in their growth rate, rather than changes in response to their nutrient environment (Pulkkinen et al., 2018). Microbes are expected to invest more in their growth rates when they are faced with direct competition for resources (Pekkonen et al., 2013). *X. nematophila* may not invest in growth rate since its primary form of competition is exclusion, as evidenced by its production of an array of antibiotics that create a sterile investment for its symbiont vector, *Steinernema carpocapsae* (Jubelin et al., 2011; Lanois et al., 2008). Nutrient environments cause changes in microbial behaviour through environmental sensing systems that regulate switches between phenotypically differing states (Cezairliyan and Ausubel, 2017; New et al., 2014). Due to the nature of its life cycle, this pathogen may have evolved to react to changes in its nutrient environment as cues for state variation rather than proliferation speed.

This idea is supported by the primary effect of nutrient variation on *K* despite similar growth rates across most of our treatments, indicating that the final bacterial counts were determined by the time at which cells switched from an exponential growth phase to a stationary phase. This can be viewed as a form of nutrient-mediated phenotypic plasticity leading to the expression of genes that reduce virulence and cause a switch from growing to vegetative cells, most likely in preparation for uptake by its nematode symbiont *S. carpocapsae* (Richards and Goodrich-Blair, 2009). The carrying capacity, *K*, is a measure of population size sustainable in a particular environment and it decreases due to increases in the *per capita* susceptibility of individuals to a high population density (Begon et al., 2005). Although *Xenorhabdus* species are generally not subject to interspecific competition, they do experience intraspecific competition. Multiple cells colonise the receptacle of the pre-infective juvenile (pre-IJ) nematodes within the insect host, however most IJs contain a monoculture by the time they infect a new host. There appears to be a selection process inside the receptacle that occurs in the maturation of the nematode from pre-IJs to fully infective IJs in-between hosts. Rather

than a steady reduction in the number of individual bacteria, the process involves the number of bacterial cells in the IJ receptacle growing and shrinking through competition until one bacterial clone remains (Martens et al., 2003). There is evidence to suggest that this process may be mediated by nutrients fed into receptacle by *S. carpocapsae* (Stilwell et al., 2018).

Oligopeptide permease (OPP) operons, mediators of peptide binding, may provide a cross-section between nutrient sensing in the environment and bacterial population density detection (Hiron et al., 2007; Lazazzera, 2001). These OPPs allow the bacterium's phenotypic state and metabolite production to vary in response to environmental cues. *Bacillus subtilis* spore formation could be induced by introduction of an extracellular oligopeptide transcription factor, *Spo0A*, which is transported with OPPs (Fujita and Losick, 2005, but see Ababneh et al., 2015). An *in vitro* study looking at an *X. nematophila OppA* gene mutant growth in *Manduca sexta* haemolymph found that in the nutrient-rich environment of LB broth, this mutant consistently exhibited lower optical densities (a *K* analogue) than the wildtype (Orchard and Goodrich-Blair, 2004). The authors confirmed that mutants with this gene were not dying off earlier but rather were entering stationary phase sooner. *OppA* is expressed higher in later phases of growth, and mutants with this gene exhibited mutualism and pathogenicity similar to the wildtype. Primary metabolites are usually produced in the growth phase, whilst secondary metabolites are produced near the end of the growth phase or during the stationary phase (Madigan et al., 2003). In the case of *X. nematophila*, primary metabolites would include virulence factors produced during the initial stages of infection, whilst secondary metabolites, such as antibiotics, would be involved in preparing the cadaver for nematode reproduction. The OPP operon is the likely mediator of the observed 'protein effects' in our study, since it balances environmental

sensing with metabolite production and state variation. Future studies could test this idea by measuring variation in *OppA* gene expression during bacterial growth in our SHs or investigate the difference in *K* between *OppA* gene mutants and wildtype *X. nematophila* grown in our SHs.

5.4.2 Independent effect of nutrient groups

To further understand how nutrients might lead to a change in state or phase, we must fully identify *X. nematophila* population fluctuations in response to specific nutrients. Our results showed a dominant positive effect of the carbohydrate content in our synthetic haemolymph on the bacteria's carrying capacity. When the results were investigated in the context of host diet, it appeared that the pathogen performed well in a nutrient space that contained a mid-level of carbohydrate albeit with a protein interaction, meaning that both nutrients were important for pathogen fitness. Our findings align with both a previous study investigating *X. nematophila* use of glucose (Kooliyottil et al., 2014), as well as our own studies of the *in vivo* pathogen nutrient use (**Chapters 2 & 3**), highlighting the balance between protein and carbohydrate as the determinant of pathogen load in the host. This calls into question the primary focus on sugars as the main energy source and primary determinant of bacterial fitness (Aidelberg et al., 2014). In fact, simple sugars were not varied in our diets, reflecting the limited variation observed in the haemolymph (Chapter 4) since this pathogen would not experience fluctuations in this nutrient group inside its host environment. Together, there appears to be a plausible link between *S. littoralis* larvae choosing to alter their haemolymph nutrient composition during infection (Lee et al., 2006), and the intake target of at least one of its pathogens, resulting in an increased chance of host survival.

Pathogen growth rate increases with increasing concentration across all nutrients examined, however growth rate was poorest in the single variable haemolymphs that

measured growth rate with increasing protein concentration (**Figure 5.1a**). In a protease production optimization experiment, Pranaw et al., (2014) found that *Xenorhabdus indica* enzyme production varied depending on the substrate provided, and soya casein hydrolysate induced a higher protease production than media containing other proteins. The author did not provide bacterial growth rate data, limiting comparability with our assay, nonetheless, it is possible that rather than a general protein effect, the poor bacterial growth rate and carrying capacity observed in our high protein environments could be a specific reaction to BSA, our chosen protein. Some bacterial groups, including Enterobacteriaceae, such as *Escherichia coli*, have specific binding sites for albumins (Myhre and Kronvall, 1980). *Xenorhabdus nematophila*, also an Enterobacteriaceae, may have analogous binding sites. Consistent with our findings of positive BSA effects on *K* at low concentrations (**Figure 5.1b**), BSA increased *E. coli* resilience to a peptide antibiotic (Mannion et al., 1990). The question remains whether the same result would have been produced at high concentrations of BSA due to the nature of our results. Enzymatic production and growth rate of *Xenorhabdus* species in protein complexes must be further be investigated to understand how protein sources alter investment in growth rate and carrying capacity.

Some protein is necessary for a high *K*, which quickly becomes negative with further increases in protein concentration (**Figure 5.1b**). It remains unclear whether the protein effect is due to whole proteins, protein intermediates, or the amino acid products of protein hydrolysis. Although we did not investigate intermediate peptides, amino acids (except serine) tended to reduce *K* consistently at high concentrations, both as aggregates and individually (**Figures 5.3-5.5**). The effects of amino acids on bacterial carrying capacity depended on the specific amino acids provided. Glutamic acid (a non-EAA; Section 5.3.3.1), arginine, lysine and valine (EAA; Section 5.3.3.2) all increased

K at a low concentration but decreased it at concentrations above the mean. Serine, a non-EAA, was the only amino acid to cause an increase in *K* at a high concentration. The grouping of these amino acids did not seem to fit the classical view of their importance as essential or non-essential amino acids to the host, nor did they group in branch chain families, which may be more important in their use as a metabolic substrate by the prokaryotic pathogen (Madigan et al., 2003). Rather, the amino acids grouped by the variation in their haemolymph concentrations in response to host diet. For example, arginine, lysine and valine, which produced identical effects on *K* (**Figures 5.5e-g**), increased in response to the concentration of nutrients in the host diet rather than dietary attributes. Bacterial growth in the SVH showed *K* to increase with amino acid concentration overall (**Figure 5.1b**), with carrying capacity declining only at the highest concentrations. This suggests that rather than a direct effect of the amino acids on bacterial growth, amino acids might act as a sensor for the host protein and carbohydrate intake.

Future investigations must carefully consider the method used to investigate pathogen nutrient usage. Our study found differences in the relationship between amino acids and *K*, depending on whether the effects of amino acids were viewed individually or as interacting pairs. For example, the non-EAA glutamic acid appeared to increase bacterial carrying capacity when paired with lysine (**Figure 5.7**), but decrease carrying capacity when paired with serine (**Figure 5.11**). Pranaw et al., (2014) increased *X. indica* protease production by 66% by altering growth media components simultaneously rather than individually. There has been little advancement in the area of microbial nutrient-use in the past half century, due to a limited focus on this area (Kovárová-Kovar and Egli, 1998). This could be rectified by applying a systematic approach such as the GF to microbial population dynamics. Future studies in this host-pathogen system could provide empirical evidence for the *X. nematophila* intake-target.

One way is to use thin plate regression splines, as were used in this study (**Figures 5.6-5.11),** to provide a value for the maximal expression of a life-history trait in a nutritional space (Rapkin et al., 2018). The significant linear and non-linear effects of nutrients on the trait can be tested statistically (Rapkin et al., 2018; South et al., 2011). And then by measuring the angles between the nutrient regions in which traits are expressed at their optima, the global conditions optimising the trait can be identified (Rapkin et al., 2018).

5.4.3 Protein may interfere with osmoregulation

Abisgold & Simpson (1987) found that increasing protein concentration in the diet of *Locusta migratoria* increased haemolymph amino acid concentration, which in turn raised haemolymph osmolality. Osmoregulation, or a cell's ability to adapt to changes in their osmotic environment, is important for the maintenance of turgor pressure across the cellular membrane (Csonka and Hanson, 1991; Kempf and Bremer, 1998). The osmoregulatory ability of a cell, in turn, determines its ability to counteract osmotic stress and therefore its ability to proliferate (Csonka, 1989; Tempest et al., 1970). The findings of Abisgold & Simpson (1987) highlight changes in osmolality as a possible mechanism for the observed 'protein effect'. Since the feeding interval of insects is decided by haemolymph osmolality (Simpson and Abisgold, 1985), this must be very tightly regulated. A host-dependent entomopathogen like *X. nematophila* would be sensitive to osmotic stress, due to limited variability in its osmotic environment. The reduction in bacterial carrying capacity in response to mid-to-high protein levels and high amino acid levels may be partially due to cells changing state upon sensing a high osmotic environment.

Prokaryotic organisms depend on the uptake of free amino acids, such as glutamine and proline, for osmoregulation (Kempf and Bremer, 1998; Krell et al., 2010; Tempest et

al., 1970). This means that after amino acids from a host meal raise haemolymph osmolality, the pathogen absorbs these very amino acids in reaction to the osmotic changes. This would cause a reduction in the haemolymph amino acid concentration signalling to the host to seek out more protein. Consistent with this, Cotter *et al.* (2011) failed to observe a change in host protein diet-choice using an immune elicitor, unlike previous experiments that used live pathogens (Lee et al., 2006; Povey et al., 2009). Investigating the effect of amino acids rather than whole proteins may provide clues as to how protein may be altering the reaction of *X. nematophila* to its osmotic environment.

5.4.4 Conclusion

To our knowledge, this study is the first to apply the geometric framework (GF) to a pathogen in response to its host's nutritional intake. The aim was to use an *in vitro* system to determine whether the host nutritional effects on the pathogen observed in previous experiments (Chapters 2 & 3) could be due to direct (bottom-up) effects in addition to the previously observed host-mediated (top-down) immunological effects. We provide strong evidence that the carrying capacity for this pathogen is in a high-carbohydrate, low-protein space, in contract to the host nutritional optima during infection: high-protein, low-carbohydrate (Chapter 2). Although the mechanisms through which nutrients alter bacterial carrying capacity are yet to be determined, it can be concluded that there are bottom-up nutritional effects determining the infection dynamics of *X. nematophila* and one of its hosts, *S. littoralis*. More importantly, we have provided an experimental framework for testing the role of nutrition in host-pathogen and host-commensal relationships. For example, one potential use of this system is to elucidate the nutritional requirements of the nematode symbionts, such as *S. carpocapsae* that remain unknown (Richards and Goodrich-Blair, 2009).

5.5 SUPPLEMENTARY MATERIAL

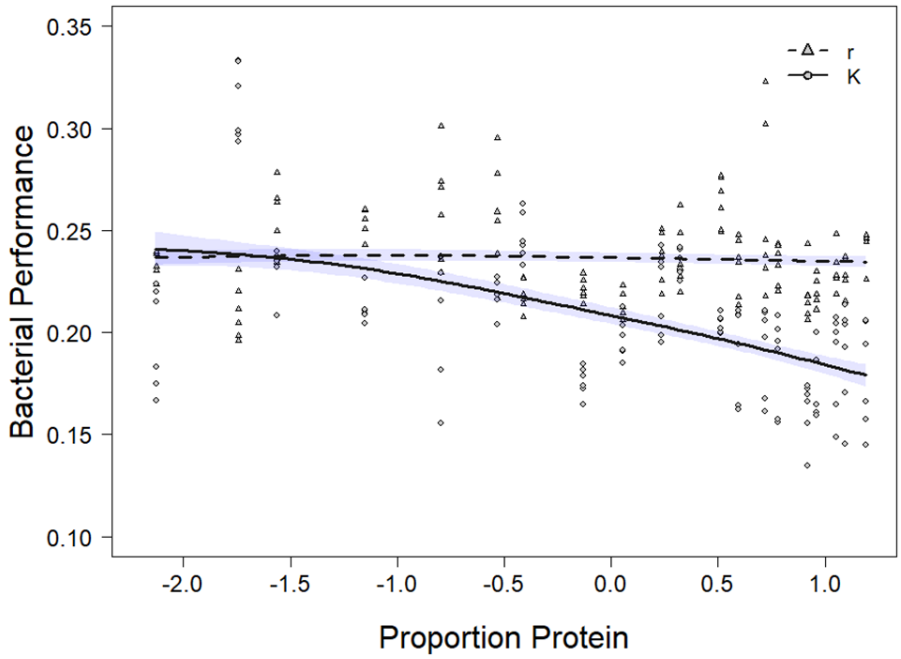

Figure S5.1: GAM models representing the effect of proportion of synthetic haemolymph (SH) protein on bacterial growth rate (*r*) and carrying capacity (*K*). There was no effect of increasing the proportion of EAA in SH on *r*. *K* decreased non-linearly (edf = 1.861) with an increasing proportion of SH protein.

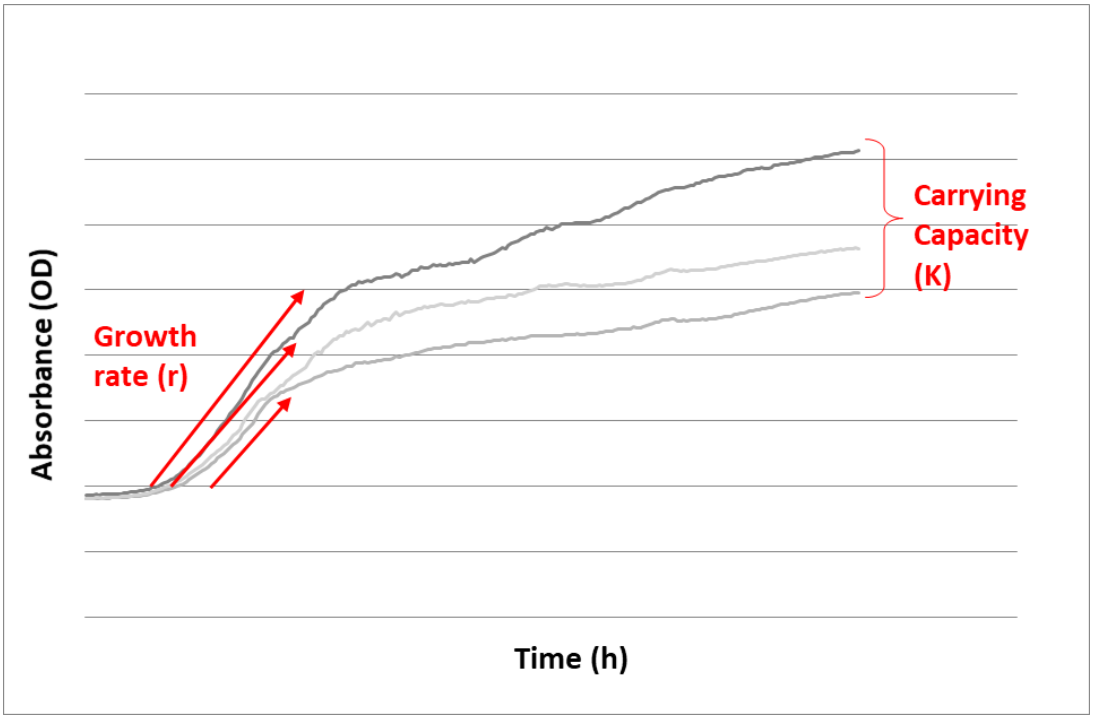

Figure S5.2: Illustrative plot showing bacterial growth in our various environments. Growth rates were similar but with varying carrying capacities. Of the metrics introduced in chapter 1, growth rate and carrying capacity were chosen for analysis. Growth rate represents the period in which bacteria are replicating exponentially and so place a high demand on the host. Carrying capacity represents the population size that a given nutrient environment can support.

Table S5.1: Twenty diets fed to *Spodoptera littoralis* caterpillars to produce varying haemolymph nutritional environments on which the synthetic haemolymphs were based.

Diet.no	P:C	P:C ratio	conc	ratio prot	%prot	%carb
1	10.5 : 52.5	1:5	63	0.17	10.5	52.5
2	7:35	1:5	42	0.17	7	35
3	5.6 : 28	1:5	33.6	0.17	5.6	28
4	2.8 :14	1:5	16.8	0.17	2.8	14
5	21:42	1:2	63	0.33	21	42
6	14:28	1:2	42	0.33	14	28
7	11.2 : 22.4	1:2	33.6	0.33	11.2	22.4
8	5.6 : 11.2	1:2	16.8	0.33	5.6	11.2
9	31.5 : 31.5	1:1	63	0.50	31.5	31.5
10	21:21	1:1	42	0.50	21	21
11	16.8 : 16.8	1:1	33.6	0.50	16.8	16.8
12	8.4 : 8.4	1:1	16.8	0.50	8.4	8.4
13	42 : 21	2:1	63	0.67	42	21
14	28:14	2:1	42	0.67	28	14
15	22.4 : 11.2	2:1	33.6	0.67	22.4	11.2
16	11.2 : 5.6	2:1	16.8	0.67	11.2	5.6
17	52.5 : 10.5	5:1	63	0.83	52.5	10.5
18	35:7	5:1	42	0.83	35	7
19	28 : 5.6	5:1	33.6	0.83	28	5.6
20	14 : 2.8	5:1	16.8	0.83	14	2.8

Table S5.2: Concentrations of nutrients that were added in the same amounts to all the synthetic haemolymphs

Inorganic salts	Concentration (g/L)	Vitamins	Concentration (g/L)	Sugars	Concentration (g/L)	Amino acids	Concentration (g/L)
CaCl2	1.00E+00	Aminobenzoic acid	2.00E-05	Glucose	9.65E-02	Asparagine	1.79E-06
KCl	2.24E+00	Biotin	1.00E-05	Fructose	1.59E-02	Glutamine	2.31E-05
MgCl2	1.07E+00	Choline chloride	2.00E-04	Lactose	2.40E-02	Glycine	3.61E-03
MgSO4	1.36E+00	Folic acid	2.00E-05	Sucrose	2.62E-03	Histidine	2.36E-02
NaHCO3	3.50E-01	myo-inositol	2.00E-05	Trehalose	3.22E-02	Methionine	4.72E-04
Na2HPO4	8.76E-01	Nicotinic acid	2.00E-05			Proline	6.43E-04
		Pantothenic acid	2.00E-05			Threonine	1.71E-03
		Pyridoxine	2.00E-05			Tyrosine	5.66E-04
		Riboflavin	2.00E-05				
		Thiamine	2.00E-05				

Table S5.3: Concentrations (g/L) of the amino acids that were added in variable amounts to the synthetic haemolymphs.

SH	Aspartic acid	Glutamic acid	Serine	Arginine	Alanine	Cysteine	Valine	Tryptophan	Phenylalanine	Isoleucine	Leucine	Lysine
1	1.81E-04	7.11E-04	2.92E-02	8.17E-03	1.40E-02	3.02E-03	7.40E-03	3.74E-08	2.25E-03	2.42E-03	6.72E-03	7.16E-02
2	1.72E-04	5.28E-04	2.27E-02	5.51E-03	1.06E-02	3.02E-03	5.02E-03	4.80E-08	1.41E-03	1.48E-03	3.95E-03	5.37E-02
3	1.68E-04	4.66E-04	2.04E-02	4.70E-03	9.37E-03	3.02E-03	4.30E-03	5.22E-08	1.17E-03	1.21E-03	3.04E-03	4.78E-02
4	1.61E-04	3.59E-04	1.61E-02	3.41E-03	7.13E-03	3.02E-03	3.14E-03	6.07E-08	7.82E-04	7.93E-04	1.57E-03	3.80E-02
5	2.47E-04	7.04E-04	2.49E-02	8.17E-03	1.40E-02	3.41E-03	7.40E-03	3.93E-07	2.60E-03	2.73E-03	7.96E-03	7.16E-02
6	2.36E-04	5.23E-04	1.90E-02	5.51E-03	1.06E-02	3.41E-03	5.02E-03	2.50E-07	1.64E-03	1.67E-03	4.92E-03	5.37E-02
7	2.31E-04	4.61E-04	1.69E-02	4.70E-03	9.37E-03	3.41E-03	4.30E-03	1.93E-07	1.35E-03	1.37E-03	3.90E-03	4.78E-02
8	2.23E-04	3.55E-04	1.30E-02	3.41E-03	7.13E-03	3.41E-03	3.14E-03	7.97E-08	9.16E-04	9.06E-04	2.21E-03	3.80E-02
9	3.32E-04	6.97E-04	2.08E-02	8.17E-03	1.40E-02	3.88E-03	7.40E-03	7.70E-07	3.01E-03	3.11E-03	9.38E-03	7.16E-02
10	3.18E-04	5.17E-04	1.54E-02	5.51E-03	1.06E-02	3.88E-03	5.02E-03	4.65E-07	1.91E-03	1.91E-03	6.05E-03	5.37E-02
11	3.13E-04	4.56E-04	1.35E-02	4.70E-03	9.37E-03	3.88E-03	4.30E-03	3.43E-07	1.58E-03	1.56E-03	4.92E-03	4.78E-02
12	3.03E-04	3.51E-04	1.00E-02	3.41E-03	7.13E-03	3.88E-03	3.14E-03	9.98E-08	1.08E-03	1.04E-03	3.00E-03	3.80E-02
13	4.36E-04	6.90E-04	1.70E-02	8.17E-03	1.40E-02	4.42E-03	7.40E-03	1.15E-06	3.49E-03	3.52E-03	1.09E-02	7.16E-02
14	4.19E-04	5.11E-04	1.22E-02	5.51E-03	1.06E-02	4.42E-03	5.02E-03	6.80E-07	2.22E-03	2.17E-03	7.31E-03	5.37E-02
15	4.13E-04	4.51E-04	1.05E-02	4.70E-03	9.37E-03	4.42E-03	4.30E-03	4.94E-07	1.85E-03	1.78E-03	6.06E-03	4.78E-02
16	4.01E-04	3.47E-04	7.47E-03	3.41E-03	7.13E-03	4.42E-03	3.14E-03	1.20E-07	1.27E-03	1.19E-03	3.91E-03	3.80E-02
17	5.55E-04	6.83E-04	1.38E-02	8.17E-03	1.40E-02	4.99E-03	7.40E-03	1.50E-06	4.00E-03	3.97E-03	1.25E-02	7.16E-02
18	5.35E-04	5.06E-04	9.51E-03	5.51E-03	1.06E-02	4.99E-03	5.02E-03	8.83E-07	2.56E-03	2.45E-03	8.59E-03	5.37E-02
19	5.28E-04	4.46E-04	8.01E-03	4.70E-03	9.37E-03	4.99E-03	4.30E-03	6.35E-07	2.13E-03	2.02E-03	7.24E-03	4.78E-02
20	5.12E-04	3.43E-04	5.39E-03	3.41E-03	7.13E-03	4.99E-03	3.14E-03	1.39E-07	1.47E-03	1.35E-03	4.87E-03	3.80E-02

Table S5.4: Concentrations of the macronutrients added to the synthetic haemolymphs

SH	Proportion Protein	Conc	Protein (g/L)	Total carbs (g/L)	Lipids (g/L)	Sum of simple sugars (g/L)	Glycogen (g/L)
1	0.17	63	22.841	1.66951	1.0068	0.1768	1.49271
2	0.17	42	19.841	1.65672	1.0068	0.1768	1.47991
3	0.17	33.6	18.750	1.65160	1.0068	0.1768	1.47479
4	0.17	16.8	16.735	1.64137	1.0068	0.1768	1.46456
5	0.33	63	29.468	1.42074	1.0068	0.1768	1.24393
6	0.33	42	25.635	1.40794	1.0068	0.1768	1.23114
7	0.33	33.6	24.240	1.40283	1.0068	0.1768	1.22602
8	0.33	16.8	21.665	1.39259	1.0068	0.1768	1.21578
9	0.5	63	34.976	1.15641	1.0068	0.1768	0.97961
10	0.5	42	30.450	1.14362	1.0068	0.1768	0.96681
11	0.5	33.6	28.803	1.13850	1.0068	0.1768	0.96169
12	0.5	16.8	25.763	1.12827	1.0068	0.1768	0.95146
13	0.67	63	37.541	0.89209	1.0068	0.1768	0.71528
14	0.67	42	32.692	0.87930	1.0068	0.1768	0.70249
15	0.67	33.6	30.927	0.87418	1.0068	0.1768	0.69737
16	0.67	16.8	27.671	0.86394	1.0068	0.1768	0.68714
17	0.83	63	36.625	0.64332	1.0068	0.1768	0.46651
18	0.83	42	31.891	0.63052	1.0068	0.1768	0.45371
19	0.83	33.6	30.168	0.62540	1.0068	0.1768	0.44860
20	0.83	16.8	26.989	0.61517	1.0068	0.1768	0.43836

Table S5.5: Calculations used to decide nutrient concentrations that would be used in the single-variable haemolymphs.

Range	min	max	SD	max + 2SD	Value at % of max + 2SD						Mean
					0%	20%	40%	60%	80%	100%	
Protein (g/L)	1.67E+01	3.75E+01	5.82E+00	4.92E+01	0.00E+00	9.84E+00	1.97E+01	2.95E+01	3.93E+01	4.92E+01	2.77E+01
Glycogen (g/L)	4.38E-01	1.49E+00	3.75E-01	2.24E+00	0.00E+00	4.48E-01	8.97E-01	1.35E+00	1.79E+00	2.24E+00	9.65E-01
Lipids (g/L)	6.98E-01	1.74E+00	2.93E-01	2.32E+00	0.00E+00	4.64E-01	9.29E-01	1.39E+00	1.86E+00	2.32E+00	1.01E+00
Aspartic acid (g/L)	1.61E-04	5.55E-04	1.33E-04	8.21E-04	0.00E+00	1.64E-04	3.28E-04	4.92E-04	6.57E-04	8.21E-04	3.34E-04
Glutamic acid (g/L)	3.43E-04	7.11E-04	1.29E-04	9.70E-04	0.00E+00	1.94E-04	3.88E-04	5.82E-04	7.76E-04	9.70E-04	5.05E-04
Serine (g/L)	5.39E-03	2.92E-02	6.21E-03	4.16E-02	0.00E+00	8.31E-03	1.66E-02	2.49E-02	3.33E-02	4.16E-02	1.53E-02
Arginine (g/L)	3.41E-03	8.17E-03	1.79E-03	1.17E-02	0.00E+00	2.35E-03	4.70E-03	7.05E-03	9.40E-03	1.17E-02	5.45E-03
Alanine (g/L)	7.13E-03	1.40E-02	2.55E-03	1.91E-02	0.00E+00	3.82E-03	7.65E-03	1.15E-02	1.53E-02	1.91E-02	1.03E-02
Cysteine (g/L)	3.02E-03	4.99E-03	7.21E-04	6.43E-03	0.00E+00	1.29E-03	2.57E-03	3.86E-03	5.15E-03	6.43E-03	3.95E-03
Valine (g/L)	3.14E-03	7.40E-03	1.60E-03	1.06E-02	0.00E+00	2.12E-03	4.24E-03	6.35E-03	8.47E-03	1.06E-02	4.96E-03
Tryptophan (g/L)	3.74E-08	1.50E-06	4.09E-07	2.32E-06	0.00E+00	4.64E-07	9.28E-07	1.39E-06	1.86E-06	2.32E-06	4.20E-07
Phenylalanine (g/L)	7.82E-04	4.00E-03	8.61E-04	5.72E-03	0.00E+00	1.14E-03	2.29E-03	3.43E-03	4.58E-03	5.72E-03	1.93E-03
Isoleucine (g/L)	7.93E-04	3.97E-03	8.76E-04	5.72E-03	0.00E+00	1.14E-03	2.29E-03	3.43E-03	4.58E-03	5.72E-03	1.93E-03
Leucine (g/L)	1.57E-03	1.25E-02	2.91E-03	1.83E-02	0.00E+00	3.66E-03	7.32E-03	1.10E-02	1.46E-02	1.83E-02	5.95E-03
Lysine (g/L)	3.80E-02	7.16E-02	1.25E-02	9.67E-02	0.00E+00	1.93E-02	3.87E-02	5.80E-02	7.74E-02	9.67E-02	5.28E-02

Table S5.6: Concentration of nutrients added to each of the single-variable haemolymphs (split into two parts).

SH	Lipids (g/L)	Protein (g/L)	Glycogen (g/L)	Aspartic acid (g/L)	Glutamic acid (g/L)	Serine (g/L)	Arginine (g/L)	Alanine (g/L)
1	1.01E+00	2.77E+01	0.00E+00	3.34E-04	5.05E-04	1.53E-02	5.45E-03	1.03E-02
2	1.01E+00	2.77E+01	4.48E-01	3.34E-04	5.05E-04	1.53E-02	5.45E-03	1.03E-02
3	1.01E+00	2.77E+01	8.97E-01	3.34E-04	5.05E-04	1.53E-02	5.45E-03	1.03E-02
4	1.01E+00	2.77E+01	1.35E+00	3.34E-04	5.05E-04	1.53E-02	5.45E-03	1.03E-02
5	1.01E+00	2.77E+01	1.79E+00	3.34E-04	5.05E-04	1.53E-02	5.45E-03	1.03E-02
6	1.01E+00	2.77E+01	2.24E+00	3.34E-04	5.05E-04	1.53E-02	5.45E-03	1.03E-02
7	1.01E+00	2.77E+01	9.65E-01	0.00E+00	0.00E+00	0.00E+00	0.00E+00	0.00E+00
8	1.01E+00	2.77E+01	9.65E-01	1.64E-04	1.94E-04	8.31E-03	2.35E-03	3.82E-03
9	1.01E+00	2.77E+01	9.65E-01	3.28E-04	3.88E-04	1.66E-02	4.70E-03	7.65E-03
10	1.01E+00	2.77E+01	9.65E-01	4.92E-04	5.82E-04	2.49E-02	7.05E-03	1.15E-02
11	1.01E+00	2.77E+01	9.65E-01	6.57E-04	7.76E-04	3.33E-02	9.40E-03	1.53E-02
12	1.01E+00	2.77E+01	9.65E-01	8.21E-04	9.70E-04	4.16E-02	1.17E-02	1.91E-02
13	1.01E+00	0.00E+00	9.65E-01	3.34E-04	5.05E-04	1.53E-02	5.45E-03	1.03E-02
14	1.01E+00	9.84E+00	9.65E-01	3.34E-04	5.05E-04	1.53E-02	5.45E-03	1.03E-02
15	1.01E+00	1.97E+01	9.65E-01	3.34E-04	5.05E-04	1.53E-02	5.45E-03	1.03E-02
16	1.01E+00	2.95E+01	9.65E-01	3.34E-04	5.05E-04	1.53E-02	5.45E-03	1.03E-02
17	1.01E+00	3.93E+01	9.65E-01	3.34E-04	5.05E-04	1.53E-02	5.45E-03	1.03E-02
18	1.01E+00	4.92E+01	9.65E-01	3.34E-04	5.05E-04	1.53E-02	5.45E-03	1.03E-02
19	0.00E+00	2.77E+01	9.65E-01	3.34E-04	5.05E-04	1.53E-02	5.45E-03	1.03E-02
20	4.64E-01	2.77E+01	9.65E-01	3.34E-04	5.05E-04	1.53E-02	5.45E-03	1.03E-02
21	9.29E-01	2.77E+01	9.65E-01	3.34E-04	5.05E-04	1.53E-02	5.45E-03	1.03E-02
22	1.39E+00	2.77E+01	9.65E-01	3.34E-04	5.05E-04	1.53E-02	5.45E-03	1.03E-02
23	1.86E+00	2.77E+01	9.65E-01	3.34E-04	5.05E-04	1.53E-02	5.45E-03	1.03E-02
24	2.32E+00	2.77E+01	9.65E-01	3.34E-04	5.05E-04	1.53E-02	5.45E-03	1.03E-02

SH	Cysteine (g/L)	Valine (g/L)	Tryptophan (g/L)	Phenylalanine (g/L)	Isoleucine (g/L)	Leucine (g/L)	Lysine (g/L)
1	3.95E-03	4.96E-03	4.20E-07	1.93E-03	1.93E-03	5.95E-03	5.28E-02
2	3.95E-03	4.96E-03	4.20E-07	1.93E-03	1.93E-03	5.95E-03	5.28E-02
3	3.95E-03	4.96E-03	4.20E-07	1.93E-03	1.93E-03	5.95E-03	5.28E-02
4	3.95E-03	4.96E-03	4.20E-07	1.93E-03	1.93E-03	5.95E-03	5.28E-02
5	3.95E-03	4.96E-03	4.20E-07	1.93E-03	1.93E-03	5.95E-03	5.28E-02
6	3.95E-03	4.96E-03	4.20E-07	1.93E-03	1.93E-03	5.95E-03	5.28E-02
7	0.00E+00	0.00E+00	0.00E+00	0.00E+00	0.00E+00	0.00E+00	0.00E+00
8	1.29E-03	2.12E-03	4.64E-07	1.14E-03	1.14E-03	3.66E-03	1.93E-02
9	2.57E-03	4.24E-03	9.28E-07	2.29E-03	2.29E-03	7.32E-03	3.87E-02
10	3.86E-03	6.35E-03	1.39E-06	3.43E-03	3.43E-03	1.10E-02	5.80E-02
11	5.15E-03	8.47E-03	1.86E-06	4.58E-03	4.58E-03	1.46E-02	7.74E-02
12	6.43E-03	1.06E-02	2.32E-06	5.72E-03	5.72E-03	1.83E-02	9.67E-02
13	3.95E-03	4.96E-03	4.20E-07	1.93E-03	1.93E-03	5.95E-03	5.28E-02
14	3.95E-03	4.96E-03	4.20E-07	1.93E-03	1.93E-03	5.95E-03	5.28E-02
15	3.95E-03	4.96E-03	4.20E-07	1.93E-03	1.93E-03	5.95E-03	5.28E-02
16	3.95E-03	4.96E-03	4.20E-07	1.93E-03	1.93E-03	5.95E-03	5.28E-02
17	3.95E-03	4.96E-03	4.20E-07	1.93E-03	1.93E-03	5.95E-03	5.28E-02
18	3.95E-03	4.96E-03	4.20E-07	1.93E-03	1.93E-03	5.95E-03	5.28E-02
19	3.95E-03	4.96E-03	4.20E-07	1.93E-03	1.93E-03	5.95E-03	5.28E-02
20	3.95E-03	4.96E-03	4.20E-07	1.93E-03	1.93E-03	5.95E-03	5.28E-02
21	3.95E-03	4.96E-03	4.20E-07	1.93E-03	1.93E-03	5.95E-03	5.28E-02
22	3.95E-03	4.96E-03	4.20E-07	1.93E-03	1.93E-03	5.95E-03	5.28E-02
23	3.95E-03	4.96E-03	4.20E-07	1.93E-03	1.93E-03	5.95E-03	5.28E-02
24	3.95E-03	4.96E-03	4.20E-07	1.93E-03	1.93E-03	5.95E-03	5.28E-02

Table S5.7: Variation in bacterial carrying capacity (K) explained by lysine, valine and arginine concentration in the synthetic haemolymph (SH) model summary tables. (a) AIC comparison table for models containing each of the amino acids in the SH as explanatory variables. df is the degrees of freedom used by the model to produce a fit and not the degrees of freedom based on the number of explanatory variables. K is the number terms in the model. AICc is the model Aikake values. Delta represents the difference between a model and the model explaining the most variation. Weight is determined by the amount of variation a model explains penalized for the degrees of freedom used by the model. The edf provides information about the shape of the curve, relating to the basis dimensions used by the model to fit the curve; for example, an edf close to 1 represents a linear effect, whilst an edf close to 2 represents a quadratic effect. This comparison was used to select which of these 3 amino acids would be used in the description of interactions between SH amino acids (Section 5.3.5). Lysine was chosen due to the marginally higher variation in K it explained compared to valine and arginine, but the choice was arbitrary since there was a direct correlation between the concentrations of these three amino acids in the SH.

AIC model comparison between Arginine, Lysine and Valine									
Model	**df**	**k**	**AICc**	**delta**	**weight**	**edf**	**F-value**	**P-value**	**R^2**
m2 *Lysine*	3	1	-468.3	0.00	0.382	1.814	7.874	<0.001	0.166
m3 *Valine*	3	1	-467.9	0.42	0.310	1.804	7.710	<0.001	0.163
m1 *Arginine*	3	1	-467.8	0.44	0.307	1.804	7.702	<0.001	0.163
m0 *Null*	2	0	-448.9	19.37	0.000				0.000

6 General Discussion

6.1 Introduction

Pathogens cause reductions in host fitness by impacting life-history traits such as reproduction, survival and growth (Hall et al., 2009; Hughes et al., 2008; Sheldon and Verhulst, 1996). Pathogen consumption of host resources may reduce the energy available to the host for metabolic and homeostatic processes (Rynkiewicz et al., 2015). Further costs of pathogenicity may occur due to the host's need to divert key resources from growth, metabolism and homeostasis to account for the increased metabolic demands of an upregulated immune response (Moret and Schmid-Hempel, 2000; Rynkiewicz et al., 2015). As such, hosts have developed a range of strategies to limit the costs of infection by pathogens. Aside from the broadly studied resistance mechanisms involved in the active clearance of the pathogens (Ayres and Schneider, 2008), hosts may increase their overall resilience (defensive capacity) by tolerating the health impacts of infection (Ayres and Schneider, 2008; Louie et al., 2016; Sheldon and Verhulst, 1996). Behavioural mechanisms such as zoopharmacognosy (self-medication) also decrease infection costs, improving relative host-fitness (Huffman, 2003). The emerging field of nutritional immunology applies frameworks such as nutritional geometry to understand animal behavioural responses to infection and examine the consequences of those behaviours (Ponton et al., 2013, 2011a; Raubenheimer and Boggs, 2009).

Studies using nutritional geometry in insect-pathogen interactions have found a role for dietary nutrients, such as lipids (Miller and Cotter, 2017), carbohydrates (Graham et al., 2014) and proteins (Povey et al., 2014), in reducing the costs of infection. Insects and their symbiotic interactions provide model systems for the study of both nutrition and immunology (Litchman et al., 2015; Ramarao et al., 2012; Stilwell et al., 2018). The discovery of macronutrient self-medication in insects has been of great interest because

of the increase in host resilience resulting from this behaviour (Lee et al., 2006; Povey et al., 2014, 2009). The caveats of these studies have been restriction to a limited range of diets as well as a largely host focused perspective, due to a necessity to simplify the system, to understand the complex multi-faceted interactions involved. However, results produced by such studies can be built upon with increasing complexity, yielding further insights, such as the discovery of nutrient-mediated trade-offs in immune responses (Cotter et al., 2011).

Using the lepidopteran insect model, *Spodoptera littoralis* and its natural bacterial pathogen, *Xenorhabdus nematophila*, this project aimed to further explore the role of nutrition in host-pathogen interactions. The key difference between this project and previous nutritional immunological studies using this host, was the pathogen-focused perspective applied to the system. Although the top-down effects of nutrition on the improvement of host defence are increasingly well understood, there has been limited focus on the bottom-up effects of resource availability on pathogen success. Initial experiments involved *in vivo* studies, that aimed to clarify the effects of pathogen numbers (through various infection doses) on the time-course of infection (Chapter 2). To increase understanding of the influence of nutrition on host defence-strategy, diets covering a broader range of macronutrient ratios and concentrations were used (Chapter 3). With a clearer understanding of the role of dietary macronutrients in host and pathogen success, a more focused perspective could be taken. The effects of dietary macronutrient variation on the haemolymph resource pool were characterised, providing information on the nutrients available to the host for investment in homeostatic, metabolic and defence mechanisms (Chapter 4). *X. nematophila* was chosen for this project due to its nature as a haemolymph-obligate parasite, meaning it directly depends on and impacts the host haemolymph resource pool. As such, the study ended with a

characterization of pathogen resource-use *in vitro,* in nutrient environments that were produced based on variation in host haemolymph nutrients (Chapter 5).

Both dietary protein and carbohydrate were found to be important for host defence, with nutrient effects becoming clearer at higher pathogen burdens (Chapters 2 &3). For the first time, diet-mediated tolerance effects were revealed in *Spodoptera*, adding to the complexity of the role of nutrition in this host's defence. *Xenorhabdus* growth rate *in vivo* appeared to be dependent on host nutrient intake, with evidence showing effects of both protein (Chapter 2) and carbohydrate (Chapter 3). Host diet altered the concentration of key haemolymph nutrient groups in different ways, implying regulation of nutrients by the host. However, diet explained more variation in haemolymph nutrients, when nutrient groups consisted of a mix of covarying amino acids and sugars (Chapter 4). *In vitro* experiments revealed a negative impact of protein and amino acids, and a positive impact of carbohydrate, on the performance of *X. nematophilus*, demonstrating apparent nutrient-mediated bottom-up effects on this pathogen (Chapter 5). The general ecological implications of these findings are discussed below.

6.2 Diet choice

6.2.1 Influence of microbes on diet choice

The presence of gut bacteria of the genera *Lactobacilli* and *Acetobacter* reduced the appetite for protein in *D. melanogaster* flies lacking essential amino acids (Leitão-Gonçalves et al., 2017). In this way the nutrient activity of commensal bacteria influenced the food choice of their host. This study found that individuals with a high parasite burden appeared to abandon carbohydrate regulation (Chapter 2); larvae ate more carbohydrates with increasing dietary carbohydrate concentration. Initially, this

result appears to contradict the previous knowledge of *Spodoptera* feeding behaviour during infection, which found a preference for protein-rich diets during both viral and bacterial infection (Lee et al., 2006; Povey et al., 2014, 2009). However, the nutrient requirements of pathogens must be taken into consideration, since they may influence host diet-choice in a similar way to commensal microorganisms. Both *in vivo* (Chapters 2 & 3) and *in vitro* (Chapter 5) *X. nematophila* growth rates increase with increasing carbohydrate availability. Combined with previous *in vitro* findings for this pathogen (Bowen et al., 2012; Kooliyottil et al., 2014), it can be assumed that *X. nematophila* uses carbohydrate for replication, placing a nutritional burden on *S. littoralis* at high population densities. Due to it stronger preference for amino acid usage for growth in *Bacillus subtilis* compared to Enterobacteriaceae (Fisher, 1999), it is possible that *B. subtilis* places a higher nitrogen burden on *S. exempta* during infection than *X. nematophila* placed on *S. littoralis* in our study. Therefore, the preferential protein self-medication observed by Povey et al., (2009) may have occurred partially to replace bacterial nutrient use. Matching the findings of Lee et al., (2006) and Povey et al., (2009), there was an increase in the survival time of infected hosts due to an increased protein intake (Chapters 2 & 3). In both cases, the 'protein effect' was more pronounced at higher pathogen loads. There is consistent evidence to suggest that ingested protein increases aspects of the insect immune response, such as lysozyme and phenoloxidase activity (Cotter et al., 2011; Lee et al., 2006; Povey et al., 2009). In other words, the role of protein in the top-down modulation of infection is well established. Replicating our *in vitro* growth assay with *B. subtilis* may reveal possible bottom-up effects in the interaction of this bacterium with *S. exempta*, due to competition between the host and pathogen for protein.

6.2.2 Self-medication

Self-medication can occur either prophylactically in organisms, preventing the onset of disease, or therapeutically, in response to infection (Abbott, 2014). In this study, the level of protein in the diet appeared to influence the pathogen burden associated with a given dose (Chapter 2). This indicates that protein levels in the haemolymph at the time of infection determine the chances that an infection will establish. Glutamic acid is important for synthesising 85% of nitrogenous contents in enteric bacteria such as *Escherichia coli* (Fisher, 1999). The importance of this amino acid for cell function may explain why it increased *X. nematophila* performance in comparison with lysine and tryptophan, only showing a relatively negative impact on performance in comparison with serine (Chapter 5). The low abundance of glutamic acid maintained in the haemolymph in healthy insects, in contrast to lysine which is kept in a high abundance (Chapter 4), is one example of how a pathogen entering the haemolymph would be at a disadvantage. Further evidence was provided by the comparison of the variation in bacterial load explained by diet eaten pre- and post-infection (Chapter 3), which revealed greater explanatory power of diet eaten pre-infection in predicting bacterial load and host fitness in general. Self-medication in *Spodoptera* has so far been reported therapeutically, due to a focus on diet mediation of infection costs (Lee et al., 2006; Povey et al., 2009). The findings of this project indicate advantages in increased explanatory power by shifting focus to the prophylactic effects of diet choice.

6.3 Haemolymph nutrients

6.3.1 Feeding Intervals

This study found the principal sugar in the haemolymph to be glucose, similar to mammalian blood, unlike most insects whose primary blood sugar is trehalose (Boctor, 1974; Thompson, 2003). Although not the only case that identifies glucose as the

primary haemolymph sugar (Wyatt, 1961), the results presented in Chapter 4 differed from those of an earlier experiment by Boctor (1974), who found trehalose to be the most abundant sugar in *S. littoralis* haemolymph. A similar difference was observed in amino acid concentrations. Boctor (1980) found the most abundant amino acid in *S. littoralis* haemolymph to be asparagine, whereas this study found lysine to be the principal haemolymph amino acid; asparagine making up less than 1% of the haemolymph amino acid pool. The difference is likely due to food availability, since castor oil leaves were the only diet source used in both the assays performed by Boctor. Indeed, on certain diets, trehalose concentration was higher than glucose concentration. The use of more diets in this study, makes a stronger case for glucose as the primary sugar and lysine as the primary amino acid in *S. littoralis* haemolymph. However, all three experiments failed to account for temporal fluctuations in haemolymph nutrient levels in response to feeding.

Abisgold and Simpson, (1987) found that amino acid constitution of *Locusta migratoria* haemolymph varied depending on the protein composition of the diet. This corresponds with the results (Chapter 4) indicating that dietary protein has a stronger effect on haemolymph nutrients than dietary carbohydrates, especially on the proportions and concentrations of essential amino acids. Lysine, the most abundant amino acid, was also found by Abisgold and Simpson, (1987) to vary in haemolymph concentration, depending on time since the last meal. By sampling at a single timepoint from larvae fed *ad libitum*, this study didn't consider feeding intervals of the experimental larvae. Lysine levels in *L. migratoria* were highest one hour after feeding, therefore sampling at different timepoints may have produced a different nutrient profile across our 20 diets for this and other amino acids. A stronger relationship between larval diet and haemolymph sugar concentrations might have also been detected.

6.3.2 Amino acid regulation

Amino acids and sugars are important phagostimulants in herbivorous insects, and they adjust their dietary intake to compensate for deficiencies in amino acid and sugar levels (Simmonds et al., 1992; Simpson and Simpson, 1992). Essential amino acid intake is important for holometabolous insects, given that the deposits acquired during the larval stage are used by adults in processes such as reproduction (O'Brien et al., 2002). As such, dietary protein intake during the larval stage can determine fecundity. For example, protein supplementation in the form of dietary yeast increased both egg production rate and overall lifetime egg production in *D. melanogaster* (Kwang Pum Lee et al., 2008). Although most amino acids in the blood of *S. littoralis* infected with nucleopolyhedrovirus decreased in concentration, proline, lysine, aspartic acid and histidine levels increased (Boctor, 1980). In this study, lysine and alanine and serine levels decreased at high levels of protein intake, implying a possible role of these amino acids in enantiostasis (Chapter 4). Abisgold and Simpson, (1987) identified these amongst a group of 11 amino acids that rose in the haemolymph directly after a meal. These amino acids regulated feeding-behaviour in *L. migratoria*; injection into the haemolymph reduced the feeding of protein-deficient locusts on high protein diets. Serine was another amino acid identified by Abisgold and Simpson, (1987) in the regulation of feeding behaviour.

6.4 Nutrients in non-immune host defences

6.4.1 Serine and host tolerance

The high performance of a bacterial pathogen when haemolymph levels of serine are high (Chapter 5) indicates that regulation of this amino acid may also be useful for host defence. Serine is important as a glucose source in mammals and the availability of this amino acid affects the function of mammalian lymphocytes and macrophages which use

glucose as an energy source (Li et al., 2007). Since serine synthesis directly corresponds with glucose availability in insects (Chapman, 2012), this amino acid may also be important in cellular immune responses in insects. The possible tolerance effect observed due to increasing survival of infected larvae (Chapter 3), may be related to carbohydrate intake providing more energy for the activity of melanin-producing cascades involving phenoloxidase (PO). This idea is based on previous findings using the same diets showing *S. littoralis* PO activity to be upregulated on carbohydrate-biased diets (Cotter et al., 2011). Dietary carbohydrate may be acting through serine since PO activity depends on serine protease enzymes (González-Santoyo and Córdoba-Aguilar, 2012). Survival during infection with *Photorhabdus luminescens* was higher in burying beetles (*Nicrophorus vespilloides*) on a diet containing a higher ratio of fat-to-protein (Miller and Cotter, 2017). These effects seemed to be mediated by tolerance. Though there was also increased PO activity on the higher fat diets, there was no direct relationship between PO and survival. There have been multiple cases in which PO activity has been a poor indicator of resistance (González-Santoyo and Córdoba-Aguilar, 2012). This may be due to the general treatment of phenoloxidase as a single enzyme, although phenoloxidases are various enzymes that perform diverse functions (Dittmer et al., 2004; González-Santoyo and Córdoba-Aguilar, 2012). Future research into the specific investment of phenoloxidase enzymes in nodulation, melanism and wound repair may simultaneously reveal mechanisms behind tolerance in insects.

6.4.2 Osmolality

A raised haemolymph amino acid level after feeding accounted for 40% of the increase in haemolymph osmolality that occurred in *L. migratoria* (Abisgold and Simpson, 1987). Furthermore, feeding intervals in *S. littoralis* and *L. migratoria* can be controlled by altering haemolymph osmolality (Abisgold and Simpson, 1987; Simmonds et al.,

1992). Enterobacteriaceae nutrient absorption is affected by the osmolality of a solution (Forst and Roberts, 1994). The osmolality of a solution can also negatively impact cell shape and growth, due to changes in turgor pressure of cells under osmotic stress (Pilizota and Shaevitz, 2014). It is likely that there is an interaction between host nutrition and pathogen nutrient demand, mediated by osmolality. Mortality was halved in larvae of the gypsy moth (*Lymantria dispar*) infected with baculovirus, when diets were supplemented with casein or various salts (Keating et al., 1989). Although the haemolymph osmolality was not measured, dietary salt can be assumed to influence haemolymph osmolality, since osmotic regulation depends on ion balance (Beyenbach, 2016). More direct evidence for the role of osmolality on host-microbe interactions has been found in mammalian research; high salt diets causing hypertension in mice and humans was also associated with reduced populations of gut endosymbiotic *Lactobacilli* (Wilck et al., 2017). An *in vitro* experiment performed with the microbial species normally found in the gut, revealed a direct inhibitory effect of osmolality on some *Lactobacillus* species, although other species performed well in a high salt environment (Wilck et al., 2017). Altogether, the role of osmolality in host defence is an area in need of further exploration.

6.4.3 Amino acid interactions

Reducing the concentration of amino acids in a growth medium increased the mean lifespan of replicating yeast cells. This effect was replicated by reducing methionine concentration alone (Lee et al., 2014). Results from this project showed interactions between amino acids in the variation they explained on bacterial carrying capacity. For example, increasing glutamic acid concentration increased bacterial carrying capacity in the presence of the EAA, lysine and tryptophan, but decreased carrying capacity in the presence of serine (Chapter 5). Considering interactive effects of nutrients has

implications for the applications of scientific findings. For example, arginine and lysine belong to different branch-chain families in their metabolic and catabolic functions (Madigan et al., 2003), and are mainly considered together in their role as essential amino acids. However, they share a transport system in mammalian immune cells. Their relationship is antagonistic, whereby increasing extracellular lysine concentrations reduces intracellular arginine concentration in macrophages (Li et al., 2007). This knowledge has allowed treatment of herpes simplex virus infections through the application of lysine, since the virus requires arginine for replication (Griffith et al., 1981).

6.5 Bottom-up effects

6.5.1 Pathogen intake targets

Bacteria are faced with constant fluctuations in their resource availability (Katz and Springer, 2016; Litchman et al., 2015). Application of the Monod Law to bacterial cultures indicates that the substrate that becomes limiting first in the growth medium is the one that determines the proliferation rate (Monod, 1949). In this study, growth rate increased with increasing concentrations of both proteins and carbohydrates, however the mean growth rate was lower in the growth solutions that varied solely in their protein concentrations (Chapter 5). The ‘protein effect’ cannot be explained by carbohydrate limitation since the protein series contained a concentration of carbohydrate equal to the mean of the carbohydrate-variation series. Overall, there was limited application of the Monod law to this system, given that within the range that nutrients vary in insect haemolymph, growth rate tended to be unaffected by fluctuations in specific nutrients. Rather, the results showed greater effects of nutrition on carrying capacity. Increasing concentrations of protein and individual essential amino acids resulted in a reduced carrying capacity for *X. nematophila*. Based on

current knowledge of oligopeptide permease (OPP) operons on the mediation of nutrient sensing in *X. nematophila*, it was hypothesised that the increased protein reduced the duration of time bacteria spent in the exponential growth phase; higher protein environments resulted in an earlier cessation of exponential growth and entry into stationary phase.

Although it is accepted that microbes are exposed to a pool of mixed resources in their natural environment, *in vitro* cultivation still focuses on carbohydrate sources and fails to account for mixed effects (Kovárová-Kovar and Egli, 1998). Growth medium optimisation studies found improvements in performance of commercially important *Xenorhabdus* (Pranaw et al., 2014) and *Bacillus* (Nickerson' and Bulla, 1974) species, indicating advantages in considering the nutritional composition of the growth media. Divergent evolution occurs when microorganisms are placed in environments that fluctuate in their resource composition, leading to individuals highly adapted to one resource environment, that perform poorly in other environments (Cooper and Lenski, 2010). The resource ratio competition model argues that the competitive ability of an organism is determined by the ratio of available nutrients (Hibbing et al., 2010; Tilman, 1982). These arguments indicate that microbes (including pathogens) can adapt to certain nutritional ratios in which they maximise their competitive ability. For example, based on the results of this study, *Xenorhabdus* competitive ability was lower in a resource ratio containing a balance of proteins and carbohydrate than one that was low in protein and high in carbohydrate. Further exploration of the nutrient ratios that maximise *Xenorhabdus* performance could apply the ideas from the geometric framework that involve identifying the intake targets of this and other bacteria, and therefore rules of compromise they employ when faced with nutrient imbalance.

6.5.2 PharmEcology

The description of a substance as a nutrient or toxin is dose-dependent (Simpson and Raubenheimer, 2012). Bertrand's rule (Figure 6.1a) states that there are costs associated with a nutrient deficiency that are alleviated by increasing intake of the deficient nutrient. The nutrient supplementation reaches a plateau at a given dose, at which point traits requiring that nutrient are optimised. Further exposure to the nutrient leads to increasing costs due to a toxic response to nutrient excess (Mertz, 1981; Raubenheimer and Simpson, 2009). The carrying capacity of *X. nematophila* in response to increasing concentrations of haemolymph amino acids (Chapter 5) corresponds with Bertrand's rule. Although Bertrand's rule was created with mineral nutrients in mind, it appears to apply to other nutrients. For example, the right experimental framework revealed a negative performance (growth and survival) of *S. littoralis* ingesting excess carbohydrate (Raubenheimer et al., 2005). Similarly, the deleterious effects associated with obesity in humans can be linked with an increased carbohydrate and fat intake as well as a reduced expenditure of the excess energy gained from diet (Simpson and Raubenheimer, 2005).

Bertand's rule bears a similarity to recent understanding of hormetic responses in the field of toxicology, creating a link between this field and nutritional ecology (Raubenheimer and Simpson, 2009). Hormesis (Figure 6.1b) is observed when a low dose of a substance leads to a stimulatory response that plateaus. Further increasing the dose causes an inhibitory response that is exacerbated with increasing dose (Calabrese and Baldwin, 2003). The shape of the carrying capacity in response to protein in our single-variable haemolymphs (Chapter 5) is similar to the shape of the dose response curve in hormesis. This indicates that the self-medication response in *S. littoralis* has a medicinal effect by shifting the nutrient availability of this pathogen into a region of the nutrient space in which protein levels are higher than the bacterium's optimal

requirement and so are deleterious. The proposed field of PharmEcology incorporates findings such as these, involving ecological concepts that can be linked with pharmacology, the scientific study of the composition and effects of drugs (Raubenheimer and Simpson, 2009). Based on the evidence provided by this project, investigating the concentrations at which Bertrand's rule applies to nutrient uptake by pathogenic bacteria may yield pharmacological advancements.

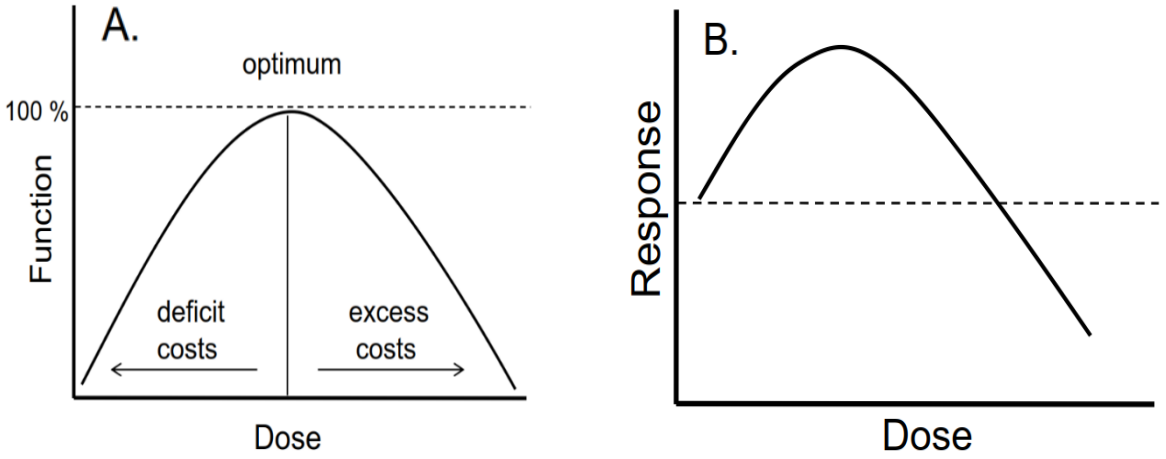

Figure 6.1: Illustrative figure showing dose-response curves. (a) Bertrand's rule. This is the notion that there is a dose at which a mineral nutrient produces an optimal function. Reducing or increasing the concentration of the nutrient away from the optimal concentration bears costs that are greater with further deviation from the optimum. (b)Hormesis. This is the idea that at a low dose, there are benefits to the intake of a toxin until an optimal is reached. Further increasing the concentration of the toxin results in costs until there are deleterious effects (indicated by the curve falling below the dashed line). (Raubenheimer and Simpson, 2012).

6.6 Research application and future directions

Current predictions estimate a global population of 9 billion by 2050, further increasing the unmet demand for food (Godfray et al., 2010; Tilman et al., 2011). One possible route to resolve this issue is to address the 40% loss of annual crop yield that occurs due to pests (Maxmen, 2013; Oerke, 2006). At the same time, gaps in the pesticide markets are being created due to increased pest resistance and changes in environmental and health legislation (Chandler et al., 2011). There is therefore an increased demand for biopesticides, naturally occurring organisms or their derivatives used in pest control (Wilson et al., 2013). *Xenorhabdus* and its nematode host *Steinernerma carpocapsae* are widely used in the biological control of lepidopteran pests (Nielsen-LeRoux et al., 2012). The ability to mass culture *Xenorhabdus* in diverse artificial growth media, that also support nematode growth makes them economically suitable for mass production (Couche and Gregson, 1987). Entomopathogenic nematode production is expensive and unreliable, limiting uptake (Yoo et al., 2000). Due to the importance of nutrition in the lifecycle of both the nematode and the bacterium (Martens et al., 2003), this and other studies focusing on microbial nutrient use can contribute to increased efficacy in the production process (Pranaw et al., 2014).

Due to the discovery that carbohydrate is a key resource for both this host and pathogen, future studies could focus on the direct competition that might occur between the host and pathogen for resources. There was evidence to show that the activity of amino acids in the haemolymph reflects the activity in haemolymph proteins both in abundance and in impacts on pathogenic activity. Investigating the effects of protein on diet choice, that have been consistently observed in *Spodoptera* (Lee et al., 2006; Povey et al., 2014, 2009), and seem to be conserved across different taxa (Ambrus, 2004; Clough et al., 2016; Goosen et al., 2014; Lochmiller et al., 1993), could progress at the level of amino

acids. Amino acid balances were found to be important for homeostasis in the host and interactions between amino acids may dictate the pathogen burden. There is also an intricate understanding of the roles amino acids play in mammalian immune defence (Li et al., 2007), allowing direct comparison of future findings with mammalian systems.

6.7 Concluding remarks

This study identified specific functions for individual dietary macronutrients in host defence. The role of dietary protein was reiterated in increasing host survival during infection. A more detailed coverage of the nutritional landscape also revealed a possible role for dietary carbohydrate in improving host resilience to infection through tolerance. This study adds to the growing pool of research indicating the importance of tolerance as a strategy used by hosts to reduce the impacts of infection.

Detailed information was provided on haemolymph resource availability and the fluctuations that occur in key nutrient groups in response to variation in dietary macronutrients were explored. The ability of host diet-choice to directly alter pathogen performance is a dimension that must be considered in future studies with greater importance as it has impacts across the fields of ecology, pharmacology and agronomy. This study highlights the importance of host nutrition on pathogen performance and reaffirms the importance of nutrition in the outcome of host pathogen-relationships.

7 References

Ababneh, Q.O., Tindall, A.J., Herman, J.K., 2015. A Secreted Factor Coordinates Environmental Quality with Bacillus Development. PLOS ONE 10, e0144168. https://doi.org/10.1371/journal.pone.0144168

Abbott, J., 2014. Self-medication in insects: current evidence and future perspectives. Ecol. Entomol. 39, 273–280. https://doi.org/10.1111/een.12110

Abisgold, J.D., Simpson, S.J., 1988. The Effect of Dietary Protein Levels and Haemolymph Composition on the Sensitivity of the Maxillary Palp Chemoreceptors of Locusts. J. Exp. Biol. 135, 215–229.

Abisgold, J.D., Simpson, S.J., 1987. The Physiology of Compensation by Locusts for Changes in Dietary Protein. J. Exp. Biol. 129, 329–346.

Adamo, S.A., 2008. 6 - Bidirectional Connections Between the Immune System and the Nervous System in Insects, in: Beckage, N.E. (Ed.), Insect Immunology. Academic Press, San Diego, pp. 129–149.

Adamo, S.A., 2006. Comparative Psychoneuroimmunology: Evidence From the Insects. Behav. Cogn. Neurosci. Rev. 5, 128–140. https://doi.org/10.1177/1534582306289580

Adamo, S.A., Bartlett, A., Le, J., Spencer, N., Sullivan, K., 2010. Illness-induced anorexia may reduce trade-offs between digestion and immune function. Anim. Behav. 79, 3–10. https://doi.org/10.1016/j.anbehav.2009.10.012

Adamo, S.A., Roberts, J.L., Easy, R.H., Ross, N.W., 2008. Competition between immune function and lipid transport for the protein apolipophorin III leads to stress-induced immunosuppression in crickets. J. Exp. Biol. 211, 531–538. https://doi.org/10.1242/jeb.013136

Aderem, A., Ulevitch, R.J., 2000. Toll-like receptors in the induction of the innate immune response. Nature 406, 782–787. https://doi.org/10.1038/35021228

Aidelberg, G., Towbin, B.D., Rothschild, D., Dekel, E., Bren, A., Alon, U., 2014. Hierarchy of non-glucose sugars in Escherichia coli. BMC Syst. Biol. 8, 133. https://doi.org/10.1186/s12918-014-0133-z

Akhurst, R.J., 1980. Morphological and Functional Dimorphism in Xenorhabdus spp., Bacteria Symbiotically Associated with the Insect Pathogenic Nematodes Neoaplectana and Heterorhabditis. J. Gen. Micobiology 121, 303–309.

Allen, J.E., Wynn, T.A., 2011. Evolution of Th2 Immunity: A Rapid Repair Response to Tissue Destructive Pathogens. PLOS Pathog. 7, e1002003. https://doi.org/10.1371/journal.ppat.1002003

Ambrus, J.L., 2004. Nutrition and Infectious Diseases in Developing Countries and Problems of Acquired Immunodeficiency Syndrome. Exp. Biol. Med. 229, 464–472.

Anderson, T.R., Boersma, M., Raubenheimer, D., 2004. Stoichiometry: Linking Elements to Biochemicals. Ecology 85, 1193–1202. https://doi.org/10.1890/02-0252

Anstead, G.M., Chandrasekar, B., Zhao, W., Yang, J., Perez, L.E., Melby, P.C., 2001. Malnutrition Alters the Innate Immune Response and Increases Early

Visceralization following Leishmania donovani Infection. Infect. Immun. 69, 4709–4718. https://doi.org/10.1128/IAI.69.8.4709-4718.2001

Archie, E.A., 2013. Wound healing in the wild: stress, sociality and energetic costs affect wound healing in natural populations. Parasite Immunol. 35, 374–385. https://doi.org/10.1111/pim.12048

Aryani, D.C., den Besten, H.M.W., Hazeleger, W.C., Zwietering, M.H., 2015. Quantifying strain variability in modeling growth of Listeria monocytogenes. Int. J. Food Microbiol. 208, 19–29. https://doi.org/10.1016/j.ijfoodmicro.2015.05.006

Ashida, M., Brey, P.T., 1995. Role of the integument in insect defense: pro-phenol oxidase cascade in the cuticular matrix. Proc. Natl. Acad. Sci. U. S. A. 92, 10698–10702.

Ayres, J.S., Schneider, D.S., 2012. Tolerance of Infections. Annu. Rev. Immunol. 30, 271–294. https://doi.org/10.1146/annurev-immunol-020711-075030

Ayres, J.S., Schneider, D.S., 2009. The Role of Anorexia in Resistance and Tolerance to Infections in Drosophila. PLoS Biol. 7. https://doi.org/10.1371/journal.pbio.1000150

Ayres, J.S., Schneider, D.S., 2008. Two ways to survive an infection: what resistance and tolerance can teach us about treatments for infectious diseases. Nat. Rev. Immunol. 8, 889–895. https://doi.org/10.1038/nri2432

Azeez, O.I., Meintjes, R., Chamunorwa, J.P., 2014. Fat body, fat pad and adipose tissues in invertebrates and vertebrates: the nexus. Lipids Health Dis. 13, 71. https://doi.org/10.1186/1476-511X-13-71

Barletta, A.B.F., Alves, L.R., Silva, M.C.L.N., Sim, S., Dimopoulos, G., Liechocki, S., Maya-Monteiro, C.M., Sorgine, M.H.F., 2016. Emerging role of lipid droplets in Aedes aegypti immune response against bacteria and Dengue virus. Sci. Rep. 6, 19928. https://doi.org/10.1038/srep19928

Bartoń, K., 2018. MuMIn: Multi-Model Inference.

Batool, R., Butt, M.S., Sultan, M.T., Saeed, F., Naz, R., 2013. Protein–Energy Malnutrition: A Risk Factor for Various Ailments. Crit. Rev. Food Sci. Nutr. 55, 242–253. https://doi.org/10.1080/10408398.2011.651543

Beck, M.A., Handy, J., Levander, O.A., 2004. Host nutritional status: the neglected virulence factor. Trends Microbiol. 12, 417–423. https://doi.org/10.1016/j.tim.2004.07.007

Begon, M., Townsend, C.R., Harper, J.L., 2005. Ecology: From Individuals to Ecosystems. Wiley, Oxford, UNITED KINGDOM.

Behnke, J.M., Barnard, C.J., Wakelin, D., 1992. Understanding chronic nematode infections: Evolutionary considerations, current hypotheses and the way forward. Int. J. Parasitol. 22, 861–907. https://doi.org/10.1016/0020-7519(92)90046-N

Bernardo, M.A., Singer, M.S., 2017. Parasite-altered feeding behavior in insects: integrating functional and mechanistic research frontiers. J. Exp. Biol. 220, 2848–2857. https://doi.org/10.1242/jeb.143800

Berne, R.M., Koeppen, Bruce M, Stanton, B.A., 2010. Berne & Levy physiology. Mosby/Elsevier, Philadelphia, PA.

Beyenbach, K.W., 2016. The plasticity of extracellular fluid homeostasis in insects. J. Exp. Biol. 219, 2596–2607. https://doi.org/10.1242/jeb.129650

Bird, A.F., Akhurst, R.J., 1983. The nature of the intestinal vesicle in nematodes of the family steinernematidae. Int. J. Parasitol. 13, 599–606. https://doi.org/10.1016/S0020-7519(83)80032-0

Blössner, M., de Onis, M., 2005. Quantifying the health impact at national and local levels. World Health Organ. 51.

Blum, H.E., 2017. The human microbiome. Adv. Med. Sci. 62, 414–420. https://doi.org/10.1016/j.advms.2017.04.005

Boctor, I.Z., 1980. Free amino acids of the haemolymph of the cotton leaf-worm,Spodoptera littoralis Boisduval full-grown larvae, infected with nuclear-polyhedrosis virus. Experientia 36, 638–639. https://doi.org/10.1007/BF01970106

Boctor, I.Z., 1974. Carbohydrates in the haemolymph of the prepupal and pupal stages ofSpodoptera littoralis Boisduval. J. Comp. Physiol. 94, 353–356. https://doi.org/10.1007/BF00710648

Boemare, N.E., Akhurst, R.J., Mourant, R.G., 1993. DNA Relatedness between Xenorhabdus spp. (Enterobacteriaceae), Symbiotic Bacteria of Entomopathogenic Nematodes, and a Proposal To Transfer Xenorhabdus luminescens to a New Genus, Photorhabdus gen. nov. Int. J. Syst. Bacteriol. 43, 249–255. https://doi.org/10.1099/00207713-43-2-249

Boman, H.G., Hultmark, D., 1987. Cell-Free Immunity in Insects. Annu. Rev. Microbiol. 41, 103–126. https://doi.org/10.1146/annurev.mi.41.100187.000535

Bowen, M., Co, D., Inman, F., Holmes, L., 2012. Microbial kinetics of Photorhabdus luminescens in glucose batch cultures. Explorations 7, 14–22.

Bren, A., Hart, Y., Dekel, E., Koster, D., Alon, U., 2013. The last generation of bacterial growth in limiting nutrient. BMC Syst. Biol. 7, 27. https://doi.org/10.1186/1752-0509-7-27

Bronstein, S.M., Conner, W.E., 1984. Endotoxin-induced behavioural fever in the Madagascar cockroach, Gromphadorhina portentosa. J. Insect Physiol. 30, 327–330. https://doi.org/10.1016/0022-1910(84)90134-3

Brown, E.S., Dewhurst, C.F., 1975. The genus spodoptera (Lepidoptera, Noctuidae) in Africa and the Near East. Bull. Entomol. Res. 65, 221–262. https://doi.org/10.1017/S0007485300005939

Brunner, F.S., Schmid-Hempel, P., Barribeau, S.M., 2014. Protein-poor diet reduces host-specific immune gene expression in Bombus terrestris. Proc. R. Soc. B Biol. Sci. 281. https://doi.org/10.1098/rspb.2014.0128

Bryce, J., Boschi-Pinto, C., Shibuya, K., Black, R.E., 2005. WHO estimates of the causes of death in children. The Lancet 365, 1147–1152. https://doi.org/10.1016/S0140-6736(05)71877-8

Burnham, K.P., Anderson, D.R., 2004. Multimodel Inference: Understanding AIC and BIC in Model Selection. Sociol. Methods Res. 33, 261–304. https://doi.org/10.1177/0049124104268644

Burnham, K.P., Anderson, D.R., 2002. Model Selection and Multimodel Inference: A Practical Information-Theoretic Approach, 2nd ed. Springer-Verlag, New York.

Calabrese, E.J., Baldwin, L.A., 2003. Toxicology rethinks its central belief. Nature 421, 691–692. https://doi.org/10.1038/421691a

Calder, P.C., Jackson, A.A., 2000. Undernutrition, infection and immune function. Nutr. Res. Rev. 13, 3. https://doi.org/10.1079/095442200108728981

Cezairliyan, B., Ausubel, F.M., 2017. Investment in secreted enzymes during nutrient-limited growth is utility dependent. Proc. Natl. Acad. Sci. U. S. A. 114, E7796–E7802. https://doi.org/10.1073/pnas.1708580114

Chagnon, P.-L., U'Ren, J.M., Miadlikowska, J., Lutzoni, F., Arnold, A.E., 2016. Interaction type influences ecological network structure more than local abiotic conditions: evidence from endophytic and endolichenic fungi at a continental scale. Oecologia 180, 181–191. https://doi.org/10.1007/s00442-015-3457-5

Chai, L.Y.A., Netea, M.G., Vonk, A.G., Kullberg, B.-J., 2009. Fungal strategies for overcoming host innate immune response. Med. Mycol. 47, 227–236. https://doi.org/10.1080/13693780802209082

Chandler, D., Bailey, A.S., Tatchell, G.M., Davidson, G., Greaves, J., Grant, W.P., 2011. The development, regulation and use of biopesticides for integrated pest management. Philos. Trans. R. Soc. B Biol. Sci. 366, 1987–1998. https://doi.org/10.1098/rstb.2010.0390

Chandra, R.K., 1997. Nutrition and the immune system: an introduction. Am. J. Clin. Nutr. 66, 460S-463S. https://doi.org/10.1093/ajcn/66.2.460S

Chapman, R.F., 2012. The Insects: Structure and Function, 5 edition. ed. Cambridge University Press, Cambridge.

Chapman, R.F., 2003. Contact Chemoreception in Feeding by Phytophagous Insects. Annu. Rev. Entomol. 48, 455–484. https://doi.org/10.1146/annurev.ento.48.091801.112629

Chapman, R.F., Boer, G.D., 2012. Regulatory Mechanisms in Insect Feeding. Springer Science & Business Media.

Chaston, J.M., Murfin, K.E., Heath-Heckman, E.A., Goodrich-Blair, H., 2013. Previously unrecognized stages of species-specific colonization in the mutualism between Xenorhabdus bacteria and Steinernema nematodes. Cell. Microbiol. 15, 1545–1559. https://doi.org/10.1111/cmi.12134

Chen, B., Teh, B.-S., Sun, C., Hu, S., Lu, X., Boland, W., Shao, Y., 2016. Biodiversity and Activity of the Gut Microbiota across the Life History of the Insect Herbivore *Spodoptera littoralis*. Sci. Rep. 6, 29505. https://doi.org/10.1038/srep29505

Cheon, H.-M., Shin, S.W., Bian, G., Park, J.-H., Raikhel, A.S., 2006. Regulation of Lipid Metabolism Genes, Lipid Carrier Protein Lipophorin, and Its Receptor during

Immune Challenge in the Mosquito Aedes aegypti. J. Biol. Chem. 281, 8426–8435. https://doi.org/10.1074/jbc.M510957200

Cho, S., Kim, Y., 2004. Hemocyte Apoptosis Induced by Entomopathogenic Bacteria, Xenorhabdus and Photorhabdus, in Bombyx mori. J. Asia-Pac. Entomol. 7, 195–200. https://doi.org/10.1016/S1226-8615(08)60215-0

Chown, S.L., Nicolson, S., 2004. Insect Physiological Ecology: Mechanisms and Patterns. OUP Oxford.

Chubukov, V., Gerosa, L., Kochanowski, K., Sauer, U., 2014. Coordination of microbial metabolism. Nat. Rev. Microbiol. 12, 327–340. https://doi.org/10.1038/nrmicro3238

Chubukov, V., Sauer, U., 2014. Environmental Dependence of Stationary-Phase Metabolism in Bacillus subtilis and Escherichia coli. Appl. Environ. Microbiol. 80, 2901–2909. https://doi.org/10.1128/AEM.00061-14

Clough, D., Prykhodko, O., Råberg, L., 2016. Effects of protein malnutrition on tolerance to helminth infection. Biol. Lett. 12, 20160189. https://doi.org/10.1098/rsbl.2016.0189

Cooper, T.F., Lenski, R.E., 2010. Experimental evolution with E. coli in diverse resource environments. I. Fluctuating environments promote divergence of replicate populations. BMC Evol. Biol. 10, 11. https://doi.org/10.1186/1471-2148-10-11

Corby-Harris, V., Habel, K.E., Ali, F.G., Promislow, D.E.L., 2007. Alternative measures of response to Pseudomonas aeruginosa infection in Drosophila melanogaster. J. Evol. Biol. 20, 526–533. https://doi.org/10.1111/j.1420-9101.2006.01267.x

Cotter, S.C., Kruuk, L.E.B., Wilson, K., 2004. Costs of resistance: genetic correlations and potential trade-offs in an insect immune System. J. Evol. Biol. 17, 421–429. https://doi.org/10.1046/j.1420-9101.2003.00655.x

Cotter, S.C., Myatt, J.P., Benskin, C.M.H., Wilson, K., 2008. Selection for cuticular melanism reveals immune function and life-history trade-offs in Spodoptera littoralis. J. Evol. Biol. 21, 1744–1754. https://doi.org/10.1111/j.1420-9101.2008.01587.x

Cotter, S.C., Simpson, S.J., Raubenheimer, D., Wilson, K., 2011. Macronutrient balance mediates trade-offs between immune function and life history traits. Funct. Ecol. 25, 186–198. https://doi.org/10.1111/j.1365-2435.2010.01766.x

Couche, G.A., Gregson, R.P., 1987. Protein inclusions produced by the entomopathogenic bacterium Xenorhabdus nematophilus subsp. nematophilus. J. Bacteriol. 169, 5279–5288.

Couche, G.A., Lehrbach, P.R., Forage, R.G., Cooney, G.C., Smith, D.R., Gregson, R.P., 1987. Occurrence of Intracellular Inclusions and Plasmids in Xenorhabdus spp. Microbiology 133, 967–973. https://doi.org/10.1099/00221287-133-4-967

Couteur, L., G, D., Solon-Biet, S., Wahl, D., Cogger, V.C., Willcox, B.J., Willcox, D.C., Raubenheimer, D., Simpson, S.J., 2016. New Horizons: Dietary protein, ageing and the Okinawan ratio. Age Ageing 45, 443–447. https://doi.org/10.1093/ageing/afw069

Cowieson, A.J., 2014. The geometric framework: An in vivo approach. J. Appl. Poult. Res. 23, 295–300. https://doi.org/10.3382/japr.2014-00939

Cowles, K.N., Cowles, C.E., Richards, G.R., Martens, E.C., Goodrich-Blair, H., 2007. The global regulator Lrp contributes to mutualism, pathogenesis and phenotypic variation in the bacterium Xenorhabdus nematophila. Cell. Microbiol. 9, 1311–1323. https://doi.org/10.1111/j.1462-5822.2006.00873.x

Crawford, J.M., Portmann, C., Zhang, X., Roeffaers, M.B.J., Clardy, J., 2012. Small molecule perimeter defense in entomopathogenic bacteria. Proc. Natl. Acad. Sci. U. S. A. 109, 10821–10826. https://doi.org/10.1073/pnas.1201160109

Cressler, C.E., Nelson, W.A., Day, T., McCauley, E., 2014. Disentangling the interaction among host resources, the immune system and pathogens. Ecol. Lett. 17, 284–293. https://doi.org/10.1111/ele.12229

Crosa, J.H., 1997. Signal Transduction and Transcriptional and Posttranscriptional Control of Iron-Regulated Genes in Bacteria. MICROBIOL MOL BIOL REV 61, 18.

Csonka, L.N., 1989. Physiological and genetic responses of bacteria to osmotic stress. Microbiol. Rev. 53, 121–147.

Csonka, L.N., Hanson, A.D., 1991. Prokaryotic Osmoregulation: Genetics and Physiology. Annu. Rev. Microbiol. 45, 569–606. https://doi.org/10.1146/annurev.mi.45.100191.003033

Cunningham-Rundles, S., McNeeley, D.F., Moon, A., 2005. Mechanisms of nutrient modulation of the immune response. J. Allergy Clin. Immunol. 115, 1119–1128. https://doi.org/10.1016/j.jaci.2005.04.036

da Silva, C.C.A., Dunphy, G.B., Rau, M.E., 2000. Interaction of Xenorhabdus nematophilus (Enterobacteriaceae) with the Antimicrobial Defenses of the House Cricket, Acheta domesticus. J. Invertebr. Pathol. 76, 285–292. https://doi.org/10.1006/jipa.2000.4975

Dadd, R.H., 1961. The nutritional requirements of locusts—IV. Requirements for vitamins of the B complex. J. Insect Physiol. 6, 1–12. https://doi.org/10.1016/0022-1910(61)90086-5

de Brito, N.J.N., Rocha, É.D., de Araújo Silva, A., Costa, J.B.S., França, M.C., das Graças Almeida, M., Brandão-Neto, J., 2014. Oral Zinc Supplementation Decreases the Serum Iron Concentration in Healthy Schoolchildren: A Pilot Study. Nutrients 6, 3460–3473. https://doi.org/10.3390/nu6093460

de Roode, J.C., de Castillejo, C.L.F., Faits, T., Alizon, S., 2011. Virulence evolution in response to anti-infection resistance: toxic food plants can select for virulent parasites of monarch butterflies. J. Evol. Biol. 24, 712–722. https://doi.org/10.1111/j.1420-9101.2010.02213.x

DeGrandi-Hoffman, G., Chen, Y., 2015. Nutrition, immunity and viral infections in honey bees. Curr. Opin. Insect Sci., Social Insects * Vectors and Medical and Veterinary Entomology 10, 170–176. https://doi.org/10.1016/j.cois.2015.05.007

Dittmer, N.T., Suderman, R.J., Jiang, H., Zhu, Y.-C., Gorman, M.J., Kramer, K.J., Kanost, M.R., 2004. Characterization of cDNAs encoding putative laccase-like multicopper oxidases and developmental expression in the tobacco hornworm, Manduca sexta,

and the malaria mosquito, Anopheles gambiae. Insect Biochem. Mol. Biol. 34, 29–41. https://doi.org/10.1016/j.ibmb.2003.08.003

Dunphy, G.B., Webster, J.M., 1991. Antihemocytic surface components of Xenorhabdus nematophilus var. dutki and their modification by serum of nonimmune larvae of Galleria mellonella. J. Invertebr. Pathol. 58, 40–51. https://doi.org/10.1016/0022-2011(91)90160-R

Dunphy, G.B., Webster, J.M., 1989. The monoxenic culture of Neoaplectana carpocapsae DD 136 and Heterorhabditis heliothidis. Rev. Nematol 12, 113–123.

Eleftherianos, I., Boundy, S., Joyce, S.A., Aslam, S., Marshall, J.W., Cox, R.J., Simpson, T.J., Clarke, D.J., ffrench-Constant, R.H., Reynolds, S.E., 2007. An antibiotic produced by an insect-pathogenic bacterium suppresses host defenses through phenoloxidase inhibition. Proc. Natl. Acad. Sci. U. S. A. 104, 2419–2424. https://doi.org/10.1073/pnas.0610525104

Elser, J., 2006. Biological Stoichiometry: A Chemical Bridge between Ecosystem Ecology and Evolutionary Biology. Am. Nat. 168, S25–S35. https://doi.org/10.1086/509048

Emson, H.E., 1987. Health, disease and illness: matters for definition. CMAJ Can. Med. Assoc. J. 136, 811–813.

Evans, D.H., Claiborne, J.B., 2005. The Physiology of Fishes, Third Edition. CRC Press.

Fellous, S., Lazzaro, B.P., 2010. Larval food quality affects adult (but not larval) immune gene expression independent of effects on general condition. Mol. Ecol. 19, 1462–1468. https://doi.org/10.1111/j.1365-294X.2010.04567.x

Fisher, S.H., 1999. Regulation of nitrogen metabolism in Bacillus subtilis: vive la différence! Mol. Microbiol. 32, 223–232. https://doi.org/10.1046/j.1365-2958.1999.01333.x

Folch, J., Lees, M., Stanley, G.H.S., 1957. A Simple Method for the Isolation and Purification of Total Lipides from Animal Tissues. J. Biol. Chem. 226, 497–509.

Forst, S., Dowds, B., Boemare, N., Stackebrandt, E., 1997. XENORHABDUS AND PHOTORHABDUS SPP.:Bugs That Kill Bugs. Annu. Rev. Microbiol. 51, 47–72. https://doi.org/10.1146/annurev.micro.51.1.47

Forst, S.A., Roberts, D.A., 1994. Signal transduction by the EnvZ-OmpR phosphotransfer system in bacteria. Res. Microbiol. 145, 363–373. https://doi.org/10.1016/0923-2508(94)90083-3

Freitak, D., Ots, I., Vanatoa, A., Hõrak, P., 2003. Immune response is energetically costly in white cabbage butterfly pupae. Proc. R. Soc. B Biol. Sci. 270, S220–S222. https://doi.org/10.1098/rsbl.2003.0069

Friedman, S., Waldbauer, G.P., Eertmoed, J.E., Naeem, M., Ghent, A.W., 1991. Blood trehalose levels have a role in the control of dietary self-selection by Heliothis zea larvae. J. Insect Physiol. 37, 919–928. https://doi.org/10.1016/0022-1910(91)90007-M

Frost, P.C., Ebert, D., Smith, V.H., 2008. Responses of a Bacterial Pathogen to Phosphorus Limitation of Its Aquatic Invertebrate Host. Ecology 89, 313–318. https://doi.org/10.1890/07-0389.1

Fujita, M., Losick, R., 2005. Evidence that entry into sporulation in Bacillus subtilis is governed by a gradual increase in the level and activity of the master regulator Spo0A. Genes Dev. 19, 2236–2244. https://doi.org/10.1101/gad.1335705

Georgis, R., Koppenhöfer, A.M., Lacey, L.A., Bélair, G., Duncan, L.W., Grewal, P.S., Samish, M., Tan, L., Torr, P., van Tol, R.W.H.M., 2006. Successes and failures in the use of parasitic nematodes for pest control. Biol. Control, Third International Symposium on Entomopathogenic Nematodes and Symbiotic Bacteria 38, 103–123. https://doi.org/10.1016/j.biocontrol.2005.11.005

Gilbert, J.A., Blaser, M.J., Caporaso, J.G., Jansson, J.K., Lynch, S.V., Knight, R., 2018. Current understanding of the human microbiome. Nat. Med. 24, 392–400. https://doi.org/10.1038/nm.4517

Godfray, H.C.J., Beddington, J.R., Crute, I.R., Haddad, L., Lawrence, D., Muir, J.F., Pretty, J., Robinson, S., Thomas, S.M., Toulmin, C., 2010. Food Security: The Challenge of Feeding 9 Billion People. Science 327, 812–818. https://doi.org/10.1126/science.1185383

González-Santoyo, I., Córdoba-Aguilar, A., 2012. Phenoloxidase: a key component of the insect immune system. Entomol. Exp. Appl. 142, 1–16. https://doi.org/10.1111/j.1570-7458.2011.01187.x

Goodrich-Blair, H., Clarke, D.J., 2007. Mutualism and pathogenesis in Xenorhabdus and Photorhabdus: two roads to the same destination. Mol. Microbiol. 64, 260–268. https://doi.org/10.1111/j.1365-2958.2007.05671.x

Goosen, N.J., de Wet, L.F., Görgens, J.F., 2014. Rainbow trout silage as immune stimulant and feed ingredient in diets for Mozambique tilapia (Oreochromis mossambicus). Aquac. Res. n/a–n/a. https://doi.org/10.1111/are.12497

Gotz, P., Boman, A., Boman, H.G., 1981. Interactions between insect immunity and an insect-pathogenic nematode with symbiotic bacteria. Proc R Soc Lond B 212, 333–350. https://doi.org/10.1098/rspb.1981.0043

Graham, R.I., Deacutis, J.M., Pulpitel, T., Ponton, F., Simpson, S.J., Wilson, K., 2014. Locusts increase carbohydrate consumption to protect against a fungal biopesticide. J. Insect Physiol., Mechanisms of Nutritional Homeostasis in Insects 69, 27–34. https://doi.org/10.1016/j.jinsphys.2014.05.015

Graham, R.I., Deacutis, J.M., Simpson, S.J., Wilson, K., 2015. Body condition constrains immune function in field populations of female Australian plague locust Chortoicetes terminifera. Parasite Immunol. 37, 233–241. https://doi.org/10.1111/pim.12179

Griffith, R.S., DeLong, D.C., Nelson, J.D., 1981. Relation of arginine-lysine antagonism to herpes simplex growth in tissue culture. Chemotherapy 27, 209–213. https://doi.org/10.1159/000237979

Haine, E.R., Moret, Y., Siva-Jothy, M.T., Rolff, J., 2008a. Antimicrobial Defense and Persistent Infection in Insects. Science 322, 1257–1259. https://doi.org/10.1126/science.1165265

Haine, E.R., Pollitt, L.C., Moret, Y., Siva-Jothy, M.T., Rolff, J., 2008b. Temporal patterns in immune responses to a range of microbial insults (Tenebrio molitor). J. Insect Physiol. 54, 1090–1097. https://doi.org/10.1016/j.jinsphys.2008.04.013

Hall, S.R., Simonis, J.L., Nisbet, R.M., Tessier, A.J., Cáceres, C.E., 2009. Resource Ecology of Virulence in a Planktonic Host-Parasite System: An Explanation Using Dynamic Energy Budgets. Am. Nat. 174, 149–162. https://doi.org/10.1086/600086

Harrison, J.F., Woods, H.A., Roberts, S.P., 2012. Ecological and Environmental Physiology of Insects. OUP Oxford.

Hastie, T.J., Tibshirani, R.J., 1990. Generalized Additive Models. CRC Press.

Haydon, D.T., Matthews, L., Timms, R., Colegrave, N., 2003. Top-down or bottom-up regulation of intra-host blood-stage malaria: do malaria parasites most resemble the dynamics of prey or predator? Proc. R. Soc. B Biol. Sci. 270, 289–298. https://doi.org/10.1098/rspb.2002.2203

Herbert, E.E., Goodrich-Blair, H., 2007. Friend and foe: the two faces of Xenorhabdus nematophila. Nat. Rev. Microbiol. 5, 634–646. https://doi.org/10.1038/nrmicro1706

Hessen, D.O., Elser, J.J., Sterner, R.W., Urabe, J., 2013. Ecological stoichiometry: An elementary approach using basic principles. Limnol. Oceanogr. 58, 2219–2236. https://doi.org/10.4319/lo.2013.58.6.2219

Hibbing, M.E., Fuqua, C., Parsek, M.R., Peterson, S.B., 2010. Bacterial competition: surviving and thriving in the microbial jungle. Nat. Rev. Microbiol. 8, 15–25. https://doi.org/10.1038/nrmicro2259

Hiron, A., Borezée-Durant, E., Piard, J.-C., Juillard, V., 2007. Only One of Four Oligopeptide Transport Systems Mediates Nitrogen Nutrition in Staphylococcus aureus. J. Bacteriol. 189, 5119–5129. https://doi.org/10.1128/JB.00274-07

Hoffmann, J.A., Reichhart, J.-M., 2002. Drosophila innate immunity: an evolutionary perspective. Nat. Immunol. 3, 121–126. https://doi.org/10.1038/ni0202-121

Holland, J.N., DeAngelis, D.L., 2009. Consumer-resource theory predicts dynamic transitions between outcomes of interspecific interactions. Ecol. Lett. 12, 1357–1366. https://doi.org/10.1111/j.1461-0248.2009.01390.x

Hosny, M.M., Topper, C.P., Moawad, G.M., El-Saadany, G.B., 1986. Economic damage thresholds of Spodoptera littoralis (Boisd.) (Lepidoptera: Noctuidae) on cotton in Egypt. Crop Prot. 5, 100–104. https://doi.org/10.1016/0261-2194(86)90088-8

Huffman, M.A., 2003. Animal self-medication and ethno-medicine: exploration and exploitation of the medicinal properties of plants. Proc. Nutr. Soc. 62, 371–381. https://doi.org/10.1079/PNS2003257

Huffman, M.A., Caton, J.M., 2001. Self-induced Increase of Gut Motility and the Control of Parasitic Infections in Wild Chimpanzees. Int. J. Primatol. 18.

Hughes, D.P., Pierce, N.E., Boomsma, J.J., 2008. Social insect symbionts: evolution in homeostatic fortresses. Trends Ecol. Evol. 23, 672–677. https://doi.org/10.1016/j.tree.2008.07.011

Ignell, R., Okawa, S., Englund, J.-E., Hill, S.R., 2010. Assessment of diet choice by the yellow fever mosquito Aedes aegypti. Physiol. Entomol. 35, 274–286. https://doi.org/10.1111/j.1365-3032.2010.00740.x

Iwasaki, A., Medzhitov, R., 2010. Regulation of Adaptive Immunity by the Innate Immune System. Science 327, 291–295. https://doi.org/10.1126/science.1183021

Jackman, S., Tahk, with contributions from A., Zeileis, A., Maimone, C., Meers, J.F. and Z., 2017. pscl: Political Science Computational Laboratory.

Jensen, K., McClure, C., Priest, N.K., Hunt, J., 2015. Sex-specific effects of protein and carbohydrate intake on reproduction but not lifespan in Drosophila melanogaster. Aging Cell 14, 605–615. https://doi.org/10.1111/acel.12333

Ji, D., Kim, Y., 2004. An entomopathogenic bacterium, Xenorhabdus nematophila, inhibits the expression of an antibacterial peptide, cecropin, of the beet armyworm, Spodoptera exigua. J. Insect Physiol. 50, 489–496. https://doi.org/10.1016/j.jinsphys.2004.03.005

Johnson, P.T.J., Roode, J.C. de, Fenton, A., 2015. Why infectious disease research needs community ecology. Science 349, 1259504. https://doi.org/10.1126/science.1259504

Joseph, A., Philip, R., 2007. Acute salinity stress alters the haemolymph metabolic profile of Penaeus monodon and reduces immunocompetence to white spot syndrome virus infection. Aquaculture 272, 87–97. https://doi.org/10.1016/j.aquaculture.2007.08.047

Jubelin, G., Pagès, S., Lanois, A., Boyer, M.-H., Gaudriault, S., Ferdy, J.-B., Givaudan, A., 2011. Studies of the dynamic expression of the Xenorhabdus FliAZ regulon reveal atypical iron-dependent regulation of the flagellin and haemolysin genes during insect infection. Environ. Microbiol. 13, 1271–1284. https://doi.org/10.1111/j.1462-2920.2011.02427.x

Kambara, T., McFarlane, R.G., Abell, T.J., McAnulty, R.W., Sykes, A.R., 1993. The effect of age and dietary protein on immunity and resistance in lambs vaccinated with Trichostrongylus colubriformis. Int. J. Parasitol., Special Issue: Proceedings of the Joint Conference of the Australian and New Zealand Societies for Parasitology, 1992 23, 471–476. https://doi.org/10.1016/0020-7519(93)90035-W

Karowe, D.N., Martin, M.M., 1989. The effects of quantity and quality of diet nitrogen on the growth, efficiency of food utilization, nitrogen budget, and metabolic rate of fifth-instar Spodoptera eridania larvae (Lepidoptera: Noctuidae). J. Insect Physiol. 35, 699–708. https://doi.org/10.1016/0022-1910(89)90089-9

Kassambara, A., Mundt, F., 2017. factoextra: Extract and Visualize the Results of Multivariate Data Analyses.

Katz, Y., Springer, M., 2016. Probabilistic adaptation in changing microbial environments. PeerJ 4. https://doi.org/10.7717/peerj.2716

Kaufmann, C., Brown, M.R., 2008. Regulation of carbohydrate metabolism and flight performance by a hypertrehalosaemic hormone in the mosquito Anopheles gambiae. J. Insect Physiol. 54, 367–377. https://doi.org/10.1016/j.jinsphys.2007.10.007

Keating, S.T., McCarthy, W.J., Yendol, W.G., 1989. Gypsy moth (Lymantria dispar) larval susceptibility to a baculovirus affected by selected nutrients, hydrogen lons (pH), and plant allelochemicals in artificial diets. J. Invertebr. Pathol. 54, 165–174. https://doi.org/10.1016/0022-2011(89)90026-8

Kempf, B., Bremer, E., 1998. Uptake and synthesis of compatible solutes as microbial stress responses to high-osmolality environments. Arch. Microbiol. 170, 319–330. https://doi.org/10.1007/s002030050649

Kerkut, G.A., 2013. Regulation: Digestion, Nutrition, Excretion. Elsevier.

Khosravi, S., Bui, H.T.D., Rahimnejad, S., Herault, M., Fournier, V., Kim, S.-S., Jeong, J.-B., Lee, K.-J., 2015. Dietary supplementation of marine protein hydrolysates in fish-meal based diets for red sea bream (Pagrus major) and olive flounder (Paralichthys olivaceus). Aquaculture 435, 371–376. https://doi.org/10.1016/j.aquaculture.2014.10.019

Kleino, A., Silverman, N., 2014. The Drosophila IMD pathway in the activation of the humoral immune response. Dev. Comp. Immunol. 42, 25–35. https://doi.org/10.1016/j.dci.2013.05.014

Koch, A.L., 1982. Multistep kinetics: Choice of models for the growth of bacteria. J. Theor. Biol. 98, 401–417. https://doi.org/10.1016/0022-5193(82)90127-8

Koella, J.C., Sørensen, F.L., 2002. Effect of adult nutrition on the melanization immune response of the malaria vector Anopheles stephensi. Med. Vet. Entomol. 16, 316–320. https://doi.org/10.1046/j.1365-2915.2002.00381.x

Kogut, M.H., Klasing, K., 2009. An immunologist's perspective on nutrition, immunity, and infectious diseases: Introduction and overview. J. Appl. Poult. Res. 18, 103–110. https://doi.org/10.3382/japr.2008-00080

Kooijman, S.A.L.M., 2001. Quantitative aspects of metabolic organization: a discussion of concepts. Philos. Trans. R. Soc. B Biol. Sci. 356, 331–349. https://doi.org/10.1098/rstb.2000.0771

Kooliyottil, R., Inman, F., Mandjiny, S., Holmes, L., 2014. Physiological Constants of the Entomopathogenic Bacterium Xenorhabdus nematophila Determined by Microbial Growth Kinetics [WWW Document]. Int. Sch. Res. Not. https://doi.org/10.1155/2014/834054

Kovárová-Kovar, K., Egli, T., 1998. Growth Kinetics of Suspended Microbial Cells: From Single-Substrate-Controlled Growth to Mixed-Substrate Kinetics. Microbiol Mol Biol Rev 62, 646–666.

Kraaijeveld, A.R., Elrayes, N.P., Schuppe, H., Newland, P.L., 2011. l-Arginine enhances immunity to parasitoids in Drosophila melanogaster and increases NO production in lamellocytes. Dev. Comp. Immunol. 35, 857–864. https://doi.org/10.1016/j.dci.2011.03.019

Krell, T., Lacal, J., Busch, A., Silva-Jiménez, H., Guazzaroni, M.-E., Ramos, J.L., 2010. Bacterial Sensor Kinases: Diversity in the Recognition of Environmental Signals. Annu. Rev. Microbiol. 64, 539–559. https://doi.org/10.1146/annurev.micro.112408.134054

Krenn, H.W., 2010. Feeding Mechanisms of Adult Lepidoptera: Structure, Function, and Evolution of the Mouthparts. Annu. Rev. Entomol. 55, 307–327. https://doi.org/10.1146/annurev-ento-112408-085338

Kristan, D.M., 2007. Chronic calorie restriction increases susceptibility of laboratory mice (Mus musculus) to a primary intestinal parasite infection. Aging Cell 6, 817–825. https://doi.org/10.1111/j.1474-9726.2007.00345.x

Kussell, E., Leibler, S., 2005. Phenotypic Diversity, Population Growth, and Information in Fluctuating Environments. Science 309, 2075–2078. https://doi.org/10.1126/science.1114383

Lafferty, K.D., DeLeo, G., Briggs, C.J., Dobson, A.P., Gross, T., Kuris, A.M., 2015. A general consumer-resource population model. Science 349, 854–857. https://doi.org/10.1126/science.aaa6224

Lanois, A., Jubelin, G., Givaudan, A., 2008. FliZ, a flagellar regulator, is at the crossroads between motility, haemolysin expression and virulence in the insect pathogenic bacterium Xenorhabdus. Mol. Microbiol. 68, 516–533. https://doi.org/10.1111/j.1365-2958.2008.06168.x

Lapointe, J.F., Dunphy, G.B., Mandato, C.A., 2012. Hemocyte–hemocyte adhesion and nodulation reactions of the greater wax moth, Galleria mellonella are influenced by cholera toxin and its B-subunit. Results Immunol. 2, 54–65. https://doi.org/10.1016/j.rinim.2012.02.002

Lavine, M.D., Strand, M.R., 2002. Insect hemocytes and their role in immunity. Insect Biochem. Mol. Biol., Recent Progress in Insect Molecular Biology 32, 1295–1309. https://doi.org/10.1016/S0965-1748(02)00092-9

Lazazzera, B.A., 2001. The intracellular function of extracellular signaling peptides. Peptides, Bacterial and anti bacterial peptides 22, 1519–1527. https://doi.org/10.1016/S0196-9781(01)00488-0

Le Gall, M., Behmer, S.T., 2014. Effects of Protein and Carbohydrate on an Insect Herbivore: The Vista from a Fitness Landscape. Integr. Comp. Biol. 54, 942–954. https://doi.org/10.1093/icb/icu102

Lee, B.C., Kaya, A., Ma, S., Kim, G., Gerashchenko, M.V., Yim, S.H., Hu, Z., Harshman, L.G., Gladyshev, V.N., 2014. Methionine restriction extends lifespan of Drosophila melanogaster under conditions of low amino acid status. Nat. Commun. 5, 3592. https://doi.org/10.1038/ncomms4592

Lee, K.P., Behmer, S.T., Simpson, S.J., Raubenheimer, D., 2002. A geometric analysis of nutrient regulation in the generalist caterpillar Spodoptera littoralis (Boisduval). J. Insect Physiol. 48, 655–665. https://doi.org/10.1016/S0022-1910(02)00088-4

Lee, K.P., Cory, J.S., Wilson, K., Raubenheimer, D., Simpson, S.J., 2006. Flexible diet choice offsets protein costs of pathogen resistance in a caterpillar. Proc. R. Soc. B Biol. Sci. 273, 823–829. https://doi.org/10.1098/rspb.2005.3385

Lee, K.P., Raubenheimer, D., Simpson, S.J., 2004. The effects of nutritional imbalance on compensatory feeding for cellulose-mediated dietary dilution in a generalist caterpillar. Physiol. Entomol. 29, 108–117. https://doi.org/10.1111/j.0307-6962.2004.00371.x

Lee, Kwang Pum, Simpson, S.J., Clissold, F.J., Brooks, R., Ballard, J.W.O., Taylor, P.W., Soran, N., Raubenheimer, D., 2008. Lifespan and reproduction in Drosophila: New insights from nutritional geometry. Proc. Natl. Acad. Sci. 105, 2498–2503. https://doi.org/10.1073/pnas.0710787105

Lee, K. P, Simpson, S.J., Wilson, K., 2008. Dietary protein-quality influences melanization and immune function in an insect. Funct. Ecol. 22, 1052–1061. https://doi.org/10.1111/j.1365-2435.2008.01459.x

Leisman, G.B., Waukau, J., Forst, S.A., 1995. Characterization and environmental regulation of outer membrane proteins in Xenorhabdus nematophilus. Appl. Environ. Microbiol. 61, 200–204.

Leitão-Gonçalves, R., Carvalho-Santos, Z., Francisco, A.P., Fioreze, G.T., Anjos, M., Baltazar, C., Elias, A.P., Itskov, P.M., Piper, M.D.W., Ribeiro, C., 2017. Commensal bacteria and essential amino acids control food choice behavior and reproduction. PLOS Biol. 15, e2000862. https://doi.org/10.1371/journal.pbio.2000862

Lemaitre, B., Hoffmann, J., 2007. The Host Defense of Drosophila melanogaster. Annu. Rev. Immunol. 25, 697–743. https://doi.org/10.1146/annurev.immunol.25.022106.141615

Letnic, M., Dickman, C.R., 2010. Resource pulses and mammalian dynamics: conceptual models for hummock grasslands and other Australian desert habitats. Biol. Rev. 85, 501–521. https://doi.org/10.1111/j.1469-185X.2009.00113.x

Li, P., Yin, Y.-L., Li, D., Kim, S.W., Wu, G., 2007. Amino acids and immune function. Br. J. Nutr. 98, 237–252. https://doi.org/10.1017/S000711450769936X

Lihoreau, M., Buhl, J., Charleston, M.A., Sword, G.A., Raubenheimer, D., Simpson, S.J., Eubanks, M., 2015. Nutritional ecology beyond the individual: a conceptual framework for integrating nutrition and social interactions. Ecol. Lett. 18, 273–286. https://doi.org/10.1111/ele.12406

Litchman, E., Edwards, K.F., Klausmeier, C.A., 2015. Microbial resource utilization traits and trade-offs: implications for community structure, functioning, and biogeochemical impacts at present and in the future. Front. Microbiol. 6. https://doi.org/10.3389/fmicb.2015.00254

Lochmiller, R.L., Deerenberg, C., 2000. Trade-Offs in Evolutionary Immunology: Just What Is the Cost of Immunity? Oikos 88, 87–98.

Lochmiller, R.L., Vestey, M.R., Boren, J.C., 1993. Relationship between Protein Nutritional Status and Immunocompetence in Northern Bobwhite Chicks. The Auk 110, 503–510. https://doi.org/10.2307/4088414

Louie, A., Song, K.H., Hotson, A., Tate, A.T., Schneider, D.S., 2016. How Many Parameters Does It Take to Describe Disease Tolerance? PLOS Biol. 14, e1002435. https://doi.org/10.1371/journal.pbio.1002435

MacKinnon, L.T., 2000. Overtraining effects on immunity and performance in athletes. Immunol. Cell Biol. 78, 502–509. https://doi.org/10.1111/j.1440-1711.2000.t01-7-.x

Madigan, M.T., Martinko, J.M., Parker, J., 2003. Brock Biology of Microorganisms. Prentice Hall/Pearson Education.

Mannion, B.A., Weiss, J., Elsbach, P., 1990. Separation of sublethal and lethal effects of the bactericidal/permeability increasing protein on Escherichia coli. J. Clin. Invest. 85, 853–860.

Maranga, L., Mendonça, R.Z., Bengala, A., Peixoto, C.C., Moraes, R.H.P., Pereira, C.A., Carrondo, M.J.T., 2003. Enhancement of Sf-9 Cell Growth and Longevity through Supplementation of Culture Medium with Hemolymph. Biotechnol. Prog. 19, 58–63. https://doi.org/10.1021/bp025583q

Marcogliese, D.J., Pietrock, M., 2011. Combined effects of parasites and contaminants on animal health: parasites do matter. Trends Parasitol. 27, 123–130. https://doi.org/10.1016/j.pt.2010.11.002

Martens, E.C., Heungens, K., Goodrich-Blair, H., 2003. Early Colonization Events in the Mutualistic Association between Steinernema carpocapsae Nematodes and Xenorhabdus nematophila Bacteria. J. Bacteriol. 185, 3147–3154. https://doi.org/10.1128/JB.185.10.3147-3154.2003

Martin, L.B., Scheuerlein, A., Wikelski, M., 2003. Immune activity elevates energy expenditure of house sparrows: a link between direct and indirect costs? Proc. R. Soc. Lond. B Biol. Sci. 270, 153–158. https://doi.org/10.1098/rspb.2002.2185

Martinez, S.S., Emden, V., F, H., 2001. Growth disruption, abnormalities and mortality of Spodoptera littoralis (Boisduval) (Lepidoptera: Noctuidae) caused by Azadirachtin. Neotrop. Entomol. 30, 113–125. https://doi.org/10.1590/S1519-566X2001000100017

Maxmen, A., 2013. Crop pests: Under attack. Nature 501, S15–S17. https://doi.org/10.1038/501S15a

McGill, B.J., Enquist, B.J., Weiher, E., Westoby, M., 2006. Rebuilding community ecology from functional traits. Trends Ecol. Evol. 21, 178–185. https://doi.org/10.1016/j.tree.2006.02.002

Medzhitov, R., Janeway Jr, C.A., 1998. Innate immune recognition and control of adaptive immune responses. Semin. Immunol. 10, 351–353. https://doi.org/10.1006/smim.1998.0136

Medzhitov, R., Schneider, D.S., Soares, M.P., 2012. Disease Tolerance as a Defense Strategy. Science 335, 936–941. https://doi.org/10.1126/science.1214935

Merrill, A.L., Watt, B.K., 1955. Energy value of foods: basis and derivation. U.S. Dept. of Agriculture.

Mertz, W., 1981. The essential trace elements. Science 213, 1332–1338. https://doi.org/10.1126/science.7022654

Mideo, N., Reece, S.E., 2011. Plasticity in parasite phenotypes: evolutionary and ecological implications for disease. Future Microbiol. 7, 17–24. https://doi.org/10.2217/fmb.11.134

Miller, C.V.L., Cotter, S.C., 2017. Resistance and tolerance: The role of nutrients on pathogen dynamics and infection outcomes in an insect host. J. Anim. Ecol. 87, 500–510. https://doi.org/10.1111/1365-2656.12763

Mills, D.S., Marchant-Forde, J.N., 2010. The Encyclopedia of Applied Animal Behaviour and Welfare. CABI.

Moatt, J.P., Nakagawa, S., Lagisz, M., Walling, C.A., 2016. The effect of dietary restriction on reproduction: a meta-analytic perspective. BMC Evol. Biol. 16, 199. https://doi.org/10.1186/s12862-016-0768-z

Monod, J., 1949. The Growth of Bacterial Cultures. Annu. Rev. Microbiol. 3, 371–394. https://doi.org/10.1146/annurev.mi.03.100149.002103

Moret, Y., Schmid-Hempel, P., 2000. Survival for Immunity: The Price of Immune System Activation for Bumblebee Workers. Science 290, 1166–1168. https://doi.org/10.1126/science.290.5494.1166

Münch, A., Stingl, L., Jung, K., Heermann, R., 2008. Photorhabdus luminescens genes induced upon insect infection. BMC Genomics 9, 229. https://doi.org/10.1186/1471-2164-9-229

Muñoz-Elías, E.J., McKinney, J.D., 2006. Carbon metabolism of intracellular bacteria. Cell. Microbiol. 8, 10–22. https://doi.org/10.1111/j.1462-5822.2005.00648.x

Myhre, E.B., Kronvall, G., 1980. Demonstration of specific binding sites for human serum albumin in group C and G streptococci. Infect. Immun. 27, 6–14.

Narr, C.F., Krist, A.C., 2015. Host diet alters trematode replication and elemental composition. Freshw. Sci. 34, 81–91. https://doi.org/10.1086/679411

New, A.M., Cerulus, B., Govers, S.K., Perez-Samper, G., Zhu, B., Boogmans, S., Xavier, J.B., Verstrepen, K.J., 2014. Different Levels of Catabolite Repression Optimize Growth in Stable and Variable Environments. PLOS Biol. 12, e1001764. https://doi.org/10.1371/journal.pbio.1001764

Nguyen, K.B., Smart, G.C., 1992. Life Cycle of Steinernema scapterisci Nguyen &Smart, 1990. J. Nematol. 24, 160–169.

Nicholson, J.K., Holmes, E., Kinross, J., Burcelin, R., Gibson, G., Jia, W., Pettersson, S., 2012. Host-Gut Microbiota Metabolic Interactions. Science 336, 1262–1267. https://doi.org/10.1126/science.1223813

Nickerson', K.W., Bulla, L.A., 1974. Physiology of Sporeforming Bacteria Associated with Insects: Minimal Nutritional Requirements for Growth, Sporulation, and Parasporal Crystal Formation of Bacillus thuringiensis. APPL MICROBIOL 28, 5.

Nielsen-LeRoux, C., Gaudriault, S., Ramarao, N., Lereclus, D., Givaudan, A., 2012. How the insect pathogen bacteria Bacillus thuringiensis and Xenorhabdus/Photorhabdus occupy their hosts. Curr. Opin. Microbiol., Ecology and industrial microbiology/Special section: Microbial proteomics 15, 220–231. https://doi.org/10.1016/j.mib.2012.04.006

Nisbet, R.M., Muller, E.B., Lika, K., Kooijman, S.A.L.M., 2000. From Molecules to Ecosystems through Dynamic Energy Budget Models. J. Anim. Ecol. 69, 913–926.

Nnadi, P.A., Ezeh, I.O., Kalu, K.C., Ngene, A.A., 2010. The impact of dietary protein on the pathophysiology of porcine trypanosome infection. Vet. Parasitol. 173, 193–199. https://doi.org/10.1016/j.vetpar.2010.07.004

Novoselov, A., Becker, T., Pauls, G., von Reuß, S.H., Boland, W., 2015. Spodoptera littoralis detoxifies neurotoxic 3-nitropropanoic acid by conjugation with amino acids. Insect Biochem. Mol. Biol. 63, 97–103. https://doi.org/10.1016/j.ibmb.2015.05.013

Nychka, D., 2016. fields: Tools for Spatial Data. https://doi.org/10.5065/D6W957CT

O'Brien, D.M., Fogel, M.L., Boggs, C.L., 2002. Renewable and nonrenewable resources: Amino acid turnover and allocation to reproduction in Lepidoptera. Proc. Natl. Acad. Sci. 99, 4413–4418. https://doi.org/10.1073/pnas.072346699

Oerke, E.-C., 2006. Crop losses to pests. J. Agric. Sci. 144, 31–43. https://doi.org/10.1017/S0021859605005708

Orchard, S.S., Goodrich-Blair, H., 2004. Identification and Functional Characterization of a Xenorhabdus nematophila Oligopeptide Permease. Appl. Environ. Microbiol. 70, 5621–5627. https://doi.org/10.1128/AEM.70.9.5621-5627.2004

Pant, R., Agrawal, H.C., 1964. Free amino acids of the haemolymph of some insects. J. Insect Physiol. 10, 443–446. https://doi.org/10.1016/0022-1910(64)90069-1

Park, Y., Herbert, E.E., Cowles, C.E., Cowles, K.N., Menard, M.L., Orchard, S.S., Goodrich-Blair, H., 2006. Clonal variation in Xenorhabdus nematophila virulence and suppression of Manduca sexta immunity. Cell. Microbiol. 9, 645–656. https://doi.org/10.1111/j.1462-5822.2006.00815.x

Park, Y., Kim, Y., Putnam, S.M., Stanley, D.W., 2003. The bacterium Xenorhabdus nematophilus depresses nodulation reactions to infection by inhibiting eicosanoid biosynthesis in tobacco hornworms, Manduca sexta. Arch. Insect Biochem. Physiol. 52, 71–80. https://doi.org/10.1002/arch.10076

Pastor, J., 2017. Ecosystem Ecology and Evolutionary Biology, a New Frontier for Experiments and Models. Ecosystems 20, 245–252. https://doi.org/10.1007/s10021-016-0069-9

Peck, M.D., Babcock, G.F., Alexander, J.W., 1992. The role of protein and calorie restriction in outcome from Salmonella infection in mice. JPEN J. Parenter. Enteral Nutr. 16, 561–565. https://doi.org/10.1177/0148607192016006561

Pekkonen, M., Ketola, T., Laakso, J.T., 2013. Resource Availability and Competition Shape the Evolution of Survival and Growth Ability in a Bacterial Community. PLoS ONE 8. https://doi.org/10.1371/journal.pone.0076471

Penczykowski, R.M., Lemanski, B.C.P., Sieg, R.D., Hall, S.R., Ochs, J.H., Kubanek, J., Duffy, M.A., 2014. Poor resource quality lowers transmission potential by changing foraging behaviour. Funct. Ecol. 28, 1245–1255. https://doi.org/10.1111/1365-2435.12238

Pernice, M., Simpson, S.J., Ponton, F., 2014. Towards an integrated understanding of gut microbiota using insects as model systems. J. Insect Physiol., Mechanisms of Nutritional Homeostasis in Insects 69, 12–18. https://doi.org/10.1016/j.jinsphys.2014.05.016

Petersen, A.J., Rimkus, S.A., Wassarman, D.A., 2012. ATM kinase inhibition in glial cells activates the innate immune response and causes neurodegeneration in Drosophila. Proc. Natl. Acad. Sci. 109, E656–E664. https://doi.org/10.1073/pnas.1110470109

Pigliucci, M., Pigliucci, P. of E. and E.D. of B.M., 2001. Phenotypic Plasticity: Beyond Nature and Nurture. JHU Press.

Pilizota, T., Shaevitz, J.W., 2014. Origins of Escherichia coli Growth Rate and Cell Shape Changes at High External Osmolality. Biophys. J. 107, 1962–1969. https://doi.org/10.1016/j.bpj.2014.08.025

Poissonnier, L.-A., Lihoreau, M., Gomez-Moracho, T., Dussutour, A., Buhl, J., 2018. A theoretical exploration of dietary collective medication in social insects. J. Insect Physiol., SI: Nutritional Homeostasis 106, 78–87. https://doi.org/10.1016/j.jinsphys.2017.08.005

Polis, G.A., Myers, C.A., Holt, R.D., 1989. The Ecology and Evolution of Intraguild Predation: Potential Competitors That Eat Each Other. Annu. Rev. Ecol. Syst. 20, 297–330. https://doi.org/10.1146/annurev.es.20.110189.001501

Ponton, F., Lalubin, F., Fromont, C., Wilson, K., Behm, C., Simpson, S.J., 2011a. Hosts use altered macronutrient intake to circumvent parasite-induced reduction in fecundity. Int. J. Parasitol. 41, 43–50. https://doi.org/10.1016/j.ijpara.2010.06.007

Ponton, F., Wilson, K., Cotter, S.C., Raubenheimer, D., Simpson, S.J., 2011b. Nutritional Immunology: A Multi-Dimensional Approach. PLOS Pathog. 7, e1002223. https://doi.org/10.1371/journal.ppat.1002223

Ponton, F., Wilson, K., Holmes, A., Raubenheimer, D., Robinson, K.L., Simpson, S.J., 2014. Macronutrients mediate the functional relationship between Drosophila and Wolbachia. Proc. R. Soc. B Biol. Sci. 282, 20142029–20142029. https://doi.org/10.1098/rspb.2014.2029

Ponton, F., Wilson, K., Holmes, A.J., Cotter, S.C., Raubenheimer, D., Simpson, S.J., 2013. Integrating nutrition and immunology: A new frontier. J. Insect Physiol., Immune Interactions Between Insects and Their Natural Antagonists: a Workshop Honoring Professor Stuart E. Reynolds 59, 130–137. https://doi.org/10.1016/j.jinsphys.2012.10.011

Popham, H.J.R., Shelby, K.S., 2006. Uptake of dietary micronutrients from artificial diets by larval Heliothis virescens. J. Insect Physiol. 52, 771–777. https://doi.org/10.1016/j.jinsphys.2006.04.005

Popham, H.J.R., Shelby, K.S., Popham, T.W., 2005. Effect of dietary selenium supplementation on resistance to baculovirus infection. Biol. Control 32, 419–426. https://doi.org/10.1016/j.biocontrol.2004.12.011

Povey, S., Cotter, S.C., Simpson, S.J., Lee, K.P., Wilson, K., 2009. Can the protein costs of bacterial resistance be offset by altered feeding behaviour? J. Anim. Ecol. 78, 437–446. https://doi.org/10.1111/j.1365-2656.2008.01499.x

Povey, S., Cotter, S.C., Simpson, S.J., Wilson, K., 2014. Dynamics of macronutrient self-medication and illness-induced anorexia in virally infected insects. J. Anim. Ecol. 83, 245–255. https://doi.org/10.1111/1365-2656.12127

Pranaw, K., 2013. Extracellular Novel Metalloprotease from Xenorhabdus indica and Its Potential as an Insecticidal Agent. J. Microbiol. Biotechnol. 23, 1536–1543. https://doi.org/10.4014/jmb.1306.06062

Pranaw, K., Singh, S., Dutta, D., Chaudhuri, S., Ganguly, S., Nain, L., 2014. Statistical Optimization of Media Components for Production of Fibrinolytic Alkaline Metalloproteases from Xenorhabdus indica KB-3 [WWW Document]. Biotechnol. Res. Int. https://doi.org/10.1155/2014/293434

Pulkkinen, K., Pekkala, N., Ashrafi, R., Hämäläinen, D.M., Nkembeng, A.N., Lipponen, A., Hiltunen, T., Valkonen, J.K., Taskinen, J., 2018. Effect of resource availability on evolution of virulence and competition in an environmentally transmitted pathogen. FEMS Microbiol. Ecol. 94. https://doi.org/10.1093/femsec/fiy060

R Core Team, 2014. R: A Language and Environment for Statistical Computing. R Foundation for Statistical Computing, Vienna, Austria.

Rahimnejad, S., Lee, K.-J., 2014. Dietary arginine requirement of juvenile red sea bream Pagrus major. Aquaculture 434, 418–424. https://doi.org/10.1016/j.aquaculture.2014.09.003

Rahnamaeian, M., Cytryńska, M., Zdybicka-Barabas, A., Dobslaff, K., Wiesner, J., Twyman, R.M., Zuchner, T., Sadd, B.M., Regoes, R.R., Schmid-Hempel, P., Vilcinskas, A., 2015. Insect antimicrobial peptides show potentiating functional interactions against Gram-negative bacteria. Proc R Soc B 282, 20150293. https://doi.org/10.1098/rspb.2015.0293

Ramarao, N., Nielsen-Leroux, C., Lereclus, D., 2012. The Insect Galleria mellonella as a Powerful Infection Model to Investigate Bacterial Pathogenesis. J. Vis. Exp. JoVE. https://doi.org/10.3791/4392

Rang, H.P., Ritter, J.M., Flower, R.J., Henderson, G., 2011. Rang & Dale's Pharmacology, 7e, 7 edition. ed. Churchill Livingstone, Edinburgh; New York.

Rapkin, J., Jensen, K., Archer, C.R., House, C.M., Sakaluk, S.K., Castillo, E. del, Hunt, J., 2018. The Geometry of Nutrient Space–Based Life-History Trade-Offs: Sex-Specific Effects of Macronutrient Intake on the Trade-Off between Encapsulation Ability and Reproductive Effort in Decorated Crickets. Am. Nat. 191, 452–474. https://doi.org/10.1086/696147

Raubenheimer, D., Boggs, C., 2009. Nutritional ecology, functional ecology and Functional Ecology. Funct. Ecol. 23, 1–3. https://doi.org/10.1111/j.1365-2435.2009.01530.x

Raubenheimer, D., Lee, K.P., Simpson, S.J., 2005. Does Bertrand's rule apply to macronutrients? Proc. R. Soc. Lond. B Biol. Sci. 272, 2429–2434. https://doi.org/10.1098/rspb.2005.3271

Raubenheimer, D., Simpson, S.J., 2009. Nutritional PharmEcology: Doses, nutrients, toxins, and medicines. Integr. Comp. Biol. 49, 329–337. https://doi.org/10.1093/icb/icp050

Raubenheimer, D., Simpson, S.J., 2003. Nutrient balancing in grasshoppers: behavioural and physiological correlates of dietary breadth. J. Exp. Biol. 206, 1669–1681. https://doi.org/10.1242/jeb.00336

Raubenheimer, D., Simpson, S.J., 1998. Nutrient transfer functions: the site of integration between feeding behaviour and nutritional physiology: Chemoecology 8, 61–68. https://doi.org/10.1007/PL00001805

Raubenheimer, D., Simpson, S.J., Le Couteur, D.G., Solon-Biet, S.M., Coogan, S.C.P., 2016. Nutritional ecology and the evolution of aging. Exp. Gerontol., Perspectives in Aging: Mechanisms Nutritional Interventions 86, 50–61. https://doi.org/10.1016/j.exger.2016.04.007

Raubenheimer, D., Simpson, S.J., Mayntz, D., 2009. Nutrition, ecology and nutritional ecology: toward an integrated framework. Funct. Ecol. 23, 4–16. https://doi.org/10.1111/j.1365-2435.2009.01522.x

Raubenheimer, D., Simpson, S.J., Tait, A.H., 2012. Match and mismatch: conservation physiology, nutritional ecology and the timescales of biological adaptation. Philos. Trans. R. Soc. B Biol. Sci. 367, 1628–1646. https://doi.org/10.1098/rstb.2012.0007

Raubenheimer, D., Simpson, S.L., 1992. Analysis of covariance: an alternative to nutritional indices. Entomol. Exp. Appl. 62, 221–231. https://doi.org/10.1111/j.1570-7458.1992.tb00662.x

Read, A.F., Graham, A.L., Råberg, L., 2008. Animal Defenses against Infectious Agents: Is Damage Control More Important Than Pathogen Control. PLOS Biol. 6, e1000004. https://doi.org/10.1371/journal.pbio.1000004

Redfield, A.C., 1958. The Biological Control Of Chemical Factors In The Environment. Am. Sci. 46, 230A–221.

Reece, S.E., Ramiro, R.S., Nussey, D.H., 2009. Plastic parasites: sophisticated strategies for survival and reproduction? Evol. Appl. 2, 11–23. https://doi.org/10.1111/j.1752-4571.2008.00060.x

Ribeiro, C., Brehélin, M., 2006. Insect haemocytes: What type of cell is that? J. Insect Physiol. 52, 417–429. https://doi.org/10.1016/j.jinsphys.2006.01.005

Richards, G.R., Goodrich-Blair, H., 2009. Masters of conquest and pillage: Xenorhabdus nematophila global regulators control transitions from virulence to nutrient acquisition. Cell. Microbiol. 11, 1025–1033. https://doi.org/10.1111/j.1462-5822.2009.01322.x

Rinderer, T.E., Dell Elliott, K., 1977. Worker Honey Bee Response to Infection with Nosema apis: Influence of Diet. J. Econ. Entomol. 70, 431–433. https://doi.org/10.1093/jee/70.4.431

Ripley, B., Venables, B., Bates, D.M., ca 1998), K.H. (partial port, ca 1998), A.G. (partial port, Firth, D., 2018. MASS: Support Functions and Datasets for Venables and Ripley's MASS.

Rock, G.C., King, K.W., 1967. Qualitative amino acid requirements of the red-banded leaf roller, Argyrotaenia velutinana (Lepidoptera: Tortricidae). J. Insect Physiol. 13, 59–68. https://doi.org/10.1016/0022-1910(67)90003-0

Rockstein, M., 2012. Biochemistry of Insects. Elsevier.

Rodríguez, R.A., Duncan, J.M., Delgado, J.D., Vanni, M.J., Riera, R., González, M.J., 2018. Additional empirical evidence on the intrinsic trend to stationarity in the long run and the nested relationship between abiotic, biotic and anthropogenic factors starting from the organic biophysics of ecosystems (OBEC). Ecol. Model. 383, 23–30. https://doi.org/10.1016/j.ecolmodel.2018.05.014

Rynkiewicz, E.C., Pedersen, A.B., Fenton, A., 2015. An ecosystem approach to understanding and managing within-host parasite community dynamics. Trends Parasitol. 31, 212–221. https://doi.org/10.1016/j.pt.2015.02.005

Ryu, J.-H., Kim, S.-H., Lee, H.-Y., Bai, J.Y., Nam, Y.-D., Bae, J.-W., Lee, D.G., Shin, S.C., Ha, E.-M., Lee, W.-J., 2008. Innate Immune Homeostasis by the Homeobox Gene Caudal and Commensal-Gut Mutualism in Drosophila. Science 319, 777–782. https://doi.org/10.1126/science.1149357

Saito, S., 1963. Trehalose in the body fluid of the silkworm, Bombyx mori L. J. Insect Physiol. 9, 509–519. https://doi.org/10.1016/0022-1910(63)90061-1

Sakkas, P., Houdijk, J.G.M., Jones, L.A., Knox, D.P., Kyriazakis, I., 2011. Dietary protein and energy supplies differentially affect resistance to parasites in lactating mammals. Br. J. Nutr. 106, 1207–1215. https://doi.org/10.1017/S0007114511001565

Salama, H.S., Shoukry, A., 1972. Flight Range of the Moth of the Cotton Leaf Worm Spodoptera littoralis (Bois.). Z. Für Angew. Entomol. 71, 181–184. https://doi.org/10.1111/j.1439-0418.1972.tb01739.x

Schmid-Hempel, P., 2005. Evolutionary Ecology of Insect Immune Defenses. Annu. Rev. Entomol. 50, 529–551. https://doi.org/10.1146/annurev.ento.50.071803.130420

Schowalter, T.D., 2016. Insect Ecology: An Ecosystem Approach. Academic Press.

Semba, R.D., 2012. The Historical Evolution of Thought Regarding Multiple Micronutrient Nutrition. J. Nutr. 142, 143S-156S. https://doi.org/10.3945/jn.110.137745

Serbus, L.R., White, P.M., Silva, J.P., Rabe, A., Teixeira, L., Albertson, R., Sullivan, W., 2015. The Impact of Host Diet on Wolbachia Titer in Drosophila. PLOS Pathog. 11, e1004777. https://doi.org/10.1371/journal.ppat.1004777

Sergeant, M., Baxter, L., Jarrett, P., Shaw, E., Ousley, M., Winstanley, C., Morgan, J.A.W., 2006. Identification, Typing, and Insecticidal Activity of Xenorhabdus Isolates from Entomopathogenic Nematodes in United Kingdom Soil and Characterization of the xpt Toxin Loci. Appl. Environ. Microbiol. 72, 5895–5907. https://doi.org/10.1128/AEM.00217-06

Shankar, A.H., Prasad, A.S., 1998. Zinc and immune function: the biological basis of altered resistance to infection. Am. J. Clin. Nutr. 68, 447S-463S. https://doi.org/10.1093/ajcn/68.2.447S

Sheldon, B.C., Verhulst, S., 1996. Ecological immunology: costly parasite defences and trade-offs in evolutionary ecology. Trends Ecol. Evol. 11, 317–321. https://doi.org/10.1016/0169-5347(96)10039-2

Shi, Y., Gao, G.F., 2012. Linking innate and adaptive immunity. Chin. Sci. Bull. 57, 4100–4102. https://doi.org/10.1007/s11434-012-5480-9

Sicard, M., Ferdy, J.-B., Pagès, S., Le Brun, N., Godelle, B., Boemare, N., Moulia, C., 2004. When mutualists are pathogens: an experimental study of the symbioses between Steinernema (entomopathogenic nematodes) and Xenorhabdus (bacteria). J. Evol. Biol. 17, 985–993. https://doi.org/10.1111/j.1420-9101.2004.00748.x

Silverman, N., Paquette, N., 2008. The Right Resident Bugs. Science 319, 734–735. https://doi.org/10.1126/science.1154209

Simcock, N.K., Gray, H.E., Wright, G.A., 2014. Single amino acids in sucrose rewards modulate feeding and associative learning in the honeybee. J. Insect Physiol., Mechanisms of Nutritional Homeostasis in Insects 69, 41–48. https://doi.org/10.1016/j.jinsphys.2014.05.004

Simmonds, M.S., Simpson, S.J., Blaney, W.M., 1992. Dietary selection Behaviour in Spodoptera Littoralis: The Effects of conditioning Diet and conditioning period on Neural Responsiveness and selection Behaviour. J. Exp. Biol. 162, 73–90.

Simpson, C.L., Simpson, S.J., Abisgold, J.D., 1991. The role of various amino acids in the protein compensatory response of Locusta migratoria. Insect-Plants 39, 39–46.

Simpson, S.J., Abisgold, J.D., 1985. Compensation by locusts for changes in dietary nutrients: behavioural mechanisms. Physiol. Entomol. 10, 443–452. https://doi.org/10.1111/j.1365-3032.1985.tb00066.x

Simpson, S.J., Clissold, F.J., Lihoreau, M., Ponton, F., Wilder, S.M., Raubenheimer, D., 2015. Recent Advances in the Integrative Nutrition of Arthropods [WWW Document]. Httpdxdoiorg101146annurev-Ento-010814-020917. URL http://www.annualreviews.org/doi/10.1146/annurev-ento-010814-020917 (accessed 2.22.17).

Simpson, S.J., Raubenheimer, D., 2012. The Nature of Nutrition: A Unifying Framework from Animal Adaptation to Human Obesity. Princeton University Press, Princeton.

Simpson, S.J., Raubenheimer, D., 2005. Obesity: the protein leverage hypothesis. Obes. Rev. 6, 133–142. https://doi.org/10.1111/j.1467-789X.2005.00178.x

Simpson, S.J., Raubenheimer, D., 1995. The geometric analysis of feeding and nutrition: a user's guide. J. Insect Physiol. 41, 545–553. https://doi.org/10.1016/0022-1910(95)00006-G

Simpson, S.J., Raubenheimer, D., 1993a. A multi-level analysis of feeding behaviour: the geometry of nutritional decisions. Philos. Trans. R. Soc. Lond. B. Biol. Sci. 342, 381–402. https://doi.org/10.1098/rstb.1993.0166

Simpson, S.J., Raubenheimer, D., 1993b. The central role of the haemolymph in the regulation of nutrient intake in insects. Physiol. Entomol. 18, 395–403. https://doi.org/10.1111/j.1365-3032.1993.tb00613.x

Simpson, S.J., Sibly, R.M., Lee, K.P., Behmer, S.T., Raubenheimer, D., 2004. Optimal foraging when regulating intake of multiple nutrients. Anim. Behav. 68, 1299–1311. https://doi.org/10.1016/j.anbehav.2004.03.003

Simpson, S.J., Simpson, C.L., 1992. Mechanisms controlling modulation by haemolymph amino acids of gustatory responsiveness in the locust. J. Exp. Biol. 168, 269'287.

Singer, M.S., Mace, K.C., Bernays, E.A., 2009. Self-Medication as Adaptive Plasticity: Increased Ingestion of Plant Toxins by Parasitized Caterpillars. PLOS ONE 4, e4796. https://doi.org/10.1371/journal.pone.0004796

Singer, M.S., Mason, P.A., Smilanich, A.M., 2014. Ecological Immunology Mediated by Diet in Herbivorous Insects. Integr. Comp. Biol. 54, 913–921. https://doi.org/10.1093/icb/icu089

Singh, J., Banerjee, N., 2008. Transcriptional Analysis and Functional Characterization of a Gene Pair Encoding Iron-Regulated Xenocin and Immunity Proteins of Xenorhabdus nematophila. J. Bacteriol. 190, 3877–3885. https://doi.org/10.1128/JB.00209-08

Smigielski, A.J., Akhurst, R.J., Boemare, N.E., 1994. Phase Variation in Xenorhabdus nematophilus and Photorhabdus luminescens: Differences in Respiratory Activity and Membrane Energization. Appl. Environ. Microbiol. 60, 120–125.

Smilanich, A.M., Mason, P.A., Sprung, L., Chase, T.R., Singer, M.S., 2011. Complex effects of parasitoids on pharmacophagy and diet choice of a polyphagous caterpillar. Oecologia 165, 995–1005. https://doi.org/10.1007/s00442-010-1803-1

Smith, V.H., 1993. Resource Competition between Host and Pathogen. BioScience 43, 21–30. https://doi.org/10.2307/1312103

Smith, V.H., Holt, R.D., 1996. Resource competition and within-host disease dynamics. Trends Ecol. Evol. 11, 386–389. https://doi.org/10.1016/0169-5347(96)20067-9

Snyder, H., Stock, S.P., Kim, S.-K., Flores-Lara, Y., Forst, S., 2007. New Insights into the Colonization and Release Processes of Xenorhabdus nematophila and the Morphology and Ultrastructure of the Bacterial Receptacle of Its Nematode Host, Steinernema carpocapsae. Appl. Environ. Microbiol. 73, 5338–5346. https://doi.org/10.1128/AEM.02947-06

Solomon, E.P., Berg, L.R., Martin, D.W., 2005. Biology. Brooks/Cole Thomson Learning, Belmont, CA.

Solon-Biet, S.M., McMahon, A.C., Ballard, J.W.O., Ruohonen, K., Wu, L.E., Cogger, V.C., Warren, A., Huang, X., Pichaud, N., Melvin, R.G., Gokarn, R., Khalil, M., Turner, N., Cooney, G.J., Sinclair, D.A., Raubenheimer, D., Le Couteur, D.G., Simpson, S.J., 2014. The Ratio of Macronutrients, Not Caloric Intake, Dictates Cardiometabolic Health, Aging, and Longevity in Ad Libitum-Fed Mice. Cell Metab. 19, 418–430. https://doi.org/10.1016/j.cmet.2014.02.009

Solon-Biet, S.M., Mitchell, S.J., Cabo, R. de, Raubenheimer, D., Couteur, D.G.L., Simpson, S.J., 2015. Macronutrients and caloric intake in health and longevity. J. Endocrinol. 226, R17–R28. https://doi.org/10.1530/JOE-15-0173

South, S.H., House, C.M., Moore, A.J., Simpson, S.J., Hunt, J., 2011. Male Cockroaches Prefer a High Carbohydrate Diet That Makes Them More Attractive to Females: Implications for the Study of Condition Dependence. Evolution 65, 1594–1606. https://doi.org/10.1111/j.1558-5646.2011.01233.x

Sperfeld, E., Wagner, N.D., Halvorson, H.M., Malishev, M., Raubenheimer, D., 2016. Bridging Ecological Stoichiometry and Nutritional Geometry with homeostasis concepts and integrative models of organism nutrition. Funct. Ecol. 31, 286–296. https://doi.org/10.1111/1365-2435.12707

Sprouffske, K., Wagner, A., 2016. Growthcurver: an R package for obtaining interpretable metrics from microbial growth curves. BMC Bioinformatics 17. https://doi.org/10.1186/s12859-016-1016-7

Srygley, R.B., Lorch, P.D., 2011. Weakness in the band: nutrient-mediated trade-offs between migration and immunity of Mormon crickets, Anabrus simplex. Anim. Behav. 81, 395–400. https://doi.org/10.1016/j.anbehav.2010.11.006

Stabler, D., Paoli, P.P., Nicolson, S.W., Wright, G.A., 2015. Nutrient balancing of the adult worker bumblebee (Bombus terrestris) depends on the dietary source of essential amino acids. J. Exp. Biol. 218, 793–802. https://doi.org/10.1242/jeb.114249

Stączek, S., Grygorczuk, K., Zdybicka-Barabas, A., Siemińska-Kuczer, A., Vertyporokh, L., Andrejko, M., Wojda, I., Cytryńska, M., 2017. [Different faces of phenoloxidase in animals]. Postepy Biochem. 63, 315–325.

Steeb, B., Claudi, B., Burton, N.A., Tienz, P., Schmidt, A., Farhan, H., Mazé, A., Bumann, D., 2013. Parallel Exploitation of Diverse Host Nutrients Enhances Salmonella Virulence. PLOS Pathog. 9, e1003301. https://doi.org/10.1371/journal.ppat.1003301

Sterner, R.W., Elser, J.J., 2002. Ecological Stoichiometry: The Biology of Elements from Molecules to the Biosphere. Princeton University Press.

Stilwell, M.D., Cao, M., Goodrich-Blair, H., Weibel, D.B., 2018. Studying the Symbiotic Bacterium Xenorhabdus nematophila in Individual, Living Steinernema carpocapsae Nematodes Using Microfluidic Systems. mSphere 3, e00530-17. https://doi.org/10.1128/mSphere.00530-17

Stoler, A.B., Relyea, R.A., 2013. Bottom-up meets top-down: leaf litter inputs influence predator–prey interactions in wetlands. Oecologia 173, 249–257. https://doi.org/10.1007/s00442-013-2595-x

Tang, X., Freitak, D., Vogel, H., Ping, L., Shao, Y., Cordero, E.A., Andersen, G., Westermann, M., Heckel, D.G., Boland, W., 2012. Complexity and Variability of Gut Commensal Microbiota in Polyphagous Lepidopteran Larvae. PLoS ONE 7. https://doi.org/10.1371/journal.pone.0036978

Tanji, T., Hu, X., Weber, A.N.R., Ip, Y.T., 2007. Toll and IMD Pathways Synergistically Activate an Innate Immune Response in Drosophila melanogaster. Mol. Cell. Biol. 27, 4578–4588. https://doi.org/10.1128/MCB.01814-06

Tempest, D.W., Meers, J.L., Brown, C.M., 1970. Influence of Environment on the Content and Composition of Microbial Free Amino Acid Pools. Microbiology 64, 171–185. https://doi.org/10.1099/00221287-64-2-171

Therneau, T.M., 2018. A Package for Survival Analysis in S.

Thomas, G.M., 1979. Xenorhabdus gen. nov., a Genus of Entornopathogenic, Nematophilic Bacteria of the Family Enterobacteriaceae. Int. J. Syst. Bacteriol. 29, 352–360.

Thompson, S.N., 2003. Trehalose – The Insect 'Blood' Sugar, in: Physiology, B.-A. in I. (Ed.), . Academic Press, pp. 205–285. https://doi.org/10.1016/S0065-2806(03)31004-5

Thompson, S.N., 2000. Pyruvate Cycling and Implications for Regulation of Gluconeogenesis in the Insect, Manduca sexta L. Biochem. Biophys. Res. Commun. 274, 787–793. https://doi.org/10.1006/bbrc.2000.3238

Thompson, S.N., Redak, R.A., 2000. Interactions of dietary protein and carbohydrate determine blood sugar level and regulate nutrient selection in the insect Manduca sexta L. Biochim. Biophys. Acta BBA - Gen. Subj. 1523, 91–102. https://doi.org/10.1016/S0304-4165(00)00102-1

Thompson, S.N., Redak, R.A., Wang, L.-W., 2001. Altered dietary nutrient intake maintains metabolic homeostasis in parasitized larvae of the insect Manduca sexta L. J. Exp. Biol. 204, 4065–4080.

Tilman, D., 1986. A Consumer-Resource Approach to Community Structure. Am. Zool. 26, 5–22. https://doi.org/10.1093/icb/26.1.5

Tilman, D., 1982. Resource Competition and Community Structure. Princeton University Press.

Tilman, D., Balzer, C., Hill, J., Befort, B.L., 2011. Global food demand and the sustainable intensification of agriculture. Proc. Natl. Acad. Sci. U. S. A. 108, 20260–20264. https://doi.org/10.1073/pnas.1116437108

Tremaroli, V., Bäckhed, F., 2012. Functional interactions between the gut microbiota and host metabolism. Nature 489, 242–249. https://doi.org/10.1038/nature11552

Trichet, V.V., 2010. Nutrition and immunity: an update. Aquac. Res. 41, 356–372. https://doi.org/10.1111/j.1365-2109.2009.02374.x

Tritschler, M., Vollmann, J.J., Yañez, O., Chejanovsky, N., Crailsheim, K., Neumann, P., 2017. Protein nutrition governs within-host race of honey bee pathogens. Sci. Rep. 7. https://doi.org/10.1038/s41598-017-15358-w

Valtonen, T.M., Kleino, A., Rämet, M., Rantala, M.J., 2010. Starvation Reveals Maintenance Cost of Humoral Immunity. Evol. Biol. 37, 49–57. https://doi.org/10.1007/s11692-009-9078-3

van der Meer, J., 2006. An introduction to Dynamic Energy Budget (DEB) models with special emphasis on parameter estimation. J. Sea Res. 56, 85–102. https://doi.org/10.1016/j.seares.2006.03.001

Vásquez, A., Forsgren, E., Fries, I., Paxton, R.J., Flaberg, E., Szekely, L., Olofsson, T.C., 2012. Symbionts as Major Modulators of Insect Health: Lactic Acid Bacteria and Honeybees. PLOS ONE 7, e33188. https://doi.org/10.1371/journal.pone.0033188

Wake, A., Morgan, H.R., 1986. Host-Parasite Relationship, in: Host-Parasite Relationships and the Yersinia Model, Springer Series in Molecular Biology. Springer, Berlin, Heidelberg, pp. 9–11. https://doi.org/10.1007/978-3-642-71344-6_2

Waldbauer, G.P., Cohen, R.W., Friedman, S., 1984. Self-Selection of an Optimal Nutrient Mix from Defined Diets by Larvae of the Corn Earworm, Heliothis zea (Boddie). Physiol. Zool. 57, 590–597.

Waldbauer, G.P., Friedman, S., 1991. Self-Selection of Optimal Diets by Insects. Annu. Rev. Entomol. 36, 43–63. https://doi.org/10.1146/annurev.en.36.010191.000355

Weathers, K.C., Groffman, P.M., Dolah, E.V., Bernhardt, E., Grimm, N.B., McMahon, K., Schimel, J., Paolisso, M., Maranger, R., Baer, S., Brauman, K., Hinckley, E., 2016. Frontiers in Ecosystem Ecology from a Community Perspective: The Future is Boundless and Bright. Ecosystems 19, 753–770. https://doi.org/10.1007/s10021-016-9967-0

Wei, T., Simko, V., 2016. Visualization of a corrletiaon matrix [WWW Document]. URL https://cran.r-project.org/web/packages/corrplot/corrplot.pdf (accessed 2.22.17).

Weinberg, E.D., Weinberg, G.A., 1995. The role of iron in infection. Curr. Opin. Infect. Dis. 8, 164.

Whittingham, M.J., Stephens, P.A., Bradbury, R.B., Freckleton, R.P., 2006. Why do we still use stepwise modelling in ecology and behaviour? J. Anim. Ecol. 75, 1182–1189. https://doi.org/10.1111/j.1365-2656.2006.01141.x

Wilck, N., Matus, M.G., Kearney, S.M., Olesen, S.W., Forslund, K., Bartolomaeus, H., Haase, S., Mähler, A., Balogh, A., Markó, L., Vvedenskaya, O., Kleiner, F.H., Tsvetkov, D., Klug, L., Costea, P.I., Sunagawa, S., Maier, L., Rakova, N., Schatz, V., Neubert, P., Frätzer, C., Krannich, A., Gollasch, M., Grohme, D.A., Côrte-Real, B.F., Gerlach, R.G., Basic, M., Typas, A., Wu, C., Titze, J.M., Jantsch, J., Boschmann, M., Dechend, R., Kleinewietfeld, M., Kempa, S., Bork, P., Linker, R.A., Alm, E.J., Müller, D.N., 2017. Salt-responsive gut commensal modulates T_H17 axis and disease. Nature 551, 585. https://doi.org/10.1038/nature24628

Willott, E., Hallberg, C.A., Tran, H.Q., 2002. Influence of calcium on Manduca sexta plasmatocyte spreading and network formation. Arch. Insect Biochem. Physiol. 49, 187–202. https://doi.org/10.1002/arch.10019

Willott, E., Tran, H.Q., 2002. Zinc and Manduca sexta hemocyte functions. J. Insect Sci. 2.

Wilson, K., Benton, T.G., Graham, R.I., Grzywacz, D., 2013. Pest Control: Biopesticides' Potential. Science 342, 799–799. https://doi.org/10.1126/science.342.6160.799-a

Wood, S., 2006. Generalized additive models: an introduction with R. CRC press.

World Health Organization, 2004. Inheriting the world : the atlas of children's health and the environment. Geneva : World Health Organization, Geneva.

Wyatt, G.R., 1961. The Biochemistry of Insect Hemolymph. Annu. Rev. Entomol. 6, 75–102. https://doi.org/10.1146/annurev.en.06.010161.000451

Wyatt, G.R., Loughheed, T.C., Wyatt, S.S., 1956. THE CHEMISTRY OF INSECT HEMOLYMPH. J. Gen. Physiol. 39, 853–868.

Yamanaka, S., Hagiwara, A., Nishimura, Y., Tanabe, H., Ishibashi, N., 1992. Biochemical and physiological characteristics of Xenorhabdus species, symbiotically associated with entomopathogenic nematodes including Steinernema kushidai and their pathogenicity against Spodoptera litura (Lepidoptera: Noctuidae). Arch. Microbiol. 158. https://doi.org/10.1007/BF00276297

Yoo, S.K., Brown, I., Gaugler, R., 2000. Liquid media development for Heterorhabditis bacteriophora : lipid source and concentration. Appl. Microbiol. Biotechnol. 54, 759–763. https://doi.org/10.1007/s002530000478

Zanotto, F.P., Raubenheimer, D., Simpson, S.J., 1996. Haemolymph amino acid and sugar levels in locusts fed nutritionally unbalanced diets. J. Comp. Physiol. B 166, 223–229. https://doi.org/10.1007/BF00263986

Zanotto, F.P., Raubenheimer, D., Simpson, S.J., 1994. Selective egestion of lysine by locusts fed nutritionally unbalanced foods. J. Insect Physiol. 40, 259–265. https://doi.org/10.1016/0022-1910(94)90049-3

Zhang, Q.-G., Buckling, A., 2016. Migration highways and migration barriers created by host–parasite interactions. Ecol. Lett. 19, 1479–1485. https://doi.org/10.1111/ele.12700

Zhao, J., Yang, X., Auh, S.L., Kim, K.D., Tang, H., Fu, Y.-X., 2009. Do adaptive immune cells suppress or activate innate immunity? Trends Immunol. 30, 8–12. https://doi.org/10.1016/j.it.2008.10.003

Zhong, H., Marcus, S.L., Li, L., 2005. Microwave-assisted acid hydrolysis of proteins combined with liquid chromatography MALDI MS/MS for protein identification. J. Am. Soc. Mass Spectrom. 16, 471–481. https://doi.org/10.1016/j.jasms.2004.12.017